BRNO UNIVERSITY OF TECHNOLOGY

VYSOKÉ UČENÍ TECHNICKÉ V BRNĚ

FACULTY OF MECHANICAL ENGINEERING

FAKULTA STROJNÍHO INŽENÝRSTVÍ

INSTITUTE OF PHYSICAL ENGINEERING

ÚSTAV FYZIKÁLNÍHO INŽENÝRSTVÍ

SCANNING ELECTRON MICROSCOPY AND ITS APPLICATIONS FOR SENSITIVE SAMPLES

RASTROVACÍ ELEKTRONOVÁ MIKROSKOPIE A JEJÍ APLIKACE PRO SENSITIVNÍ VZORKY

DOCTORAL THESIS

DIZERTAČNÍ PRÁCE

AUTHOR   Mgr. Kamila Hrubanová
AUTOR PRÁCE

SUPERVISOR   Ing. Vladislav Krzyžánek, Ph.D.
ŠKOLITEL

BRNO 2019

This doctoral thesis was created

at the Institute of Scientific Instruments of the CAS, v. v. i.,

Electron Microscopy department,

under supervision of Ing. Vladislav Krzyžánek, Ph.D.

Statement

I declare that I have written the Doctoral Thesis titled *"Scanning electron microscopy and its applications for sensitive samples"* independently, under the guidance of the supervisor Ing. Vladislav Krzyžánek, Ph.D., and using exclusively the technical references and other sources of information cited in the thesis and listed in the comprehensive bibliography at the end of the thesis. As the author I furthermore declare that, with respect to the creation of this Doctoral Thesis, I have not infringed any copyright or violated anyone's personal and/or ownership rights. In this context, I am fully aware of the consequences of breaking Regulation§ 11 of the Copyright Act No. 121/2000 Coll. of the Czech Republic, as amended, and of any breach of rights related to intellectual property or introduced within amendments to relevant Acts such as the Intellectual Property Act or the Criminal Code, Act No. 40/2009 Coll., Section 2, Head VI, Part 4.

--   --

In Brno   Kamila Hrubanová

Acknowledgements

Herein, I would like to express my sincere gratitude to my supervisor Ing. Vladislav Krzyžánek, Ph.D. for his support, motivation and valuable advice during my Ph.D. studies and to all of my colleagues, especially to Mgr. Bc. Kateřina Adámková and Mgr. Ing. Radim Skoupý, because good team is essential in scientific research. I would also like to thank Mgr. Ota Samek, Ph.D. for his advice and support with the Raman spectroscopy results. I would like to thank the staff at the Biological Centre of the CAS in České Budějovice for their support in my initial efforts with the cryo-SEM technique. A very special gratitude goes to my children for their generous patience with my continuous work commitment and to my husband for his endless support, help and understanding in difficult times. Finally, I would like to thank my family and my friends for being in my life and making me the person that I am.

Abstract

The presented dissertation thesis titled "*Scanning electron microscopy and its applications for sensitive samples*" describes an instrumental and methodological development in the field of scanning electron microscopy leading to an innovative solution that could be particularly applicable in microbiological research. A summary of the history and current state of electron microscopy (EM) as a scientific imaging and analytical technique is provided in the introductory chapters. The undeniable contribution of EM in the biological and medical sciences is evidenced by many cited scientific publications. This dissertation thesis contains innovations and improvements in specimen preparation and cryogenic scanning electron microscopy (cryo-SEM) produced at the Institute of Scientific Instruments of the CAS in Brno. In particular, the new constructions of special sample holders together with methodological development in the field of microbiological sample preparation resulted in finding optimal parameters for individual processes. In the experimental part there is showed a verification of methodological procedures in the study of hydrated and electron beam sensitive specimens. Subsequent comparison of different methodological approaches on a defined microbiological system contributes to extending the interpretation of the hitherto known results. Among the microbiological strains investigated were the biofilm positive bacteria *Staphylococcus epidermidis* and yeasts such as *Candida albicans* and *Candida parapsilosis*, which are considered to be clinically significant because they are often involved in serious infections and especially threaten immunocompromised patients. Furthermore, the effect of the biofilm formation of *Bacillus subtilis* on the biodeterioration and biodegradation of poly-ε-caprolactone films was studied. The new development in low temperature cryo-SEM was employed in the research of microbes with biotechnological potential such as *Cupriavidus necator* and *Sporobolomyces shibatanus*.

Key words

Bibliographic record

Abstrakt

Předložená dizertační práce s názvem *"Rastrovací elektronová mikroskopie a její aplikace pro senzitivní vzorky"* pojednává o problematice rastrovací elektronové mikroskopie v kontextu instrumentálního a metodologického vývoje vedoucího k inovativnímu řešení, které je dobře aplikovatelné zejména v mikrobiologickém výzkumu. Součástí práce je rozprava o historii a současném stavu elektronové mikroskopie (EM) jakožto vědecké zobrazovací a analytické techniky, tato část se nachází v úvodních kapitolách. Nepopiratelný přínos EM v biologických a lékařských oborech je dokazován mnoha citovanými vědeckými publikacemi. Předložená dizertační práce přináší novinky z oblasti přípravy preparátů a kryogenní rastrovací elektronové mikroskopie (cryo-SEM) vyvinuté na pracovišti Ústavu přístrojové techniky AV ČR, v.v.i. v Brně. Jedná se především o návrhy a výrobu speciálních držáků vzorků a vývoj nových metodik v oblasti přípravy mikrobiologických preparátů vedoucích k nalezení optimálních parametrů jednotlivých procesů. V experimentální části se nachází ověření metodologických postupů při studiu hydratovaných a na elektronový svazek senzitivních preparátů. Následné srovnání různých přístupů na definovaném biologickém systému z oblasti mikrobiologie přispívá k rozšíření interpretace doposud známých výsledků. Mezi zkoumanými mikrobiologickými kmeny byly biofilm-pozitivní bakterie *Staphylococcus epidermidis* a kvasinky jako *Candida albicans* a *Candida parapsilosis*, jež jsou považovány za klinicky významné, protože se podílejí na vzniku závažných infekcí zejména u imunokompromitovaných pacientů. Dále byl studován vliv růstu biofilmu bakterie *Bacillus subtilis* na biodeteriorizaci a biodegradaci poly-ε-kaprolaktonových fólií. Vývoj v oblasti cryo-SEM byl aplikován ve výzkumu mikrobů s biotechnologickým potenciálem, jako jsou např. *Cupriavidus necator* a *Sporobolomyces shibatanus*.

Klíčová slova

Elektronová mikroskopie, cryo-SEM, příprava preparátů, mikrobiologie, biofilm

Bibliografický záznam

Contents

Contribution of the thesis

The research merit of this doctoral thesis is supported by authoring and co-authoring 34 scientific publications. Most of these are directly linked with basic and applied research in the field of microbiology and scanning electron microscopy, especially with the use of low temperatures during sample preparation as well as imaging. Out of the 34 publications, eight were published in impacted journals, one in a non-impacted journal and 25 were published in several international conference proceedings. The engineering contribution related to cryogenic scanning electron microscopy (cryo-SEM) is resulted in the valid utility model no. 32258 and two functional samples (RIV/68081731:_____/18:00498266 and RIV/68081731:_____/17:00483558). Moreover, there are some important specific contributions to the field of clinical and environmental microbiology:

- A methodology for the preparation and visualization of clinically significant and biofilm positive microbial strains using scanning electron microscopy was developed with the aim of visualizing under high magnification the ultrastructure of the extracellular matrix produced during cultivation and the relationships among the microbial cells in the biofilm as well as to study areas of the biofilm where the microbial cells adhere to the substrate/surface.
- A methodology for the preparation and visualization of microbial cultures connected with an environmental/biotechnological potential using scanning electron microscopy was improved with the intention to study polymer production as well as polymer biodeterioration.

The educational contribution of this doctoral thesis is represented by supervising one bachelor thesis which was successfully defended in 2014 and two master theses where the author acted as a consultant. Several students' measurements resulted in co-authoring conference papers. Furthermore, authors educational activities were connected with the preparation of two workshops "*Recent trends in cryo-SEM applied to biology and chemistry, 2016*" and "*Correlative microscopy of beam sensitive samples, 2018*" organized by the research group Microscopy for biomedicine (BioEM) at the ISI of CAS. Both events were aimed at students and professional public and drew nearly one hundred participants. Last but not least, participating in the establishment of a new BioEM lab can be considered to be an indirect contribution by this work's author.

List of publications

The following information were available in Scopus database and ASEP database.

Date: 04.06.2019

Impacted journal article

1. Hrubanová, K., Krzyžánek, V., Nebesářová, J., Růžička, F., Pilát, Z., Samek, O. Monitoring *Candida parapsilosis* and *Staphylococcus epidermidis* Biofilms by a Combination of Scanning Electron Microscopy and Raman Spectroscopy. *Sensors*. 2018, 18(12), 4089. ISSN 1424-8220 doi: 10.3390/s18124089

2. Hrubanová, K., Nebesářová, J., Růžička, F., Krzyžánek, V. The innovation of cryo-SEM freeze-fracturing methodology demonstrated on high pressure frozen biofilm. *Micron*. 2018, 110(JUL), 28-35. ISSN 0968-4328
doi: 10.1016/j.micron.2018.04.006

3. Obruča, S., Sedláček, P., Krzyžánek, V., Mravec, F., Hrubanová, K., Samek, O., Kučera, D., Benešová, P., Márová, I. Accumulation of Poly(3-hydroxybutyrate) Helps Bacterial Cells to Survive Freezing. *PLoS ONE*. 2016, 11(6), 0157778:1-16. E-ISSN 1932-6203
doi: 10.1371/journal.pone.0157778

4. Obruča, S., Sedláček, P., Mravec, F., Krzyžánek, V., Nebesářová, J., Samek, O., Kučera, D., Benešová, P., Hrubanová, K., Milerová, M., Márová, I. The presence of PHB granules in cytoplasm protects non-halophilic bacterial cells against the harmful impact of hypertonic environments. *New Biotechnology*. 2017, 39(OCT), 68-80. ISSN 1871-6784
doi: 10.1016/j.nbt.2017.07.008

5. Samek, O., Bernatová, S., Ježek, J., Šiler, M., Šerý, M., Krzyžánek, V., Hrubanová, K., Zemánek, P., Holá, V., Růžička, F. Identification of individual biofilm-forming bacterial cells using Raman tweezers. *Journal of Biomedical Optics*. 2015, 20(5), 051038:1-6.
ISSN 1083-3668
doi: 10.1117/1.JBO.20.5.051038

6. Mravec, F., Obruča, S., Krzyžánek, V., Sedláček, P., Hrubanová, K., Samek, Ota, Kučera, D., Benešová, P., Nebesářová, Jana. Accumulation of PHA granules in *Cupriavidus necator* as seen by confocal fluorescence microscopy. *FEMS Microbiology Letters*. 2016, 363(10), fnw094:1-7. ISSN 0378-1097
doi: 10.1093/femsle/fnw094.

7. Voběrková, S., Hermanová, S., <u>Hrubanová, K.</u>, Krzyžánek, V. Biofilm formation and extracellular polymeric substances (EPS) production by *Bacillus subtilis* depending on nutritional conditions in the presence of polyester film. *Folia Microbiologica*. 2016, 61(2), 91-100. ISSN 0015-5632
doi: 10.1007/s12223-015-0406-y

8. Pořízka, P., Procházka, D., Pilát, Z., Krajčarová, L., Kaiser, J., Malina, R., Novotný, J., Zemánek, P., Ježek, J., Šerý, M., Bernatová, S., Krzyžánek, V., <u>Dobranská, K.</u>, Novotný, K., Trtílek, M., Samek, O. Application of laser-induced breakdown spectroscopy to the analysis of algal biomass for industrial biotechnology. *Spectrochimica Acta Part B: Atomic Spectroscopy*. 2012, 74-75(AUG-SEP), 169-176. ISSN 0584-8547. Available: doi: 10.1016/j.sab.2012.06.014

Journal article

1. <u>Hrubanová, K.</u>, Krzyžánek, V. Inovativní metodika mrazového lámání a cryo-SEM demonstrovaná na biofilmu *Candidy parapsilosis*. *Jemná mechanika a optika*. 2019, 64(1), 15-17. ISSN 0447-6441.

Proceedings

1. Adámková, K., <u>Hrubanová, K.</u>, Samek, O., Trudičová, M., Sedláček, P., Krzyžánek, V. Structure investigation of hydrogels using a cryo-SEM. In: Recent Trends in Charged Particle Optics and Surface Physics Instrumentation. Proceedings of the 16th International Seminar. Brno: Institute of Scientific Instruments The Czech Academy of Sciences, 2018, S. 26-28. ISBN 978-80-87441-23-7.

2. <u>Hrubanová, K.</u>, Bernatová, S., Samek, O., Šerý, M., Zemánek, P., Nebesářová, J., Růžička, F., Krzyžánek, V. Monitoring of Multilayered Bacterial Biofilm Morphology by Cryo-SEM for Raman Spectroscopy Measurements. *Microscopy and Microanalysis*. 2015, 21(S3), 187-188. ISSN 1431-9276.

3. <u>Hrubanová, K.</u>, Krzyžánek, V., Samek, O., Skoupý, R., Šiler, M., Ježek, J., Obruča, S., Zemánek, P. Morphological and Production Changes in Planktonic and Biofilm Cells Monitored Using SEM and Raman Spectroscopy. *Microscopy and Microanalysis*. 2017, 23(S1), 1158-1159. ISSN 1431-9276
doi: 10.1017/S1431927617006456

4. <u>Hrubanová, K.</u>, Samek, O., Haroniková, A., Bernatová, S., Zemánek, P., Márová, I., Krzyžánek, V. Morphological and Production Changes in Stressed Red Yeasts Monitored Using SEM and Raman Spectroscopy. *Microscopy and Microanalysis*. 2016, 22(S3), 1146-1147. ISSN 1431-9276
doi: 10.1017/S1431927616006577

5. Burdiková, Z., Hickey, C., Auty, M. A. E., Pala, J., Švindrych, Z., Steinmetz, I., Krzyžánek, V., Hrubanová, K., Sheehan, J. J. Cheese Matrix Microstructure Studied by Advanced Microscopic Techniques. *Microscopy and Microanalysis*. 2014, 20(S3), 1336-1337. ISSN 1431-9276
doi: 10.1017/S1431927614008411

6. Hrubanová, K., Voberková, S., Hermanová, S., Krzyžánek, V. Characterization of Polycaprolactone Films Biodeterioration by Scanning Electron Microscopy. *Microscopy and Microanalysis*. 2014, 20(S3), 1950-1951. ISSN 1431-9276 doi: 10.1017/S1431927614011489

7. Hrubanová, K., Nebesářová, J., Růžička, F., Dluhoš, J., Krzyžánek, V. Characterization of Yeast Biofilm by Cryo-SEM and FIB-SEM. *Microscopy and Microanalysis*. 2013, 19(S2), 226-227. ISSN 1431-9276
doi: 10.1017/S1431927613003127

8. Hrubanová, K., Nebesářová, J., Růžička, F., Dluhoš, J., Samek, O., Krzyžánek, V. Comparison of biofilm formation of mixed yeast/bacterial cultures by FIB-SEM tomography. In: Microscopy conference (MC) 2013. Proceedings. Vol. 2. Regensburg: University of Regensburg, 2013, S. 424-425.

9. Hrubanová, K., Nebesářová, J., Růžička, F., Krzyžánek, V. Comparison of freeze fracture images of mixed bacterial/yeast biofilm in cryo-SEM with high pressure freezing fixation. In: 18th International Microscopy Congres. Proceedings. Praha: Czechoslovak Microscopy Society, 2014. ISBN 978-80-260-6720-7.

10. Hrubanová, K., Růžička, F., Nebesářová, J., Burdíková, Z., Dluhoš, J., Collakova, J., Samek, O., Krzyžánek, V. Electron and light microscopy of yeast biofilm. In: Microscopy conference (MC) 2013. Proceedings. Vol. 2. Regensburg: University of Regensburg, 2013, S. 19-20.

11. Hrubanová, K., Krzyžánek, V., Samek, O., Šiler, M., Zemánek, P., Hároniková, A., Marová, I. Monitoring lipid production in yeast using SEM and Raman spectroscopy. In: Gajović, A., Weber, I., Kovačević, G., Čadež, V., Šegota, S., Peharec Štefanić, P., Vidoš, A., eds. 13th Multinational Congress on Microscopy: Book of Abstracts. Zagreb: Ruder Bošković Institute, Croatian Microscopy Society, 2017, S. 308-309. ISBN 978-953-7941-19-2.

12. Hrubanová, K., Samek, O., Obruča, S., Hároniková, A., Krzyžánek, V. Scanning electron microscopy and Raman spectroscopy of microorganisms related to biofuels and biopolymer production. In: MC 2015. Microscopy Conference Proceedings. Göttingen: DGE, 2015, S. 700-701.

13. Hrubanová, K, Skoupý, R., Nebesářová, J., Růžička, F., Krzyžánek, V. The sample preparation for cryo-SEM: the real ultrastructure of microbial biofilm or just artifacts? In: EMC2016. The 16th European Microscopy Congress. Proceedings. Oxford: Wiley, 2016, S. 203-204. ISBN 9783527808465
doi: 10.1002/9783527808465.EMC2016.6907.

14. Krzyžánek, V., Novotná, V., Hrubanová, K., Nebesářová, J. Beam damage of embedding media sections and their investigations by SEM. In: 18th International Microscopy Congres. Proceedings. Praha: Czechoslovak Microscopy Society, 2014.
ISBN 978-80-260-6720-7.

15. Krzyžánek, V., Skoupý, R., Hrubanová, K., Kočová, L., Nebesářová, J. Influence of ultrathin resin section aging and its reduction for imaging in the low voltage STEM. In: MC 2015. Microscopy Conference Proceedings. Göttingen: DGE, 2015, S. 817-818.

16. Obruča, S., Doskočil, L., Krzyžánek, V., Hrubanová, K., Sedláček, P., Mravec, F., Samek, O., Kučera, J., Benešová, P., Márová, I. Polyhydroxyalkanoates in bacterial cells – more than just storage materials. In: Materials Science Forum. Vol. 851. London: Trans Tech Publications, 2016, S. 20-25. ISSN 1662-9752
doi: 10.4028/www.scientific.net/MSF.851.20

17. Šiler, M., Samek, O., Bernatová, S., Mlynariková, K., Ježek, J., Šerý, Mojmír, Krzyžánek, V., Hrubanová, K., Holá, M., Růžička, F., Zemánek, P. Principal component analysis of Raman spectroscopy data for determination of biofilm forming bacteria and yeasts. In: Mika, Filip, ed. Proceedings of the 15th International Seminar on Recent Trends in Charged Particle Optics and Surface Physics Instrumentation. Brno: Institute of Scientific Instruments CAS, 2016, S. 66-67. ISBN 978-80-87441-17-6.

18. Krzyžánek, V., Tacke, S., Hrubanová, K., Reichelt, R. Beyond Imaging: Scanning Electron Microscope for the Quantitative Mass Measurement. *Microscopy and Microanalysis*. 2013, 19(S2), 130-131. ISSN 1431-9276
doi: 10.1017/S143192761300264X

19. Krzyžánek, V., Hrubanová, K., Nebesářová, J., Růžička, F. Cryo-SEM of Perpendicular Cross Freeze-Fractures Through a High-Pressure-frozen Biofilm. *Microscopy and Microanalysis*. 2014, 20(S3), 1232-1233. ISSN 1431-9276
doi: 10.1017/S1431927614007892

20. Novotná, V., Hrubanová, K., Nebesářová, J., Krzyžánek, V. Investigation of Electron Beam Induced Mass Loss of Embedding Media in the Low Voltage STEM. *Microscopy and Microanalysis*. 2014, 20(S3), 1270-1271. ISSN 1431-9276
doi: 10.1017/S1431927614008083

21. Samek, O., Hároniková, A., Vaškovicová, N., <u>Hrubanová, K.</u>, Ježek, Jan, Márová, I., Krzyžánek, V., Zemánek, P. SEM and Raman Spectroscopy Applied to Biomass Analysis for Application in the Field of Biofuels and Food Industry. *Microscopy and Microanalysis*. 2015, 21(S3), 1775-1776. ISSN 1431-9276.

22. Vaškovicová, N., Skoupý, R., Paták, A., <u>Hrubanová, K.</u>, Krzyžánek, V. Cathodoluminescence Study of Microdiamonds and Improvements of Signal Detection by Lowering Temperature of the Sample. *Microscopy and Microanalysis*. 2017, 23(S1), 2284-2285. ISSN 1431-9276
doi: 10.1017/S1431927617012089

23. Vaškovicová, N., <u>Hrubanová, K.</u>, Krzyžánek, V. Is Sputtering Sufficient for Production of Replicas? *Microscopy and Microanalysis*. 2016, 22(S3), 44-45. ISSN 1431-9276
doi: 10.1017/S1431927616001070

24. Vaškovicová, N., <u>Hrubanová, K.</u>, Krzyžánek, V. Processing a Biological Tissue from Cryo-SEM to Replica. *Microscopy and Microanalysis*. 2016, 22(S3), 236-237.
ISSN 1431-9276
doi: 10.1017/S1431927616002038

25. Vaškovicová, N., Skoupý, R., <u>Hrubanová, K.</u>, Kulich, P., Turánek, J., Krzyžánek, V. Localization of nanodiamonds inside cancer cells using cathodoluminescence imaging in the cryo-SEM. In: Gajović, A., Weber, I., Kovačević, G., Čadež, V., Šegota, S., Peharec Štefanić, P., Vidoš, A., eds. 13th Multinational Congress on Microscopy: Book of Abstracts. Zagreb: Ruder Bošković Institute, Croatian Microscopy Society, 2017, S. 80-81. ISBN 978-953-7941-19-2.

The engineering contribution

1. Krzyžánek, V., Skoupý, R., <u>Hrubanová, K.</u>, Vaškovicová, N. Kryo-držák pro SEM umožňující zobrazování tenkých vzorků v transmisním módu s možností prvkové a kato-doluminiscenční analýzy. 2017.

2. Krzyžánek, V., Skoupý, R., <u>Hrubanová, K.</u> Sestava pro regulaci teploty vzorku. 2018. Brno: Ústav přístrojovén techniky AV ČR, v.v.i., 07.11.2018. 32258.

3. Skoupý, R., <u>Hrubanová, K.</u>, Krzyžánek, V. Systém kryo-držáku a antikontaminačního štítu pro katodoluminiscenční analýzu v SEM při velmi nízkých teplotách. 2018.

1 State of art

One of the greatest desires of a men is to explore the world around them, including the hard to reach places, such as the depths of the sea, outer space or the very nature of mass. The development of human knowledge brings a technical progress. The birth of microscopy, which falls into the end of the 16th century [1; 2], most certainly belongs among the milestones in the knowledge of the structure of matter. The invention of a spectacle lens by master Janssen, which would later become the main part of the light microscope opened the so far locked door to the microscopic world [2]. These first microscopic components could magnify objects 20 to 30 times [1]. In the following century, Antonie van Leeuwenhoek invented the first single lens microscope, which represented a vast improvement in the production of lenses and allowed a magnification up to 300 times [1; 3].

At the beginning of the 20th century, samples could be magnified almost 1000 times and it was possible to distinguish two particles 0.2 µm apart [1]. This resolution ability extended also knowledge in biological sciences and medicine, for microscopes helped to reveal agents of some bacterial diseases and to study behaviour and structure of a cell during its life cycle. The maximum resolution of the microscope, however, is limited by the wavelength of the radiation used. This issue was addressed in detail by German physicist Ernst Karl Abbe at the end of the 19th century, when, based on his work [4-6], a simplified equation for the resolution determination was derived:

$$d \geq \frac{\lambda}{2}, \qquad (1)$$

according to which the resolution limit d is always greater than or equal to half the wavelength λ of the light used. This equation was originally derived for classical light microscope, but can be built on for determining resolving power of other microscope types.

A major milestone of the 1930s is the idea and construction of an electron microscope (EM) which pushed the limits of material observation and study to a subatomic resolution. EM is a very important invention for researchers in the field of microscopic and nanoscopic world observations. The path that led to its construction was relatively complicated; one single thought was not enough, only after successive combining of many physical discoveries and technological developments this useful device came into existence. The cornerstone was the discovery of the electron in 1897, which was described by the English experimental physicist, Nobel Prize winner J. J. Thompson [5; 6]. Another important finding, published by Luis de Broglie in 1925, was that the electrons have not only a corpuscular but also a wave nature, which predetermines an electron beam to be used for observing small objects. According to de Broglie hypothesis [1; 6; 7], each particle with the momentum p is bound to a planar monochromatic wave with the wavelength λ:

$$\lambda = \frac{h}{p}, \qquad (2)$$

where h is the Planck constant. This bold claim was independently confirmed two years later by Davisson experiment with electron diffraction, which demonstrated the wave nature of electrons. The works of H. Busch, which were published in 1926, dealt with the description of an electron

beam deflection using magnetic fields in comparison with a light beam and a glass lens [8; 9]. Physical notions and a description concerning the properties of electrons plus theoretical possibilities of their use had already existed, but the specific design of an electron microscope came up a few years later [3; 5; 7].

The construction of the first electron microscope falls into the 1930s, when the first photographs of transmission electron microscope (TEM) and the description of electromagnetic lenses which shaped the electron beam appeared in an article by Knoll and Ruska [9]. TEM microscopes began to be produced commercially in 1939 by the Siemens & Halske company [1; 10]. A commonly used TEM reaches today a resolution lower than 0.2 nm [11]; to compare it with theoretical resolution, the calculation of the de Broglie wavelength may be mentioned (examples in Table 1). Nonrelativistic de Broglie wavelength λ_n in (5) can be expressed by using following relation [5; 6; 11]:

$$p_n = \sqrt{2Tm} \, , \tag{3}$$

where m is the electron mass and T is its kinetic energy. As for an electron of the charge e accelerated with the voltage U, it applies:

$$T = Ue \, . \tag{4}$$

In the nonrelativistic approach the electron mass m_n is equal to its rest mass $m_e = m_n$. By substituting (4) into (3) we obtain the equation for the de Broglie wavelength [6]:

$$\lambda_n = \frac{h}{\sqrt{2U\,e\,m_e}} \, . \tag{5}$$

By contrast, according to the theory of relativity the momentum p_r of an electron with the kinetic energy T is equal to:

$$p_r = v_r m_r = \sqrt{2m_e T \left(1 + \frac{T}{2m_e c^2}\right)} \, , \tag{6}$$

where v_r is the relativistic velocity of an electron, m_r is the relativistic mass of an electron, $m_e c^2$ is rest energy of an electron and c is the speed of light in vacuum. By substituting (6) into (2) we obtain the expression for the relativistic wavelength [6; 11; 12]:

$$\lambda_r = \frac{h}{\sqrt{2m_e\,U\,e\left(1 + \frac{U\,e}{2m_e c^2}\right)}} \, . \tag{7}$$

Table 1: A comparison of de Broglie wavelengths for selected acceleration voltages used in a SEM.

U [kV]	λ_n [pm]	λ_r [pm]	v_n [ms^{-1}]	v_r [ms^{-1}]
1	38.78	38.76	0.19	0.19
5	17.34	17.30	0.42	0.42
30	7.08	6.98	1.03	0.98

Table 1 shows that the relativistic calculation is the more significant the closer the electron energies are to their rest energy ($m_e c^2 \approx 511$ keV). It is also evident that, taking the calculated wavelength into account, the theoretical resolution is several orders of magnitude higher compared to the real resolution of electron microscopes. This is because of the "imperfection" of electron optics which is loaded with a wide range of optical defects (discussed in further chapters) as well as the sample itself and the physical principles of electron scattering.

The path of a scanning electron microscope (SEM) was slightly more complicated. German physicist, professor Manfred von Ardenne, described in 1938 [1; 5; 13; 14] the principle of raster scanning for a transmission electron microscope, an American named Zworykin invented a photomultiplier tube for detecting secondary electrons, and the production of a commercial version of a SEM began in 1960s by Cambridge Scientific Instruments [7; 12].

From that time to the present there has been a significant progress in the field of electron microscopy; there is a range of detectors for scanning different signals emanating from the electron beam interaction with atoms of the studied preparation, and the resolution limit shifted to tenths of a nanometre. There are a number of companies engaged in their development and commercialization, such as Thermo Fisher Scientific, TESCAN, Delong Instruments, JEOL, Hitachi, and Zeiss. In addition, three of these companies are based in Brno (Thermo Fisher Scientific, TESCAN and Delong Instruments). Nowadays, electron microscopes can be considered a necessary part of equipment in laboratories that pursue imaging and research in the field of microscopic and nanoscopic world, and are useful in many fields, such as material research and biological applications. They can provide a comprehensive information on the microstructure, chemical composition and many other properties of the sample examined [12; 13; 15].

In general, electron microscopes mean two basic types, the first of which are SEMs, where the resulting image gives information mainly on the surface of the sample [1; 11; 12]. The second type are TEMs that project electrons through very thin samples [3; 11; 16]. TEM is used for the observation and analysis of the internal structure of very thin samples with atomic resolution. The transmission mode can also be applied in a scanning transmission electron microscope (STEM) or in SEM equipped with transmitted electrons detector (STEM detector in SEM, low voltage STEM), which is at present often composed of several segments whereby it is possible to detect electrons scattered in certain directions (or angles) and thus obtain further information about the sample. STEM microscopes allow to scan the sample surface and simultaneously to detect electrons transmitted through the sample – they map the material in defined regions [1; 5; 12; 17].

Roughly speaking, the electron microscopy has found a wide spectrum of applications and the future of the electron microscopy seems to be promising as well. Automated scanning of large parts of the sample at high resolution, accurate data fusion, and increase in the quality of stored images are becoming an integral part of modern microscopes, and thus extend the limits of their use in science as well. Quantitative imaging, which is becoming an automated process as well, provides a more objective view on biological systems and processes that take place inside cell compartments. The combination of SEM imaging and slicing using focused ion beam (FIB-SEM) or ultramicrotome (serial block-face SEM (SBF-SEM)) offers the possibility of spatial reconstruction of sample volume [18-22]. The electron microscopy will most likely continue to be involved in the solution of many issues in science, medicine and industry.

1.1.1 Principle of the scanning electron microscope

Scanning electron microscopes (SEM) have become very popular thanks to the possibility of taking pictures of samples which provide three-dimensional image of a surface, external structures of which are easily recognizable, and they also allow to view a rather large surface area in comparison with TEM microscopes, which are primarily used for the study of ultrastructure of very thin biological and material samples [3; 5; 11] that are "transparent" for electrons.

Although the designs of some SEM and TEM parts, such as electromagnetic lenses, are very similar, their functions can differ [5; 12]. In the case of SEM, for example, these electromagnetic lenses do not form the image of the sample surface as they do in comparison with the optical principles of more conventional light and transmission electron microscopes, but are used to shape the electron beam which subsequently scans the surface of the studied sample, and as a result of its interaction with atoms of the imaged material it induces production of a number of signals which include secondary electrons carrying topographical information [11-13]. These electrons are further collected using special detectors, processed and compiled as a series of pixels (picture elements). For each point on the sample surface that is hit by the focused electron beam and in which secondary electrons (or other elementary particles and photons) are generated there is a corresponding pixel on the monitor. Brightness intensity of a pixel is directly proportional to the number of generated secondary electrons [1; 5; 13]. In addition to the cathode as the electron source, electromagnetic lenses and detectors, essential components of the SEM design also include, for example, a chamber with a movable stage for mounting a sample, a vacuum system, electronics and a control computer with a monitor and operating software [1; 13]. Schematic drawing of an arrangement of a SEM microscope is shown in Figure 1 [23].

1.1.2 Electron-optic system and electron beam control

A vacuum system is used to maintain low pressure in a microscope interior where electrons are moving [1]. A need for a vacuum arises from several reasons. The air is not a sufficient electrical insulator, a danger of air ionization and subsequent electric discharge between nozzle cathode and anode could therefore arise [5; 12; 13]. The air contains sundry molecules including hydrocarbons which cause contamination of a column and a studied sample. The column area has to be pumped also in order to prevent accidental collisions of accelerated primary electrons with air molecules, which would lead to changes in their energy and direction of motion. A working vacuum is achieved using powerful vacuum pumps [24], which are, for example, rotary, diffusion, ion and turbomolecular [3]. There are vacuum gauges that control the vacuum quality and the whole process of air-pumping is controlled automatically. The electron gun area requires a higher degree of vacuum that is up to 10^{-9} mbar, which is usually achieved by ion vacuum pumps [3].

The image obtained using SEM depends on the signal, hence the quality of the electron source – cathode – is quite essential. Each electron in an atom is bound with an energy, and an energy larger than the binding one must be supplied to this electron, so it could be released from the bond [3; 5; 6; 12]. This may be done in several ways. In electron microscopy, mainly thermoemission methods, where heating a cathode leads to releasing electrons from its surface, and cold field emission methods, where an electrode with high positive voltage is placed against a cold metal thread etched in the "V-shape", are currently applied [12; 13]. A strong electric field is created around the tip that can pull a large number of electrons from the surface of the tip. Among the cathodes used is, e.g., the most widely used thermoemission tungsten hairpin. Input high voltage and direct current flow cause it to heat up to approx. 2 430 °C which leads to the emission of

electrons from the tungsten into the surrounding vacuum in a column [5]. Alternatively, a LaB$_6$ cathode can be used, which does not need to be heated up to as high temperatures as the tungsten one. Another option is to use the Schottky cathode, where the efficiency of the emission source is increased when the electrostatic charge is applied on the surface of a cathode made of tungsten crystal enriched with ZnO [5; 11]. Cold field emission is used mainly in high-resolution microscopes, where there is an electron source with very high efficiency and stability, on the other hand, with the highest purchase costs [5; 11; 25].

In an electron microscope column, a Wehnelt cylinder can be found, which works as an auxiliary electrode. An earthed anode with a hole in the middle is located behind the cylinder. Wehnelt cylinder creates an electric field around the cathode thread, which causes the beam of electrons emitted from the cathode to narrow before the anode opening and create a crossover (the narrowest spot of the beam) [5; 13]. This spot can then be regarded as a point source of accelerated electrons. Electrostatic optics must ensure perfect circularity of the thread projection in the crossover so that we can consider the electron source to be point and coherent. Trajectory, velocity, and width of the electron beam are further adjusted using a system of apertures and lenses [5].
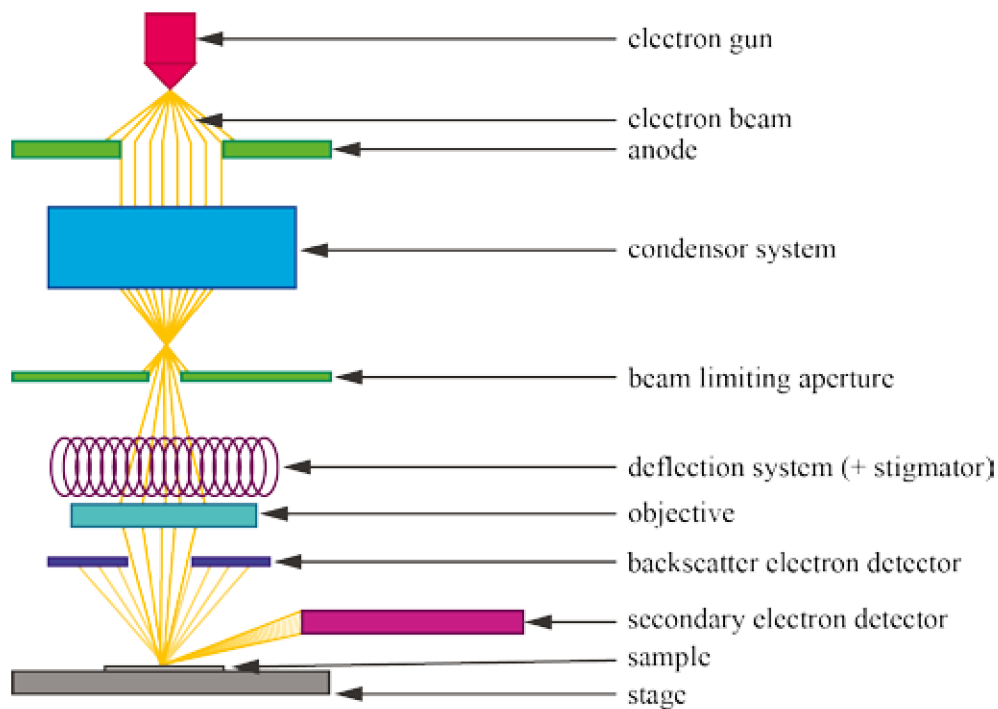
Figure 1: Schematic drawing shows the components of a scanning electron microscope.

A charge e of an electron that is moving in a magnetic field of induction $\vec{B}$ is affected by a force $\vec{F}$ the size and direction of which can be determined from the following equation:

$$\vec{F} = e(\vec{v} \times \vec{B}), \qquad (8)$$

where $\vec{v}$ is the electron velocity [6; 11]. For the magnitude of the force F the following equation applies:

$$F = evB \sin \theta, \qquad (9)$$

where θ is the angle the vectors $\vec{v}$ and $\vec{B}$ contain [6; 11]. If an electron enters a homogeneous magnetic field in the direction perpendicular to the vector of magnetic induction, then the magnetic force affecting the electron curves its trajectory so it begins to move in a circle. Thanks to the knowledge of centrifugal and magnetic forces we can express the radius of curvature of the circular trajectory of the electron motion [6]. If an electron enters the magnetic field at a certain angle, the velocity vector of the electron motion resolves into a normal and tangential component. The resulting trajectory is then a helix the projection of which is in the shape of a circle with radius r:

$$r = \frac{m_e v}{Be}, \qquad (10)$$

where m_e is the mass of the electron [6].

The ability to influence the electron trajectory through a magnetic field can be used to construct an electromagnetic lens that has a function similar to a glass lens in the case of light. The simplest electromagnetic lens is similar to a solenoid. The solenoid is an inductor with a large number of coils the diameter of which is much smaller than the inductor length. Inside the solenoid, almost homogeneous magnetic field is created. The fact that it is not perfectly homogeneous is one of the causes of the emergence of aberrations. Trajectories of all electrons that pass through the same point on the lens axis are affected by the magnetic field of the lens, so that they intersect past the lens at the same point on the lens axis again. The greater the current flowing through the lens is, the greater the magnetic induction of the field in the lens cavity is, and the shorter the focal length of the lens is. To express the focal length, the following equation can be applied:

$$\frac{1}{f} = \frac{e}{8m_e U} \int_{z_1}^{z_0} B_{z0}^2 \, dz, \qquad (11)$$

where B_{z0} is the magnetic induction in point z on the lens axis [5; 6]. Electromagnetic lenses consist of magnet pole pieces with electromagnetic coils winding (Fig. 2) [26]. In addition, smaller focal length means better optical parameters, therefore, it is required that the highest possible current flowed through the electromagnetic inductor. Its size is limited by heat losses, therefore, cooling the lenses is necessary.

The entire imaging system in SEM forms the beam with the required parameters (angular aperture, crossover diameter and current density). The sample surface is scanned by a primary electron beam that is deflected in two mutually perpendicular axes. The primary electron beam is deflected using scanning coils. The sample surface is scanned across line by line. A signal that excites the deflection coils also synchronizes the image creation in a display unit [3].

20
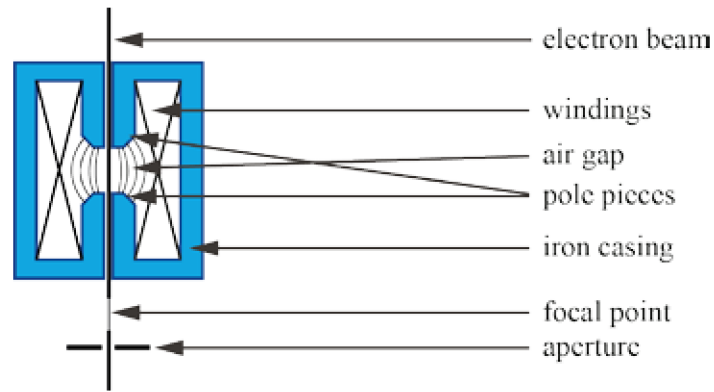
Figure 2: Schematic drawing of an electromagnetic lens used in
EM. Modification of work by James H. Wittke [26].

The objective lens is another important part of the SEM imaging system because achievable resolving power depends on it as well. The limit of the resolving power is primarily determined by the spherical defect size which decreases with decreasing focal length of the objective lens, and by maximum angular aperture of the objective lens given by the objective aperture diameter [5; 11]. Altering its size, the current density changes.

To detect the electrons (or photons), various detectors are used, e.g., ET detector (Everhart and Thornley) [11]. The detector consists of a scintillation crystal or a fluorescent substance that, upon the electron incidence, create photons of visible light which are subsequently transmitted via a light guide to a photocathode electrons are being released from thanks to the photoelectric effect [11]. The electrons are accelerated to an electrode – dynode that has a positive potential. The electron incidence on the dynode causes it to emit secondary electrons that proceed to the next dynode which has a higher potential. From the last electrode – anode – the detected current is conducted away through a decoupling capacitor. Often, this detector is permanently installed in the microscope chamber and usually works in secondary electrons (SE) and backscatter electrons (BSE) detection mode, or any combination thereof, depending on the voltage set on the grid [11]. The detector inside the column, usually referred to as "in lens" or "through the lens", is primarily intended for high resolution interface. Among other common detectors belong, e.g., a directional backscatter electron detector (CBS) which uses ring-shaped segments of the detector diode to make a distinction between BSEs reflected close to the beam axis and electrons reflected further from the beam axis, and a detector for the detection of energy-dispersive X-ray (EDX) which provides the opportunity for an elemental analysis, important for the identification of surface and subsurface features [27].

1.1.3 Aberrations in electron microscopes

Electromagnetic lenses, as well as the lenses used in light microscopes, have aberrations. The high current flowing through the winding of the electromagnetic lens produces heat which increases its temperature. As it was already mentioned in the previous text, the magnetic field inside a real electromagnetic lens is not perfectly homogeneous, which contributes to the aberrations. These defects have a negative influence on an image created by the lens, especially its contrast, depth of field and resolution limit. This topic is described in sever literature sources [3; 11-13; 16].

21

Spherical aberration means that the electromagnetic lens does not focus all the electron beams emanating from the point source on the axis to a single point on the axis again. Electrons passing through the lens further from its axis are focused to a point that lies closer to the lens, than electrons that pass through the lens very close to the optical axis. This aberration can by partially compensated by reducing the aperture diameter. In recent years, correctors of this defect have been constructed which contain multipole electromagnetic lenses.

Chromatic aberration emerges in electron microscopes as a result of different energies of electrons in the beam. In the magnetic field of the inductors, slower electrons with larger wavelength are deflected differently from those with higher speed. We can eliminate the chromatic aberration by stabilizing the accelerating voltage of the microscope making the electron beam more monochromatic and coherent.

Axial astigmatism is caused by the asymmetry of the electron beam and hence also the magnetic field that deforms it. As a result, the electron beams have different focal points. The astigmatism is corrected by the additional magnetic field of a stigmator virtually every time an image is focused, especially at large magnification, and is influenced by the parameters of the sample.
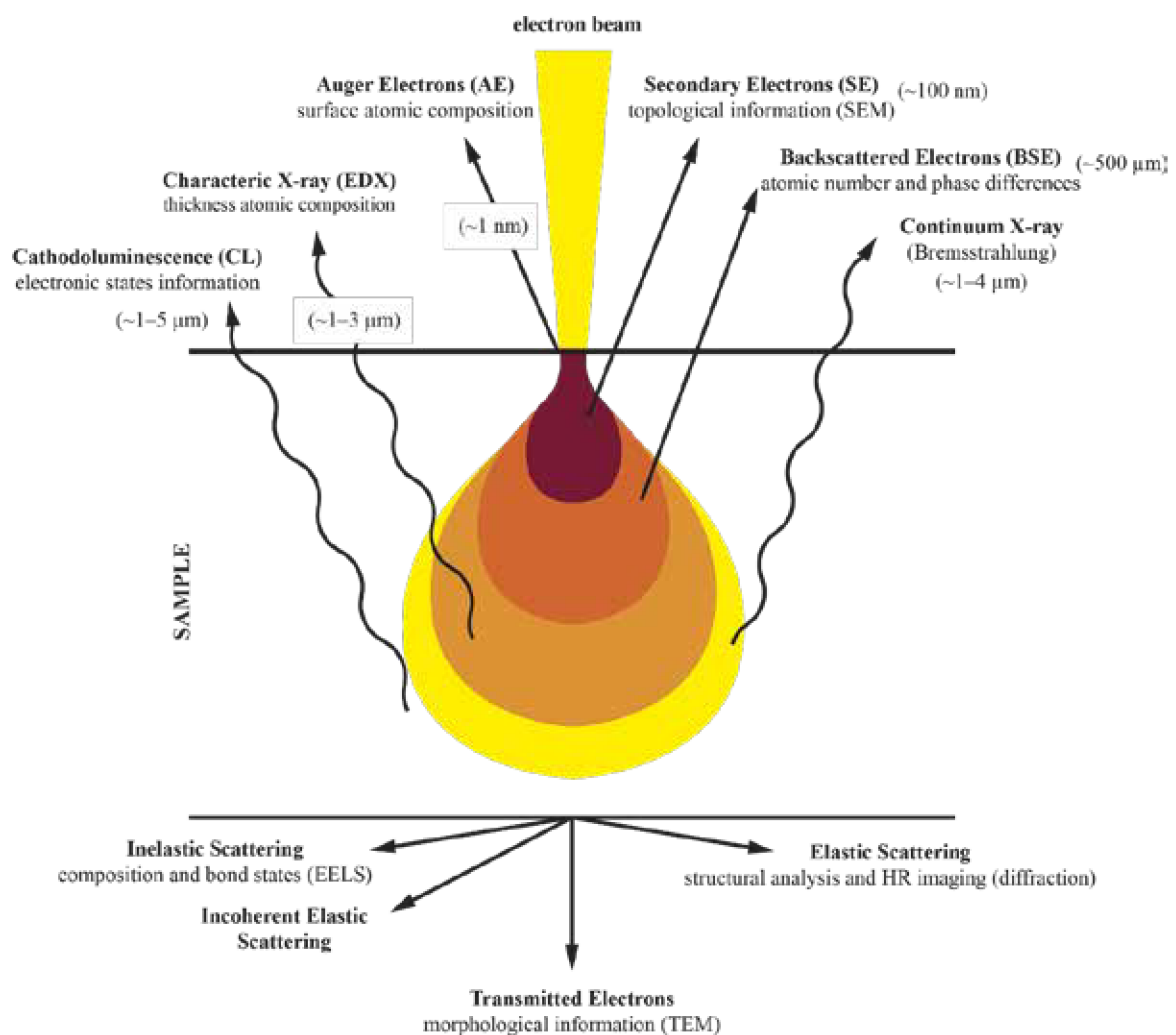
1.2 Electron beam-specimen interactions

Nowadays electron microscopy is a diversity of different imaging and analytical technique that offer unique possibilities to gain insights into structure, topology, morphology, and composition of materials. Various imaging and spectroscopic methods represent indispensable tools for the characterization of all kinds of specimens on a small size scale with the ultimate limit of a single atom. The observable specimens include inorganic and organic materials, micro and nano structures, minerals as well as biological objects. The impact of electron microscopy arises from knowledge of different information that is obtainable by the multitude detection of signals from electrons sample interactions. The different types of electron scattering are of course the basis of most electron microscopy methods and will be introduced in the following overview.

When an electron hits onto a material, different interactions can occur, as summarized in Figure 3. For a systemization, the interactions are classified into two types – elastic and inelastic interaction [3; 12]. The generation and use of selected elastic and inelastic interactions with major importance in SEM imaging is discussed in the following text in more detail.

In the ideal case of *elastic interactions,* no energy is transferred from electron to the sample. The electron has still original energy $E_0 = E_{el}$. Of course, no energy is transferred if the electron passes the sample without any interaction at all. Such electrons contribute to the direct beam which contains the electrons that passes the sample in direction of the incident beam (Fig. 3) [28]. Furthermore, elastic scattering happens if the electron is deflected from its path by Coulomb interaction with the positive potential inside the electron cloud [12]. By this, the primary electron loses only a negligible amount of energy. These signals are mainly exploited in TEM and electron diffraction methods. For the description of the elastic scattering of a single electron by an atom, it is sufficient to regard it as a negatively charged particle and neglect its wave properties. An electron penetrating into the electron cloud of a specimen atom is attracted by the positive potential of the nucleus (electrostatic or Coulombic interaction), subsequently its path is deflected towards the core. The closer the electron comes to the nucleus, the scattering angle depends on the distance between electron and the atom nucleus. The complete backscattering can occur generating back-scattered

electrons (BSE) [25]. These electrostatic electron-matter interactions can be treated as elastic. The Coulombic interaction is strong, because of its dependence on the force with which an atom attracts an electron is stronger for atoms containing more positives charges (increases with increasing atomic number Z) [5].

In the case of *inelastic interaction,* the energy is transferred from the incident electrons to the sample. After the interaction with the sample the electron energy is reduced $E_{el} < E_0$ [6]. The transferred energy can cause different signals in the specimen such as X-rays, Auger or secondary electrons, plasmons, phonons, UV radiation or cathodoluminescence [11; 13]. Inelastic electron- matter interactions are often detected by the methods of analytical electron microscopy. If a part of the energy that an electron carries is transferred to the specimen, several processes can lead to the several signal generation of inner-shell ionization, braking radiation, secondary electrons, phonons, plasmons or cathodoluminescence [12].

Figure 3: Schematic drawing illustrating different electron beam-specimen interactions that can occur when an electron hits a material. Modification of work by Claudio Nico [28].

All effects depend on the sample material, its structure and composition. Information from inelastic electron-matter interactions can be directly observed by various detectors in EM or the transferred energy from the incident electron to the specimen can be measured by electron energy loss spectroscopy (EELS) [12]. The incident electron that travels through the electron cloud of an atom might transfer a part of its energy to an electron localized in any of the shells. By a certain minimum amount of up-taken energy (threshold energy), this electron is promoted to the lowest unoccupied electron level [12].

If the transferred energy is sufficient to eject the electron into the vacuum, the atom becomes ionized. The energy transferred to an electron of an inner shell is particularly important because the resulting electronic state of the generated ion is energetically unstable: an inner shell with a low energy has an electron vacancy whereas the levels of higher energy are occupied. To achieve the energetically favourable ground state again, an electron drops down from a higher level to fill the vacancy. By this process, the atom can relax but the excess energy has to be given away. This excess energy of the electron, which dropped to a lower state, corresponds to the difference between the energy levels. The processes for getting rid of the additional energy is the generation either of a characteristic X-ray or an Auger electron [5].

Electrons located in the valence or conduction band need only transfer of a small amount of energy to gain the necessary energy to be ejected into the vacuum. Typically they carry energies below 50 eV and are called as slow SEs [29]. These SEs are utilized in scanning electron microscopy for forming images of morphology and surface topography [12; 30]. If incident electrons hit specimen atoms, atoms in crystal lattice begin to vibrate to over a large volume due to the absorbed energy. The collective vibrations are equivalent to heating up the specimen and phonons can be generated as main effect of any inelastic electron-matter interaction. The beam sensitive sample can be destroyed or modified, therefore cooling of the sample is advisable to minimize such unwanted effects [12]. It is important to understand from where in a sample the different signals that can be detected come. Auger electron and other secondary electrons with rather small energy are readily absorbed and thus only such generated close to the surface can leave the sample. Back-scattered electrons have the same energy as the electron beam and thus better penetrate the sample.

2 Introduction to SEM of beam sensitive samples

The use of electron microscopes in biology represents a chapter on its own. It is easy to forget that practically all of the organelles and cellular inclusions were actually discovered or described in detail thanks to the electron microscope. Its description laid the foundations for the design of experiments which led to the revelation of cellular functions and processes that contributed to the understanding of cell structures in natural and experimental environment. Electron microscopy in biology is not only used for imaging of preparations, but also for analysis of chemical composition or physical properties.

The use of high-vacuum scanning electron microscope, the description of which will the reader find in the following text, in biological applications where the studied samples are composed mainly of elements with low atomic number and have a high water content, brings with it many difficulties that are dealt with also within this thesis. As well as the development of microscopes themselves, detection systems, equipment and software for image processing is important, the development of specialized techniques for sample preparation and handling is also important. This area will be discussed in more detail in the following sections.

2.1 Modern scanning electron microscopes in biology

In the 1950s the scanning system was incorporated in the electron microscope thanks to a scientific group from Cambridge, led by Oatley [13; 31; 32]. His group invented an improved detector for secondary electrons (SE) and backscatter electrons (BSE) [33] and also focused on the development of electronics needed for screening with the electron beam and for recording the detected signal as an image. Today's modern SEM microscopes owe most of their important functions to the knowledge and work done by this very famous group as well.

2.1.1 The function of electrons in SEM

In comparison with light or X-rays, electrons are almost ideal excitation source for SEM imaging. Electrons in SEM include four important functions:

- They are an easily accessible and easily sustainable monoenergetic source with a high specific brightness value.
- The wavelength can be very short and microscope lenses can focus the electron beam into a Gaussian spot size with a diameter about 0.5-2 nm depending on the voltage.
- Due to the existence of the electron charge, it is possible to use electromagnetic field for fast and accurate scanning of a sample surface.
- Energetic electrons can, after they hit the sample, excite various detectable signals, such as secondary electrons [33], Auger electrons [34], backscatter electrons [35], also characteristic and continuous X-rays [36], electron-hole pairs, and cathodoluminescence [37] (Fig. 3). Because these signals are produced only in the place and time of the

interaction between the sample and the electron beam, they are immediately detected and processed in order to create an image or signal maps/curves. The image resolution depends on the size of the current spot and of the interaction volume (Fig. 4) as well as on the detected signal.

3.1.2 SEM limitations related to the use of electrons

The use of electrons in the SEM has, particularly for biological materials, limitations which are generally known and accepted, because benefits of the electron microscopy to the description of many biological structures cannot be denied. However, the success in SEM imaging depends on the efforts of researchers to induce optimal conditions for microscope imaging and eliminate effects caused by the use of electrons as signal production intermediaries [13; 25; 38].

Defects of electromagnetic lenses are one of the main reasons why the theoretical resolution cannot be achieved. The chromatic aberration is a consequence of different energies of electrons in the beam, which, as a result, are deflected at different angles. It can be minimized mainly by increasing the stability of the source. The spherical aberration results from the lens inability to focus all beams emanating from a point source back to a single point. The astigmatism is caused by an asymmetric magnetic field and is the only aberration that can be fully corrected by a magnetic field of a stigmator.

The existence of the electron charge complicates the observation of non-conductive materials, which the biological samples undoubtedly are. The negative charge which cannot be taken away due to the non-conductivity of the studied material, accumulates at the exposure area. The area around the accumulated charge can defocus or deflect the beam [13]. There is also a mutual interaction between electrons in the beam when they travel between the source and sample surface. This phenomenon can be minimized by reducing the effective brightness of the electron source and decreasing the operating voltage.

The radiation damage of the sample surface caused by the electron beam is another negative effect that manifests itself on biological materials. When the electron beam with the energy of 1-30 keV hits the sample surface, it interacts with a positive charge of atomic nuclei in the sample or a negative charge of electron shells. Because of the large disproportion between the total numbers of electrons and atomic nuclei in the sample, the electron-electron collisions occur, which lead to the transmission of significant amounts of energy from the electron beam to the sample in the form of non-elastic collisions. Since many of these collisions have higher energy than a few eV needed to break molecular bonds, the effect of this energy is very similar to that of energies with the same dose coming, for example, from X-ray or other ionizing radiation [39]. The magnitude of the ionizing radiation dose during the exposure in SEM is dependent on the accelerating voltage, beam current but also material composition. For organic materials, even a relatively low dose has a degradation effect [13]. The magnitude of the accelerating voltage affects the penetration depth and the amount of signal, and the higher is the voltage, the greater is the interaction volume. In the Figure 4 Monte Carlo simulations in Casino software [40] showing differences in interaction volumes between various materials for accelerating voltage 1 keV and 2 keV are presented.

26

The vacuum in SEM is again required because of the use of electrons. The mean free path of electrons moving in a gaseous environment is very short, because collisions with gas molecules occur very quickly, therefore samples for the SEM imaging are inserted and observed at very low pressure. That is a complication for imaging samples with a high water content, such as biological samples, which must be specially treated and dehydrated so that they can be observed in a conventional SEM, or frozen and imaged at low temperature. The exception is an environmental SEM (ESEM), where the sample is inserted into a chamber the pressure can be regulated in, which is well separated from the microscope column and the electron optical system. This technique is useful for imaging some non-conductive samples, but it also brings disadvantages associated with lower resolution and the need to use higher accelerating voltage [41].

The contamination of the sample surface which is caused by the impact of the electron beam, is not limited only to shrinkage of molecules and their evaporation from the preparation surface, but may also have a reversed, deposition effect. Despite the low pressure inside the microscope chamber, there are free hydrocarbons which are bound not only to the surfaces of internal components in the chamber, but can also be part of the studied material surface. At the room temperature, thermal excitation causes these molecules to migrate along the surface. Subsequent excitation or ionization induced by the electron beam leads to chemical reactions and frequent polymerization on the preparation surface, which can even create a thin film that covers the real sample surface. This phenomenon can be minimized by improving the vacuum, a baking process or, for example, plasma cleaning [42]. By cooling the mechanical parts inside the SEM chamber, such as an anticontaminator which is located near the sample, this process can be suppressed as well, as decreasing the temperature deprives the hydrocarbon molecules of energy needed for their migration along and clinging to the sample surface.

The chemical contrast which can be observed by detecting signals in SEM, such as BSE, cathodoluminescence and X-rays, can be used for studying biological preparations, for example, in the case of immunolabeling, where some structures and functions within a cell can be observed using special markers, contrast nanoparticles or quantum dots. To localize them, a higher acceleration voltage and current are usually needed, and the resulting dose can damage the sample irretrievably. Thanks to the high-quality preparation of biological samples and high resolution of SEM, this method of macromolecular markers localization is often preferred.

It may seem that for some, especially biological samples, electrons as intermediaries of emerging signals are not completely convenient. The effect of energetic electrons causes samples to be destroyed, we observe charging or contamination instead of the surface, the contrast is not always optimal, we need to remove water from samples with complex processes – this is a number of difficulties that researchers and microscope developers try to deal with. On the other hand, modern SEMs enable working with low energies and high resolution, and if the appropriate parametrs setting and the optimal scanning mode are selected, many of these phenomena can be suppressed. For example, if image integration is used, a dose the sample is subjected to during SEM imaging can be minimized, and thus the effect of charging and contamination can be eliminated and the resulting image with needed contrast and resolution obtained.
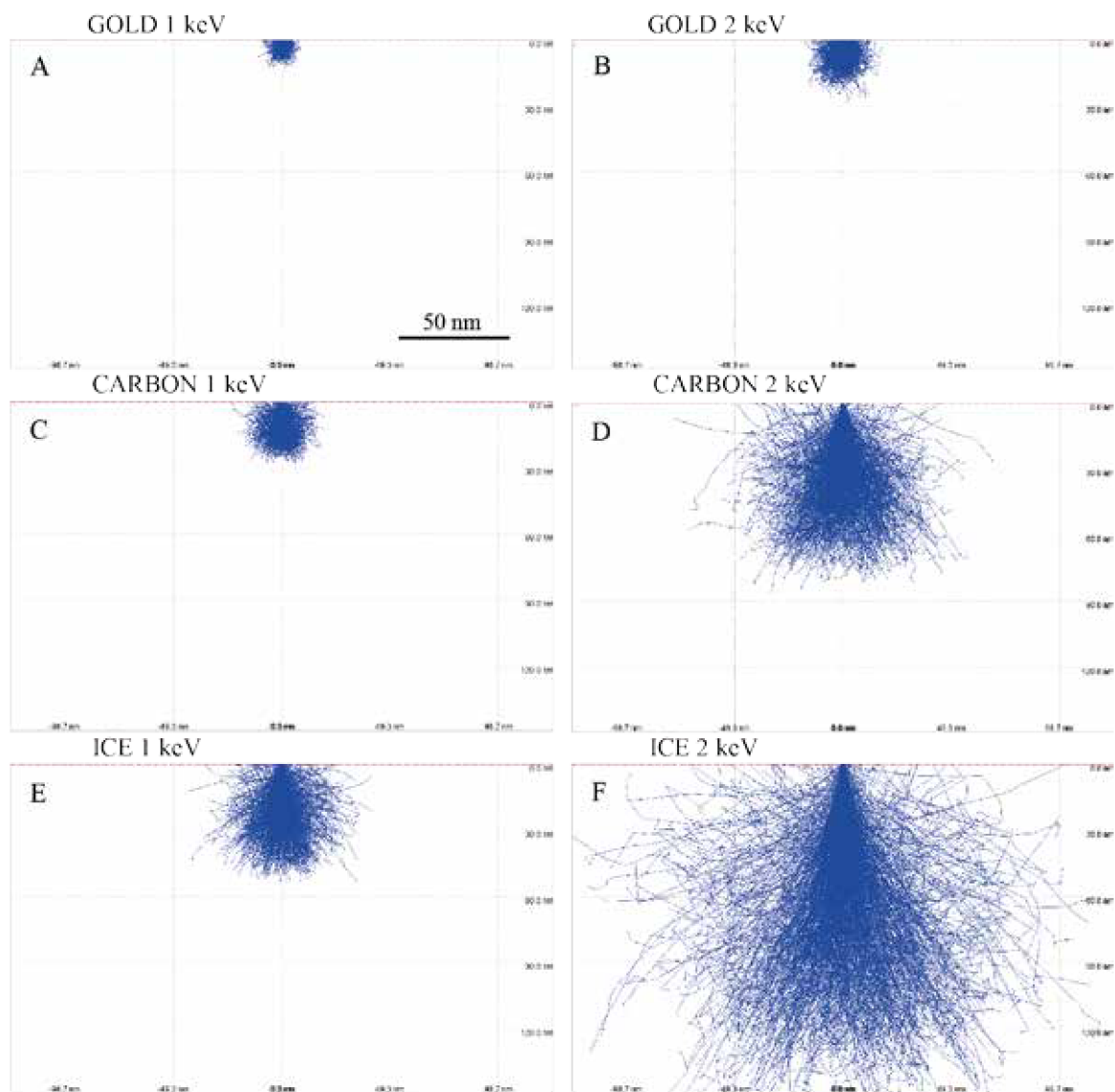
Figure 4: Monte Carlo simulations performed in Casino software for accelerating voltage 1 keV (left column) and 2 keV (right column). The table shows differences of interaction volumes between various materials: gold (A, B), carbon (C, D), water in solid state (E, F).

3 Biological sample preparation for SEM

Biological specimens, such as individual cells or tissues, usually contain a significant amount of water. For example, in the case of microbial biofilms which are, to a large extent, also a research subject within this thesis, the water amounts up to 97 % of their weight [43]. Therefore, it is no exaggeration to consider the preparation methodology of biological and other hydrated sensitive samples to be very important and extensive scientific and experimental area where a number of disciplines, such as physics, chemistry, biology, instrumental development and construction meet. A proof for this statement is a number of publications dealing with procedures and instructions for individual groups of samples, where various methods and techniques that can be used are discussed [1; 14; 44]. In the following text, there is a brief overview of processes the studied preparation must undergo before it can be inserted into the vacuum of the microscope chamber, and its surface imaged or other analysis performed. Individual approaches will be elaborated in more detail, including experimental benefits, within this dissertation in the following sections.

3.1 Sample preparation for SEM

The sample suitable for imaging in a high vacuum SEM must meet the following criteria: any external impurities and water content should be removed, it should be stable in vacuum, it should be resistant to the impact of the electron beam and it should provide a sufficient signal [13]. Some biological objects meet these requirements without problems, such as, e.g., various mineralized structures, teeth, bones, or plant material such as wood. In most cases, however, biological samples contain water which must be removed from them prior to the imaging, which means they have to be treated in some way. Which method will be chosen depends on the specimen type and the information we want to obtain about it. The preparation usually begins with sample fixation.

The conventional chemical preparation of the hydrated object for room temperature SEM includes the following steps [13; 44]:
1. Cleaning the sample surface, which is performed, for example, by blowing the gaseous nitrogen or compressed air upon the sample, or rinsing it in a buffer.
2. Fixating the preparation by immersing it in a fixative agent that binds to organic molecules such as lipids and proteins. The fixative agent is usually dissolved in a buffer with suitable pH and molarity. Sometimes multiple fixation steps can be applied, individual protocols are adapted to the sample type.
3. Washing out the fixative solutions using a buffer is a step that is usually repeated several times. It is very important that all the fixative agent is washed away from the preparation.
4. The water content is removed from the sample using a dehydration series, where in several steps the water is replaced by solutions with increasing concentrations of ethanol or acetone.

5. There are several ways for drying of the sample. For example, to use a method of a critical point drying which makes use of a good miscibility of chemicals, that are the outcome of the dehydration series with liquid carbon dioxide that has an acceptable region of the critical point, or to use chemicals with low surface tension which are also well miscible with products of the dehydration series.
6. The final step is to attach the sample to a special holder, alternatively it is possible to increase its surface conductivity by applying a thin layer of metal or carbon.

This whole process takes a few hours, sometimes even days. The specimen size is limited by the SEM chamber dimensions and the fixation quality in the sample volume, because the penetration of the fixative agent is a relatively slow process. Often, problems with complete drying occur with large samples [14; 44].

The physical preparation of a sample is represented by cryogenic methods and subsequent SEM imaging at low temperature (cryo-SEM), or at room temperature for completely dried samples. The advantage of this approach is mainly its swiftness, thanks to which we avoid a chemical preparation lasting several hours, and also possible artifacts associated with exposure to chemicals are prevented from forming. This preparation usually includes the following steps [14; 44]:
1. The first step is freeze fixation. The main requirement is to freeze the sample so that no water crystals that would damage it irreparably are created inside. The freezing technique is chosen according to the size and type of the specimen.
2. After the cryo-fixation, the sublimation process follows, which can only take a few seconds or minutes to sublime just a thin layer of ice off the sample surface according to the sublimation curve [45; 46], or it can be a multistage process, which can last many hours and at the end of which the sample is completely dried.
3. By coating the sample, its conductivity, and alternatively contrast can be increased and its topography highlighted.

The whole physical preparation lasts from a few minutes to several hours. Its main advantages include the possibility of fixating the sample swiftly so it is close to its natural state at the given moment, also the preparation can be studied in its fracture, so besides the surface, internal structures can be imaged as well. On the other hand, it is a process physically demanding to maintain the necessary rates and other parameters in individual steps so that we can avoid all artifacts. This area is discussed in more detail in Chapter 4.

3.1.1 Conventional sample preparation for room temperature SEM

Chemical fixation

The fixation is expected to "fix" the biological material in a state close to its nature in its current state (i.e. to stop all the living processes). Commonly used fixative agents include glutaraldehyde (GA), which can be classified together with, e.g., paraformaldehyde among non-coagulating agents – as a result of the chemical bonds formation between individual predominantly peptide components in the cellular cytoplasm, "a gel transparent for electrons" is created inside the cell, and thus it is stabilized [1; 44], also, for example, osmium tetroxide (OsO_4), which binds to lipids in surface areas of the biological object and strengthens it thereby, and because osmium is a heavy metal, it contributes to sample conductivity and contrast increase in the final image in SEM. In

connection with osmium tetroxide we mainly speak about post-fixation – it often follows after an aldehyde fixation. After the fixation, the samples are washed using washing solutions consisting of buffers, or containing sucrose or glucose as well [47].

Dehydration

After thorough fixation, it is necessary to wash the specimen properly several times with distilled water to completely remove the buffer and the fixative agent, including all the salts it contains. In rare cases, the sample is ready to be air-dried after the washing, but most of the biological tissues and individual cells require another step, which is dehydration. Dehydration is a process during which the water content in the sample is replaced with liquid suitable for the subsequent drying process. Therefore, the aim of this process is to remove water from the sample by successive series with increasing concentrations of organic solvent. Chemical substances well miscible with water, polar ethanol or aprotic acetone, are used to dehydrate the samples. The basic philosophy is to dehydrate the material in steps; usually a series of solvent solutions with distilled water starting at 30 %, then proceeding gradually with 50 %, 70 %, 85 % and 95 % is stated, and at the end the preparation is brought into absolute ethanol or acetone, where repeated exchange is performed [44]. The moment the highest concentration of the dehydration solution is reached, it is necessary to repeat its exchange and thus to avoid the residual amount of water to stay in the preparation. The time of each step for which it is necessary to keep the sample in the solution is directly proportional to its size and adjusted to its composition [17].

Acetone, ethanol and other dehydration solutions lead to the extraction of lipids from cells and tissues. As a result, lipid droplets may become non-homogenous or damaged. Anhydrous acetone is considered to be a stronger extractor of lipids from the cell, and thus it can contribute to the formation of artifacts; in addition, it absorbs water contained in the air more easily. For these reasons, ethanol is usually preferred as a dehydration agent to acetone. Hydroscopic nature of these agents generally causes difficulties related to the ability to absorb atmospheric water. Absolute ethanol or acetone which remains exposed to air humidity for a relatively short period of time is degraded due to the water content and becomes unsuitable for the final dehydration of the samples for electron microscopy. It is desirable to perform the post-fixation using osmium tetroxide in cases requiring preservation of lipid structures [17] as it can, at least in part, prevent the extraction phenomenon.

Drying

In many cases, it is not possible to simply air-dry the biological sample, since the surface tension of liquid would cause a rapid evaporation leading to specimen deformation, and neither the internal, nor the surface structure would be preserved any longer in the real state the specimen was fixed in. Therefore, it is necessary to proceed to the drying process after the sample is dehydrated.
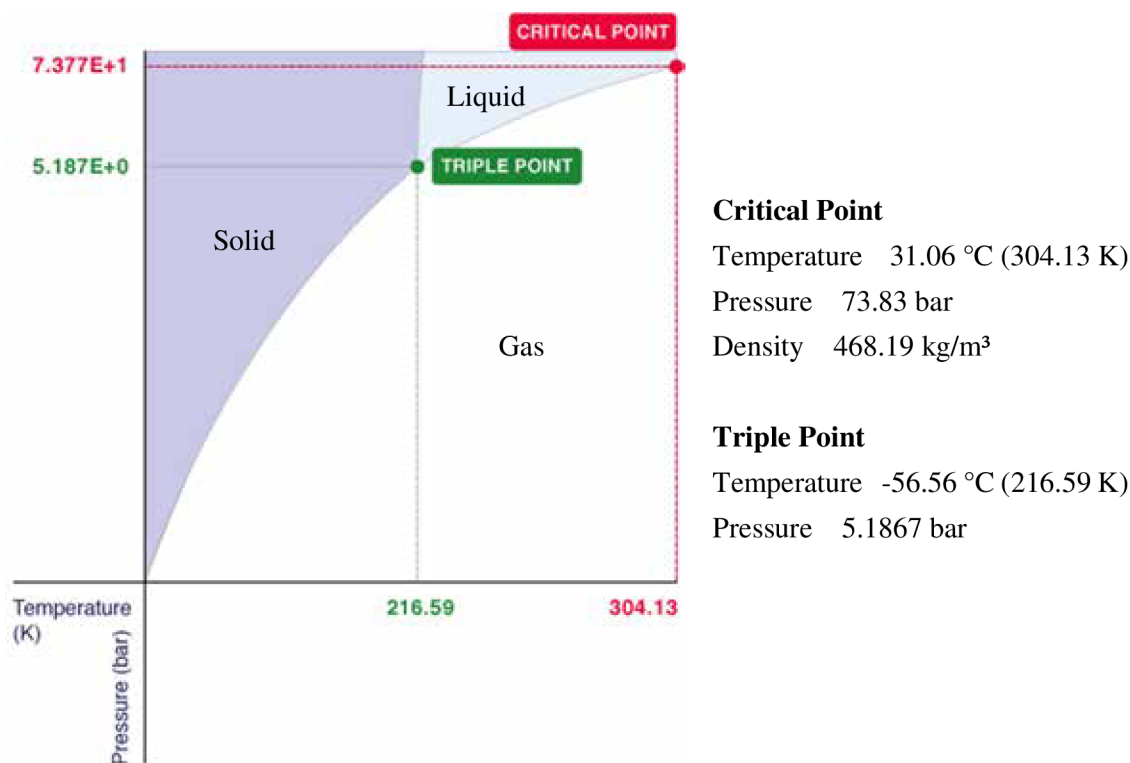
One of the most famous methods [48] used to dry a sample is a method of critical point drying (CPD), which allows to avoid the effect of surface tension of the dehydration liquid on the preparation. The CPD method is based on the principle of achieving the critical point on a characteristic curve. At this point, the difference between liquid and gaseous phases of the given substance disappears, meaning both states have the same density and specific volume, are not separated by any interface, and surface tension decreases to zero. This very moment is the most advantageous to dry the specimen. Since the critical point of water can be found in relatively

extreme values (approx. 374 °C and 220 bar), the carbon dioxide (CO_2) is usually used for CPD. Note, that the critical point of acetone is also difficult to reach (approx. 235 °C and 47 bar) [48].

The device for the CPD method consists of a pressurized CO_2 bottle, a control valve to regulate the CO_2 supply, and a chamber the sample is inserted and the entire drying process takes place in. The chamber is equipped with two meters to check the pressure and temperature, also a valve to regulate the pressure inside this chamber, and a cooling unit. The whole process begins with cooling the chamber required for liquefaction of CO_2, then a sample is inserted inside, completely immersed in 100% dehydration agent in a special bath. During the subsequent washing the dehydrating agent is replaced with liquid CO_2 and the critical point is shifted to more advantageous values thereby. Increasing the temperature and pressure at the same time turns the liquid CO_2 into a dense gaseous phase without any phase interface that would damage the preparation due to the surface tension (Fig. 5) [49]. This condition is advantageous to dry the sample. The resulting gas is released from the enclosed device chamber by controlled pressure and temperature reduction. The fact that liquid CO_2 is the optimal choice is confirmed by its good miscibility with dehydration agents; the second advantage is its good availability and relatively low price.

Instead of CPD it is possible to dry the sample using low surface tension chemicals [50; 51] which are also well miscible with organic solvents such as, for example, hexamethyldisilazane (HMDS). The second option is to use tert-butanol or commercially available Peldri II compounds which are liquid above a certain acceptable temperature (it depends on the given substance and its purity, e.g., tert-Butanol 99.5% with product number 471712-100ML from SIGMA-ALDRICH has the melting point of 23 - 26 °C), and after cooling down a few °C (e.g., 30 minutes at 4 °C in the fridge) they harden without a crystal formation. The sample is dried by subsequent sublimation in prevacuum at room temperature.

Critical Point
Temperature   31.06 °C (304.13 K)
Pressure   73.83 bar
Density   468.19 kg/m³

Triple Point
Temperature   -56.56 °C (216.59 K)
Pressure   5.1867 bar

Figure 5: Schematic drawing of the CO_2 phase diagram. Adapted [49].

Sample surface coating for SEM imaging

More than 60 years ago, Knoll [52] discovered that a piece of mica examined in an early predecessors of the commercial scanning electron microscopes (SEMs), appeared bright while the surrounding regions appeared dark. This phenomenon is a common feature of most secondary electron (SE) images of non-conducting specimens because their surface acts as an electron trap. This accumulation of electrons on the surface is called charging" and creates the extra-white regions on the sample which can influence the image information. SEs are emitted with such low energies (5–50 eV), that local potentials due to charging can have a large effect on the collection of the SE signal detector [14; 53]. Charging gives rise to many weird and distorted images. In order to remove this artifact lower vacuum level inside the chamber can be applied. This introduces positively-charged molecules near the surface of the sample. They interact with the charging electrons and neutralize them, thereby removing this charging effect. This has proven to be an effective approach, however the air molecules that are present in the vacuum chamber interact with the primary electrons and the quality of the image is reduced. If a high-quality SEM image is required, the coating is recommended because the layer of conductive material allows the electrons to be removed from the material [17].

SEMs are very versatile tools that can provide information at the nanoscale of many different samples such as ceramics, metals and alloys, semiconductors, polymers, biological samples and many more. Nevertheless, the electron beam in a SEM is highly energetic and, during its interaction with the sample, it carries part of its energy to the sample mainly in the form of heat. If the sample consists of a material that is sensitive to the electron beam, this interaction can damage part or their entire structure. Therefore certain types of samples are more challenging and require an extra step in sample preparation to enable the user to gather high-quality information from a SEM imaging and analysis. Such as in the case of charging, this extra step also involves coating the sample with an additional thin layer of a conductive material that is not beam-sensitive and can act as a protective layer against such kind of damage [1; 17].

The most used sputter coating material is gold (Au), due to its high conductivity and its relatively small grain size that enables high-resolution imaging. Nowadays, for sputter coating for SEM can be used also other electrically-conducting metals – such as gold/palladium (Au/Pd), platinum (Pt), silver (Ag), chromium (Cr) or iridium (Ir). Sputtered films for SEM typically have a thickness range of 2–20 nm [53]. Benefits for SEM samples sputtered with metal are, e.g. reduced microscope beam damage, increased thermal conduction and reduced sample charging as decribed above [54].

Besides sputtering, metal and carbon can be also evaporated. The thermal evaporation of carbon is widely used for preparing specimens for analytical electron microscopy [55; 56]. When the carbon source is heated to its evaporation temperature, a fine stream of carbon is deposited onto specimens. The main applications of carbon coating in EM electron microscopy is X-ray microanalysis and preparation of specimen support films on TEM grids. It is a directional process and has a limited surface of coated area. Usually, this technique is used in application where the directional coating is necessary (shadowing or replicas) or fines layers are required [53].

One of coating disadvantages is the fact that the sample surface does not contain the original material but the sputter-coated one, and therefore the atomic number-contrast can be lost and in extreme cases it may lead to altered surface topography or false elemental information about the sample. While uniform deposition of metal on all sides of a particle provides greater contrast, it also can produce curious artifacts. Neugebauer and Zingsheim observed these artifacts and studied the

relationship of these artifacts to the angle of shadowing, and found that it was most pronounced at low shadowing angles [57]. Nevertheless, in most cases, the parameters of the coating procedure are carefully selected and these issues do not appear and therefore the user is able to acquire high-quality images that carry the type of information that is required (Fig. 6) [58].
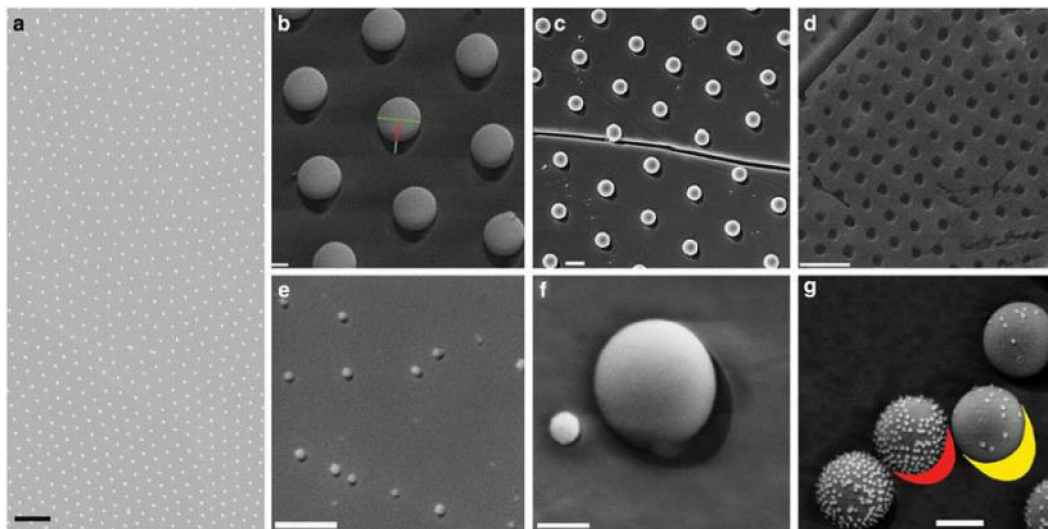
Figure 6: The shadow cast by the nanoparticles on metal deposition in the high-magnification images. (a) Low-magnification (3 μm); (b) 500 nm amidine latex (AL) nano particles (NP) (200 nm); (c) 200 nm AL NP (300 nm); (d) 500 nm AL NP (2 μm); (e) 20 nm AL NP (200 nm); (f) 100 nm hydrophilic citrate gold NP next to a 500 nm AL NP (200 nm) and (g) 500 nm AL NPs coated by 20 nm citrate gold NPs (300 nm). Modification of work [58].

4 Cryo-SEM

The SEM is primarily associated with the examination of the specimen surfaces. This section is concerned with the use of the SEM to obtain information about the surfaces of frozen specimens that retain a substantial part of their natural water content. The cryogenic scanning electron microscope (cryo-SEM) is frequently used as an instrumentation also for X-ray analytical studies, and many of the sample preparation techniques discussed here are identical. Several information about electron optics and image formation was described in previous chapters and details are available in many books and papers [5; 14; 59]. Nowadays low-temperature microanalysis, digital scanning techniques, which are now available on many modern scanning electron microscopes, provide a useful method in various scientific fields.

The versatility of the SEM for the study of solids can be derived in measurements from wide variety of electron beam-specimen interactions. The generation of back-scattered, secondary, and Auger electrons, X-ray photons, long-wavelength electro-magnetic radiation in the visible, UV, and IR regions, phonons, and plasmons can be used to obtain information about the specimen that relates to its shape, composition, crystal structure, electronic structure, and internal electric or magnetic fields as described in the Section 1.2 in more details. A relatively large depth of field in focus allows easy visualization of the three-dimensional structure of an object and at a spatial resolution better than can be obtained by confocal light microscopy. Modern SEMs are quite user-friendly and have become as imaging device of various scientists and engineers. However, interpretation of the rough fracture faces which are frequently examined in cryo-SEM is often difficult [22; 60].

SEM became commercially available 30 years after the first TEM and the first low-temperature images were published [61; 62]. One of the reasons for the advance development in cryo-SEM is the benefit of large specimen chamber – it is easier to construct cold stages. Cryogenic electron microscopy can be recognized as the only way to visualize the natural structure of materials such as lung and leaf tissue, foams and foods, and soils. The conventional preparative techniques remove the liquid phases and distort the solid phases, and even freeze-drying produces a sample in which the gaseous and liquid phases are indistinguishable. Another attribute is that it is a relatively fast technique for obtaining medium high resolution information about a wide range of samples. With the appropriate equipment, hydrated samples can be frozen, fractured, coated, and imaged in shorter time in contrary with conventional approach. Therefore, it is possible to visualize dynamic processes occurring in the aqueous phase in high-resolution. In addition, the necessary ancillary preparative equipment associated with cryo-SEM allows a single sample to be sequentially analyzed by a process of repeated fracturing further into or across the sample.

Although low-temperature microscopy is not only associated with hydrated systems, most studies are concerned with systems where water, either as ice or amorphous water, is an important structural component. For this reason, it is necessary to appreciate some basic facts about the water at normal temperatures and pressures as well as at cryogenic temperatures. Following chapters should provide an overview of the more general features of the water and show how they may relate to the processes of cryogenic microscopy. More about the subject can be found in several studies [63-67].

Water is in many aspects a substance with some unexpected properties. At 0 °C (the triple point of water) the solid, liquid, and vapour phases coexist, and whereas the hydrides of the other elements close to oxygen in the Periodic Table (e.g., HF, H_2S, NH_3, and CH_4) only exist as gases at normal temperatures and pressures, water is a liquid (Fig. 7) [68]. The apparently anomalous liquid state of water is reflected in the central role it had in terrestrial biogenesis and continues to have for the presence of life on Earth. Several characteristics of water are well known. Table 2 summarizes the properties related to the conversion of liquid water to ice [69]. The presence of hydrogen bonds affect the internal chemical energy of the water molecule and relates with the processes by which water is associated with other molecules [67]. The relatively low density is caused by continually breaking and reforming of hydrogen bonds. Because energy can be stored in hydrogen bonds, water has a high specific heat and can lose or store large amounts of thermal energy with only a small change in temperature. The large heat of vaporization, due to the fact that extra energy has to go into breaking hydrogen bonds, provides the basis for an effective cooling mechanism for many organisms and in combination with the high cohesively and tensile strength of water, provides the pathway and the mechanism to transport dissolved minerals. The viscosity and self-diffusion coefficient of water are properties that determine the rate at which water molecules are displaced from their temporary position at equilibrium. Both properties are strongly temperature dependent and have a large influence on the kinetics of crystallization. The relatively high melting and boiling points of water have provided two major points on thermometers. Another well-known fact is that the presence of solutes in water can depress the melting point and vapour pressure and elevate the boiling point. The presence of solutes lowers the free chemical energy of water and provides the basis for osmotic pressure [64].
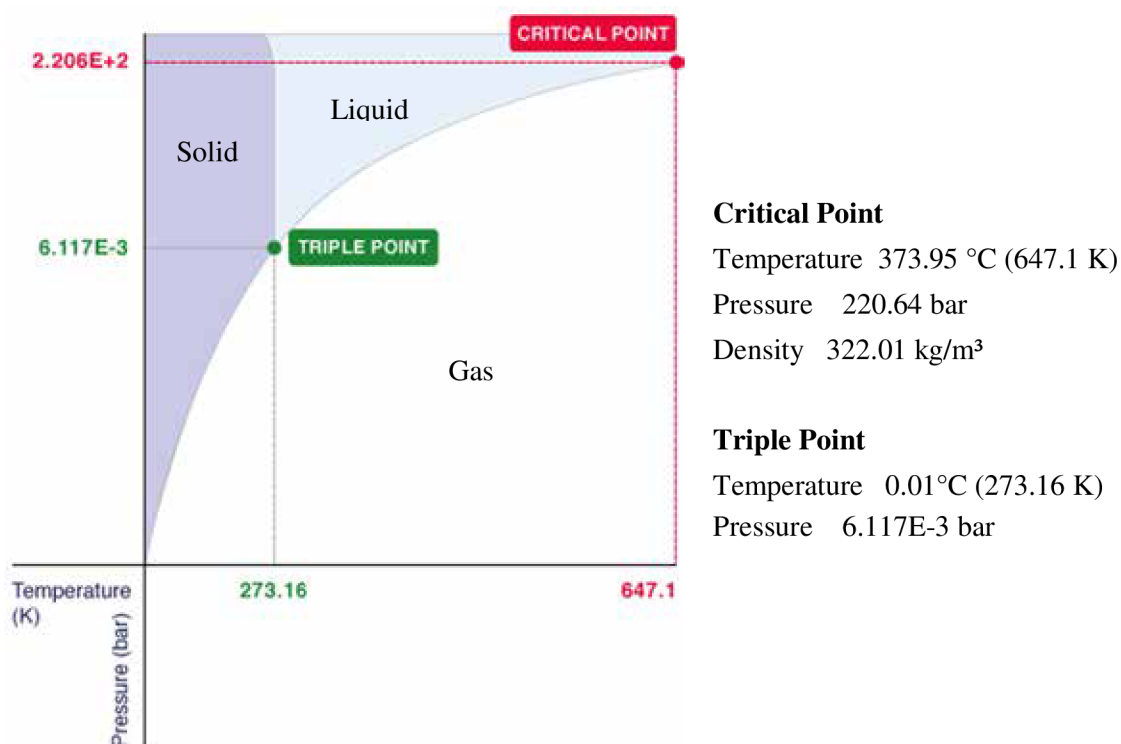
Table 2: The water properties related with the conversion of a liquid to a solid state [69].

	Liquid	**Solid**
Density [kg m^{-3}]	1000 (277 K)	978 (239 K)
Latent heat of fusion [J g^{-1}]	334 (273 K)	235 (253 K)
Self-diffusion coef. [m^{-2} s^{-1}]	2.2 x 10^{-9} (273 K)	1.0 x 10^{-14} (273 K)
Thermal conductivity [J K^{-1} m^{-1} s^{-1}]	0.58 (273 K)	2.1 (273 K)
Specific heat [J K^{-1} g^{-1}]	4.2 (273 K)	2.1 (273 K)
Viscosity [N m^{-2} s^{-1}]	0.23 (273 K)	10^7/10^{15}(273 K)
Isothermal compressibility [N m^{-2}]	4.9	2.0

The molecule of water is strongly polarized owing to the separation of the charges on the oxygen (-) and hydrogen (+). The hydrogens bonds are responsible for the dynamic structure of liquid water and for its interactions with dissolved materials and intact macroscopic surfaces [63]. The hydrogen bonding of water influences the properties of the liquid closely associated with the life processes.

The ionic, polar and apolar associations of water with a wide range of substances indicate that the pure water rarely exists. The complex interactions between liquid water and varied components of cellular systems reveal that some of the water can be in modified form. These variations influence the amount and form of the solid phases to which liquid water may be converted during cryogenic sample preparation for cryo-SEM [61].

Therefore, the discussion of the properties of liquid water is necessary to complete with how water molecules may link together into the solid phase of ice. The use of water as a matrix in low-temperature microscopy is showing that the structure and properties of this material assume greater significance. One of the water properties is that it can exist in a large number of different solid forms depending on the pressure and temperature applying at the time of its transition [70]. An attention is required to pay to the polymorphs of ice which form at normal pressures as well as a few tens of degrees below the melting point. However, the ice can be produced also when water vapour is rapidly cooled. More information can be found in references written by Echlin [64] and Hobbs [71]. When a liquid water is slowly cooled to below its freezing point, the random and dynamic tetrahedron configuration assumes a more stable form. The liquid is changed by a first-order phase transition into a solid material in which the basic tetrahedral structure is now extensively cross-linked into hexagonal crystals, which at normal pressures are characteristic of this stable polymorph of ice [64].

Critical Point

Temperature 373.95 °C (647.1 K)

Pressure   220.64 bar

Density   322.01 kg/m³

Triple Point

Temperature   0.01°C (273.16 K)

Pressure   6.117E-3 bar

Figure 7: Schematic drawing of H_2O phase diagram. Adapted from [68].

The hydrogen bonding is very labile and all of changes in pressure during the cooling process can affect the crystal structure. Depending on the temperature and pressure, solid water can exist currently in 17 experimentally-confirmed polymorphs of ice [70; 71]. Figure 8 shows the solid liquid phase diagram of water upon pressure 24 kbar) [72].

The most commonly forms of ice at ambient pressure that can be observed by cryo-EM are hexagonal ice (I_H) and cubic ice (I_C). Hexagonal ice is the polymorph of ice that forms when water is cooled quite rapidly. It is the ordinary ice in snowflakes as well as in frozen, hydrated samples prepared by low-temperature methods for cryo-EM. Cubic ice is metastable form of ice *I* which exists between -80 and -150 °C and may be formed in the laboratory when water vapour is condensed at below -130 °C, when amorphous ice (I_A) is warmed to above -150 °C and in the case high-pressure forms of ice are cooled to liquid-nitrogen temperatures, the pressure is reduced to atmospheric and the samples then are warmed to -116 °C for a few minutes [17; 59; 70].

At high pressures other forms of ice can exist, each within its own temperature and pressure range. The high pressures push the water molecules closer together and the hydrogen bonds are consequently bent and distorted. These high-pressure forms of ice are denser than liquid water and have rhomboidal, tetragonal and monoclinic crystal systems. Less is known about these high-pressure ice polymorphs. In the nature they exist just at the depths of polar ice caps. The form of ice produced by high-pressure freezing technique is required to be discussed in following chapter.

At the pressure of approximately 20 bar and the temperature in the range between -20 °C and -90 °C it should be possible to undercool water without the formation of the two polymorphs of ice. If heat is removed from water at these conditions, the liquid can crystallize to form of high-density, high-pressure polymorphs of ice (*II, III*). Although, the advantage of the high-pressure freezing comes from the substantial amount of undercooling that can occur in liquid water at specific pressure. Amorphous ice (I_A) is a monocrystalline form ice and in cryo-SEM it is considered as an ideal state of water. The term of "*vitreous ice*" (I_V) is also used to describe this state (Fig. 8) [72]. Detailed physical description related with vitreous ice and glass transition can be found in studies Johari [73], Lepault [74], Kouchi and Kuroda [75] and Hemley [17; 76].
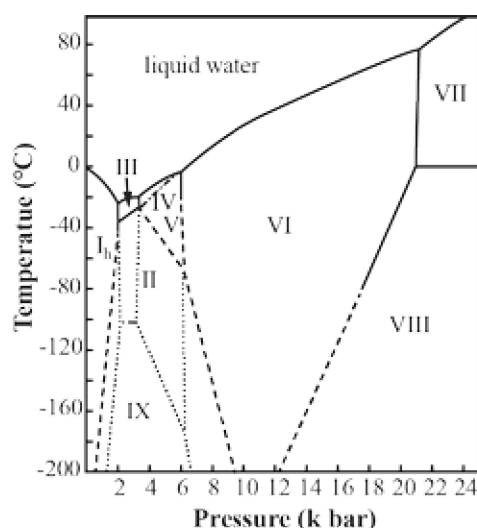
Figure 8: Solid-liquid phase diagram of water. Broken lines represent approximate and dotted lines represent estimated phase boundaries. I_h to *IX* are the unstable crystalline forms of ice. Redrawn from [72].

Cryo-fixation by vitrification is an excellent method for preserving biological material. It makes it possible to observe samples without going through the major transformations of chemical fixation, dehydration and drying. Vitrification is the process by which the viscosity of the sample is increased to such a high value that molecular movements become negligible before ice crystal formation has time to start. There are two main advantages to be gained by vitrification: the provision of a solid matrix suitable for manipulation and microscopy, and an effective immobilization of dynamic processes [64]. In principle, the method is simple. It should now be clear that if a purpose is to convert the water in a sample to a vitreous or even a microcrystalline state by lowering the temperature, then the sample must be cooled as rapidly as possible. The low thermal conductivity of water prevents high cooling rates in the centre of a thicker specimen and the gaining of undercooled water in whole bulk of specimen is impossible. Undercooled water is important in the preparation of samples for cryo-EM. The water in small droplets and thin layers when is rapidly cooled will first undercool and in the absence of any nucleating agents can be transformed to a noncrystalline, glasslike state. The existence of this phenomenon has received some support from the studies of Sceats and Rice [77]. Conditions for successful undercooling of biological tissues were specified by Sakai an Larcher [78]: small sample size with small intracellular space, low water content, an absence of intracellular as well as extracellular nucleators, freezing in small units which can freeze independently and presence of "compounds" that depress nucleation.

The cooling speeds calculated in study of Studer et al in 1995 [79] cannot be significantly increased because the limiting factor is the thermal conductivity of water. There are, however, two other parameters that can favour vitrification: the addition of a cryoprotectant and high pressure. The former acts by reducing the capability of water molecules to participate in crystal formation. For example, in a saturated sugar solution, water molecules are so involved in their interaction with the sugar that they cannot crystallize [7]. Most soluble substances act as a cryoprotectant. The material inside a cell, the cytoplasm, which typically corresponds to 15-30 % of dry weight, is a cryoprotectant that nature provides freely [7].

Cryoprotectants are substances that facilitate freezing of specimens with the formation of small or less ice crystals and acceptable preservation of cellular morphology. Their most important protective influence is, that they are able to increase the viscosity of the medium. They bind to or substitute water and thereby reduce the amount of water available for freezing. The cryoprotectants decrease the chemical potential of the water and thus reduce the growth of ice crystals [7]. Either low-molecular-weight penetrating cryoprotectants such as glycerol or high-molecular-weight polymeric, non-penetrating compounds such as sucrose can be used to suppress ice crystal formation. These reagents are employed usually at concentrations of 10-30 %, depending on the specimen under study. Glycerol is used quite commonly for freeze-fracture investigations. It has been well studied as a cryoprotectant by Luyet and Kroener in 1966 [80]. Adequate information on how to use high pressure freezing (HPF) and freeze substitution (FS) optimally can be provided by developers and methodological reports [47; 81]. However, the proper use of certain cryoprotectants for successful cryo-fixation is often essential in many experiments. Cryoprotectants remain to be studied for their systematic use in TEM sample preparation with cryo-fixation [82; 83]. There have been a number of studies on the cryoprotective properties of common solutions such as dextran, 1- hexadecene or polyvinylpyrrolidone (PVP), on various biological specimens [84]. Carbohydrates are widely used as freeze-drying protectants either individually or in combination with other solutes. Monosaccharides, such as glucose, provide good bioprotection during freezing and freeze-drying

[81]. Disaccharides are also considered as effective freeze-drying protectants. The addition of salts to formulations containing sugars will described in several studies [7; 14; 85].

There are described eight principal ways of sample freezing for EM in one of major literature sources obtained sample preparation protocols for EM [7]:

I.   *Combination of chemical preparation and freezing* into a liquefied organic gas such as propane at a temperature of from -160 °C to -190 °C, resulting in a freezing rate of ~ 100 °C/s. Although this rate of freezing can be increased by using helium, tissue specimens are still not vitrified. The thickness of the specimen should not exceed 0.5 mm.

II. *Plunge-freeze method* involves dipping the specimen into a liquid cryogen. This method is the simplest, least expensive and most widely used procedure especially for cryo-TEM applications. The specimen is dipped into the cryogen by hand or by plunging devices (Fig. 9) to increase the rate of travel of the specimen through the cryogen. Cryogens such as liquid propane, a mixture of propane and isopentane, liquid nitrogen, solid-liquid nitrogen slush and ethane have been used for plunge freezing. The cryogens are usually liquefied by liquid nitrogen. One of the best coolants is contaminated liquid propane used at about -180 °C to -190 °C. The useful heat sink capacity of propane is higher than that other commonly used liquid cryogen and for practical purposes propane is recognized as the best coolant for very thin samples.

III. *Cold metal block freeze method* involves bringing rapidly exposed, thin and flat specimens into contact with a polished metal surface (copper or silver) which has been uniformly cooled to -190 °C with liquid nitrogen or to -254 °C with liquid helium (synthetic sapphire has better thermal properties than those of copper, and can be used instead of copper [86]). The melting points of liquid helium and liquid nitrogen are -271.4 °C and -210 °C, respectively. The metal surface is protected from condensation of frost and atmospheric oxygen by passing a stream of nitrogen boil-off gas over its surface. This method provides freezing to a depth of 10-20 µm from the face of a fresh, untreated tissue block. Higher cooling rates are obtained with this method compared with those achieved by the plunge freezing method. In general, the depth of the ice crystal-free zone obtained with the cold metal block freeze method is greater than that given by the plunge freeze method.

IV. *Cryogen jet freeze method* involves spraying liquid propane, cooled by liquid nitrogen up to a temperature of -190 °C, onto the specimen at high speed. The cooling rate increases with increasing speed of the propane jet [87]. The heat exchange should be up to tens times faster than in the plunge-freeze method. The cooling rate near the specimen surface is four times greater for jet spraying compared with plunge-freezing [88]. Jet freezing allows near-vitrification of any specimen that can be prepared as a thin layer. The use of a sandwich preparation is recommended with this method in order to prevent possible loss of or damage to the specimen by the force of the propane jet. Because heat is withdrawn simultaneously from both sides of the specimen, the depth of the frozen region in the specimen should be greater than that achieved with any other method at atmospheric pressure [87]. Theoretically, the specimen volume can be frozen up to 40 µm of thickness but in practical terms, propane-jet freezing shows satisfactory freezing to a depth of 15 µm [87].

V.   *Spray-freeze method* is based on freezing in a microcrystalline state that is achieved when an efficient cryogen acts specimens of very small size (droplets). The method achieves a high surface-to-volume ratio by splitting the specimen into very small droplets (10 - 50 µm). Spray-freezing also takes advantage of increased heat convection by injecting the spray droplets into a cryogen fluid. The very low heat content of specimen droplets encourages higher cooling rates. Also, the reduced nucleation within very small spray droplets is an advantage of this method. The cooling rates achieved are fast enough to prevent observable ice crystal damage [7]. This method should be used only for special studies.

VI.   *Popsicle-freeze method* involves clamping of tissue between slabs of melting cryogen, which assume the shape of the tissue during freezing [89]. This method allows rapid freezing of organs *in situ* with a spring-loaded, hand-held clamping device which holds two apposing melting Freon 22 popsicles. Since the Freon is at the melting point while coming in contact with the tissue, the former moulds itself exactly to the unevenness of the tissue surface. A small incision is made in the animal abdomen and the Freon damper is activated to snap-freeze the tissue. The frozen specimen is plunged into liquid nitrogen. This method has only been employed for preserving elemental composition at a high spatial resolution. The preservation of tissue morphology is adequate, showing signs of rather extensive ice crystals.

VII.   *Punch-freeze method* is similar to the popsicle-freeze method in that the specimen is punched out of the living organ by means of a syringe chilled with liquid propane or liquid nitrogen [90].

VIII.   *High-pressure freezing (HPF) method* deserves special interest because of its potential to freeze near vitrification relatively thick specimens. Theoretically, specimens up to 0.6 mm thick can be immobilized in <10 ms, producing ice crystals <10 nm in diameter [7]. This thickness is 20-30 times greater than that available with plunge-freezing, cold metal block freezing or cryogen jet freezing. Although both cryogen jet and cold metal block freezing can stabilise cytoplasm uniformly in <10 ms, the maximum thickness of well-frozen cytoplasm is usually <20 µm with cold metal block freezing and 40 µm with cryogen jet freezing. Therefore, the HPF becomes to cutting edge freezing methods and for this thesis means a crucial sample preparation technique. Section 5.3.1 is devoted to describe it.

IX.   *Self-pressure freezing method* was derived according to the HPF method where the high pressure is built by the sample itself during the plunging into the liquid cryogen; the liquid sample is sealed in a capillary tube, hence it does not allow to increase its volume [91]. This method is much cheaper than HPF, however, its usefulness and variability is limited.
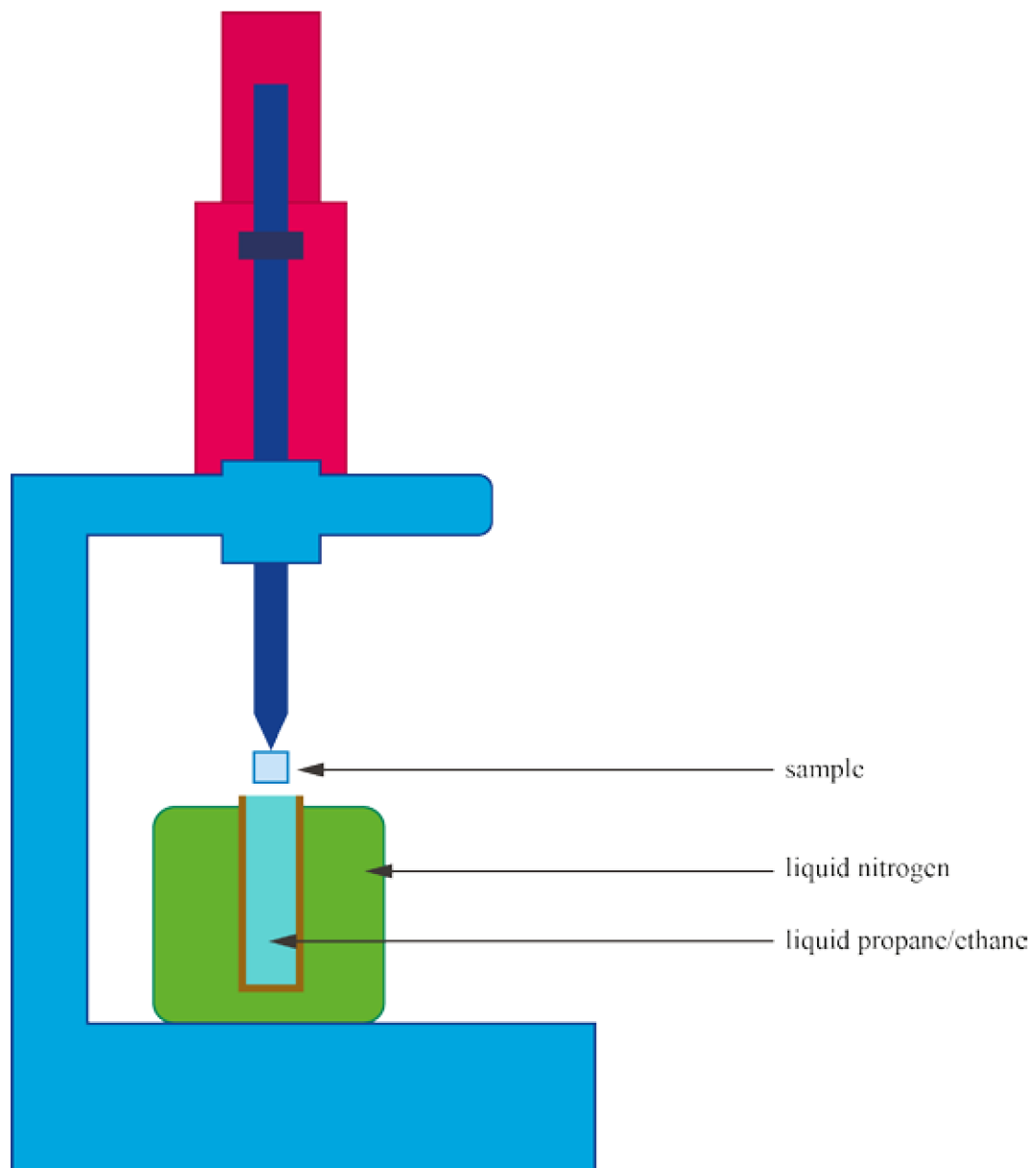
Figure 9: Schematic drawing of a typical plunge freezing machine.

5.3.1 High pressure freezing method

This chapter summarizes several studies [14; 56; 92-94] and contains a discussion about the improvements in the technology and the methodology of high-pressure freezing (HPF) nowadays. HPF is currently the only method which enables adequate low temperature immobilization of bulk hydrated samples. In the current state of HPF instrumentation and preparation methods, the technique has not still reached its full theoretical potential. Cryo sample preparation takes several requirements such as to achieve optimal freezing quality of the sample without distorting the organization of the tissue in short time.

The effect of high pressure on the critical freezing rate of aqueous samples is related to the principle of Le Chatelier – when water freezes, its volume increases. High pressure inhibits this expansion and thereby the crystallization. These changes result in less heat being produced by crystallization, thereby reducing the amount of heat that has to be extracted per unit time by cooling. The cooling rate can be reduced. The most profitable pressure zone for affecting the freezing behaviour of water is about 2 050 bar. At this pressure the melting point of water is depressed to approx. -20 °C, and the zone of possible supercooling is reduced to -90 °C [95]. Furthermore, at this pressure, water does not crystallize as ice *I* with a lower density; instead it produces ice *II* and *III*, both of which are denser than water and have lower nucleation and growth rates than ice *I* formed at lower pressures [66]. These changes result in the lowering of the critical cooling rate of pure water from -1 000 000 to -20 000 °C/s [96] and to about -100 °C/s for biological specimens. In practical terms, the application of aprox. 2 kbar pressure results in a cryoprotective effect equivalent to about 20% glycerol and allows freezing of up to 0.6 mm thick planar samples when cooling is applied from both sides [97].

The consequence of these physical effects allows freezing to greater depths, than it is possible by plunge freezing or impact against a cold metal block as described previously. In the latter methods, an optimistic average depth of good freezing is on the order of 10 μm. With any method, the actual depth of good freezing will vary with the chemistry of the particular cell type. In general, cells with less free water will freeze better than those that have more aqueous cytoplasm. Most cells also have natural cryoprotectants, such as high sugar and/or protein contents. Despite the fact, it was experimentally recognized a preserving fine ultrastructural details of bulky samples up to 200 μm without any visible deformation caused by ice crystallization. These results proved that HPF has not yet reached its full theoretical potential [92; 98].

Once frozen, cells can be treated in many different ways, such as freeze-fracturing, vitreous cryosectioning, freeze-drying, or freeze substitution [14]. Different types of samples often require different specimen carriers and/or loading strategies. A brief overview according to the various specimen types, starting with single cells and proceeding to more complex tissues together with a discussion about differences between available HPF machines finds its rightful place in this thesis. In biological research when optimal preservation of cell ultrastructure is necessary, fixation by HPF is often the only way to achieve eligible results. Vitreous cryosectioning or morphometric analysis and three-dimensional modelling by tomography or serial sections are good examples. Last but not least, for immunolabeling methods cryo fixation is required, because conventional sample preparation techniques could cause extractions of proteins, lipids and other molecules [82] and this is unacceptable for immunolabeling. Nevertheless, for the purposes of this thesis, freezing cells in suspension and cultured cells grown on substrates by HPF is primarily discussed. Because a brief introduction to mentioned types of specimen and related specimen carriers as well as HPF machines should be recognized as a "springboard" for an experimental part of this work.

Nowadays, there are currently three commercially available HPF instruments on the market: the Wohlwend Compact HPF03 from Wohlwend Engineering, Sennwald, Switzerland; the Leica EM ICE from Leica Microsystems in Vienna, Austria and the ABRA HPM010 from Fluid AG, Widnau, Switzerland. The machine BAL-TEC HPM010 has become to the most famous machine in cryogenic fixation. Because BAL-TEC, AG was acquired by Leica Microsystems ABRA has begun producing this high-pressure freezer itself since the end of the year 2007 as mentioned in company web page [99]. The machine is available through RMC (Tucson) in the United States and in Europe. The question of which high-pressure freezer to choose depends primarily on several factors such as the size and shape of the sample which needs to be frozen and for special application required light and electrical stimulation there exists only one option. Another important criteria are number of samples, which are able to be frozen in one hour, as well as a purchase price.

Although featuring some new improvements, the Wohlwend HPF03 is based on the old BAL-TEC HPF 010 (now the ABRA HPF010), it was improved significantly. It is because the director of this small company, Martin Wohlwend, was significantly involved in the production of the HPF 010 for BAL-TEC in the mid-1980s. There are still many of these machines in the world and more details about this machine and its applications can be found in McDonald [100] or Kaech [101]. The important similarity between the BAL-TEC and Wohlwend machines is the size and shape of the specimen holders for the freezing as well as the way of the freezing. The standard Wohlwend-style carriers are 3 mm in diameter with a 2 mm well for the specimen. Using two carriers in combination it is possible to freeze samples from less than 25 to 600 μm deep as shown in McDonald [56; 102] and Kaech [101]. But the latest version HPF03 is spread also for freezing of 6mm carriers as mentioned in company web page [103].

The Leica microsystems archived product HPF EM PACT2 with an optional attachment – rapid transfer system (RTS) [104] was distinctly different in design and operation than the BAL-TEC-style machines, where the pressure and cooling systems were "in-line", in the EM PACT2 they are separate as described in details by Studer et al. [105], Vanhecke and Studer [106] and Verkade [104]. In particular, the standard specimen cups were smaller and less versatile. The specimen well was 1.5 mm in diameter and depths are limited to 100 or 200 μm. Because of the small specimen size this machine has been especially used in applications where frozen samples have been processed for TEM, typically after their freeze-substitution. The HPF EM PACT2 was used in experimental part of this thesis where its usability is shown in microbiological experiments and its unique combination with cryo-SEM observation; see the Chapter 7 Results and published papers [21; 107].

The Leica microsystems HPF machine EM ICE (Fig. 10) is the most modern instrument on the market nowadays. Its centrepiece is a multipart polymer cartridge which holds the specimen carrier sandwich and guides it automatically through the freezing process until immersed frozen in liquid nitrogen storage. The cartridge can be adapted to the specimen and carrier geometry to optimize the flow of liquid nitrogen and hence rapid cooling. Dedicated cartridges are available for a variety of different carriers, including carriers for samples of up to 5 mm in diameter. Cartridge specific handling and carrier assemblies are described extensively for freezing samples in aluminium or cooper gold coated specimen carriers, cell cultures grown on sapphire discs, suspensions for freeze-fracturing, and specimens for cryo-sectioning. The EM ICE solution uses an alcohol-free freezing principle to allow a superior cryo-fixation of the specimen which promises better quality results because missing alcohol in the chamber should lead to a faster increasing of the pressure for specimen cooling and the carrier or the specimen remain without alcohol contamination [108]. The HPF EM ICE is the only one freezing machine on the market using

a pneumatic freezing principle as well as it is equipped optionally by precisely define the timing for light and electrical stimulation that becomes widely used in neuroscience [109].

The freezing rate during high-pressure freezing can be evaluated by temperature and pressure vs. time curves (Fig. 11) and it is very important to assess freezing quality. In several studies such as in the work from D. Studer et al. [79] the temperature and cooling rate profiles within biological specimens were estimated on the following assumptions:

- Tissue thermal properties correspond to those of water at 17 °C that they are homogeneous and do not change during cooling;
- The surface temperature, being a function of time on both sides of the specimen during cooling, is represented as a linear decrease of temperature with time between the initial and final temperatures (direct measurements of the temperature vs. time during cooling);
- The cylindrical disc geometry is adequately represented by a slice of infinite lateral dimensions. These estimations of cooling rates should represent a lower limit in the case of crystallization and an upper limit in the case of vitrification.
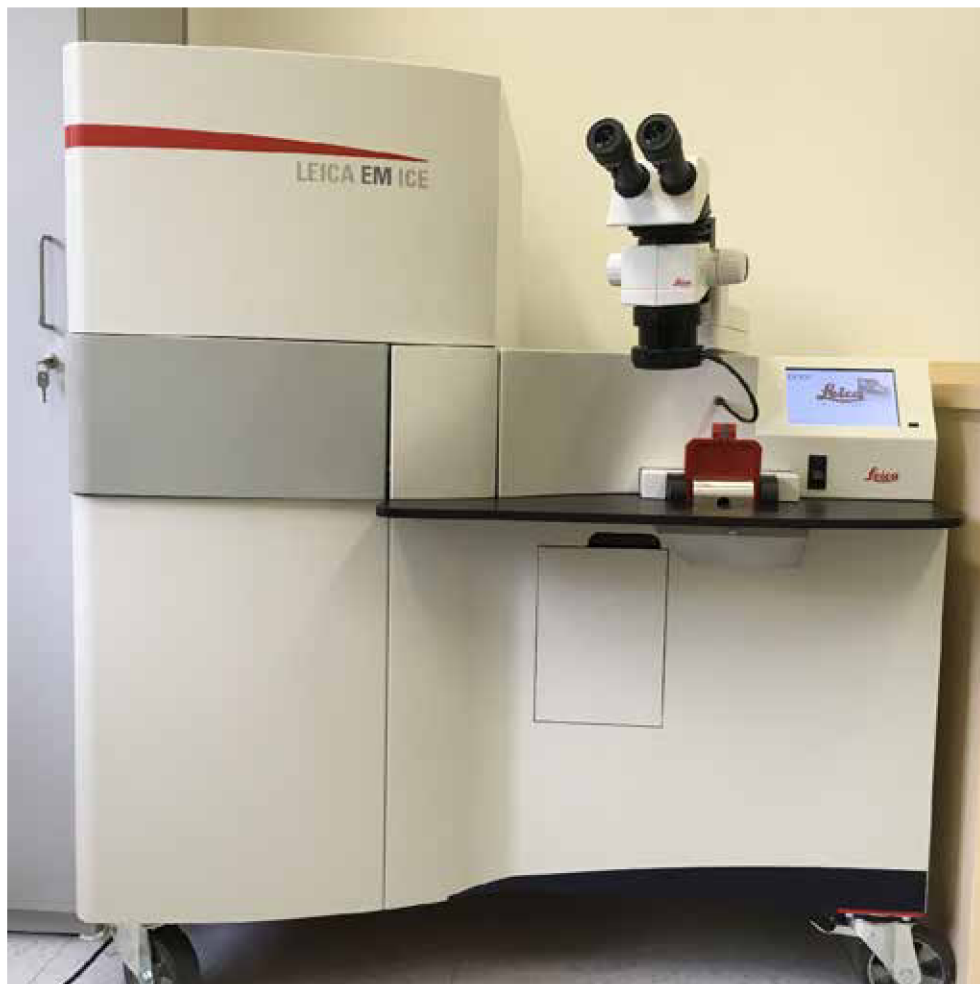
Figure 10: Photograph of HPF machine EM ICE produced by Leica microsystems.

Temperature vs pressure curve EM ICE
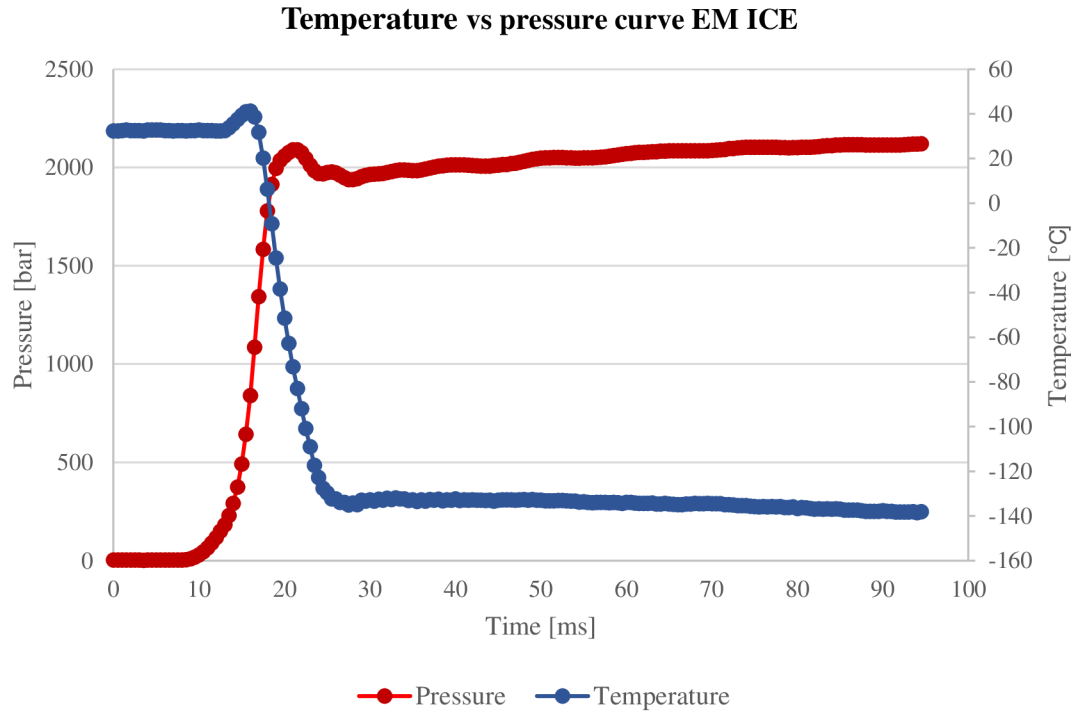
Figure 11: Record of temperature (blue line) and pressure (red line) changes during the freezing in the EM ICE high pressure freezing machine. The temperature is measured with a thermocouple located just below the specimen carriers, the pressure is measured in the pressure system that is connected to the sample. As a consequence, the measured pressure really effects on the sample, whereas the temperature serves as a reference value for evaluating of the freezing quality if both pressure and temperature were synchronized correctly.

5.4 Freeze-fracturing

Fracturing is well described as a separation of a specimen along a line of least resistance parallel to the applied force. It may be achieved either by applying tensile stress via impact with a blunt instrument, which will produce a single fracture plane, or by using a sharp tool, which will generate shear forces just ahead of the knife edge and produce a series of conchoidal fractures. Unlike sectioning, the fracturing tool should not make physical contact with the freshly exposed fracture face. This means that fractures have an undulating to rough surface in contrast to the smoother surfaces of sections. There are fewer surface defects and artifacts on a fracture face of a frozen sample, provided the fracturing process is carried out in conditions of low contamination, such as under liquid nitrogen or at a high vacuum and low temperature.

The process of fracturing is described in several studies [1; 93; 107; 110; 111]. Completely brittle material will fracture without deformation, whereas completely ductile material does not fracture but will exhibit plastic deformation. Although there are few organic and hydrated materials that are completely brittle at very low temperature up to -269 °C [64], the main aim of fracturing at low temperature is to obtain brittle fractures with a minimum of plastic deformation. In an ideal brittle fracture, deformation is limited only to the molecules that are actually pulled apart. The applied force of the fracturing tool causes stress to build up in localized regions in the sample. This stress overcomes the cohesive properties of the specimen and then suddenly spreads rapidly through

46

the sample, causing it to fracture. The way the sample fractures will depend on its brittleness, which is influenced not only by the properties of the sample but by decrease in temperature, rate of stress application, and the presence of discontinuities such as minute cracks within the sample (Fig. 12).

The fracture path follows the line of least resistance, but these pathways vary with different materials. It might be along the interface between two phases, i.e., particle-solvent, along regions where differential contraction has occurred during cooling, or along the hydrophobic inner face of biological membranes. The situation is much less clear in single-phase material, and the fracture pathway may be related to differences in the local orientation of the constituent molecules [112].

In freeze-fracturing, the actual fracture face is usually examined in cryo-SEM. The fracture face of the replica may be examined at ambient temperatures in a TEM alternatively. Both procedures can be used for morphological and analytical studies, and because of the differences in procedure, can provide complimentary information about samples [7; 14].

Freeze-fracturing can be carried out with basic equipment. The simplest and quite effective way is a fracturing the sample in liquid nitrogen by two tweezers. Nevertheless, fractures usually appear in the most unexpected places and the process is accompanied by lots of debris. Alternatively, the sample may be held in liquid nitrogen (LN_2) and a scalpel blade pressed at right angles to the proposed fracture plane until it snaps. In the case of high-pressure frozen samples which are covered in aluminium/copper sandwiches, it is possible to open the sandwiches in LN_2 by a needle or some scalpel and perform a fracture in this way. The fracture face can be "washed" in fresh liquid nitrogen to remove any debris and then it becomes ready for optional freeze-etching and coating and examination at low temperatures [64].
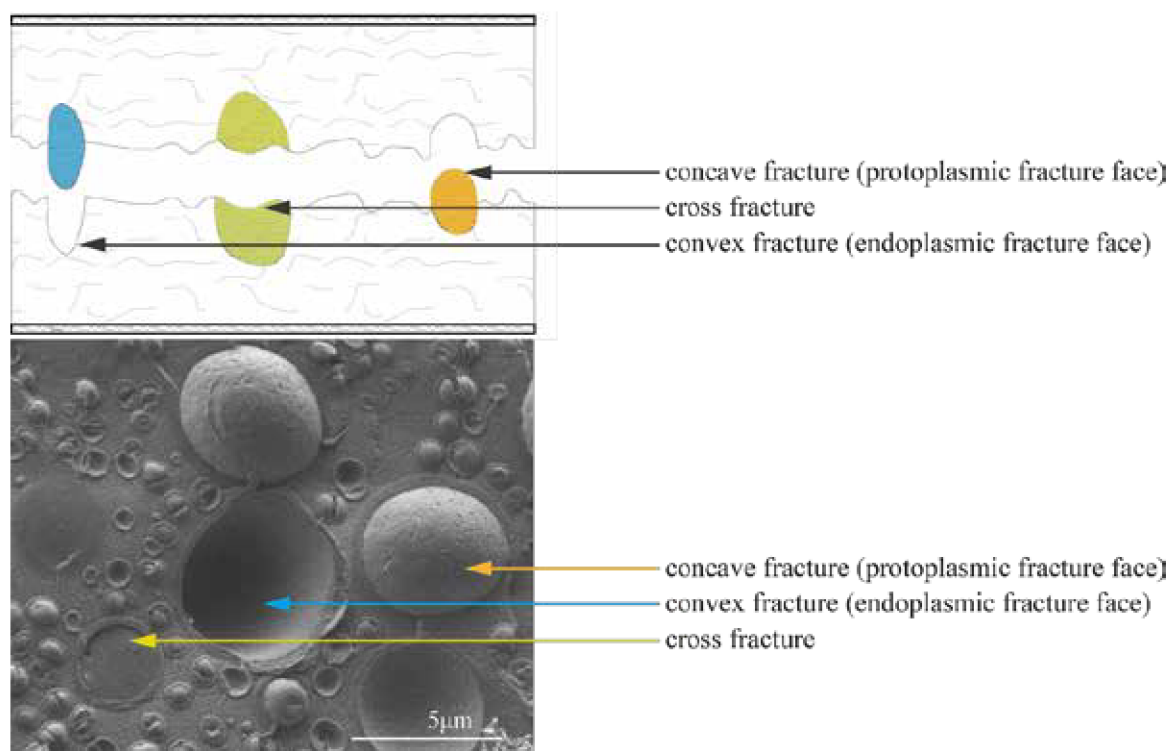
Figure 12: A principle of freeze-fracturing method.

However, in order to utilize the process effectively and to provide useful and reproducible information about the sample, it is necessary to integrate the fracturing process into a system which allows the fracture faces to be processed further before being examined and analyzed in a deep frozen state in the SEM. More controlled procedure of freeze-fracturing can be achieved in

47

cryogenic preparation chambers at precisely defined conditions such as temperature and pressure. As an example can be mentioned widely used commercial systems such as ACE600, ACE900 and BAF060 all of them produced by Leica Microsystems [113]. Main advantage of this system is that they can be used separately without the microscope being occupied because they are "freestanding" machines. There are available another two solutions: The ALTO series from Gatan and a cryo-system from Quorum Technology, UK. Both systems are based on a cryo-preparation system directly connected to the SEM chamber. In the case of ALTO series a cryo transfer system for SEM is combined with ion beam coating system [114]. The series had two models, ALTO 2500 for field emission SEM and ALTO 1000 for conventional SEM. The Quorum's market-leading PP3010 cryo preparation system is automated, column-mounted, gas-cooled cryo preparation and transfer system suitable for most SEMs. An example of freeze-fracturing system ACE600 including sample holders and carriers which were widely used in experimental part of this study are shown in Figures 13-14.
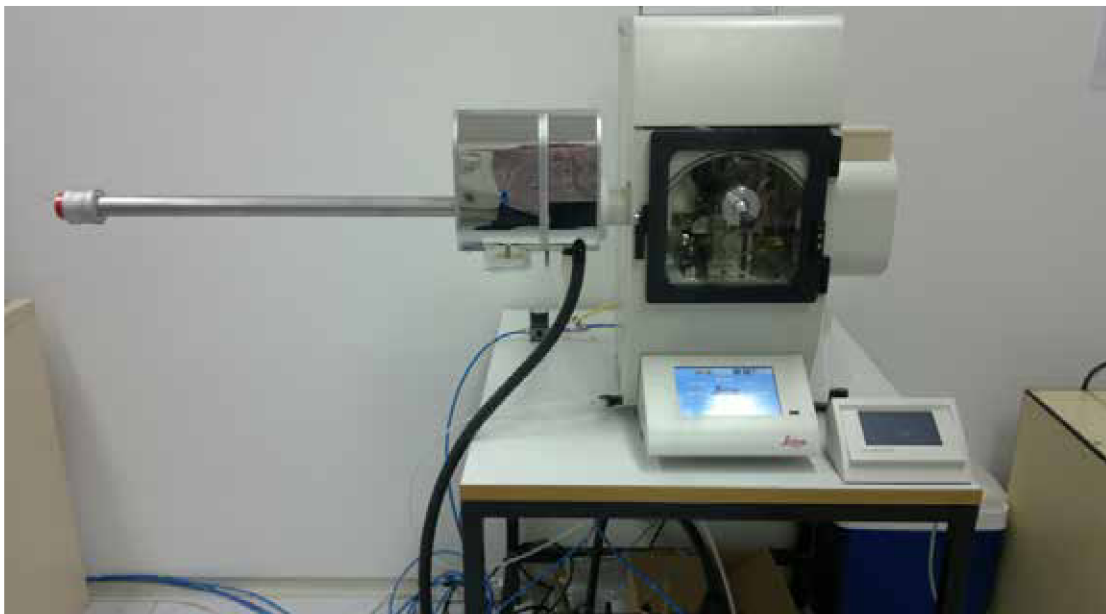
Figure 13: Photograph of ACE600 produced by Leica microsystems.
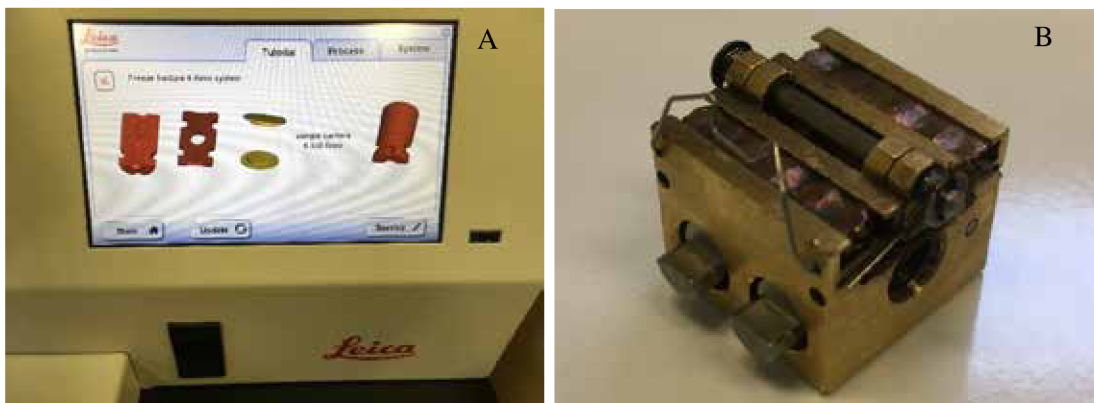
Figure 14: Photographs (A) of sample preparation using HPF for freeze-fracturing (A) and commercial sample holder (B) suitable for freeze-fracturing.

In the previous Section 5.4 several methods that enable information to be obtained from inside frozen hydrated specimens were briefly described. This section will consider the ways water may be removed from such frozen specimens using cryogenic temperature procedures and discuss the process of freeze-drying, in which ice in frozen specimens is removed by low-temperature vacuum sublimation. This controlled dehydration technique, which is an integral part of a more extended process for the preparation of hydrated specimens, serves the advantages of low temperature electron microscopy.

Because water plays such an important part in both the properties and structure of molecules in hydrated systems, its removal must be done as gently as possible in order to minimize structural damage and distortion. In some instances, such damage is unavoidable. Only the most robust samples can withstand the enormous forces (146 bar) that are generated at the air-water interface as a sample is air dried [64]. This is a consequence of the relatively high surface tension of water, although these effects can be lessened by drying from solvents with low surface tension (Table 3).

Following terminology is used: *Sublimation* is defined as a process of the transition of a substance directly from the solid to the gas phase, without passing through the intermediate liquid phase. Sublimation is an endothermic process that occurs at temperatures and pressures below a substance's triple point in its phase diagram. The reverse process of sublimation is deposition or desublimation, in which a substance passes directly from a gas to a solid phase [115]. At ambient pressure, chemical compounds and elements possess three different states at different temperatures. In these cases, the transition from the solid to the gaseous state requires an intermediate liquid state. The pressure referred to is the partial pressure P_{part} of the substance. For sublimation the saturation vapour pressure P_{sat} of water below 0 °C (273 K) is smaller as P_{part} of water in air. To obtain drying conditions, P_{part} of water in the environment has to be reduced by decreasing of the ambient pressure. The fact that P_{sat} of water is a function of temperature shows that both, specimen temperature and vacuum condition determine whether the specimen is dried or contaminated by condensing gases. When cold specimen surfaces are exposed under high vacuum, sublimation and condensation phenomena occur simultaneously. Sublimation becomes dominant if P_{sat} of the specimen is higher as P_{part} of water in the surrounding vacuum [64; 83; 116].

The *sublimation rate* is proportional to the difference of P_{sat} - P_{part} and high vacuum in cryo-preparation chamber as well as in SEM; for ice during freeze-drying under high vacuum conditions it increases rapidly with increasing specimen temperature. Although it is only 1.5 nm/s at -100 °C, it is already 50 nm/s at -80 °C and 1000 nm/s at -60 °C [64]. To avoid recrystallization of the vitrified specimen a drying temperature below -73 °C is demanded.

Freeze-drying is one of a number of dehydration processes, which include air drying, chemical drying, and solvent drying. All techniques effectively remove water from hydrated systems, but freeze-drying has the advantage that it minimizes structural collapse and the differential extraction of components during the dehydration process. Freeze-drying remains an empirical process for microscopy and analysis, and although there are general guidelines that can be followed, the experimental protocols have to be designed specifically for investigated system. A lot of studies has been written about freeze-drying for cryogenic temperature microscopy and analysis, and comprehensive reviews have been produced by MacKenzie [117] or Nermut [118]. In most of them have been already shown that molecules in hydrated systems are surrounded by a layer of water referred to as the hydration shell, which prevents the molecules sticking together. This is a particularly important phenomenon in biological material because the removal of

the hydration shell can lead to collapse of the organic matrix. These changes are a consequence of thermal movements and the natural stickiness of dehydrated biological material. In the case when the water makes the bulk, its fast removal is related to shrinkage, which can be a serious problem in freeze-drying. For example, Lee [119] showed that many cells retain their shape and volume until about 70 % of the cellular water is replaced by solvents, but when all the water is removed, the shrinkage may amount to between 20 % and 70 % of the original volume. The discussion about the term "freeze-drying" can be concluded that freeze-drying has been used in experiments where hydrated samples were completely dried during long-term sublimation under controlled conditions [120] as well as in such studies where short and very soft drying revealed cell structures and removed gas contamination caused during freezing of the specimen and its following manipulation [121].

The term "freeze-etching" is sometimes used synonymously with "freeze-fracturing". This usage, which arises for historical reasons, is to be discouraged. "Etching" is defined as removal of ice from the surface of the fractured specimen by vacuum sublimation, before making imaging by cryo-SEM or preparing the replica [121]. In the early days of the technique, it was thought that the planar aspects viewed in replicas represented true surfaces of membranes, exposed by removal of ice, hence the technique was originally designated "freeze-etching" [122]. However, it was demonstrated that the planar membrane views (fracture faces), so characteristic of the replica technique are revealed just as effectively when freeze-fracturing is carried out in the absence of etching [121]. Therefore, the term "freeze fracture" is the preferred for the major features of relief observed in the replica that are generated by the splitting of membranes. The etching (short-term freeze-drying) is a valuable method in its own right for exposing the natural surfaces of membranes or other cellular components.

Ice or frozen specimens with a temperature of -120 °C have a saturation pressure of about 10^{-7} mbar (Fig. 15) [45]. If this pressure is established in the chamber, condensation and evaporation are in equilibrium. The amount of evaporated molecules is equal to the amount of condensed molecules. At a higher pressure the condensation rate is higher than the sublimation rate – ice crystals grow on the specimen's surface (Table 3) [45]. This has to be avoided by all means. A colder (than the specimen) plate placed above the specimen reduces the local pressure and works as a condensation trap (also cooled as an anticontaminator). Water molecules driven up from the specimen preferentially attach to the colder surface of the anticontaminator and therefore it is advantage to have the area as large as possible (often such a plate is produced by sandblasting rather than polishing to maximize its surface area). At a lower pressure than the saturation pressure more molecules sublimate than condensate and freeze-etching takes place [17; 64].

Saturation vapor pressure
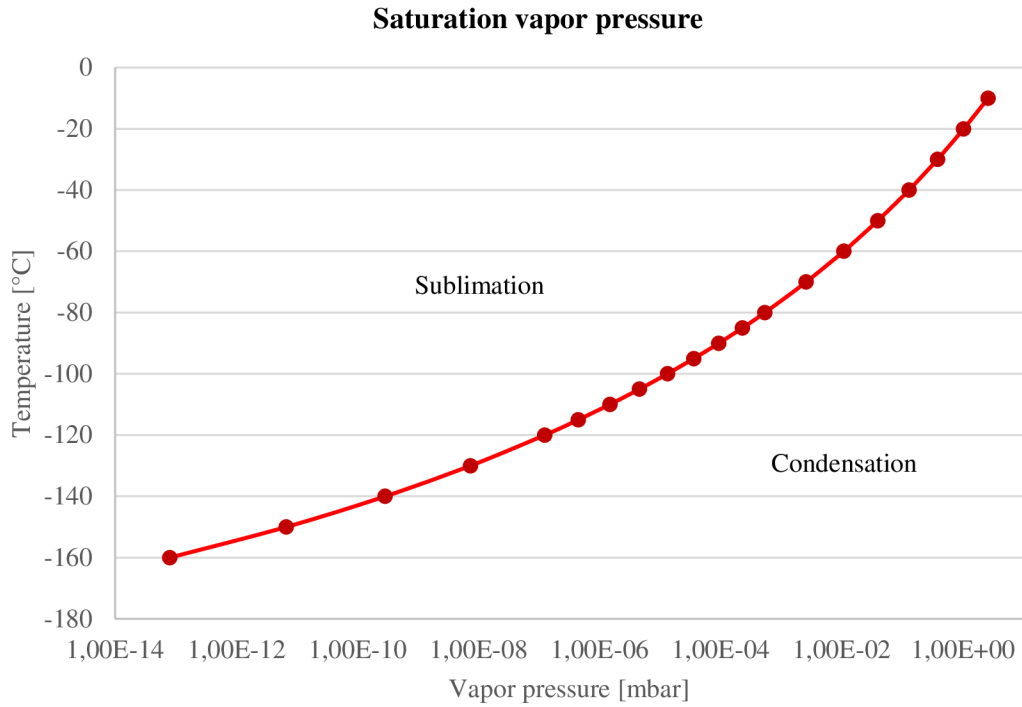
Figure 15: Curve of saturation vapour pressure of water. Redrawn from [45].

Table 3: Sublimation rates; bold parameters are usually used in cryo-SEM. Redrawn from [45].

Temperature (°C)	Saturation pressure (mbar)	Sublimation rate (g/cm²)	Increase of dry layer = Etch rate (1/s)
-10	2,60E+00	2,98E-02	324 µm
-20	1,03E+00	1,21E-02	131 µm
-30	3,81E-01	4,54E-03	49,3 µm
-40	1,29E-01	1,57E-03	17 µm
-50	3,93E-02	4,90E-04	5,3 µm
-60	1,08E-02	1,37E-04	1,48 µm
-70	2,59E-03	3,37E-05	364 nm
-80	5,36E-04	7,16E-06	77 nm
-85	2,29E-04	3,10E-06	33,3 nm
-90	**9,35E-05**	**1,28E-06**	**13,7 nm**
-95	**3,61E-05**	**5,02E-07**	**5,39 nm**
-100	**1,32E-05**	**1,87E-07**	**2 nm**
-105	**4,57E-06**	**6,55E-08**	**0,7 nm**
-110	**1,48E-06**	**2,15E-08**	**0,23 nm**
-115	4,45E-07	6,58E-09	70,4 pm
-120	1,24E-07	1,86E-09	19,9 pm
-130	7,38E-09	1,15E-10	1,22 pm
-140	2,88E-10	4,64E-12	49,5 fm
-150	6,68E-12	1,12E-13	1,19 fm
-160	8,02E-14	1,40E-15	0,01 fm

Cryogenic electron microscopy was originally developed by biologists or biophysicists, who attempted to examine biological/hydrated systems at conditions as close as possible to their native state. Among the pioneers in that area was Patrick Echlin, who developed an early methodology of cryo-SEM [59], and Robert Glaeser [123], who worked on cryogenic TEM (cryo-TEM). An important breakthrough was the demonstration of successful vitrification of cryo-TEM specimen by Jacques Dubochet and his colleagues [124]. As commercial manufacturers introduced cryo-specimen holders, it gradually became easier to perform cryo-TEM. Cryo-SEM took the same path, but has never been as widely used as cryo-TEM. While cryo-TEM is now a well-established methodology that can be applied in the study of a wide range of biological/chemical applications; note that for the often used cryo electron tomography a Nobel prize in chemistry was awarded end of 2017 [125], quite often research question needs to be completed by cryo-SEM examination. This is in experiments when the studied system is very viscous, and thus cannot be made into the very thin liquid films that are vitrified into a cryo-TEM specimen, or when the specimen is too large or when the interested is focused onto surfaces, but where looking for nanometric details are essential. Nowadays, SEM cryo-holders are available from a number of manufacturers because the need for specimen preparation under controlled conditions exists and in many scientific fields inquiries increase.

Nevertheless, some researchers have produced their own home-made sample holders because some scientific questions can be answered only by "own methodology" which requires specific holding of the sample and its investigation by EM. In several publication technological solution has been described. Group around Paul Walther developed a new type of high-pressure freezing cryo-holder [126]. This holder can take up an EM grid that has been dipped in the suspension and clamped in between two low-mass copper platelets, as used for propane-jet freezing. The new suspension holder allowed them to make cryo-fractures without visible ice crystal damage. Moreover, high-pressure frozen rat pancreas tissue samples were also examined in the frozen-hydrated state by use of a cryo-stage in an in-lens SEM. With this approach a few nanometre resolution in a near life-like state was able to achieve. Jacob Bastacky and his colleagues also developed and described innovative sample holders [127; 128]. The specimen holder [127] was designed for pre-frozen blocks of tissue up to 1×0.5×0.5 cm in size. The pure copper stub, which was the holder main part, was precooled by immersion in liquid nitrogen and screwed with forceps into a submerged preparation block. The frozen sample was cut into a rectilinear block circular saw blade under liquid nitrogen. Then sample was transferred into the specimen holder. The described specimen stub allowed good thermal contact with the cooling stage in the SEM at temperatures of liquid nitrogen (-196 °C) and therefore satisfactorily prevented warming of frozen hydrated specimens during imaging and freeze-drying using the low temperature SEM. Another sample holder produced by Jacob Bastacky [128] was a pure copper capsule with trough, slide, and securing screw was designed for pre-frozen tissue blocks up to 3.0×1.0×0.5 mm. For smoothness and rectilinearity, a slot for the slide was also produced. Precooled capsule by immersion in liquid nitrogen should be held in the trough of a large cryo-SEM specimen holder [127], which has a semicircular cut out on the face of the slide, and then screwed into an aluminium block.

The concept and practical application of freeze-fracture processing of biological specimens was introduced in several publications such as in [129]. The early apparatus appropriated disparate components into a working self-contained unit. The original apparatus was modified and refined into commercially available instruments in order to accommodate the critical need for remote

manipulation, maintenance of high vacuum, and the evaporation of carbon and metals to produce a replica suitable for examination by TEM. Freeze-fracturing technique was applied also in cryo-SEM experiments. In Tanifuji Goro et al. [130] study the freeze-fracture cryo-SEM was carried out as follows. A suspension of bacterial cells in seawater was transferred into a 1 mm deep hole in a sapphire disc at room temperature, and then cryo-fixed by flash freezing in liquid nitrogen. The cartridge-mounted disc was then transferred under vacuum to the cryo-attachment chamber then fractured using a metal spike and sublimated at -95 °C for 5 min. Freeze-fractured specimen was finally observed by cryo-SEM.

The combination of HPF fixation and freeze-fracturing together with imaging by cryo-SEM was presented in the work from Yong Wu et al [22] where four different cryo-fixation approaches for *Staphylococcus aureus* biofilm preparation were evaluated. In the case of HPF fixed biofilms grown on sapphire disks (6 mm in diameter, compatible with the Leica high-pressure freezing system used in these experiments). After freezing samples were mounted perpendicularly into a commercial sample holder then fractured and sublimated in cryo-preparation chamber MED020 (Leica microsystems). This work explored artifacts in extracellular matrix (ECM) structure of *S. aureus* biofilms depended on ice crystallization caused during sample preparation.

Müller formulated a "hierarchy of biological specimen preparation": Specimen preparation starts with sampling (excision of tissue, harvesting of cells), than it continues with immobilization and fixation (e. g. freezing), and ends with microscopy, image interpretation and analysis [13]. The final result of this chain of procedures can never be better than the first step, and at best, each step may only preserve the information density retained by the previous one [24]. Therefore, one of the main objectives solved in this thesis is focused on instrumental developments and improvements related with low temperature sample preparation. As well several presented results correspond to the statement mentioned above that understanding to processes behind sample preparation and following imaging by SEM/cryo-SEM are essential to results interpretation.

Within this thesis, also temperature measurement during freeze-etching process was performed in the cryo preparation chamber ACE600 (Leica microsystems). Behind the original temperature sensor which is an original part of the ACE600 chamber at the cryo stage that is cooled down by metal belts coupled with Dewar containing liquid nitrogen, two additional temperature Pt100 sensors were directly mounted on – the first one on the sample holder to the place of the sample (Fig. 16, the blue line) and the second one on the cryo stage near the original temperature sensor (Fig. 16, the red line). The grey line in Figure 16 shows the temperature measured by the original Leica sensor, and, in addition the set freeze-etching temperature is corresponding with this grey line. In the presented experiment the freeze-etching parameters were set as following: starting temperature at -140 °C, increasing the temperature to -90 °C with a speed of 5 °C/min, subsequent staying at -90 °C for 10 min and finally lowering down to initial temperature of -140°C with the highest possible speed. The pressure in cryo preparation chamber was 2.7×10^{-7} mbar. It is not surprising that measured red and blue curves have time shift approximately one minute at the temperature of -110 °C (time needed for cooling down the sample holder from -113 to -110 °C). On the other hand, as an unexpected result a temperature shift of original sensor has been recognized which is decisive in freeze-etching procedure. This temperature shift was verified by measurement of liquid nitrogen temperature. In conclusion, it can be summarized that real sublimation has been running at different conditions set and the sublimation speed is lower than would be expected. The temperature measurement in the chamber of cryo-SEM Magellan (Thermo Fisher Scientific) is showed in Figure 17. Temperature/time shift has been measured less than 2 °C / 30 s probably due to better thermal contact between cryo-stage and sample holder than in ACE600; pressure inside

SEM chamber was 4.3×10^{-6} mbar. This measurement raised the need to tightly control the temperature and also develop another solution temperature control.

Temperature measurement in ACE600
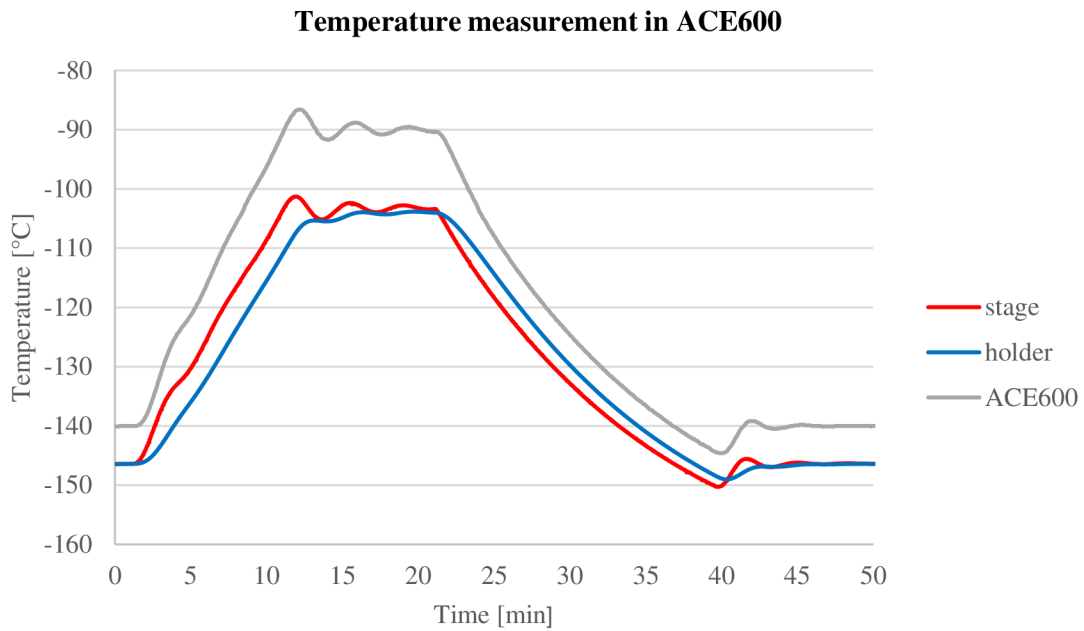
Figure 16: Temperature measurement in cryo preparation chamber ACE600. Lines show the temperature: red on the cryo-stage, blue on the sample holder, and grey line represents temperature measured by original sensor on the cryo-stage.

Temperature measurement in SEM Magellan 400/L
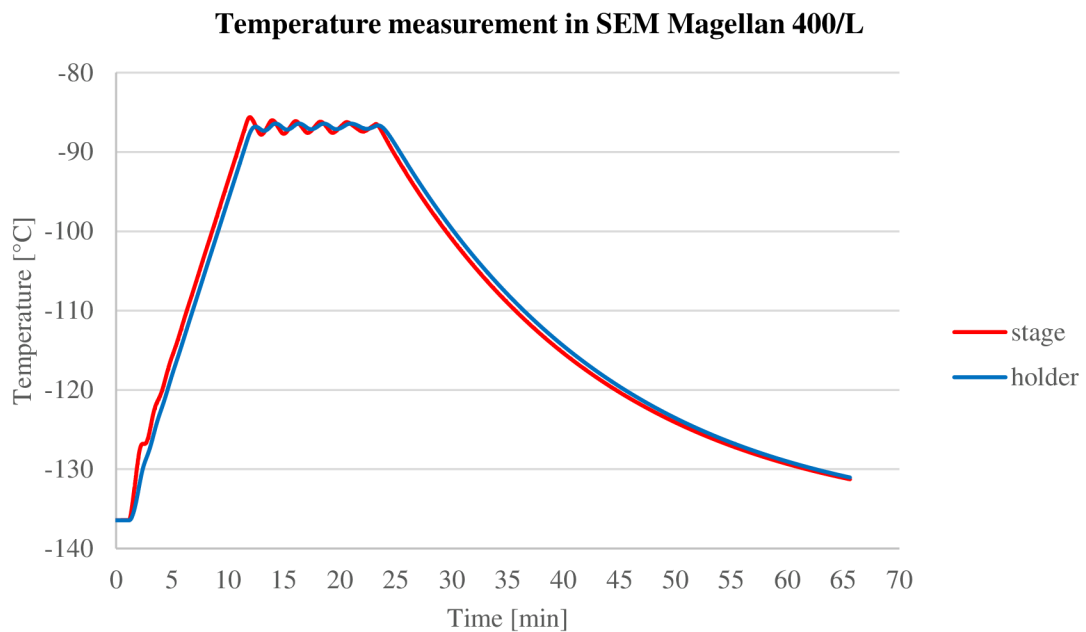
Figure 17: Temperature measurement in the cryo-SEM Magellan chamber. Lines show the temperature: red on the cryo-stage and blue on the sample holder.

Yeast and bacteria are microorganisms that can live as planktonic cells or in an organized formation called biofilm [131-133]. During their adherence to surfaces or interfaces and their subsequent proliferation, the cells embed themselves into an amorphous extracellular matrix (ECM) [132; 134; 135], which is composed of extracellular polymeric substances (EPS) produced by the cells. The presence of ECM is often considered an important characteristic of a mature biofilm [131]. Among the main components of EPS belong polysaccharides, proteins, and extracellular DNA [135; 136]. Since these substances are all highly hydrophilic, the biofilm water content can sometimes be as high as 90 % of the total biofilm mass [133; 134; 137]. Microbes in natural ecosystems appear to have a pronounced tendency to colonize various surfaces and each other. The interest in such microbial communities – biofilms – has increased over the last three decades, because the biofilms are important in many aspects of health, biotechnology, etc. [135; 138; 139].

The presence of biofilms can lead to human health problems, e.g., biofilm on teeth [140], also known as plaque and a factor in tooth decay and parodontosis, as well as the development of biofilm on medical devices such as catheters or implants [141]. On the other hand, biofilms can be useful, as they are already extensively used in wastewater treatment [142; 143] and play a role in biofuel production such as methane generation by methanogenesis [144] or in food production [145]. Life in biofilms is favourable for microbes, bringing advantages such as enhanced persistence and resistance to environmental threats such as antimicrobial agents [146], toxic substances, thermal and oxidative stress [147-149]. Studies of biofilms suggest that the biofilm matrix architecture is variable and it contains channels that enable water, nutrients and oxygen flow through the biofilm [148]. However, the detailed architecture of the channels inside the ECM, and the processes operating within them have not yet been fully elucidated [146; 148].

The yeast *Candida parapsilosis* and bacterium *Staphylococcus epidermidis* have been studied in this project as well. These species are frequently found among the normal human microbiota [139; 150]. However, in a medical context, the ability to form biofilms allows these microbes to colonize the surfaces of implants, consequently causing difficult-to-treat infections, especially in immunocompromised patients [151; 152]. The presence of EPS protects the microbial cells from the natural defences of the human immune system as well as from the effects of antibiotic treatments [133; 136] and thus it complicates the therapy [135; 139]. Understanding the biofilm structure can contribute to the research of biofilm formation and the underlying biochemical mechanisms. This will help to develop a more efficient treatment strategy for biofilm infections [153; 154].

Bacillus subtilis which is a nonpathogenic, Gram-positive soil bacterium belongs to a group of attractive microorganisms, which are also capable of forming a biofilm [155]. However, extracellular DNA production by *B. subtilis* is incorrectly understood [156]. It was stated that EPS is both secreted by bacteria and is the product of cell lysis and hydrolytic activities even without the presence of accessible solid surfaces [157]. The role of EPS in the cell surface adhesion process has been extensively researched by biofilm scientific literature [131; 135; 158]. However, up to now, only a few of these papers have provided actual information on relationship between biofilm formation, EPS production, and biodeterioration of polymer materials in relation to nutritional factors [143; 159]. Bacterial biofilm has a significant impact on utilization and lifetime period of polymer material in medical, industrial, and environmental settings [160; 161]. Although biofilm formation on polymer surfaces [161] does not lead to its biodegradation, it contributes to changes in surface conditions and in this way influences the biodegradation rate. Lefévre et al. [162] reported

that the biodegradation rate of poly(ε-caprolactone) film decreased, and also, biodegradation extent was more limited under conditions, which favoured the biofilm formation, than under those, where no biofilm was detected. A research [143] carried out to study the effect of various nutrition conditions on the biofilm formation and related PCL film biodeterioration by submerged cultivation of *B. subtilis CCM* 1999.

There is a series of various stress factors in the environment such as temperature below 0 °C that affect microorganisms. Approximately 80 % of our planet's biosphere is permanently cold with average temperatures below 5 °C [47]. Therefore, many microorganisms have developed sophisticated defence strategies for their protection. One of them is the ability to produce and accumulate cryoprotectants, e.g. amino acids, sugars, as well as high molecular weight substances [47; 81]. On the contrary, the response of most prokaryotes is passive at temperatures close to 0 °C, which is connected with the formation of ice [163]. A process of ice crystals growing in the extracellular medium results in effective osmotic stress. This induces so-called "freeze-dehydration" which is an important harmful consequence of cell freezing. Ice crystallization inside the cells causes the physical destruction of membranes, formation of gas bubbles, and might also result in organelle disruption [81]. More generally, the survival of bacterial cells during freezing depends on the cooling rate. Cell survival is maximal when cooling occurs slowly enough to avoid formation of intracellular ice but fast enough to prevent causing injury to the cells by substantial dehydration [164].

Polyhydroxyalkanoates (PHAs) are storage polymers accumulated in the form of intracellular granules by a wide range of taxonomically different groups of microorganisms. It is generally proposed that PHAs serve primarily as a carbon and energy storage material. However, there are reports that the capacity for intracellular PHA accumulation and degradation also enhances the resistance of bacterial cells to various stress conditions including low temperatures and freezing. PHAs have been observed to be essential for maintenance of the redox state in the Antarctic bacterium *Pseudomonas* sp. 14–3 during low-temperature adaptation [165]. Iustman et al. isolated and studied the Antarctic strain *Pseudomonas extremaustralis,* whose high resistance to a wide range of stress conditions including cold was attributed to its capacity to produce PHB [166]. Further, Pavez et al. reported that PHAs exert a protective effect against freezing in *Sphingopyxis chilensis* [167]. In the work [168] the cryoprotective effect of PHB–3–hydroxybutyrate (3HB) for lipase was tested as a model enzyme as well as for selected eukaryotic (*Saccharomyces cerevisiae*) and prokaryotic (*Cupriavids necator*) microorganisms. In addition, using flow cytometry, thermal analysis, and cryo-SEM, the role of intracellular PHB granules with respect to the survival of bacterial cells during freezing and thawing was studied.

Single microorganisms cells as well as microbial biofilms are usually investigated by various microscopic techniques including confocal laser scanning microscopy (CLSM) and conventional SEM [143; 169; 170], transmission electron microscopy (TEM) [171], focused ion beam SEM (FIB)-SEM [172] and by special SEM techniques, such as cryo-SEM or environmental SEM (ESEM) [107; 172; 173]. The main limitation of the light microscopy techniques is the restricted magnification [174]. This can be resolved by the use of SEM, which provides high-magnification images of the individual bacteria and yeast cells and their location and interaction within the ECM, which is important for understanding the morphology and physiology of biofilms [46].

However, a conventional SEM, where the sample is observed in high vacuum at room temperature, is limited due to the need for a dry sample [14]. Biofilms are rich in water and the conventional sample preparation for SEM that includes desiccation as a prerequisite for imaging

can cause substantial changes in the ECM and the microbial cell ultrastructure, leading to artifacts [21; 107; 172]. Chemical fixation with aldehydes and osmium tetroxide treatment help to preserve cell morphology and enhance contrast [175; 176], while dehydration with ethanol or acetone series is used for the gradual replacement of the water inside the sample. However, this phase of preparation also causes some artifacts, such as cell membrane discontinuities [177], and it has other deleterious effects on morphology.

In the case of cryo-fixation, the biofilm is not dehydrated but kept frozen to obtain high-resolution images closer to the native state of the sample [7; 14; 176]. It has been proven that in cryo-fixed biofilms, the bacterial ultrastructure preservation and the biofilm organization improved significantly [22]. To reduce the damage inherent to these treatments, various innovative cryogenic sample preparation methods have been developed [178-180]. One of the simplest cryo-fixation techniques is plunging the sample into a liquid cryogen [181]. In general, plunging into liquid nitrogen is not usually sufficient because of the Leidenfrost effect: a thermally insulating film of vaporized nitrogen forming around the sample, preventing fast cooling and allowing water ice crystals to form inside the specimen [182]; more detail regarding sample preparation are covered in Chapters 3 and 4. However, cryogens like liquid ethane/propane are often used, for example in electron tomography, for fixation of very thin layers [183]. Substantially more effective freezing can be achieved by increasing the pressure during exposure to the liquid cryogen. This can be performed by the high-pressure freezing (HPF) technique [92; 93; 97; 184]. Microscopic results published in several scientific papers have revealed that low temperature preparation of microbiological samples for electron microscopy seems to be meaningful approach.

6 Motivation and research strategy

As mentioned in the thesis assignment: *"The aim of the doctoral thesis is an instrumental and a methodological development in the field of scanning electron microscopy and its application in biomedicine and sensitive nanomaterials. An integral part of the work is the specific preparation of samples, both chemical and physical (e.g. cryofixation, immunostaining)"*; the motivation was clearly specified. A suitably selected sample preparation methodology and appropriate instrumental equipment are key for obtaining meaningful and publishable results in microscopic research, especially in biological applications.

There were several important topics and tasks related to the thesis. All the results discussed in Chapter 7 may be divided into one successive tasks depending on their contribution to the thesis:

1. *Instrumental & Methodological developments in cryo-SEM.* The motivation in this part was to design and build innovative tools, especially various sample holders, and to optimize the related methodology for the preparation of fully hydrated samples which should be applicable using available laboratory equipment. Specific tasks were the building of sample holders allowing perpendicular freeze-fracturing of small sapphire disks as well as gripping of multiple coper tubes. The author's contribution to the development of a new assembly for temperature control of the sample came from a need to have a defined temperature in the area of the examined sample that is considered to be an important parameter in most applications.

2. *The merit of SEM in microbiological research.* A demanding challenge in the field of microbiological research was to develop an optimal methodology for preparation of biofilm samples, with the aim of visualizing the internal structure of a biofilm layer at a high resolution reached by means of a scanning electron microscope. Another microbiological project required developments in sample preparation and freeze-fracturing methodology which were useful in studies of environmentally significant microbial strains.

The research strategy in this thesis started with setting out the scientific problems and identifying the research question and objectives. This part included literature studies and numerous discussions with experts in the field of microbiological/biotechnological and microscopic research. Subsequently, it could seek optimal solutions. In this work, methods and instrumental designs are proposed which were realized and tested on real samples. The new instrumentation was developed with the aim of enabling sample investigation at set conditions and of determining the answers to scientific questions. The results were published in several journals and thus recognized as useful for the scientific community.

7 Results

The main results of the thesis, which are divided into the following two sections and show the six most important achievements, are documented by the author's publications. The seven most related outputs are included in the Annexes to the thesis.

7.1 Instrumental & Methodological developments in cryo-SEM

7.1.1 Sample holder I. – perpendicular freeze-fracturing of sapphire disc

Author's contribution to the publications:

- Design of the sample holder construction
- Sample processing/installation
- Design of the experiments with microbial biofilm
- Biofilm incubation
- Imaging in cryo-SEM
- Results interpretation
- Preparation of manuscripts as a first author (full texts are available in Annex I and Annex II)

Annex I

Hrubanová, K., Nebesářová, J., Růžička, F., Krzyžánek, V. The innovation of cryo-SEM freeze-fracturing methodology demonstrated on high pressure frozen biofilm. *Micron*. 2018, 110(JUL), 28-35. ISSN 0968-4328
doi: 10.1016/j.micron.2018.04.006

Annex II

Hrubanová, K., Krzyžánek, V. Inovativní metodika mrazového lámání a cryo-SEM demonstrovaná na biofilmu *Candidy parapsilosis*. *Jemná mechanika a optika*. 2019, 64(1), 15-17. ISSN 0447-6441.

Results description

In this study an innovative method for the preparation of fully hydrated samples of the microbial biofilms of *Staphylococcus epidermidis*, *Candida parapsilosis* and *Candida albicans* cultures was presented. Cryogenic scanning electron microscopy (cryo-SEM) and high-pressure freezing (HPF) rank among the cutting-edge techniques in the electron microscopy of hydrated samples such as biofilms. However, the combination of these techniques is not always easily applicable. Therefore, a method of combining high-pressure freezing using EM PACT2 (Leica Microsystems) was presented, which fixed hydrated samples on small sapphire discs, with a high-resolution SEM equipped with the widely used cryo-preparation system ALTO 2500 (Gatan). Using a holder developed in-house, a freeze-fracturing technique was applied to image and investigate microbial cultures cultivated on the sapphire discs. Our experiments were focused on the ultrastructure of the extracellular matrix produced during cultivation and the relationships among the microbial cells in the biofilm. The main goal of these investigations was a detailed visualization of areas of the biofilm where the microbial cells adhere to the substrate/surface. The feasibility of this technique was shown and clearly demonstrated in experiments with various freeze-etching times.

A new sample holder for sapphire discs with a diameter of 1.4 mm for the HPF instrument EM PACT2 (Leica microsystems) was designed and built. Due to the small dimensions of the sapphire discs (diameter 1.4 mm, thickness 50 µm) several requirements for holder construction were specified such as easy fixing of the sapphire disc in liquid nitrogen, perpendicular fracturing of the sapphire disc with the sample in the ALTO 2500 preparation chamber using the original scalpel-manipulator, and the ability to observe both sides of the sapphire disc in the cryo-SEM without removing it from the ALTO 2500. The dimensions and material of the holder main body were analogous to the original dimensions and material, so that the disc fit in the ALTO 2500 instrument.

The holder consisted of two main parts (Fig. 18):
   (i)   the main body with a bayonet interface that fit onto the transfer rod and the rail system in the ALTO 2500 and
   (ii)   a hinged part for fastening the sapphire disc which could be easily tilted by ±5° using the ALTO 2500 manipulator, allowing one to observe the interface from both sides of the fractured sapphire disc.

The new holder and developed methodology were tested on experiments with microbial biofilms where the interior of biofilm layer was evaluated. Our study of bacterial/yeast biofilms suggests that cryo-SEM in combination with HPF and perpendicular cross freeze-fracturing through a sapphire disc is an excellent technique for imaging highly hydrated samples such as biofilms. Details of biofilm formation can be recognized and further studied in the natural hydrated state, thus allowing for detailed investigations of the ultrafine structure and morphology in near-life-like conditions (Fig. 19). Note that these experiments were performed in cooperation with the Biology centre of the Czech Academy of Sciences, Ceske Budejovice; the holder developed at ISI Brno is still being used to tackle other projects at the Biology Centre.
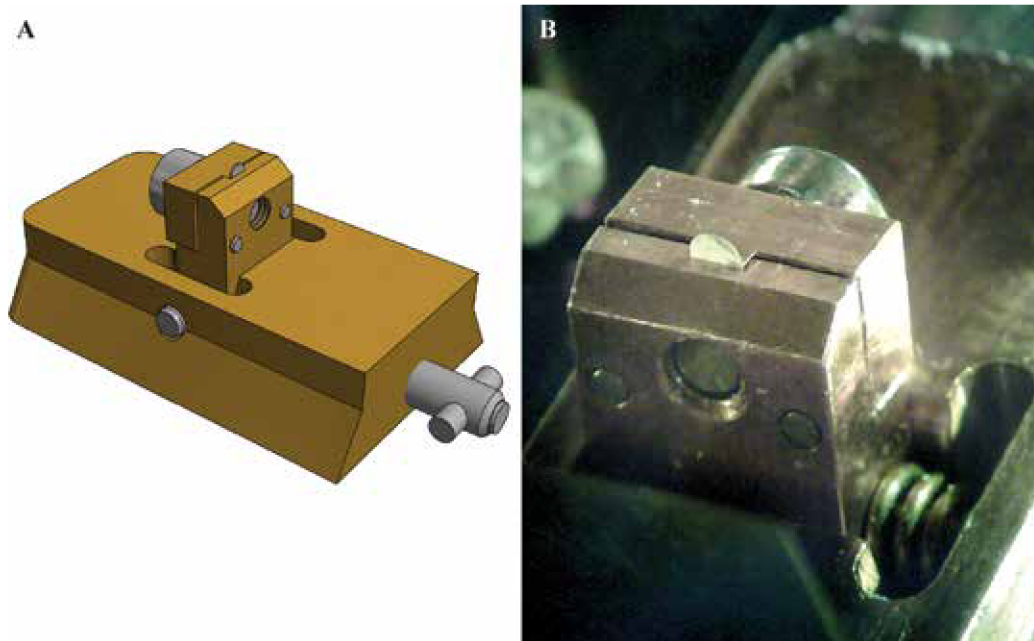
Figure 18: A holder allowing gripping and perpendicular cross freeze-fracturing of the 1.4mm sapphire disc compatible with the ALTO 2500 cryo-preparation system. (A) a schematic drawing and (B) actual picture taken during the experiments in the cryo-preparation chamber.
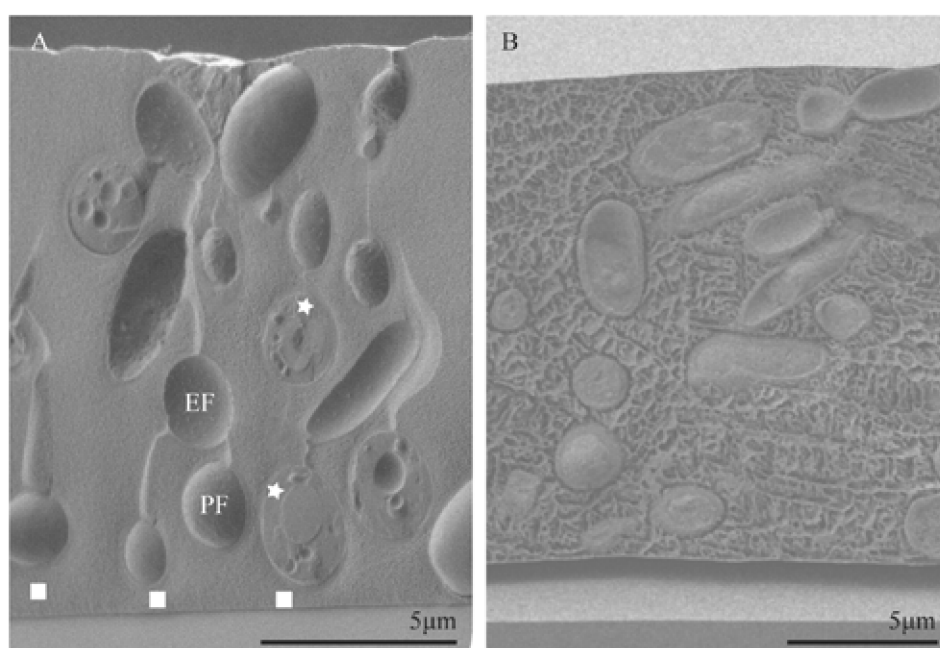
Figure 19: Freeze-fracture of *Candida parapsilosis*. (A) *Candida parapsilosis* grown on a sapphire disc and fixed using HPF. (B) *Candida parapsilosis* grown on a glass substrate and fixed by plunging in nitrogen slush. Endoplasmic (EF) and protoplasmic (PF) fracture faces exhibit typical invaginations and corresponding ridges, broken cells show a preserved ultrastructure with visible cell organelles (stars) and quite large distances between cells and an adhesion surface/substrate (square).

7.1.2 Sample holder II. – freeze-fracturing of samples in Cu tubes

Author's contribution to the publication:

- Contribution to the construction design of the sample holder
- Sample processing/installation
- Design of microbial samples preparation for cryo-SEM
- Imaging in cryo-SEM
- Cryo-SEM results interpretation
- Preparation of a SEM part of a manuscript (full text is available in Annex III)

Annex III

Obruča, S., Sedláček, P., Krzyžánek, V., Mravec, F., Hrubanová, K., Samek, O., Kučera, D., Benešová, P., Márová, I. Accumulation of Poly(3-hydroxybutyrate) Helps Bacterial Cells to Survive Freezing. *PLoS ONE*. 2016, 11(6), 0157778:1-16. E-ISSN 1932-6203 doi: 10.1371/journal.pone.0157778

Results description

A new sample holder for the cryo-SEM technique was designed and built (Fig. 20). It enables investigation of frozen samples covered in small copper tubes (Cu tubes) with various diameters ranging from 0.8 mm to 1.2 mm. The main body of the new holder fits onto the transfer rod and the rail system of the VCT100 cryo high-vacuum transfer system and the ACE600 cryo preparation chamber (both Leica Microsystems). Its upper part allows one to attach up to eight samples at a time. Therefore, it is possible to observe eight samples in cryo-SEM under the same conditions. Cryogenic fixation of the samples in the Cu tubes by plunging into liquid cryogen can be applied. Although that is not the ideal freezing methodology, it could be beneficial in some experiments. The usage of the sample and the related methodology of sample preparation is demonstrated in the following study on microbial systems. However, its potential was also demonstrated through structure studies of hydrogels. Several results were presented in a master thesis written by Kateřina Adamková under the supervision of Vladislav Krzyžánek and with the technical support of Kamila Hrubanová [185].

Accumulation of polyhydroxybutyrate (PHB) seems to be a common metabolic strategy adopted by many bacteria to cope with cold environments. This work aimed at evaluating and understanding the cryoprotective effect of PHB. At first a monomer of PHB, 3-hydroxybutyrate, was identified as a potent cryoprotectant capable of protecting model enzyme (lipase), yeast (*Saccharomyces cerevisiae*) and bacterial cells (*Cupriavidus necator*) against the adverse effects of freezing-thawing cycles. Further, the viability of the frozen/thawed PHB-accumulating strain of *C. necator* was compared to that of the PHB non-accumulating mutant. The presence of PHB granules in cells was revealed to be a significant advantage during freezing. This might be attributed to the higher intracellular level of 3-hydroxybutyrate in PHB-accumulating cells (due to the action of parallel PHB synthesis and degradation, the so-called PHB cycle), but the cryoprotective effect of PHB granules seems to be more complex. Since intracellular PHB granules retain highly flexible properties even at extremely low temperatures (observed by cryo-SEM), it can be expected that PHB granules protect cells against injury from extracellular ice. Finally, thermal analysis indicates that PHB-containing cells exhibit a higher rate of transmembrane water transport, which protects cells against the formation of intracellular ice, something that usually has fatal consequences.

Figure 21 shows cryo-SEM microphotographs of PHB non-containing (*C. necator* PHB-4) and containing (*C. necator* H16) bacterial cells. In PHB-containing cells, needle-like plastic deformations were observed, while these structures were absent in cells without the polymer, which indicates that these deformations can be clearly attributed to PHB granules. Despite the fact that the mechanism of the genesis of these deformations during freeze-fraction has not yet been explained, we can state that frozen PHB granules exhibit completely different mechanical and physico-chemical properties than any other components of bacterial cytoplasm and that their flexibility, even in deeply-frozen states, is significantly higher than that of PHB isolated from bacterial cells. In cryo-SEM microphotographs we observed elongation corresponding to a value of more than 100%.

Figure 20: A holder is able to grip up to 8 copper tubes in order to freeze-fracture and image the sample inside.
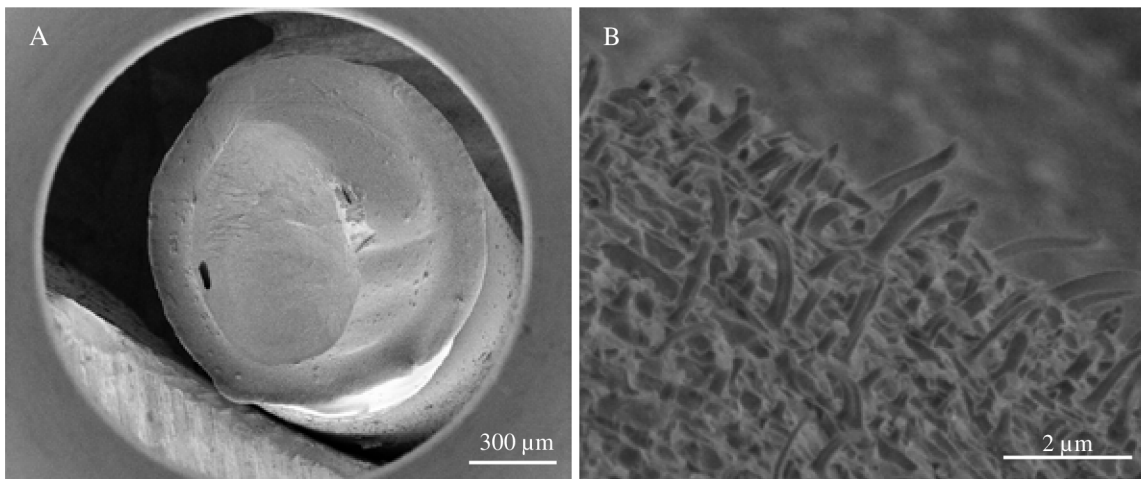
Figure 21: Cryo-SEM images of freeze-fracture of *Cupriavidus necator* sample frozen in copper tube: (A) an overview magnification and (B) a fracture face of bacterial cells containing intracellular PHB granules.

7.1.3 A sample temperature control assembly

Author's contribution to the utility model:

- Contribution to the shape design of the assembly for sample temperature control
- Sample processing/installation
- Preparation of the technical documentation (full text is available in Annex IV)

Annex IV

Krzyžánek, V., Skoupý, R., <u>Hrubanová, K.</u> Sestava pro regulaci teploty vzorku. 2018. Brno: Ústav přístrojovén techniky AV ČR, v.v.i., 07.11.2018. 32258.
https://isdv.upv.cz/doc/FullFiles/UtilityModels/FullDocuments/FDUM0032/uv032258.pdf

Results description

Cryogenic electron microscopy is recognized as an important technique in the biological as well as material sciences. It is particularly useful for analysing biological samples or polymers with a high water content. The precise control of a defined temperature in the area of the examined sample is important for most samples, but it seems to be essential in some applications like investigation of hydrogels that are very sensitive to sublimation.

Currently, commercial cryo-attachments have a temperature control located in the area of the stage where the sample holder with a specimen is placed on. The main disadvantage of this solution is that the temperature is measured quite far away from the specimen, therefore the measured temperature means the value of the complete system including table + holder + sample. The rate of temperature control is burdened by the whole entire system including a large mass of the material consisted on. Moreover, during sublimation the sample holder as well as the stage is heated and cooled, therefore this standard solution leads to a delay in temperature response (temperature measurements using the commercial system are shown in Figures 16 and 17). Moreover, it does not allow the analysis of a frozen sample in the transmission mode, i.e. using the STEM detector, with the temperature control.

Our main innovations in the presented sample temperature control assembly are new designs for a cryo-stage and the sample holder where a heating element and a temperature sensor are a new part thereof. Both elements are electrically interconnected with the cryo-stage as well as with a temperature controller using a set of connectors. The cryo-stage is connected to the Dewar containing liquid nitrogen via the cooling bands. The main body of the sample holder is based on a commercial solution in order to maintain compatibility with the VCT100 high-vacuum transfer system and other cryo-equipment produced by Leica Microsystems. The construction of the sample holder's upper part is completely innovative (Fig. 22; documentation of the Utility Model No. 32258 can be found in Annex IV). The assembly is made of a gold-plated copper alloy.
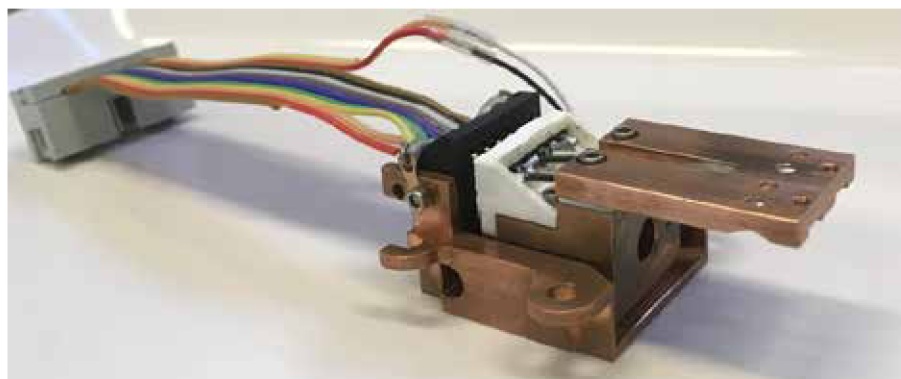
Figure 22: The new sample temperature control assembly.

7.2.1 Biological application I – Medical significant biofilm positive microbial strains

Author's contribution to the publication:

- Design of the experimental concept
- Biofilm cultivation
- Sample preparation for SEM and cryo-SEM
- Imaging using SEM and cryo-SEM
- SEM and cryo-SEM results interpretation
- Preparation of the manuscript as the first author (full text is available in Annex V)

Annex V

Hrubanová, K., Krzyžánek, V., Nebesářová, J., Růžička, F., Pilát, Z., Samek, O. Monitoring *Candida parapsilosis* and *Staphylococcus epidermidis* Biofilms by a Combination of Scanning Electron Microscopy and Raman Spectroscopy. *Sensors*. 2018, 18(12), 4089. ISSN 1424-8220 doi: 10.3390/s18124089

Results description
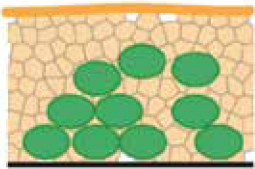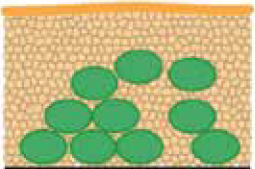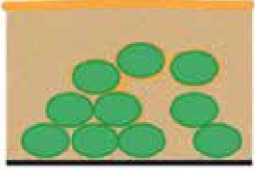
The biofilm-forming microbial species *Candida parapsilosis* and *Staphylococcus epidermidis* have been recently linked to serious infections associated with implanted medical devices. In this work, microbial biofilms were studied using high-resolution SEM. Observation using SEM allowed us to visualize the biofilm structure, including the distribution of cells inside the extracellular matrix and the areas of surface adhesion. The work evaluated the merits of a classical SEM involving chemically fixed samples with cryo-SEM, including physical sample preparation based on plunging the sample into various liquid cryogens as well as high-pressure freezing (HPF). For imaging the biofilm interior, the freeze-fracture technique was applied. In this study, it was shown that the different means of sample preparation have a fundamental influence on the observed biofilm structure. The SEM was employed to study the ECM content and distribution in the biofilm, and the way it translates into a Raman spectral characteristics. The SEM images helped us to estimate the relative proportion of the ECM, which in most cases ranges between 20 % and 50 % of the total biofilm volume. This means that in the Raman spectra the signal was observed both from the bacterial cells and from the ECM, the proportion of which depends on the growth stage of the biofilm. The proportion of the ECM increased with the age of the biofilm.

All the samples were imaged by SEM, both at room temperature and at low temperature. Figure 23 describes all the sample preparation protocols for SEM and the limitations of these six different preparation techniques on bacterial and yeast biofilms (M1–M6). The benefits and influence on the biofilm structure are summarized in Table 4. A comparison of the applied techniques for microbial biofilm studies was presented and it showed that a combination of Raman spectroscopy with selected SEM techniques can provide a deeper insight into the chemistry and composition of biofilms.
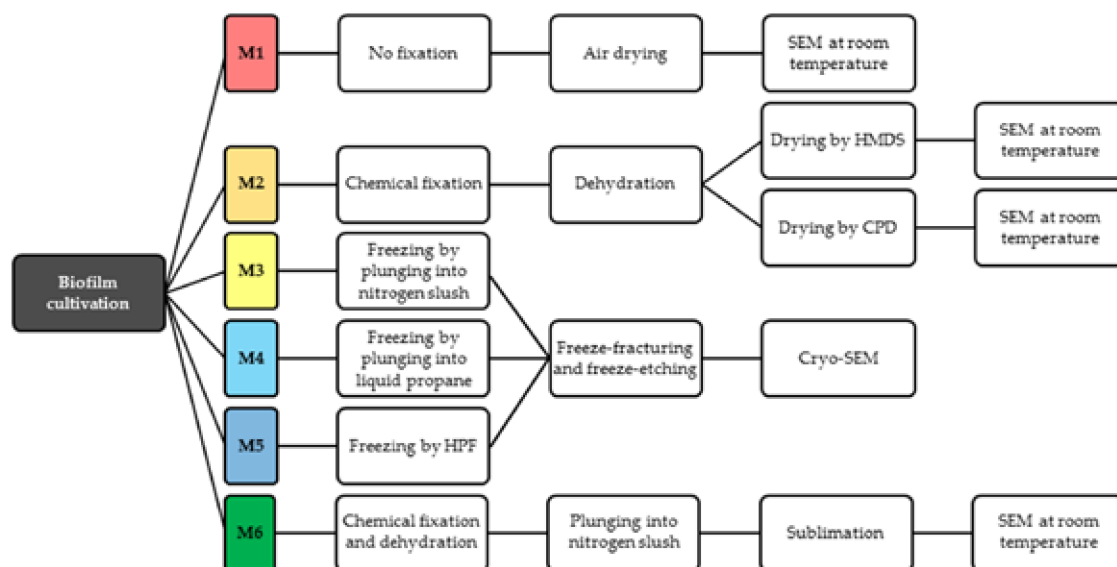
Figure 23: Diagram of microbial biofilm sample preparation for SEM.

Table 4: Comparison of benefits and limitations of sample preparation protocols for SEM (Methods M1-M6) and their influence on biofilm structure as shown in schematic drawings. Our best candidates for sample preparation techniques are labelled green.

M	Advantage	Disadvantage	Schema
M1 – air-drying	Speed of sample preparation Simplicity Repeatability of measurement in SEM at room temperature Suitable for **surface imaging**	The loss of the 3D structure Deformation of microbial biofilm Deformation of ECM The possibility of imaging only the sample surface (not interior)	Deformation of biofilm
M2 - conventional chemical preparation	Repeatability of measurement in SEM at room temperature The 3D structure is preserved. Suitable for **surface imaging**	Long-term procedure Damage of soft biofilm sample due to multi-steps washing Artifacts with chemicals treatment (the change of gel-like ECM into fiber structures) The sample surface imaging	Biofilm is washed out
M3 – plunging LN₂; cryo-SEM	Speed of sample preparation The 3D structure of microbial cells is preserved Possibility of biofilm **interior imaging** (used freeze-fracturing technique also suitable for M3-M5)	Artifacts with freezing procedure Freezing is sufficient for very thin samples Limitation for surface imaging because of water content in biofilm samples	"Large" ice crystals
M4– plung. Ethane; cryo-SEM	Speed of sample preparation The 3D structure of microbial cells is preserved Possibility of biofilm **interior imaging**	Artifacts with freezing procedure (smaller ice crystals inside biofilm than by M3) Freezing of thin samples Limitation in surface imaging because of water content in biofilm samples	"Small" ice crystals
M5 – HPF freezing and cryo-SEM	Speed of sample preparation 3D structure of microbial cells / ECM is nicely preserved The best freezing technique for samples with thickness up to 200 µm (exp. tested) Biofilm **interior imaging**	Limitation in surface imaging (water content in biofilm) Limitations connected with HPF machine – cultivation substrate (sapphire discs for freeze-fracturing; Al or Cu-gold discs)	**Optimal** prep. of biofilm for **interior imaging**
M6 - Combined preparation	Speed of sample preparation 3D structure of biofilm Biofilm **surface imaging** Repeatability of measurement in SEM at room temperature after freeze-drying Less washed out biofilm	Artifacts from chemical fixation (the change of gel-like ECM) The imaging of sample surface	**Optimal** prep. of chemically fixed biofilm for **surface imaging.**

7.2.2 Biological application II – Environmentally significant microbial strains

Author's contribution to the publication:

- Microbial samples preparation for SEM
- Sample processing/installation
- Imaging using SEM
- SEM results interpretation
- Preparation of a SEM part of the manuscript (full text is available in Annex VI)

Annex VI

Voběrková, S., Hermanová, S., Hrubanová, K., Krzyžánek, V. Biofilm formation and extracellular polymeric substances (EPS) production by Bacillus subtilis depending on nutritional conditions in the presence of polyester film. *Folia Microbiologica*. 2016, 61(2), 91-100. ISSN 0015-5632 doi: 10.1007/s12223-015-0406-y

Results description

Widespread studies on the biodegradation of plastics have been carried out in order to confront the environmental problems associated with synthetic plastic waste. From this point of view aliphatic polyesters represent a class of biodegradable materials with various potential applications. Research interest has been also paid to enhancement of biodegradation of resistant plastics by incorporation of aliphatic ester linkages to aromatic ones or modification of polyolefins with aliphatic polyesters. Polycaprolactone (PCL) as a representative of aliphatic polyesters undergoes biodegradation by the action of enzymes and microorganisms and hence it is a suitable candidate for the study of biodeterioration and biodegradation.

The biodeterioration activity of a *Bacillus* strain, naturally occurring in the soil environment, on the surface of polycaprolactone films in mineral salt and mineral salt-yeast extract enriched media at 30 °C after 21 days was studied. Polyester square specimens (10×10 mm) were sectioned from film prepared by melt pressing. Control abiotic tests were carried out by immersion of the studied samples into the media in the absence of microorganisms. As described in [145, 187] the surface erosion pattern which developed is ascribed to the formation of degradation products ended with carboxylic groups in dissociated forms as the first step. Subsequently, the accumulation of more hydrophilic species supports both the acceleration of chain degradation through autocatalysis and the diffusion of water. Changes in the film surface were evaluated by means of SEM using a Magellan 400/L (Thermo Fisher Scientific) at a primary energy of 2 keV. For characterization of the material surface, here the presented samples lacked any chemical treatment and were air-dried, and they were coated with 4 nm of platinum.

For the characterization of the investigated material surface structure by SEM, several parameters were evaluated. The deformations recognized and described in the study were as follows:
  (i)   Microcracks on the surface with sharp edges (0.1–5.0 μm long, 0.5 μm in width, the depth of cracks up to a few μm) and their directional orientation;
  (ii) holes in the surface (often annular);
  (iii) the lamellar structure of the surface (incidence of long fibres with a diameter of up to 0.1 μm and their clusters);
  (iv) the surface roughness;
  (v)   places with smooth surfaces and
  (vi) the occurrence of bacteria (biofilm).

The flat surface of PCL films is presented in Fig. 24. The microcracks which developed on the surface of biotically-aged films in mineral salt and mineral salt with yeast extract media were randomly distributed. The formation of irregular holes on the surface may be associated with higher enzymatic activity in a mineral salt medium enriched with yeast extract. The polycaprolactone sample, due to its semicrystalline and hydrophobic character, displayed only a low water uptake in abiotic control media and consequently no weight loss along with no surface erosion proceeded.
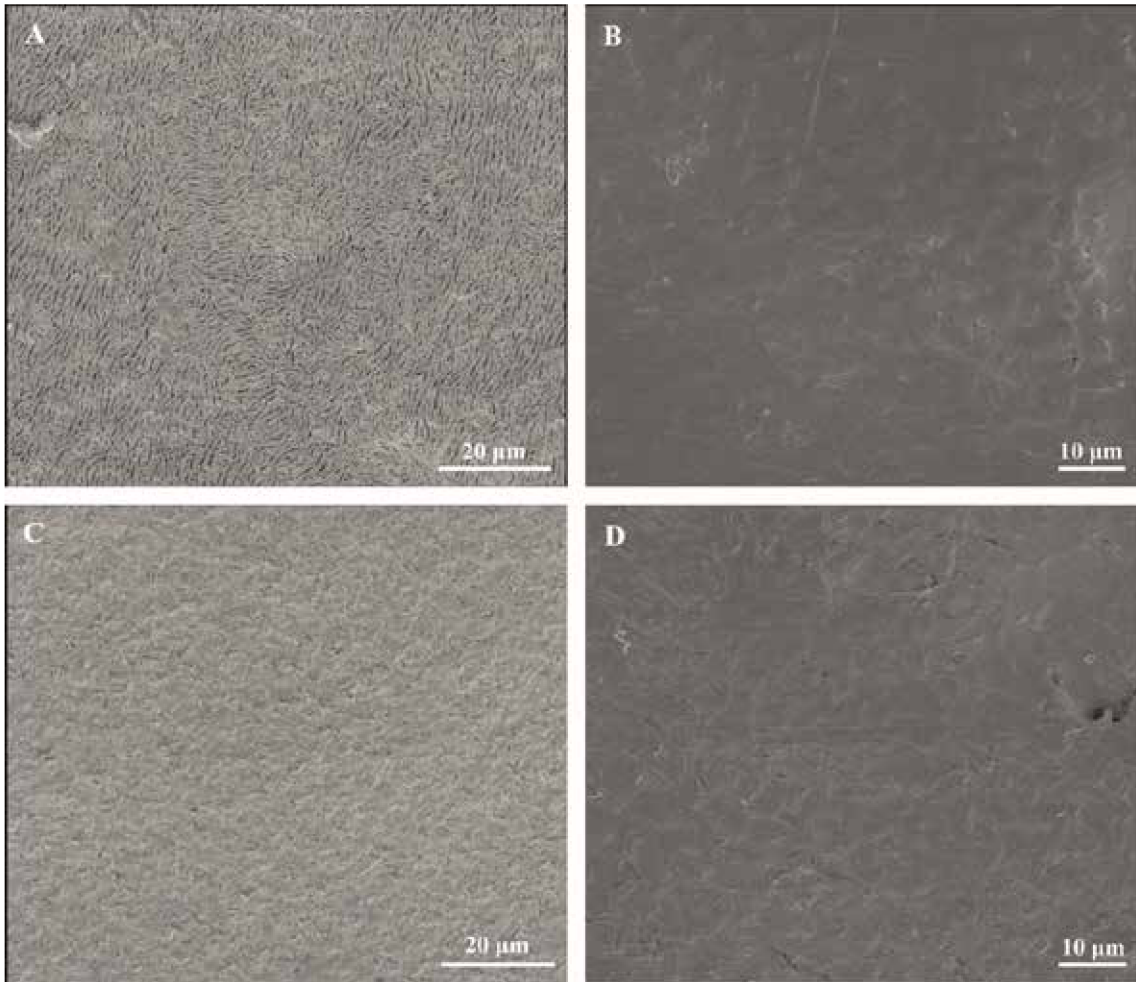
Figure 24: SEM micrographs of polycaprolactone films. (A) PCL sample after 21 days in mineral salt medium inoculated with *Bacillus* strain, (B) the control sample in mineral salt medium, (C) PCL sample after 21 days in mineral salt medium supplemented with *Bacillus* strain, (D) the control sample in mineral salt medium supplemented with yeast extract.

7.2.3 Biological application III – Environmentally significant red yeast strains

Author's contribution to the publication:

- Microbial samples preparation for SEM and cryo-SEM
- Sample processing/installation
- Imaging using SEM and cryo-SEM
- SEM and cryo-SEM results interpretation
- Preparation of the abstract and poster (full text is available in Annex VII)

Annex VII

Hrubanová, K., Samek, O., Haroniková, A., Bernatová, S., Zemánek, P., Márová, I., Krzyžánek, V. Morphological and Production Changes in Stressed Red Yeasts Monitored Using SEM and Raman Spectroscopy. *Microscopy and Microanalysis*. 2016, 22(S3), 1146-1147. ISSN 1431-9276 doi: 10.1017/S1431927616006577

Results description

Several investigations of the influence of different cultivation conditions on lipids production by red yeasts, using SEM and Raman spectroscopy techniques, have been reported. Here, SEM uses an electron beam to gain information about the morphology of cells which reflects the cells' response to the applied stress. Consequently, Raman spectroscopy was used for the determination of carotenoids and lipids present in the biomass. Thus, this study presented some factors which could lead to efficient industrial production of carotenoids and lipids in selected biotechnological production.

Applied stress can induce changes in cell composition, metabolism and physiology. These investigations were focused on red yeasts which also could produce a high amount of lipid compounds. Carotenoids are membrane-bound lipid-soluble pigments, which can act as effective antioxidants and scavenge singlet oxygen. In red yeast, controlled physiological and nutrition stress can be used for enhanced pigment and also oil production. Namely, in the presented experiments osmotic stress was induced by incubation in two different media which led to production of lipids or carotenoids. Note that also the morphology of cells can be changed. Both media contain the same: salts, glucose and ammonium sulphate with different C/N ratios. The first growth medium (medium 1) indicated positive results for carotenoid production and the second medium (medium 2) with a high C/N ratio led to an increased lipid production. Our experimental results were presented as a Poster in Figure 25.

For SEM imaging the samples of *Cystofilobasidium infirmominiatum* were prepared in the following way: (a) the samples were cultivated aerobically at 25 °C in the two different media for 144 hours; (b) cell suspensions were fixed in 2.5% glutaraldehyde in PBS for 2 hours and 30 min in 1% OsO_4, dehydrated by ethanol series and dried using HDMS on the glass slides. Both images of prepared samples were scanned without any metal coating at an electron beam energy of 1 keV and a beam current of 6.3 pA in a SEM Magellan (FEI). The samples of *Sporobolomyces shibatanus* were cultivated as mentioned above and observed by cryo-SEM. The sample was quickly frozen in liquid nitrogen, moved into a vacuum chamber (ACE600, Leica Microsystems) where it was freeze-fractured and sublimated at -95 °C for 5 minutes. In the next step, the sample was moved under high vacuum using a shuttle (VCT100, Leica Microsystems) into the SEM (Magellan, FEI) equipped with a cold stage and the fractured structure was observed with a 1 keV electron beam at -120 °C and a beam current of 6.3 pA without any metal coating.

Our results showed that systematic studies are required in order to fully monitor cell response mechanisms on applied stress and a combination of SEM and Raman spectroscopy approaches could be applied.

Figure 25: Poster demonstrated the morphological and production changes in stressed red yeasts monitored by SEM and Raman Spectroscopy; it was presented at Microscopy and Microanalysis 2016 meeting in Columbus, Ohio, USA.

8 Conclusions

Electron microscopy in biology can provide high-resolution images and other specific information originating from electron-sample interactions that are useful for a deeper understanding of the structural and functional quintessence of complex biological systems. Consequently, specimen preparation protocols related to this powerful technique and imaging procedures should form the basis for the correct interpretation of the hydrated sample images and analyzed data.

In the introductory part, the author describes sample immobilization techniques such as the preparation protocols of aqueous materials that are necessary for their transition to a solid state in which a specimen can resist physical conditions during imaging and analysis. These techniques are divided into two main groups depending on the means of sample fixation and on the observation temperature under a scanning electron microscope (SEM). For conventional SEM, i.e. under room temperature, a chemical fixation to preserve soft structures, subsequent dehydration and metal coating is required. All of these steps have their own limits and often create a lot of artifacts which have been identified in several studies which are cited in the thesis. Many of the problems associated with conventional preparation techniques of hydrated electron beam sensitive materials can be avoided by using cryogenic SEM (cryo-SEM), which allows observation of an aqueous specimen close to its native state. However, to understand the imaged structures properly, it is important to determine the main processes that occur during the cryo-preparation, because potential pitfalls in cryo-SEM can be also recognized. In addition, this theoretical section of the thesis also includes an overview of already extant instruments for SEM sample preparation, such as critical point dryers and cryo-related equipment which are designed with the aim of dealing with the water content in biological and other liquid-based specimens.

This dissertation thesis contains innovations and improvements in the field of specimen preparation and cryo-SEM technique that were produced at the Institute of Scientific Instruments of the CAS in Brno. The most important results, including the developed tools and their verification in real experiments, are described in Chapter 7.

In particular, the new constructions of two sample holders are presented. The functionality of the first sample holder for perpendicular freeze-fracturing of small sapphire discs, which are usually used for high pressure freezing (HPF), is presented in experiments with microbial samples. Among the investigated microbiological strains are the biofilm positive bacteria *Staphylococcus epidermidis* and yeasts such as *Candida albicans* and *Candida parapsilosis*, which are considered to be clinically significant because they are often involved in serious infections. The main aim of this study is to suggest that cryo-SEM in combination with HPF and perpendicular cross freeze-fracturing through a sapphire disc is an excellent technique for imaging highly hydrated samples. Details of biofilm formation can be recognized and further studied in the natural hydrated state, thus allowing for detailed investigations of the ultrafine structure and morphology in near-life-like conditions.

These strains were used also in the methodological study where positives and limits of a room temperature SEM and cryo-SEM technique are evaluated on the quality of biofilm structure. The author compared the merit of various sample preparation protocols including chemical fixation as well as physical fixation by plunging into various liquid cryogens and freezing by HPF. It was shown that the different means of sample preparation have a fundamental influence on the observed

biofilm structure. SEM was employed to study the ECM content and distribution in the biofilm, and the way it translates into Raman spectral characteristics.

The second presented sample holder was designed with the aim of improving and increasing the reproducibility of experiments which required the same temperature/sublimation conditions. It was proved successful in the field of microbiological samples with biotechnological potential. Its upper part allows one to attach up to eight samples covered in copper tubes at a time. Therefore, it is possible to observe eight samples in cryo-SEM under the same conditions. Its usefulness is shown in the evaluation of the cryoprotective effect of polyhydroxybutyrate (PHB) inside bacterial cells of *Cupriavidus necator*. In this case, the cryogenic fixation in Cu tubes by plunging into liquid cryogen can be applied. Even though it is not the ideal freezing methodology, it is beneficial in these experiments.

A sample temperature control assembly presents an innovation in the area of increasing temperature control during sublimation as well as imaging by cryo-SEM. This valid utility model couples a new design of the cryo-stage and a sample holder which is enhanced by means of a temperature sensor and heating element.

The merits of the methodological improvements are proven also in other experimental applications such as the investigation of the influence of different cultivation conditions on lipid production by red yeasts such as *Cystofilobasidium infirmominiatum* and *Sporobolomyces shibatanus*, using a combination of SEM and Raman spectroscopy. Furthermore, the effect of the biofilm formation of *Bacillus subtilis* on biodeterioration and biodegradation of poly-ε-caprolactone films was studied.

The author would like to note that the carefully selected sample preparation methodology and appropriate instrumental equipment described within this thesis are key in obtaining meaningful and publishable results in microscopic research, especially in biological applications. Besides the author's results, which have been published and therefore recognized as useful for the scientific community, the presented thesis can be considered to represent a review of the current state in the area of high-vacuum SEM in the life sciences as well.

9 List of abbreviations

AE	Auger electron
BSE	Backscatter electron
CBS detector	Circular/directional backscatter electron detector
CL (detector)	Cathodoluminescence (detector)
CLEM	Correlative light-electron microscopy
CLSM	Confocal laser scanning microscopy
CPD	Critical point drying
cryo-SEM	Cryogenic scanning electron microscopy
DNA	Deoxyribonucleic acid
ECM	Extracellular matrix
EDX (detector)	Energy-dispersive X-ray (detector)
EELS	Electron energy loss spectroscopy
EM	Electron microscopy
EPS	Extracellular polymeric substances
ESEM	Environmental scanning electron microscopy
ET detector	Everhart Thornley detector
FIB-SEM	Focused ion beam scanning electron microscopy
FS	Freeze substitution
GA	Glutaraldehyde
HMDS	Hexamethyldisilazane
HPF	High-pressure freezing
IR (radiation)	Infrared (radiation)
LVSEM	Low voltage scanning electron microscopy
PBS	Phosphate-buffered saline
PCL	Polycaprolactone
PHA	Polyhydroxyalkanoates
PHB	Polyhydroxybutyrate
PVP	Polyvinylpyrrolidon
SBF-SEM	Serial block-face scanning electron microscopy
SE	Secondary electron
SEM	Scanning electron microscopy
STEM	Scanning transmission electron microscopy
TEM	Transmission electron microscopy
UV (radiation)	Ultraviolet (radiation)

10 List of figures and tables

10.2 List of tables

11 References

[1]   BOZZOLA, J. J. AND L. D. RUSSELL. *Electron Microscopy: Principles and Techniques for Biologists*. Jones and Bartlett, 1999. ISBN 9780763701925.

[2]   HAWKES, P. W. Complementary Accounts of the History of Electron-Microscopy. *Advances in Electronics and Electron Physics*, 1985, Suppl. 16, 589-618.

[3]   ECHLIN, P. The development of biological scanning electron microscopy and X-ray microanalysis. *Advances in Imaging and Electron Physics*, 2004, 133, 469-484.

[4]   AMELINCKX, S. *Electron microscopy: principles and fundamentals*. VCH, 1997. ISBN 9783527294794.

[5]   GOLDSTEIN, J., D. E. NEWBURY, D. C. JOY, C. E. LYMAN, et al. *Scanning Electron Microscopy and X-Ray Microanalysis*. Springer US, 2003. ISBN 978-0-306-47292-3.

[6]   HALLIDAY, D., R. RESNICK AND J. WALKER. *Fundamentals of Physics, Part 4, Chapters 34 - 38, Enhanced Problems Version*. Wiley, 2003. ISBN 9780471228561.

[7]   HAYAT, M. A. *Principles and techniques of scanning electron microscopy: biological applications*. Van Nostrand Reinhold Co., 1976. ISBN 9780442256920.

[8]   BUSCH, H. Calculation of the channel of the cathode rays in axial symmetric electromagnetic fields. *Annalen Der Physik*, 1926, 81(25), 974-993.

[9]   KNOLL, M. AND E. RUSKA. The Electron Microscope. *Zeitschrift Fur Physik*, 1932, 78(5-6), 318-339.

[10]   BOZZOLA, J. J., M. C. JOHNSON AND I. L. SHECHMEI. In-Situ Multiple Sampling of Attached Bacteria for Scanning and Transmission Electron-Microscopy. *Stain Technology*, 1973, 48(6), 317-325.

[11]   EGERTON, R. F. *Physical Principles of Electron Microscopy: An Introduction to TEM, SEM, and AEM*. Springer US, 2006. ISBN 9780387260167.

[12]   REIMER, L. Scanning electron microscopy: physics of image formation and microanalysis. *Measurement Science and Technology*, 2000, 11(12), 1826.

[13]   PAWLEY, J. AND H. SCHATTEN. *Biological Low-Voltage Scanning Electron Microscopy*. Springer New York, 2007. ISBN 9780387729725.

[14]   KUO, J. *Electron microscopy: Methods and protocols*. Springer Science & Business Media, 2007. ISBN 1597452947.

[15]   WALTHER, P. AND M. MÜLLER. Biological ultrastructure as revealed by high resolution cryo-SEM of block faces after cryo-sectioning. *Journal of Microscopy*, 1999, 196, 279-287.

[16]   REIMER, L. *Transmission electron microscopy: physics of image formation and microanalysis*. Springer, 2013. ISBN 3662135531.

[17] ECHLIN, P. *Handbook of Sample Preparation for Scanning Electron Microscopy and X-Ray Microanalysis.* Springer US, 2011. ISBN 9780387857312.

[18] CHAFFEY, N. Hayat MA. 2000. Principles and techniques of electron microscopy: biological applications. 4th edn. 543pp. Cambridge. *Annals of Botany* [online]. 87(4), 546-548 [cit. 2019-05-30]. DOI: 10.1006/anbo.2001.1367. ISSN 03057364. Available: http://academic.oup.com/aob/article-lookup/doi/10.1006/anbo.2001.1367

[19] TAKAHASHI, C., G. KALITA, N. OGAWA, K. MORIGUCHI, et al. Electron microscopy of *Staphylococcus epidermidis* fibril and biofilm formation using image-enhancing ionic liquid. *Analytical and Bioanalytical Chemistry*, 2015, 407(6), 1607-1613.

[20] OI, T., S. ENOMOTO, T. NAKAO, S. ARAI, et al. Three-dimensional intracellular structure of a whole rice mesophyll cell observed with FIB-SEM. *Annals of Botany*, 2017, 120(1), 21-28.

[21] HRUBANOVA, K., V. KRZYZANEK, J. NEBESAROVA, F. RUZICKA, et al. Monitoring *Candida parapsilosis* and *Staphylococcus epidermidis* Biofilms by a Combination of Scanning Electron Microscopy and Raman Spectroscopy. *Sensors*, 2018, 18(12), 4089.

[22] WU, Y., J. LIANG, K. RENSING, T. M. CHOU, et al. Extracellular Matrix Reorganization during Cryo Preparation for Scanning Electron Microscope Imaging of *Staphylococcus aureus* Biofilms. *Microscopy and Microanalysis*, 2014, 20(5), 1348-1355.

[23] Figure 12. These schematic illustrations compare the components of transmission electron microscopes and scanning electron microscopes. Courses.lumenlearning [online]. Rice University, Houston, USA: OpenStax CNX, 2019 [cit. 2019-05-01]. Available: https://courses.lumenlearning.com/suny-microbiology/chapter/instruments-of-microscopy/.

[24] WALTHER, P. High-Resolution Cryoscanning Electron Microscopy of Biological Samples. In H. SCHATTEN AND J.B. PAWLEY eds. *Biological Low-Voltage Scanning Electron Microscopy.* New York, NY: Springer New York, 2008, p. 245-261.

[25] JOY, D. C. AND J. I. GOLDSTEIN. Scanning Electron-Microscopy. *Journal of Metals*, 1988, 40(7), A10-A10.

[26] WITTKE, J. H. Condenser Lens. Schematic of a condenser lens, showing upper spray aperture and lower limiting aperture. 2.nau [online]. Arizona, USA: The NAU Electron Microanalysis Core Facility, 2015 [cit. 2019-05-30]. Available: https://www2.nau.edu/micro-analysis/wordpress/index.php/instrumentation/.

[27] FEI COMPANY. Magellan 400, Magellan 400L: User Operation Manual. 1. Hillsboro, OR 97124, 2011, 178 s.

[28] NICO, C. Illustration of the phenomena that occur from the interaction of highly energetic electrons with matter, also depicting the pear shape interaction volume which is typically observed in this type of interactions. Commons.wikimedia [online]. Wikimedia, 2013, 17 December 2013, 24 August 2017 [cit. 2019-05-07]. Available: https://commons.wikimedia.org/wiki/File:Electron_Interaction_with_Matter.svg.

[29] MULLEROVA, I., M. LENC AND M. FLORIAN. Collection of Backscattered Electrons with a Single Polepiece Lens and a Multiple Detector. *Scanning Microscopy*, 1989, 3(2), 419-428.

[30] MULLEROVA, I. AND L. FRANK. Scanning low-energy electron microscopy. *Advances in Imaging and Electron Physics*, 2003, 128, 309-443.

[31] MCMULLAN, D., J. THEWLIS, A. W. AGAR, D. GABOR, et al. An Improved Scanning Electron Microscope for Opaque Specimens. *Proceedings of the Institution of Electrical Engineers-London*, 1953, 100(75), 245-259.

[32] WELLS, O. C. Xy Table and Tilting Stage for Scanning Electron-Microscope (Sem). *Review of Scientific Instruments*, 1975, 46(1), 77-79.

[33] EVERHART, T. E. AND R. F. M. THORNLEY. Wide-Band Detector for Micro-Microampere Low-Energy Electron Currents. *Journal of Scientific Instruments*, 1960, 37(7), 246-248.

[34] MACDONALD, N. C. AND J. R. WALDROP. Auger Electron Spectroscopy in Scanning Electron Microscope - Auger Electron Images. *Applied Physics Letters*, 1971, 19(9), 315.

[35] BALL, M. D. AND D. G. MCCARTNEY. The Measurement of Atomic-Number and Composition in an Sem Using Backscattered Detectors. *Journal of Microscopy-Oxford*, 1981, 124(Oct), 57-68.

[36] STATHAM, P. J. Pitfalls and Advances in Quantitative Elemental Mapping. *Scanning*, 1988, 10(6), 245-252.

[37] JAKUBOWICZ, A. Theory of Electron-Beam Induced Current and Cathodoluminescence Contrasts from Structural Defects of Semiconductor Crystals - Steady-State and Time-Resolved Problems. *Scanning Microscopy*, 1987, 1(2), 515-533.

[38] JOY, D. C. Resolution in Low-Voltage Scanning Electron-Microscopy. *Journal of Microscopy-Oxford*, 1985, 140, 283-292.

[39] GLAESER, R. M. Limitations to Significant Information in Biological Electron Microscopy as a Result of Radiation Damage. *Journal of Ultrastructure Research*, 1971, 36(3-4), 466.

[40] DEMERS, H., N. POIRIER-DEMERS, A. R. COUTURE, D. JOLY, et al. Three-Dimensional Electron Microscopy Simulation with the CASINO Monte Carlo Software. *Scanning*, 2011, 33(3), 135-146.

[41] DANILATOS, G. D. Foundations of Environmental Scanning Electron-Microscopy. *Advances in Electronics and Electron Physics*, 1988, 71, 109-250.

[42] ISABELL, T. C., P. E. FISCHIONE, C. O'KEEFE, M. U. GURUZ, et al. Plasma cleaning and its applications for electron microscopy. *Microscopy and Microanalysis*, 1999, 5(2), 126-135.

[43] RUZICKA, F., V. HOLA, M. VOTAVA AND R. TEJKALOVA. Importance of biofilm in *Candida parapsilosis* and evaluation of its susceptibility to antifungal agents by colorimetric method. *Folia Microbiol*, 2007, 52(3), 209-214.

[44] NEBESAROVA, J. Elektronová mikroskopie pro biology. Paru.cas [online]. České Budějovice, Czech Republic: Biology Centre CAS, 2001, 13.1.2002 [cit. 2019-05-30]. Available: http://triton.paru.cas.cz/old-lem/book/.

[45] UMRATH, W. Calculation of the Freeze-Drying Time for Electron-Microscopical Preparations. *Mikroskopie*, 1983, 40(1-2), 9-34.

[46] HAWSER, S. P. AND L. J. DOUGLAS. Biofilm Formation by *Candida Species* on the Surface of Catheter Materials in-Vitro. *Infection and Immunity*, 1994, 62(3), 915-921.

[47] HUBALEK, Z. Protectants used in the cryopreservation of microorganisms. *Cryobiology*, 2003, 46(3), 205-229.

[48] HAWKINS, D. M., E. A. ELLIS, D. STEVENSON, A. HOLZENBURG, et al. Novel critical point drying (CPD) based preparation and transmission electron microscopy (TEM) imaging of protein specific molecularly imprinted polymers (HydroMIPs). *Journal of Materials Science*, 2007, 42(22), 9465-9468.

[49] Physical Properties: Carbon dioxide. Encyclopedia.airliquide [online]. Paris, France: L'AIR LIQUIDE S.A., 2019 [cit. 2019-05-30]. Available: https://encyclopedia.airliquide.com/carbon-dioxide.

[50] HAZRIN-CHONG, N. H. AND M. MANEFIELD. An alternative SEM drying method using hexamethyldisilazane (HMDS) for microbial cell attachment studies on sub-bituminous coal. *Journal of Microbiological Methods*, 2012, 90(2), 96-99.

[51] BRAY, D. F., J. BAGU AND P. KOEGLER. Comparison of Hexamethyldisilazane (Hmds), Peldri-Ii, and Critical-Point Drying Methods for Scanning Electron-Microscopy of Biological Specimens. *Microscopy Research and Technique*, 15 1993, 26(6), 489-495.

[52] KNOLL, M. Controlling effect of a loaded particle in the field of a secondary emission cathode. *Naturwissenschaften*, 1941, 29, 335-336.

[53] ECHLIN, P. Scanning Electron Microscopy and Analysis of Moist, Wet and Liquid Specimens. *Microscopy and Microanalysis*, 2009, 15, 1116-1117.

[54] FISCHER, E. R., B. T. HANSEN, V. NAIR, F. H. HOYT, et al. Scanning electron microscopy. *Curr Protoc Microbiol*, 2012, Chapter 2, Unit 2B.2. DOI: 10.1002/9780471729259.mc02b02s25

[55] ZHANG, B. Z., R. WEPF, K. FISCHER, M. SCHMIDT, et al. The Largest Synthetic Structure with Molecular Precision: Towards a Molecular Object. *Angewandte Chemie-International Edition*, 2011, 50(3), 737-740.

[56] MCDONALD, K. L. A review of high-pressure freezing preparation techniques for correlative light and electron microscopy of the same cells and tissues. *Journal of Microscopy-Oxford*, 2009, 235(3), 273-281.

[57] NEUGEBAUER, D. C. AND H. P. ZINGSHEIM. Apparent Holes in Rotary Shadowed Proteins - Dependence on Angle of Shadowing and Replica Thickness. *Journal of Microscopy-Oxford*, 1979, 117(Nov), 313-315.

[58] ISA, L., F. LUCAS, R. WEPF AND E. REIMHULT. Measuring single-nanoparticle wetting properties by freeze-fracture shadow-casting cryo-scanning electron microscopy. *Nature Communications*, 2011, 2, 438.

[59] ECHLIN, P. Low-Temperature Scanning Electron-Microscopy - Review. *Journal of Microscopy*, 1978, 112, 47-61.

[60] SRIAMORNSAK, P., N. THIRAWONG, K. CHEEWATANAKORNKOOL, K. BURAPAPADH, et al. Cryo-scanning electron microscopy (cryo-SEM) as a tool for studying the ultrastructure during bead formation by ionotropic gelation of calcium pectinate. *International Journal of Pharmaceutics*, 2008, 352(1), 115-122.

[61] ECHLIN, P. Scanning Electron-Microscopy and X-Ray Microanalysis at Low-Temperatures. *Journal of Cell Biology*, 1972, 55(2), A66.

[62] ECHLIN, P. Application of Scanning Electron Microscopy to Biological Research. *Philosophical Transactions of the Royal Society of London Series B-Biological Sciences*, 1971, 261(837), 51.

[63] READ, N. D. AND C. E. JEFFREE. Low-temperature scanning electron microscopy in biology. *Journal of Microscopy*, 1991, 161(1), 59-72.

[64] ECHLIN, P. *Low-Temperature Microscopy and Analysis*. Springer, 1992. ISBN 9780306439841.

[65] FRANKS, F. Bound Water - Fact and Fiction. *Cryo-Letters*, 1983, 4(2), 73-74.

[66] FRANKS, F. Water Activity - Towards a More Realistic Description of Resistance and Survival. *Cryobiology*, 1983, 20(6), 700-701.

[67] EISENBERG, D. AND W. KAUZMANN. *The Structure and Properties of Water*. OUP Oxford, 2005. ISBN 9780198570264.

[68] Physical Properties: Water. Encyclopedia.airliquide [online]. Paris, France: L'AIR LIQUIDE S.A., 2019 [cit. 2019-05-30]. Available: https://encyclopedia.airliquide.com/water.

[69] CHAPLIN, M. Water Phase Diagram. Lsbu.ac [online]. 03 Borough Road, London, Great Britain: London South Bank University, 2000, 12 May 2019 [cit. 2019-05-30]. Available: http://www1.lsbu.ac.uk/water/water_phase_diagram.html.

[70] KOHL, I., E. MAYER AND A. HALLBRUCKER. Ice XII forms on compression of hexagonal ice at 77 K via high-density amorphous water. *Physical Chemistry Chemical Physics*, 2001, 3(4), 602-605.

[71] HOBBS, P. V., S. CHANG AND J. D. LOCATELLI. Dimensions and Aggregation of Ice Crystals in Natural Clouds. *Journal of Geophysical Research*, 1974, 79(15), 2199-2206.

[72] BRUGGELLER, P. AND E. MAYER. Complete Vitrification in Pure Liquid Water and Dilute Aqueous-Solutions. *Nature*, 1980, 288(5791), 569-571.

[73] JOHARI, G. P., A. HALLBRUCKER AND E. MAYER. The Glass Liquid Transition of Hyperquenched Water. *Nature*, 10 1987, 330(6148), 552-553.

[74] LEPAULT, J., R. FREEMAN AND J. DUBOCHET. Electron-Beam Induced Vitrified Ice. *Journal of Microscopy-Oxford*, 1983, 132(Dec), Rp3-Rp4.

[75] KOUCHI, A. AND T. KURODA. Amorphous Ar Produced by Vapor-Deposition. *Japanese Journal of Applied Physics Part 2-Letters*, 1990, 29(5), L807-L809.

[76] HEMLEY, R. J., L. C. CHEN AND H. K. MAO. New Transformations between Crystalline and Amorphous Ice. *Nature*, 1989, 338(6217), 638-640.

[77] SCEATS, M. G. AND S. RICE. Amorphous Solid Water and Its Relationship to Liquid Water: A Random Network Model for Water. In. *Water and Aqueous Solutions at Subzero Temperatures*, 1982, p. 83-214.

[78] SAKAI, A. AND W. LARCHER. Frost Survival of Plants, Responses and Adaptation to Freezing Stress. In *Ecological Studies*. Springer-Verlag Berlin Heidelberg, 1987.

[79] STUDER, D., M. MICHEL, M. WOHLWEND, E. B. HUNZIKER, et al. Vitrification of Articular-Cartilage by High-Pressure Freezing. *Journal of Microscopy*, 1995, 179, 321-332.

[80] LUYET, B. J., E. AMRHEIN AND C. KROENER. Problems in Study of Nucleation in Cryobiology. *Cryobiology*, 1966, 2(6), 308.

[81] FULLER, B. J. Cryoprotectants: The essential antifreezes to protect life in the frozen state. *Cryoletters*, 2004, 25(6), 375-388.

[82] DAY, J. G. AND G. STACEY. *Cryopreservation and Freeze-Drying Protocols*. Humana Press, 2007. ISBN 9781588293770.

[83] CAVALIER, A., D. SPEHNER AND B. M. HUMBEL. *Handbook of Cryo-Preparation Methods for Electron Microscopy*. Taylor & Francis, 2008. ISBN 9780849372278.

[84] ASHWOOD-SMITH, M. J., C. WARBY, K. W. CONNOR AND G. BECKER. Low-temperature preservation of mammalian cells in tissue culture with polyvinylpyrrolidone (PVP), dextrans, and hydroxyethyl starch (HES). *Cryobiology*, 1972, 9(5), 441-449.

[85] PFEIFFER, S., G. VIELHABER, F. PFLUCKER, R. WEPF, et al. Structural conservation of human skin: A comparison of chemical fixation with cryoimmobilization and different cryopreservation methods. *European Journal of Cell Biology*, 1997, 74, 101-101.

[86] MEISNER, J. AND W. A. HAGINS. Fast Freezing of Thin Tissues by Thermal Conduction into Sapphire Crystals at 77-Degrees-K. *Biophysical Journal*, 1978, 21(3), A149.

[87] GILKEY, J. C. AND L. A. STAEHELIN. Advances in Ultra-Rapid Freezing for the Preservation of Cellular Ultrastructure. *Journal of Electron Microscopy Technique*, 1986, 3(2), 177-210.

[88] BALD, W. B. The Relative Merits of Various Cooling Methods. *Journal of Microscopy*, 1985, 140, 17-40.

[89] SOMLYO, A. V. AND C. FRANZINIARMSTRONG. New Views of Smooth-Muscle Structure Using Freezing, Deep-Etching and Rotary Shadowing. *Experientia*, 1985, 41(7), 841-856.

[90] VON ZGLINICKI, T., M. RIMMLER AND H. J. PURZ. Fast cryofixation technique for X-ray microanalysis. *Journal of microscopy*, 1986, 141, 79-90.

[91] LEUNISSEN, J. AND H. YI. Self-pressurized rapid freezing (SPRF): a novel cryofixation method for specimen preparation in electron microscopy. *Journal of Microscopy*, 2009, 235(1), 25-35.

[92] SHIMONI, E. AND M. MULLER. On optimizing high-pressure freezing: from heat transfer theory to a new microbiopsy device. *Journal of Microscopy*, 1998, 192(Pt 3), 236-247.

[93] DAHL, R. AND L. A. STAEHELIN. High-pressure freezing for the preservation of biological structure: Theory and practice. *Journal of Electron Microscopy Technique*, 1989, 13(3), 165-174.

[94] KUO, J. Processing Plant Tissues for Ultrastructural Study. *Electron Microscopy: Methods and Protocols*, 2014, 1117, 39-55.

[95] KANNO, H., R. J. SPEEDY AND C. A. ANGELL. Supercooling of Water to -92°C under Pressure. *Science*, 1975, 189(4206), 880-881.

[96] RIEHLE, U. Rapid Cooling of Thin Slices of Organic Preparations for Electron Microscopy - Vitrification of Diluted Aqueous Solutions. *Chemie Ingenieur Technik*, 1968, 40(5), 213.

[97] MOOR, H. Theory and Practice of High Pressure Freezing. In R. STEINBRECHT AND K. ZIEROLD eds. *Cryotechniques in Biological Electron Microscopy*. Springer Berlin Heidelberg, 1987, p. 175-191.

[98] DUBOCHET, J. High-Pressure Freezing for Cryoelectron Microscopy. *Trends in Cell Biology*, 1995, 5(9), 366-368.

[99] ABRA Fluid AG - The Swiss manufacturer of the High Pressure Freezing Machine HPM 010. High-pressure-freezing-machine-hpm-010 [online]. Espenstrasse 135, CH-9443 Widnau: ABRA Fluid, 2016 [cit. 2019-05-20]. Available: http://www.high-pressure-freezing-machine-hpm-010.com/.

[100] MCDONALD, K. High-Pressure Freezing for Preservation of High Resolution Fine Structure and Antigenicity for Immunolabeling. In M.A. NASSER HAJIBAGHERI ed. *Electron Microscopy Methods and Protocols*. Totowa, NJ: Humana Press, 1999, p. 77-97.

[101] KAECH, A. AND U. ZIEGLER. High-Pressure Freezing: Current State and Future Prospects. *Electron Microscopy: Methods and Protocols*, 2014, 1117, 151-171.

[102] MCDONALD, K. Cryopreparation methods for electron microscopy of selected model systems. *Cellular Electron Microscopy*, 2007, 79, 23-56.

[103] WOHLWEND, M. High Pressure Freezing Machine HPF Compact 03. Wohlwend-hpf [online]. Bifig 14, Sennwald, Switzerland: Engineering Office M. Wohlwend [cit. 2019-05-27]. Available: http://www.wohlwend-hpf.ch/.

[104] VERKADE, P. Moving EM: the Rapid Transfer System as a new tool for correlative light and electron microscopy and high throughput for high-pressure freezing. *Journal of Microscopy*, 2008, 230(2), 317-328.

[105] STUDER, D., W. GRABER, A. AL-AMOUDI AND P. EGGLI. A new approach for cryofixation by high-pressure freezing. *Journal of Microscopy*, 2001, 203, 285-294.

[106] VANHECKE, D., W. GRABER AND D. STUDER. Close-to-native ultrastructural preservation by high pressure freezing. *Methods in Cell Biology*, 2008, 88, 151-164.

[107] HRUBANOVA, K., J. NEBESAROVA, F. RUZICKA AND V. KRZYZANEK. The innovation of cryo-SEM freeze-fracturing methodology demonstrated on high pressure frozen biofilm. *Micron*, 2018, 110, 28-35.

[108] EM Sample Preparation. Leica-microsystems [online]. Vienna, Austria: Leica Mikrosysteme, July 2013 [cit. 2019-05-31]. Available: https://www.leica-microsystems.com/fileadmin/academy/2013/WF_HighPressureFreezing_07_13.pdf.

[109] ZHAO, S. T., D. STUDER, X. J. CHAI, W. GRABER, et al. Structural plasticity of hippocampal mossy fiber synapses as revealed by high-pressure freezing. *Journal of Comparative Neurology*, 2012, 520(11), 2340-2351.

[110] BRAUN, A., P. C. STENGER, H. E. WARRINER, J. A. ZASADZINSKI, et al. A freeze-fracture transmission electron microscopy and small angle X-ray diffraction study of the effects of albumin, serum, and polymers on clinical lung surfactant microstructure. *Biophysical Journal*, 2007, 93(1), 123-139.

[111] BIEL, S. S., K. KAWASCHINSKI, K. P. WITTERN, U. HINTZE, et al. From tissue to cellular ultrastructure: closing the gap between micro- and nanostructural imaging. *Journal of Microscopy-Oxford*, 2003, 212, 91-99.

[112] ZASADZINSKI, J. A. N. AND S. M. BAILEY. Applications of Freeze-Fracture Replication to Problems in Materials and Colloid Science. *Journal of Electron Microscopy Technique*, 1989, 13(4), 309-334.

[113] Leica EM ACE: Coater Family. Leica-microsystems [online]. Vienna, Austria: Leica Mikrosysteme, 2017, 2017 [cit. 2019-05-30]. Available: https://www.leica-microsystems.com/fileadmin/downloads/Leica%20EM%20ACE600/Brochures/EMACECoaters_Brochure_09_17_EN.pdf.

[114] Alto 2500. Operators Handbook. In. Oxon, UK: Gatan UK, 2005, p. 35.

[115] BOREYKO, J. B., R. R. HANSEN, K. R. MURPHY, S. NATH, et al. Controlling condensation and frost growth with chemical micropatterns. *Scientific Reports*, 2016, 6(1), 19131.

[116] MULLER, J. H., U. D. SCHWARZ, R. WEPF AND R. WIESENDANGER. A cryogenic scanning force microscope for the characterization of frozen biological samples. *Applied Physics a-Materials Science & Processing*, 2003, 76(6), 893-898.

[117] MACKENZIE, A. P., W. DERBYSHIRE AND D. S. REID. Nonequilibrium Freezing Behavior of Aqueous Systems. *Philosophical Transactions of the Royal Society of London Series B-Biological Sciences*, 1977, 278(959), 167.

[118] NERMUT, M. V. Negative Staining in Freeze-Drying and Freeze-Fracturing. *Micron*, 1977, 8(4), 211-212.

[119] LEE, D. L., K. A. WRIGHT AND R. R. SHIVERS. A Freeze-Fracture Study of the Body Wall of *Trichinella Spiralis*. *Parasitology*, 1984, 89(Oct), R42.

[120] KRZYZANEK, V., N. SPORENBERG, U. KELLER, J. GUDDORF, et al. Polyelectrolyte multilayer capsules: nanostructure and visualisation of nanopores in the wall. *Soft Matter*, 2011, 7(15), 7034-7041.

[121] SEVERS, N. J. Freeze-fracture electron microscopy. *Nature Protocols*, 2007, 2(3), 547-576.

[122] MOOR, H. AND K. MUHLETHALER. Fine Structure in Frozen-Etched Yeast Cells. *Journal of Cell Biology*, 1963, 17(3), 609.

[123] GLAESER, R. M. AND R. J. HALL. Reaching the information limit in cryo-EM of biological macromolecules: experimental aspects. *Biophysical Journal*, 2011, 100(10), 2331-2337.

[124] DUBOCHET, J., M. ADRIAN, J. J. CHANG, J. C. HOMO, et al. Cryo-Electron Microscopy of Vitrified Specimens. *Quarterly Reviews of Biophysics*, 1988, 21(2), 129-228.

[125] The Nobel Prize in Chemistry 2017. NobelPrize [online]. Nobel Media AB, 2019, 5 June 2019 [cit. 2019-06-06]. Available: https://www.nobelprize.org/prizes/chemistry/2017/summary/.

[126] WALTHER, P. Cryo-fracturing and cryo-planing for in-lens cryo-SEM, using a newly designed diamond knife. *Microscopy and Microanalysis*, 2003, 9(4), 279-285.

[127] BASTACKY, J., C. GOODMAN AND T. L. HAYES. A Specimen Holder for Low-Temperature Scanning Electron-Microscopy. *Journal of Electron Microscopy Technique*, 1990, 14(1), 83-84.

[128] BASTACKY, J., C. LEE, T. FREEMAN, G. WEBER, et al. A Specimen Holder for High-Resolution Low-Temperature Scanning Electron-Microscopy. *Microscopy Research and Technique*, 1995, 32(5), 457-458.

[129] WALTHER, P. Recent progress in freeze-fracturing of high-pressure frozen samples. *Journal of Microscopy*, 2003, 212, 34-43.

[130] TANIFUJI, G., U. CENCI, D. MOOG, S. DEAN, et al. Genome sequencing reveals metabolic and cellular interdependence in an amoeba-kinetoplastid symbiosis. *Scientific Reports*, 2017, 7, 11688.

[131] DONELLI, G. *Microbial biofilms: methods and protocols*. Edtion ed. New York: Humana Press ; Springer, 2014, 380. ISBN 9781493904662, 1493904663 (hbk alk. paper), 1064-3745.

[132] PAIVA, L. C. F., P. G. VIDIGAL, L. DONATTI, T. I. E. SVIDZINSKI, et al. Assessment of in vitro biofilm formation by *Candida species* isolates from vulvovaginal candidiasis and ultrastructural characteristics. *Micron*, 2012, 43(2), 497-502.

[133] PAIVA, L. C. F., L. DONATTI, E. V. PATUSSI, T. I. E. SVIZDINSKI, et al. Scanning Electron and Confocal Scanning Laser Microscopy Imaging of the Ultrastructure and Viability of Vaginal Candida albicans and Non-Albicans Species Adhered to an Intrauterine Contraceptive Device. *Microscopy and Microanalysis*, 2010, 16(5), 537-549.

[134] COSTERTON, J. W., P. S. STEWART AND E. P. GREENBERG. Bacterial biofilms: A common cause of persistent infections. *Science*, 1999, 284(5418), 1318-1322.

[135] DONLAN, R. M. AND J. W. COSTERTON. Biofilms: Survival mechanisms of clinically relevant microorganisms. *Clinical Microbiology Reviews*, 2002, 15(2).

[136] DELEO, F. AND M. W. OTTO. *Bacterial pathogenesis: methods and protocols*. Edtion ed. Totowa, N.J.: Humana Press, 2008. ISBN 9781588297402, 1588297403 (hbk.), 9781603270328 (ebook).

[137] WU, W. Z., L. H. YANG AND J. L. WANG. Denitrification using PBS as carbon source and biofilm support in a packed-bed bioreactor. *Environmental Science and Pollution Research*, 2013, 20(1), 333-339.

[138] DONLAN, R. M. Biofilms: Microbial life on surfaces. *Emerging Infectious Diseases*, 2002, 8(9), 881-890.

[139] HOLA, V., F. RUZICKA, R. TEJKALOVA AND M. VOTAVA. Biofilm formation in nosocomial pathogens of respiratory tract. *International Journal of Antimicrobial Agents*, 2007, 29, S142.

[140] MARSH, P. D. Plaque as a biofilm: pharmacological principles of drug delivery and action in the sub- and supragingival environment. *Oral Diseases*, 2003, 9, 16-22.

[141] FRANCOLINI, I. AND G. DONELLI. Prevention and control of biofilm-based medical-device-related infections. *FEMS Immunology and Medical Microbiology*, 2010, 59(3), 227-238.

[142] BARGHI, A., R. SADATI AND R. A. LARKI. Biological Wastewater Treatment through Biofilm. *Iranian Journal of Public Health*, 2016, 45, 101-101.

[143] VOBĚRKOVÁ, S., S. HERMANOVÁ, K. HRUBANOVÁ AND V. KRZYŽÁNEK. Biofilm formation and extracellular polymeric substances (EPS) production by Bacillus subtilis depending on nutritional conditions in the presence of polyester film. *Folia Microbiol*, 2015, 61(20), 1-10.

[144] CRESSON, R., P. DABERT AND N. BERNET. Microbiology and performance of a methanogenic biofilm reactor during the start-up period. *Journal of Applied Microbiology*, 2009, 106(3), 863-876.

[145] BAO, J., N. LIU, L. ZHU, Q. XU, et al. Programming a Biofilm-Mediated Multienzyme-Assembly-Cascade System for the Biocatalytic Production of Glucosamine from Chitin. *J Agric Food Chem*, 2018, 66(30), 8061-8068.

[146] DE LA FUENTE-NUNEZ, C., M. H. CARDOSO, E. DE SOUZA CANDIDO, O. L. FRANCO, et al. Synthetic antibiofilm peptides. *Biochim Biophys Acta*, 2016, 1858(5), 1061-1069.

[147] HUQ, A., C. A. WHITEHOUSE, C. J. GRIM, M. ALAM, et al. Biofilms in water, its role and impact in human disease transmission. *Current Opinion in Biotechnology*, 2008, 19(3), 244-247.

[148] SUTHERLAND, I. W. Biofilm exopolysaccharides: a strong and sticky framework. *Microbiology-Uk*, 2001, 147, 3-9.

[149] BRANDA, S. S., A. VIK, L. FRIEDMAN AND R. KOLTER. Biofilms: the matrix revisited. *Trends in Microbiology*, 2005, 13(1), 20-26.

[150] ADAM, B., G. S. BAILLIE AND L. J. DOUGLAS. Mixed species biofilms of *Candida albicans* and *Staphylococcus epidermidis*. *Journal of Medical Microbiology*, 2002, 51(4), 344-349.

[151] LIU, H. Y., Y. F. ZHAO, D. ZHAO, T. GONG, et al. Antibacterial and anti-biofilm activities of thiazolidione derivatives against clinical staphylococcus strains. *Emerging Microbes & Infections*, 2015, 4(1), 1-6.

[152] RUZICKA, F., M. HORKA, V. HOLA, A. KUBESOVA, et al. The differences in the isoelectric points of biofilm-positive and biofilm-negative *Candida parapsilosis* strains. *Journal of Microbiological Methods*, 2010, 80(3), 299-301.

[153] BANDARA, H. M. H. N., O. L. T. LAM, R. M. WATT, L. J. JIN, et al. Bacterial lipopolysaccharides variably modulate in vitro biofilm formation of *Candida species*. *Journal of Medical Microbiology*, 2010, 59(10), 1225-1234.

[154] LATTIF, A. A., P. K. MUKHERJEE, J. CHANDRA, K. SWINDELL, et al. Characterization of biofilms formed by *Candida parapsilosis*, *C. metapsilosis*, and *C. orthopsilosis*. *International Journal of Medical Microbiology*, 2010, 300(4), 265-270.

[155] KEARNS, D. B., F. CHU, S. S. BRANDA, R. KOLTER, et al. A master regulator for biofilm formation by *Bacillus subtilis*. *Molecular Microbiology*, 2005, 55(3), 739-749.

[156] ZAFRA, O., M. LAMPRECHT-GRANDIO, C. G. DE FIGUERAS AND J. E. GONZALEZ-PASTOR. Extracellular DNA Release by Undomesticated *Bacillus subtilis* Is Regulated by Early Competence. *Plos One*, 2012, 7(11), e48716.

[157] FLEMMING, H. C., T. R. NEU AND D. J. WOZNIAK. The EPS matrix: The "House of Biofilm cells". *Journal of Bacteriology*, 2007, 189(22), 7945-7947.

[158] FLEMMING, H.-C., J. WINGENDER AND U. SZEWZYK. *Biofilm highlights*. Edtion ed. Heidelberg ; New York: Springer, 2011, 243. ISBN 9783642199394.

[159] ALLAN, V. J. M., M. E. CALLOW, L. E. MACASKIE AND M. PATERSON-BEEDLE. Effect of nutrient limitation on biofilm formation and phosphatase activity of a *Citrobacter sp. Microbiology-Sgm*, 2002, 148, 277-288.

[160] RINAUDI, L., N. A. FUJISHIGE, A. M. HIRSCH, E. BANCHIO, et al. Effects of nutritional and environmental conditions on *Sinorhizobium meliloti* biofilm formation. *Research in Microbiology*, 2006, 157(9), 867-875.

[161] SIVAN, A. New perspectives in plastic biodegradation. *Current Opinion in Biotechnology*, 2011, 22(3), 422-426.

[162] LEFEVRE, C., A. TIDJANI, C. VANDER WAUVEN AND C. DAVID. The interaction mechanism between microorganisms and substrate in the biodegradation of polycaprolactone. *Journal of Applied Polymer Science*, 2002, 83(6), 1334-1340.

[163] PANOFF, J. M., B. THAMMAVONGS, M. GUEGUEN AND P. BOUTIBONNES. Cold stress responses in mesophilic bacteria. *Cryobiology*, 1998, 36(2), 75-83.

[164] MORI, S., J. CHOI, R. V. DEVIREDDY AND J. C. BISCHOF. Calorimetric measurement of water transport and intracellular ice formation during freezing in cell suspensions. *Cryobiology*, 2012, 65(3), 242-255.

[165] AYUB, N. D., P. M. TRIBELLI AND N. I. LOPEZ. Polyhydroxyalkanoates are essential for maintenance of redox state in the Antarctic bacterium *Pseudomonas* sp 14-3 during low temperature adaptation. Extremophiles, 2009, 13(1), 59-66.

[166] RAIGER-IUSTMAN, L. J. AND J. A. RUIZ. The alternative sigma factor, sigma(S), affects polyhydroxyalkanoate metabolism in *Pseudomonas putida. FEMS Microbiology Letters*, 2008, 284(2), 218-224.

[167] PAVEZ, P., J. L. CASTILLO, C. GONZALEZ AND M. MARTINEZ. Poly-beta-Hydroxyalkanoate Exert a Protective Effect Against Carbon Starvation and Frozen Conditions in *Sphingopyxis chilensis. Current Microbiology*, 2009, 59(6), 636-640.

[168] OBRUCA, S., P. SEDLACEK, V. KRZYZANEK, F. MRAVEC, et al. Accumulation of Poly(3-hydroxybutyrate) Helps Bacterial Cells to Survive Freezing. *Plos One*, 2016, 11(6), e0157778.

[169] DOHNALKOVA, A. C., M. J. MARSHALL, B. W. AREY, K. H. WILLIAMS, et al. Imaging hydrated microbial extracellular polymers: Comparative analysis by electron microscopy. *Applied and Environmental Microbiology*, 2011, 77(4), 1254-1262.

[170] SCHAUDINN, C., P. STOODLEY, L. HALL-STOODLEY, A. GORUR, et al. Death and Transfiguration in Static *Staphylococcus epidermidis Cultures. Plos One*, 2014, 9(6), e100002.

[171] LAWRENCE, J. R., G. D. W. SWERHONE, G. G. LEPPARD, T. ARAKI, et al. Scanning transmission X-ray, laser scanning, and transmission electron microscopy mapping of the exopolymeric matrix of microbial biofilms. *Applied and Environmental Microbiology*, 2003, 69(9), 5543-5554.

[172] ALHEDE, M., K. QVORTRUP, R. LIEBRECHTS, N. HOIBY, et al. Combination of microscopic techniques reveals a comprehensive visual impression of biofilm structure and composition. *FEMS Immunology and Medical Microbiology*, 2012, 65(2), 335-342.

[173] KARCZ, J., T. BERNAS, A. NOWAK, E. TALIK, et al. Application of lyophilization to prepare the nitrifying bacterial biofilm for imaging with scanning electron microscopy. *Scanning*, 2012, 34(1), 26-36.

[174] BIEL, S. S., K. WILKE, K. DUNCKELMANN, K. P. WITTERN, et al. Light and electron microscopy: Histochemistry on the identical biopsy after high-pressure freezing. *Journal of Histochemistry & Cytochemistry*, 2004, 52, S62-S62.

[175] MONTESINOS, E., I. ESTEVE AND R. GUERRERO. Comparison between Direct Methods for Determination of Microbial Cell-Volume - Electron-Microscopy and Electronic Particle Sizing. *Applied and Environmental Microbiology*, 1983, 45(5), 1651-1658.

[176] WEBSTER, P., S. WU, S. WEBSTER, K. RICH, et al. Ultrastructural preservation of biofilms formed by non-typeable Hemophilus influenzae. *Biofilms*, 2004, 1(03), 165-182.

[177] GRAHAM, L. L. AND T. J. BEVERIDGE. Effect of Chemical Fixatives on Accurate Preservation of *Escherichia Coli* and *Bacillus Subtilis* Structure in Cells Prepared by Freeze-Substitution. *Journal of Bacteriology*, 1990, 172(4), 2150-2159.

[178] HAYAT, M. A. *Principles and techniques of scanning electron microscopy. Biological applications. Volume 1*. Van Nostrand Reinhold Company, 1974. ISBN 0442256779.

[179] FASSEL, T. A. AND C. E. EDMISTON. Bacterial biofilms: Strategies for preparing glycocalyx for electron microscopy. *Methods in enzymology*, 1999, 310, 194-203.

[180] REESE, S. AND B. GUGGENHEIM. A novel TEM contrasting technique for extracellular polysaccharides in in vitro biofilrns. *Microscopy Research and Technique*, 2007, 70(9), 816-822.

[181] GALWAY, M. E., J. W. HECKMAN JR, G. J. HYDE AND L. C. FOWKE. Advances in High-Pressure and Plunge-Freeze Fixation. *Methods in Cell Biology*, 1995, 49, 3-19.

[182] WANG, A. B., C. H. LIN AND C. C. CHEN. The critical temperature of dry impact for tiny droplet impinging on a heated surface. *Physics of Fluids*, 2000, 12(6), 1622-1625.

[183] WU, Y., J. R. LIU, J. JIANG, J. HU, et al. Role of the two-component regulatory system arlRS in ica operon and aap positive but non-biofilm-forming *Staphylococcus epidermidis* isolates from hospitalized patients. *Microbial Pathogenesis*, 2014, 76, 89-98.

[184] STUDER, D., M. MICHEL AND M. MULLER. High pressure freezing comes of age. *Scanning Microsc Suppl*, 1989, 3, 253-268.

[185] ADÁMKOVÁ, K. *Structure investigation of hydrogels using a cryo-SEM*. Brno, 2018. Master thesis. Masaryk University. Supervisor Vladislav Krzyžánek.

12 Annexes

Hrubanová, K., Nebesářová, J., Růžička, F., Krzyžánek, V. The innovation of cryo-SEM freeze-fracturing methodology demonstrated on high pressure frozen biofilm. *Micron.* 2018, 110(JUL), 28-35. ISSN 0968-4328
doi: 10.1016/j.micron.2018.04.006

The innovation of cryo-SEM freeze-fracturing methodology demonstrated on high pressure frozen biofilm

Kamila Hrubanova[a], Jana Nebesarova[b,c], Filip Ruzicka[d], Vladislav Krzyzanek[a,*]

[a] Institute of Scientific Instruments of the Czech Academy of Sciences, Brno, Czech Republic
[b] Institute of Parasitology, Biology Centre of the Czech Academy of Sciences, Ceske Budejovice, Czech Republic
[c] Faculty of Science, University of South Bohemia, Ceske Budejovice, Czech Republic
[d] Department of Microbiology, Faculty of Medicine, Masaryk University and St. Anne's Faculty Hospital, Brno, Czech Republic

ARTICLE INFO

ABSTRACT

In this study we present an innovative method for the preparation of fully hydrated samples of microbial biofilms of cultures *Staphylococcus epidermidis*, *Candida parapsilosis* and *Candida albicans*. Cryo-scanning electron microscopy (cryo-SEM) and high-pressure freezing (HPF) rank among cutting edge techniques in the electron microscopy of hydrated samples such as biofilms. However, the combination of these techniques is not always easily applicable. Therefore, we present a method of combining high-pressure freezing using EM PACT2 (Leica Microsystems), which fixes hydrated samples on small sapphire discs, with a high resolution SEM equipped with the widely used cryo-preparation system ALTO 2500 (Gatan). Using a holder developed in house, a freeze-fracturing technique was applied to image and investigate microbial cultures cultivated on the sapphire discs. In our experiments, we focused on the ultrastructure of the extracellular matrix produced during cultivation and the relationships among microbial cells in the biofilm. The main goal of our investigations was the detailed visualization of areas of the biofilm where the microbial cells adhere to the substrate/surface. We show the feasibility of this technique, which is clearly demonstrated in experiments with various freeze-etching times.

1. Introduction

Microscopic organisms, including bacteria and yeasts, were studied in this project. In addition to adopting a planktonic mode of living, microbes are able to adhere to surfaces or interfaces and to form organized communities, so-called biofilms, which are embedded in the matrix of extracellular polymeric substances (EPS) they produce (Donelli, 2014; Paiva et al., 2012); structural investigation of this microscopic formation was the main goal of this study. In medicine, biofilm formation allows microorganisms to colonize the surface of implants, and also protects the microbial cells from attacks by the immune system and from the effects of antibiotics (Deleo and Otto, 2008; Donlan and Costerton, 2002). Therefore, biofilms are considered to be an important virulence factor in these microorganisms. The characteristic features of biofilm infections, especially high resistance to antifungal agents, can complicate a therapy (Donlan and Costerton, 2002). Understanding the biofilm structure can contribute to understanding biofilm formation and the basic biochemical mechanisms underlying this process (Holá et al., 2006). This understanding might aid in the development of more efficient treatment strategies for biofilm infections. Yeasts of the *Candida* genus (e.g., *Candida parapsilosis*, *Candida*

albicans) and bacteria such as staphylococci have recently been recognized as an important cause of severe biofilm infections associated with implanted medical devices (Bandara et al., 2010; Lattif et al., 2010).

Microbial biofilms and the matrix components are typically investigated and imaged by various microscopy techniques (Schaudinn et al., 2014), including confocal laser scanning microscopy (CLSM) and conventional scanning electron microscopy (SEM) (Dohnalkova et al., 2011), transmission electron microscopy (TEM) (Lawrence et al., 2003), and focused ion beam (FIB)-SEM (Alhede et al., 2012), and by special SEM techniques (cryo-SEM and environmental-SEM (ESEM)) that do not require dehydration (Alhede et al., 2012; Dohnalkova et al., 2011; Karcz et al., 2012; Krzyzanek et al., 2011; Schwartz et al., 2009). One limitation of CLSM is its restricted useful magnification. This limitation can be easily overcome by the use of SEM, which has the power to resolve the spatial distribution of individual biofilm-forming bacteria and yeast and their interaction in the biofilm. High magnification images are important for understanding the physiology of biofilms. However, conventional SEM is limited by the requirement of dehydration of the samples during preparation (Alhede et al., 2012). Biofilms are particularly rich in water, and sample preparation might alter

---

Micron 110 (2018) 28–35

their morphology and give rise to artefacts and structural alterations (Donelli, 2014). The conventional sample preparation for SEM, which includes dehydration as a prerequisite for imaging by high-resolution vacuum instruments, can cause substantial changes in the microbial cell ultrastructure. Chemical fixation with aldehydes and treatment with heavy metals help to preserve the cell morphology and enhance contrast. (Montesinos et al., 1983; Webster et al., 2004). Dehydration with organic solvents can extract cell constituents, cause cell membrane discontinuities (Graham and Beveridge, 1990), induce distortion of delicate structures, such as membrane-associated components (Beveridge, 2005), cause substantial shrinkage, and exert other deleterious effects on morphology; the EPS in the biofilm, which contains approximately 95% of water, will look more like fibers than like a thick gelatinous matrix surrounding the cells (Donlan and Costerton, 2002). In the case of cryo-fixation, the biofilm is not dehydrated but is kept frozen to obtain high-resolution images closer to the native state of the sample (Hayat, 1974; Kuo, 2007). It has been demonstrated that cryo-fixed biofilms show a significantly improved preservation of the bacterial ultrastructure and biofilm organization (Webster et al., 2004). To reduce the damage inherent in these treatments, various innovative cryogenic sample preparation methods have been developed (Fassel and Edmiston, 1999; Hayat, 1974; Reese and Guggenheim, 2007). One of the simplest cryo-fixation techniques is plunging the sample (e.g., biofilm) on a substrate into liquid cryogen (Galway et al., 1995). However, plunging the sample into liquid nitrogen or liquid ethane/ propane is sufficient for fixation of only very thin layers where fixation in liquid nitrogen leads to significant lateral macro-segregations of bacteria and EPS, whereas plunging into liquid ethane leads to micro-segregations of EPS and macro-segregation of bacteria (Wu et al., 2014). Substantially more effective freezing with reduced ice crystal formation can be achieved by increasing the pressure during the exposure to liquid cryogen, which can be performed by the high-pressure freezing (HPF) technique (Dahl and Staehelin, 1989; Moor, 1987; Tranfield and Walker, 2013). The application of approximately 2100 bar of pressure to a sample in the course of the freezing process is sufficient to freeze biological material more effectively (Studer et al., 1989). Experimental findings show that HPF allows to freeze samples up to 200 µm thick without visible ice crystal damage. (Shimoni and Müller, 1998; Studer et al., 1989; Studer et al., 1995; Vanhecke et al., 2008; Wu et al., 2014).

The introduction of HPF combined with the freeze-fracturing process brought revolutionary improvements to the EM-based imaging of bacterial cells and associated extracellular material. Applying these methods to biofilms of *C. parapsilosis*, *C. albicans* and *S. epidermidis* show biofilms structures that resemble the native state more closely.

2. Materials and methods

2.1. Cultivation of the biofilm

Two biofilm-positive microbial strains were examined in this study: well-characterized *ica* operon-positive, biofilm and slime producing *S. epidermidis* strain CCM 7221 (Czech Collection of Microorganisms, Brno, Czech Republic) (Ruzicka et al., 2007) and *C. parapsilosis* BC11 from Collection of Microbiology Institute, Masaryk University and St. Anna University Hospital (Brno, Czech Republic) (Ruzicka et al., 2010). The strain *C. albicans* GDH 2346, kindly provided by L. J. Douglas (University of Glasgow, Scotland), was also included (Hawser and Douglas, 1994).

The strains included in this study were stored at −70 °C in Itest cryotubes (ITEST plus, Hradec Králové, Czech Republic). Prior to each experiment, the strains were thawed quickly at 37 °C and cultivated on Mueller-Hinton agar (Oxoid, Basingstoke, United Kingdom) at 37 °C for 24 h. The microbial cultures were re-suspended in sterile physiological saline solution (PSS) to an optical density of 0.5 on the McFarland scale.

During the first experiment, the wells of 24-well polystyrene tissue

culture plates Nunclon (Nunc, Roskilde, Denmark) containing 1 mL of Yeast Nitrogen Base medium Difco (Becton, Dickinson and Co., Franklin Lakes, USA) with 4% glucose (YNBg) and sterile substrate discs were inoculated with 100 µL of a standardized cell suspension. As a substrate, we used sapphire discs with a diameter of 1.4 mm (No. 16706849, Leica Microsystems Inc., Austria) for HPF and a cover glass (No. 1014/1818, Hecht-Assistant, Paris, France) for plunge freezing. After 24 h of incubation at 37 °C, the substrate discs were removed from the wells and further processed.

In the second experiment, a mixed biofilm of *C. albicans* and *S. epidermidis* was prepared. The wells of 24-well polystyrene tissue culture plates Nunclon (Nunc, Roskilde, Denmark) containing 1 mL of brain-heart infusion (BHI) medium (Oxoid, Basingstoke, United Kingdom) with 4% glucose (BHIg) and sterile substrate discs were inoculated with 50 µL of a standardized cell suspension of *S. epidermidis* together with 50 µL of a standardized cell suspension of *C. parapsilosis*. After 24 h of incubation at 37 °C, the substrate discs were removed from the wells and further processed.

2.2. Cryo-fixation of the samples

For the cryo-fixation of the biofilm samples grown on a substrate, two methods were used: standard plunging into nitrogen slush and HPF. In both cases, substrates with the cultivated biofilm were carefully and quickly removed from the inoculated medium with the microbial culture.

2.2.1. Plunging into liquid cryogen
Freezing in nitrogen slush was performed at a slushing station as a part of the cryo-preparation system ALTO 2500 (GATAN Inc., USA). The substrate for the cultivation of biofilm samples was a cover glass with a thickness of 0.17 mm, which was removed from the medium without any rinsing right before the freezing.

2.2.2. High-pressure freezing
The high-pressure freezing was performed with an EM PACT2 HPF instrument (Leica Microsystems Inc., Austria) under standard conditions, according to instructions in the instrument manual (Studer et al., 1989). With the HPF EM PACT2, only sapphire discs with a diameter of 1.4 mm can be frozen, and therefore, these discs were used in the described experiments as a substrate for the biofilm cultivation. As in the case of the plunging fixation, the samples were not rinsed before freezing.

2.3. Freeze-fracturing and freeze-etching

The freeze-fracture technique consists of physically breaking the frozen hydrated samples and it was performed in a cryo-preparation chamber ALTO 2500 (GATAN) (Osumi et al., 2006). A suitable cryo-holder was selected depending on the substrate; in the case of the cover glass, a commercial ALTO 2500 holder with clamp facility was used for the fixing, and in the case of the sapphire disc, the developed cryo-holder was used.

The holder with the sample was moved into the ALTO 2500 preparation chamber according to the operators handbook (2005). The holder was fixed to the rod of the cryo-shuttle in liquid nitrogen and transferred via the slushing station into the cryo-preparation unit already attached to the SEM. The freeze-fracturing of the sapphire disc was performed using the blade on the manipulator of the ALTO 2500.

During the described experiment, a sequence of two freeze-etching steps was performed: one minute freeze-etching and then additional six minute freeze-etching (7 min in total) were performed at a temperature of −96 °C to expose structural details in the fracture plane. In all experiments, it was possible to image the biofilm samples uncoated; charging was not disturbing at used magnifications. This also allows to image the sample close to its native structure without any eventual
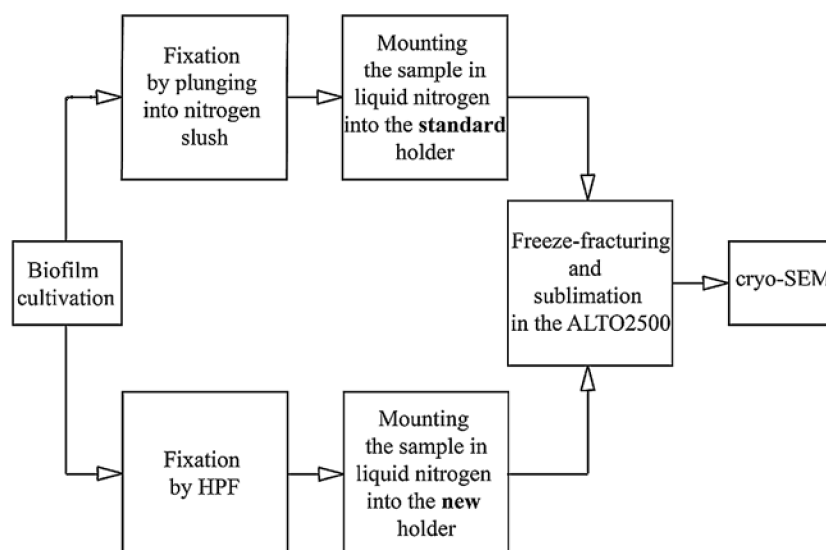
Fig. 1. Schematic workflow starting with the cultivation of biofilms for imaging by cryo-SEM.

artefacts caused by the coating and it was possible to perform multi-step sublimation.

2.4. Cryo-SEM

The imaging was performed in a high resolution SEM 7401F (JEOL, Japan) equipped with an ALTO 2500 cryo-preparation system (Pšenička et al., 2010), so the prepared samples could be directly inserted into the specimen chamber without being removed from the high vacuum. The cryo-stage in the SEM was cooled to −135 °C, and the anti-contamination aperture was cooled to −145 °C during specimen observation. Secondary electron (SE) micrographs were recorded at an electron energy range between 1 and 2 keV and the working distance of approximately 8 mm.

3. Results and discussion

The inner structure of biofilm samples was investigated by cryo-SEM techniques (Fig. 1). For cryo-fixation, simple plunging and HPF were applied. The freeze-fracture technique consists of physically breaking the frozen hydrated samples. The structural details in the fracture plane were then visualized at low temperatures using cryo-SEM (Severs, 2007). In contrast to classical freeze-fracturing, the perpendicular fracturing of the substrate allows observation of the grown sample over its entire thickness.

Our experimental results were consistent with the known fact that cryo-fixation is the best way to fix and stabilize biofilms before their examination in cryo-EM (Alhede et al., 2012; Webster et al., 2004). Simple plunging into liquid cryogen is applicable only for very thin specimens with a thickness of < 10 μm (Kuo, 2007), depending on the composition and substrate used or if the biofilm envelope is studied. In this case, when the inner structures of the matrix and bacteria interconnections were observed and the freeze-fracture technique was used, the HPF technique proved to be necessary for preserving the biofilm ultrastructure. The thickness range of the observed biofilms started at approximately 10 μm, and one side of the grown biofilm was covered with the cover glass, which reduced the cooling efficiency during the plunge freezing. The thickness of the sample carriers and the thermal conductivity are more critical for plunge freezing than for HPF. As described by (Handley et al., 1981), the ideal sample carrier for plunge freezing is made from very thin, high-strength sandwiches of titanium or other high-strength metals. Nevertheless, the cover glass is widely used as a cultivation substrate in *in vitro* biofilm experiments (Azeredo

et al., 2017; Haque et al., 2016; Lüdecke et al., 2014). The use of sapphire discs as a cultivation substrate for plunge-freezing seems to be more suitable from the perspective of its thermal conductivity and also its thickness. Several experiments, however, show that the plunge freezing fixation of cells cultivated on sapphire discs lead to ice crystal segregation as well (Kaech and Woelfel, 2007); this result also correspond to our experiments (see S2 Fig). Therefore, a technique based on HPF that allows preserving the ultrastructure of a thickness up to 300 μm (Kuo, 2007; Moor, 1987) was designed. Several experiments with the fracturing of perpendicularly oriented samples were already designed earlier (Bastacky et al., 1990; Bastacky et al., 1995; Walther, 2003), but these experiments were possible only for samples on larger sapphire discs. For 1.4 mm sapphire discs and the available instrumentation, a special cryo-holder was developed (Fig. 2).

3.1. Innovative technique and developed sample holder

A new sample holder for sapphire discs with a diameter of 1.4 mm for the HPF instrument EM PACT2 (Leica Microsystems Inc., Austria) was designed and built. Due to small dimensions of the sapphire discs and the necessity to keep them submerged in liquid nitrogen, mounting was difficult and often time consuming. The following are the requirements for the cryo-holder of sapphire discs:

(1) easy fixing of the sapphire disc in liquid nitrogen,
(2) perpendicular fracturing of the sapphire disc with the cultured sample in the preparation chamber ALTO 2500 using the original scalpel-manipulator, and
(3) the ability to observe both sides of the sapphire disc in the SEM without removing it from the ALTO 2500 (GATAN Inc., USA) cryo-attachment.

The dimensions and material of the main body were analogous to the original dimensions and material, so that the disc fit in the ALTO 2500 instrument. Fig. 2A shows the schematic drawing of the holder for the new sample preparation technique in which we imaged the perpendicular cross freeze-fractures of high-pressure frozen cultures cultivated on small sapphire discs. The holder consisted of two main parts: (i) the main body with a bayonet interface that fit to the transfer rod and the rail system in the ALTO 2500 and (ii) a hinged part for fastening the sapphire disc. Slightly less than half of the sapphire disc could be fastened in the groove and tightened using a single screw. Because of the manipulation with the sapphire disc from the HPF holder and its
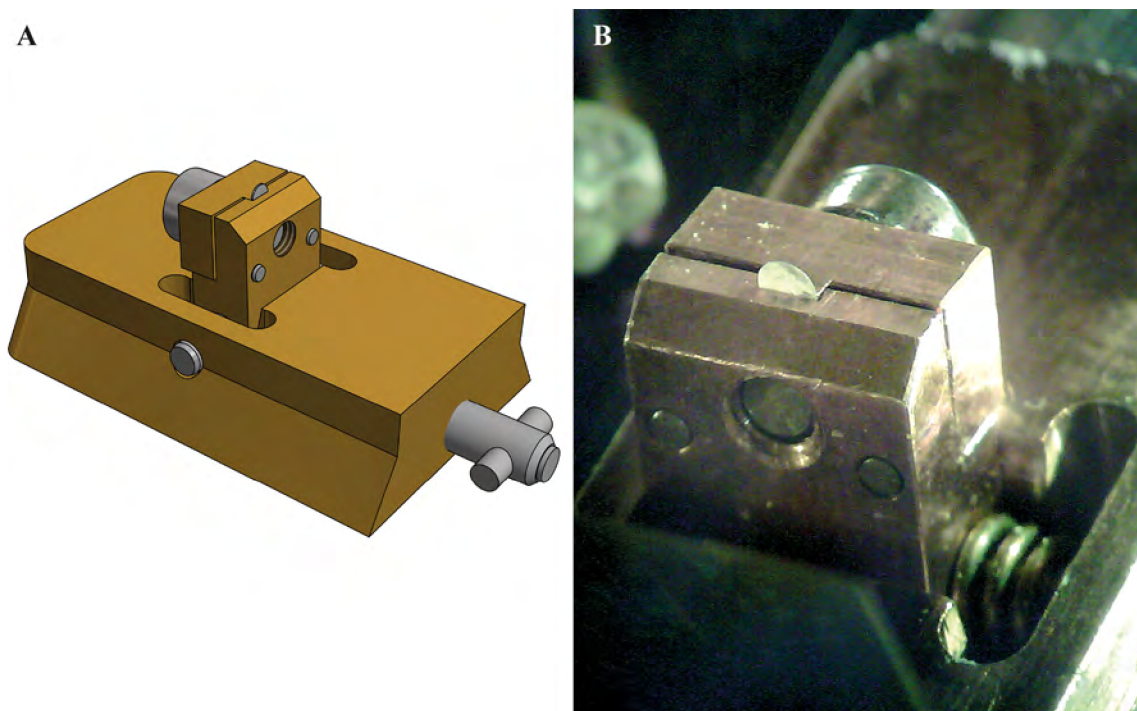
Fig. 2. A holder for gripping and perpendicular cross freeze-fracturing of the 1.4 mm sapphire disc compatible with the ALTO 2500 cryo-preparation system. (A) schematic drawing and (B) actual picture when performing the experiments in the cryo-preparation chamber.

small dimensions, it was very difficult to determine the side of the biofilm. Therefore, the tilted part containing the sapphire disc could be easily tilted by ± 5° using the ALTO 2500 manipulator, allowing to observe the interface from both sides of the fractured sapphire disc (see also S1 File), since it is not possible to do a tilting of the ALTO cryo-stage in the used SEM.

Due to the interest in the extracellular matrix structure, composition and distribution of microbes in the biofilm, the freeze-fracture technique was applied in the preparation chamber ALTO 2500 with a scalpel manipulator. This was more a random event in which it was not easy to specifically select the broken area (see, e.g., S2 File). Nevertheless, if the sapphire disk was completely covered by the biofilm, the fracturing was typically sufficient.

### 3.2. Perpendicular freeze-fracturing of microbial biofilms

In our experiments, we used two sample preparation protocols suitable for biofilm samples grown on a thin substrate and consequently imaged their perpendicular cross sections. As model samples microbial biofilms with cultivation times of 24 and 48 h were investigated where the main aim was to detect the biofilm formation at the maximum growth of the single/mixed species biofilm including *Staphylococcus epidermidis*, *Candida albicans* and *Candida parapsilosis* (Adam et al., 2002; Holá et al., 2006). Fig. 3 shows fractures of *C. parapsilosis* and its extracellular matrix fixed by the following two methods: (i) simple plunging into nitrogen slush (Fig. 3B) in which the sample was cultivated in the inoculated cultivation medium YNBg on a sterile cover glass and (ii) HPF in which the sample was cultivated on a sapphire disc under the same conditions (Fig. 3A). In the case of HPF, the use of the sapphire disc was important because of its advantages: (i) a very high coefficient of heat transfer allowing very high cooling rates that prevent ice crystallization, (ii) surface properties allowing the growth of biofilms, and (iii) relatively easy and localized freeze-fracturing due to its crystal structure. After the freeze-fracture, a freeze-etching was performed. The freeze-etching led partially to the exposure of details in the fracture plane. For more micrographs with different freezing

conditions, see S1 Fig and Fig. 3.

From Fig. 3, it is clear that the simple plunging technique causes ice crystallization; this finding is in contrast to the HPF technique, which preserves the fine structure well. Our results are in agreement with conclusions published by (Wu et al., 2014) where four different approaches are compared and used to the preparation of the *Staphylococcus aureus* hydrated biofilm cultivated on larger, 6 mm in diameter sapphire discs, for cryo-SEM imaging where the HPF EM HPM100 (Leica Microsystems) was used for the sample freezing. Also there the high-pressure freezing technique was evaluated as the method of choice capable to preserve the highly hydrated extracellular matrix of biofilms with minimal changes caused by ice crystallization effects. The re-organization of the biofilm structure observed in samples plunged in liquid cryogen can be attributed to crystallization of water and segregation effects. Fig. 3B and D reveals the artefact structure of the sample, showing a net-like structure with channels. The formation of these protrusions (Fig. 3B) may be caused by the presence of nonaqueous components in biofilm and in the rest of the cultivation medium. The artificial structures of these 24 h biofilms that are observed in samples fixed by a simple plunging appear very similar to the structures described in biofilms cultivated for much longer time (14 days) (Schaudinn et al., 2014) in both shape and dimensions of the channel like structures that were observed by various imaging techniques. However, the morphology of the 24 h biofilms fixed by plunging can be attributed to the formation of crystalline ice during the freezing process, which was also observable in images of the pure cultivation medium frozen by plunging at the same conditions that is in contrast with the well frozen smooth structure obtained by HPF (see Fig. 3C and D).

The freezing by HPF was found the most effective method in our study. Even though the crystallization of the water content in highly hydrated regions of the biofilm samples occurs as well by using this type of fixation, the ice crystals in the extracellular matrix can be revealed with higher magnifications or in the freeze-etching experiments in this work. The size of ice crystals visible mainly after longer freeze-etching samples may indicate diluted vs more concentrated regions in
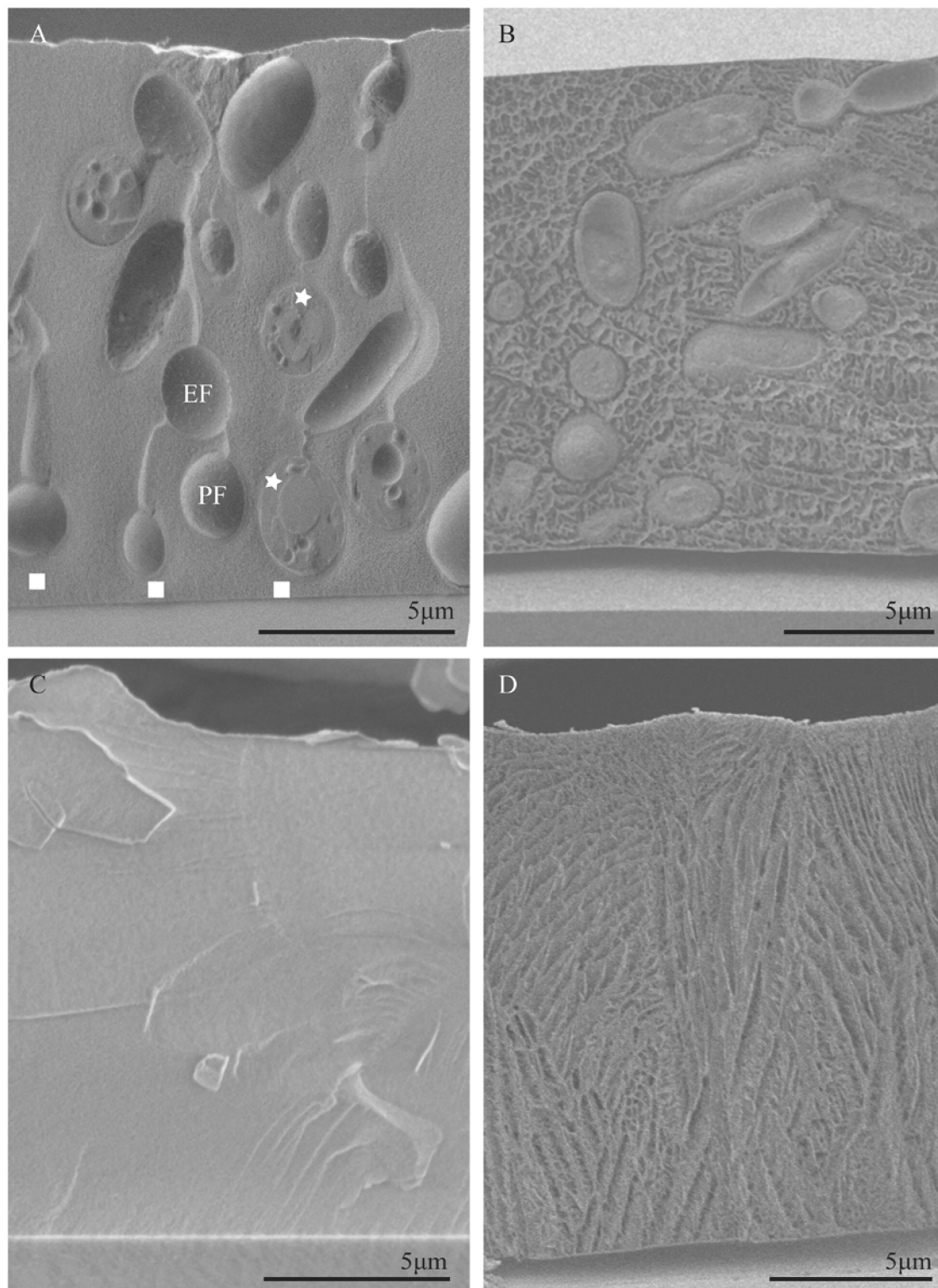
Fig. 3. Freeze-fracture of *Candida parapsilosis*. (A) *Candida parapsilosis* grown on a sapphire disc and fixed by HPF. (B) *Candida parapsilosis* grown on a glass substrate and fixed by plunging in nitrogen slush. (C) Cultivation medium on sapphire disc frozen by HPF. (D) Cultivation medium on cover glass frozen by plunging in nitrogen slush. Endoplasmic (EF) and protoplasmic (PF) fracture faces exhibit typical invaginations and corresponding ridges, broken cells show a preserved ultrastructure with visible cell organelles (stars) and quite large distances between cells and an adhesion surface/substrate (square).

the sample. For HPF, we used the instrument EM PACT2, which freezes only very small samples suitable for the specimen carriers up to a diameter of 1.5 mm (Kaech and Ziegler, 2014; McDonald, 2009). The HPF instrument EM PACT2 is widely used in laboratories for transmission electron microscopy, for which such small sample dimensions

are sufficient for the following sample preparation such as freeze-substitution and production of ultrathin sections (Kaech and Ziegler, 2014).

Small sapphire discs must be handled delicately; in addition, the biofilm grown on the surface of the substrate is a very soft and fully
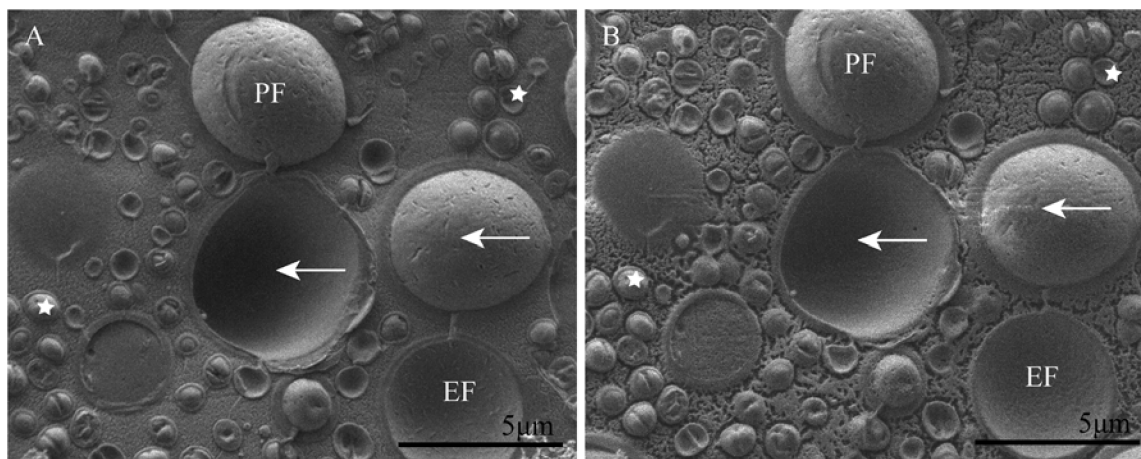
Fig. 4. Mixed bacterial − *Staphylococcus epidermidis*/yeast – *Candida albicans* biofilm with different freeze-etching times. (A) 1 min at − 96 °C and (B) 7 min at − 96 °C. Stars indicate cells of *S. epidermidis*, arrows protoplasmic (PF) and endoplasmic fracture faces (EF) of *C. albicans* with typical invaginations and corresponding ridges. Invaginations in EF disappear during longer freeze-etching.

hydrated material, so its manipulation should be rigorous it should be manipulated with extreme care. The time between removing the disc from cultivation plates and the fixation should be as short as possible, owing to the possibility of desiccation and potentially destroying the biofilm structure. In our experiments, the time of handling the biofilm samples before freezing was kept within one minute; therefore, artefacts due to drying out were avoided.

A crucial parameter in cryo-SEM techniques is sublimation. Because sublimation depends on many parameters (including temperature and time of sublimation, pressure in the cryo-preparation chamber, and composition of the sample), several tests were performed with different times for this process. The sublimation removes ice contamination and might expose structural details on the imaged surface (freeze-etching).

The structure inside of the freeze-fractured samples (mixed biofilm) is shown in Fig. 4A, with additional ultrastructure revealed after further freeze-etching shown in Fig. 4B. A fine structure proved helpful in improving the cryo-fixation technique. Moreover, it was possible to recognize differences in several parts of the extracellular matrix that are characterized by various water content (diluted vs more concentrated regions) (arrows, Fig. 5A). These differences were also visible in the experiment with two different freeze-etching times of mixed biofilms of two species (arrows, Fig. 5B). A well-known fact about biofilms is that microorganisms are able to produce and envelop themselves in an extracellular polymeric matrix. Using this method, the region near yeast or bacterial cells was clearly visible (Figs. 4 and 3A). Moreover, this method allows relationships between microbial cells, even in polymicrobial biofilms, to be revealed in detail. In the presented figures, the spatial distribution of microbial cells is visible. A relatively large distances (large gaps) than we expected at the contact between the microbial cells, as shown in Fig. 5 (rounds), as well as at the connection of the microbial cells to the adhesion surface/substrate (square, see Fig. 3A), indicates a key role of the extracellular matrix in the adhesion process.

Biofilm layers are formed by microorganism cells of which adhere to surfaces. Aggregation and proliferation of microbial cells lead to the formation of heterogeneous cell aggregates called microcolonies. These structures are embedded within a self-produced matrix of extracellular polymeric substance (EPS), which is generally composed of polysaccharides, extracellular DNA, and proteins (Donlan, 2002; Wu et al., 2014). Biofilm architecture is highly heterogeneous: microbial cells are usually organized into varied microcolonies and EPS matrix, and interstitial cavities (water channels) may also be present. Moreover, biofilm structures are variable in both space and time. The structure depends on external conditions as well as on internal processes in the

biofilm layer, e.g., cell-to-cell signaling (quorum sensing system), metabolic activity of microbial cells and oxygen or nutrient availability (Donlan and Costerton, 2002). In comparison with staphylococcal biofilms, the candida biofilm exhibits higher variability due to the differentiation of yeast cells to hyphae or pseudohyphae. This differentiation leads to a biphasic structure of candida biofilms that is composed of an adherent blastospore layer covered by hyphal elements embedded in EPS (Baillie and Douglas, 1999),

A key building component of biofilm EPS is a jelly-like or slimy substance containing up to 97% of water. This substance is responsible for most of the physical, chemical and biological properties of a biofilm (Davey and O'toole, 2000) and is generally composed of many types of polymeric substances, particularly polysaccharides, proteins and extracellular DNA (Ruzicka et al., 2011; Zarnowski et al., 2014). Therefore, the EPS composition is more complex and contains a number of polymeric substances in comparison with common culture microbiological media, such as YNB or BHI, which contain relatively simple compounds, e.g., ions, oligosaccharides, vitamins, amino acids and proteins. EPS also showed higher viscosity compared with culture media.

4. Conclusions

Our study of bacterial/yeast biofilms suggests that cryo-SEM in combination with high-pressure-freezing and perpendicular cross freeze-fracturing through a sapphire disc is an excellent technique for imaging highly hydrated samples such as biofilms.

Details of biofilm formation can be recognized and further studied in the natural hydrated state, thus allowing for detailed investigations of the ultrafine structure and morphology in near-life-like conditions. In particular, our method enables the observation of the spatial distribution of microbial cells and relatively large gaps (distances) at their mutual contact as well as at the connection of the microbial cells to the adhesion surface/substrate that indicate a key role of the extracellular matrix in the adhesion process. The developed methodology and new holder compatible with the ALTO 2500 cryopreparation system for perpendicular cross freeze-fracture of small sapphire discs with a diameter of 1.4 mm offer a unique opportunity to fully explore this method. However, this method can be easily adapted also for all other HPF and cryo-SEM instruments. Different sublimation times lead to differentiation between dilute and concentrated regions in our sample. This is related to the ability of the ice crystals to sublime. Therefore, we were able to differentiate more hydrated parts of samples, such as the cultivation medium, from denser substances and cells.
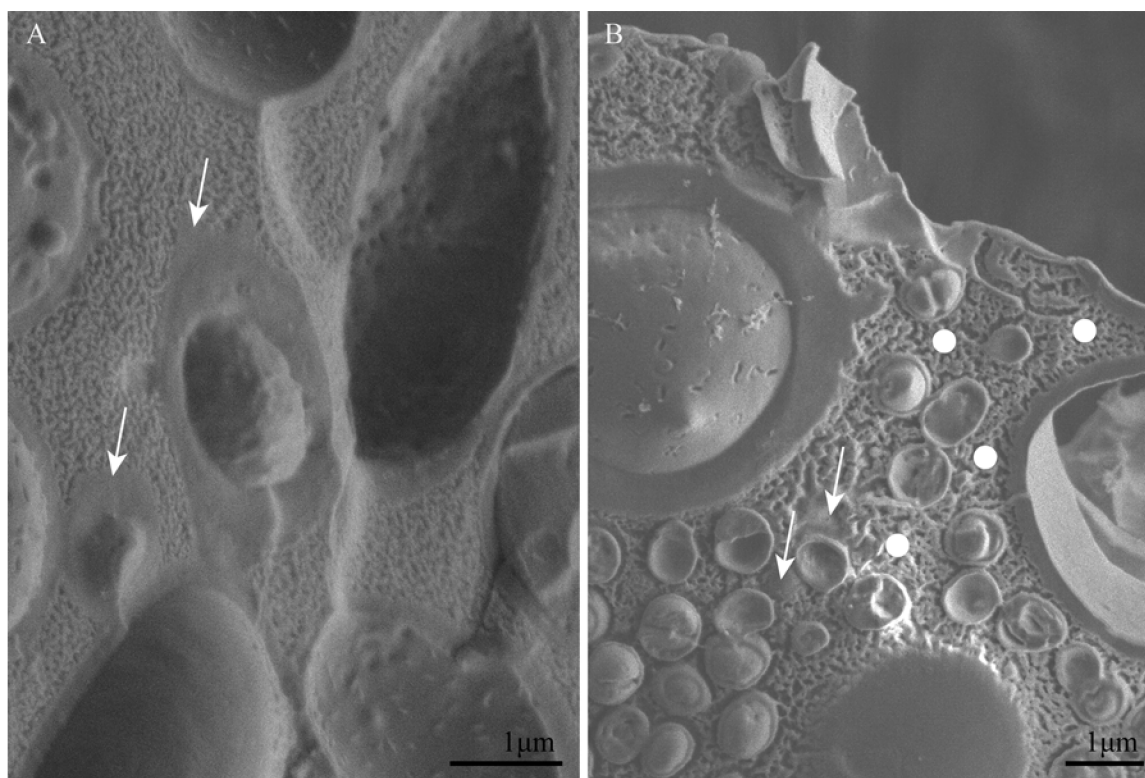
Fig. 5. (a) Freeze-fracture of *Candida parapsilosis* biofilm grown on a sapphire disc and fixed by HPF in higher magnification than in Fig. 3B with the detail of denser EPS around the yeast cells; (b) Freeze-etching experiment of mixed bacterial − *Staphylococcus epidermidis*/yeast − *Candida albicans* biofilm with the time of freeze-etching 7 min at −96 °C. Arrows show finer (probably more concentrated) regions in biofilm. Rounds show distances (large gaps (LG)) between cells of microbes.

The novel methodology suggested here, which involves the combination of high-pressure freezing fixation and freeze-fracturing, is supported by experiments using different sublimation conditions. Therefore, this approach is convenient and useful for the description of the composition of microbial biofilms on selected substrates under specific life conditions. Relationships between microbial cells (their spatial distribution, distances between cells) in biofilms and the characteristics of the microbial adhesion on adhesion surfaces can also be studied in detail.

Acknowledgements

Appendix A. Supplementary data

Supplementary data associated with this article can be found, in the online version, at https://doi.org/10.1016/j.micron.2018.04.006.

References

Adam, B., Baillie, G.S., Douglas, L.J., 2002. Mixed species biofilms of Candida albicans and Staphylococcus epidermidis. J. Med. Microbiol. 51, 344–349.

Alhede, M., Qvortrup, K., Liebrechts, R., Hoiby, N., Givskov, M., Bjarnsholt, T., 2012. Combination of microscopic techniques reveals a comprehensive visual impression of biofilm structure and composition. FEMS Immunol. Med. Microbiol. 65, 335–342.

Alto 2500, 2005. Operators Handbook. Gatan, UK, Oxon, UK p. 35.

Azeredo, J., Azevedo, N.F., Briandet, R., Cerca, N., Coenye, T., Costa, A.R., Desvaux, M., Di Bonaventura, G., Hebraud, M., Jaglic, Z., Kacaniova, M., Knochel, S., Lourenco, A., Mergulhao, F., Meyer, R.L., Nychas, G., Simoes, M., Tresse, O., Sternberg, C., 2017. Critical review on biofilm methods. Crit. Rev. Microbiol. 43, 313–351.

Baillie, G.S., Douglas, L.J., 1999. Role of dimorphism in the development of Candida albicans biofilms. J. Med. Microbiol. 48, 671–679.

Bandara, H.M.H.N., Lam, O.L.T., Watt, R.M., Jin, L.J., Samaranayake, L.P., 2010. Bacterial lipopolysaccharides variably modulate in vitro biofilm formation of Candida species. J. Med. Microbiol. 59, 1225–1234.

Bastacky, J., Goodman, C., Hayes, T.L., 1990. A specimen holder for low-temperature scanning electron microscopy. J. Electron. Microsc. Tech. 14, 83–84.

Bastacky, J., Lee, C., Freeman, T., Weber, G., Baeza, A., Hubbins, T., Chen, Y., 1995. A specimen holder for high-resolution low-temperature scanning electron microscopy. Microsc. Res. Tech. 32, 457–458.

Beveridge, T.J., 2005. Bacterial surface structure, physicochemistry and geo-reactivity. Geochim. Cosmochim. Ac 69, A668.

Dahl, R., Staehelin, L.A., 1989. High-pressure freezing for the preservation of biological structure: theory and practice. J. Electron. Microsc. Tech. 13, 165–174.

Davey, M.E., O'toole, G.A., 2000. Microbial biofilms: from ecology to molecular genetics. Microbiol. Mol. Biol. Rev. 64, 847–867.

Deleo, F., Otto, M.W., 2008. Bacterial Pathogenesis: Methods and Protocols. Humana Press, Totowa, N .J.

Dohnalkova, A.C., Marshall, M.J., Arey, B.W., Williams, K.H., Buck, E.C., Fredrickson, J.K., 2011. Imaging hydrated microbial extracellular polymers: comparative analysis by electron microscopy. Appl. Environ. Microbiol. 77, 1254–1262.

Donelli, G., 2014. Microbial Biofilms: Methods and Protocols. Humana Press ; Springer, New York.

Donlan, R.M., Costerton, J.W., 2002. Biofilms: survival mechanisms of clinically relevant microorganisms. Clin. Microbiol. Rev. 15, 167–193.

Donlan, R.M., 2002. Biofilms: microbial life on surfaces. Emerg. Infect. Dis. 8, 881–890.

Fassel, T.A., Edmiston, C.E., 1999. Bacterial biofilms: strategies for preparing glycocalyx for electron microscopy. Method Enzymol. 310, 194–203.

Galway, M.E., Heckman Jr., J.W., Hyde, G.J., Fowke, L.C., 1995. Advances in high-pressure and plunge-freeze fixation. Methods Cell Biol. 49, 3–19.

Graham, L.L., Beveridge, T.J., 1990. Effect of chemical fixatives on accurate preservation of Escherichia-Coli and Bacillus-Subtilis structure in cells prepared by freeze-substitution. J. Bacteriol. 172, 2150–2159.

Handley, D.A., Alexander, J.T., Chien, S., 1981. The design and use of a simple device for rapid quench-freezing of biological samples. J. Microsc. 121, 273–282.

Haque, F., Alfatah, M., Ganesan, K., Bhattacharyya, M.S., 2016. Inhibitory effect of sophorolipid on Candida albicans biofilm formation and hyphal growth. Sci. Rep. 6, 23575.

Hawser, S.P., Douglas, L.J., 1994. Biofilm formation by Candida Species on the surface of

catheter materials in-vitro. Infect. Immun. 62, 915–921.

Hayat, M.A., 1974. Principles and Techniques of Scanning Electron Microscopy, Biological Applications, vol.1 Van Nostrand Reinhold Company.

Holá, V., Růžička, F., Votava, M., 2006. The dynamics of Staphylococcus epidermis biofilm formation in relation to nutrition, temperature, and time. Scripta Medica Facultatis Medicae Universitatis Brunensis Masarykianae 79, 169–174.

Kaech, A., Woelfel, M., 2007. Evaluation of different freezing methods for monolayer cell cultures. Microsc. Microanal. 13, 240–241.

Kaech, A., Ziegler, U., 2014. High-pressure freezing: current state and future prospects. Methods Mol. Biol. 1117, 151–171.

Karcz, J., Bernas, T., Nowak, A., Talik, E., Woznica, A., 2012. Application of lyophilization to prepare the nitrifying bacterial biofilm for imaging with scanning electron microscopy. Scanning 34, 26–36.

Krzyzanek, V., Sporenberg, N., Keller, U., Guddorf, J., Reichelt, R., Schonhoff, M., 2011. Polyelectrolyte multilayer capsules: nanostructure and visualisation of nanopores in the wall. Soft Matter 7, 7034–7041.

Kuo, J., 2007. Electron Microscopy: Methods and Protocols. Springer Science & Business Media.

Lüdecke, C., Jandt, K.D., Siegismund, D., Kujau, M.J., Zang, E., Rettenmayr, M., Bossert, J., Roth, M., 2014. Reproducible biofilm cultivation of chemostat-grown Escherichia Coli and investigation of bacterial adhesion on biomaterials using a non-constant-depth film fermenter. PLoS One 9, e84837.

Lattif, A.A., Mukherjee, P.K., Chandra, J., Swindell, K., Lockhart, S.R., Diekema, D.J., Pfaller, M.A., Ghannoum, M.A., 2010. Characterization of biofilms formed by Candida parapsilosis C. metapsilosis, and C. orthopsilosis. Int. J. Med. Microbiol. 300, 265–270.

Lawrence, J.R., Swerhone, G.D.W., Leppard, G.G., Araki, T., Zhang, X., West, M.M., Hitchcock, A.P., 2003. Scanning transmission X-ray, laser scanning, and transmission electron microscopy mapping of the exopolymeric matrix of microbial biofilms. Appl. Environ. Microbiol. 69, 5543–5554.

McDonald, K.L., 2009. A review of high-pressure freezing preparation techniques for correlative light and electron microscopy of the same cells and tissues. J. Microsc. 235, 273–281.

Montesinos, E., Esteve, I., Guerrero, R., 1983. Comparison between direct methods for determination of microbial cell-volume – electron-microscopy and electronic particle sizing. Appl. Environ. Microbiol. 45, 1651–1658.

Moor, H., 1987. Theory and practice of high pressure freezing. In: Steinbrecht, R., Zierold, K. (Eds.), Cryotechniques in Biological Electron Microscopy. Springer Berlin Heidelberg, pp. 175–191.

Osumi, M., Konomi, M., Sugawara, T., Takagi, T., Baba, M., 2006. High-pressure freezing is a powerful tool for visualization of Schizosaccharomyces pombe cells: ultra-low temperature and low-voltage scanning electron microscopy and immunoelectron microscopy. J. Electron. Microsc. 55, 75–88.

Pšenička, M., Tesařová, M., Těšitel, J., Nebesářová, J., 2010. Size determination of Acipenser ruthenus spermatozoa in different types of electron microscopy. Micron 41, 455–460.

Paiva, L.C.F., Vidigal, P.G., Donatti, L., Svidzinski, T.I.E., Consolaro, M.E.L., 2012. Assessment of in vitro biofilm formation by Candida species isolates from vulvovaginal candidiasis and ultrastructural characteristics. Micron 43, 497–502.

Reese, S., Guggenheim, B., 2007. A novel TEM contrasting technique for extracellular polysaccharides in in vitro biofilms. Microsc. Res. Tech. 70, 816–822.

Ruzicka, F., Horka, M., Hola, V., Votava, M., 2007. Capillary isoelectric focusing-useful tool for detection of the biofilm formation in Staphylococcus epidermidis. J. Microbiol. Methods 68, 530–535.

Ruzicka, F., Horka, M., Hola, V., Kubesova, A., Pavlik, T., Votava, M., 2010. The differences in the isoelectric points of biofilm-positive and biofilm-negative Candida parapsilosis strains. J. Microbiol. Methods 80, 299–301.

Ruzicka, F., Horka, M., Hola, V., 2011. Extracellular polysaccharides in microbial biofilm and their influence on the electrophoretic properties of microbial cells. In: Volpi, N. (Ed.), Capillary Electrophoresis of Carbohydrates. Humana Press, pp. 105–126.

Schaudinn, C., Stoodley, P., Hall-Stoodley, L., Gorur, A., Remis, J., Wu, S., Auer, M., Hertwig, S., Guerrero-Given, D., Hu, F.Z., Ehrlich, G.D., Costerton, J.W., Robinson, D.H., Webster, P., 2014. Death and transfiguration in static Staphylococcus epidermidis cultures. PLoS One 9, e100002.

Schwartz, T., Jungfer, C., Heissler, S., Friedrich, F., Faubel, W., Obst, U., 2009. Combined use of molecular biology taxonomy, Raman spectrometry, and ESEM imaging to study natural biofilms grown on filter materials at waterworks. Chemosphere 77, 249–257.

Severs, N.J., 2007. Freeze-fracture electron microscopy. Nat. Protoc. 2, 547–576.

Shimoni, E., Müller, M., 1998. On optimizing high-pressure freezing: from heat transfer theory to a new microbiopsy device. J. Microsc. 192, 236–247.

Studer, D., Michel, M., Muller, M., 1989. High-pressure freezing comes of age. Scanning Microsc. Suppl. 3, 253–269.

Studer, D., Michel, M., Wohwend, M., Hunziker, E.B., Buschmann, M.D., 1995. Vitrification of articular cartilage by high-pressure freezing. J. Microsc. 179, 321–322.

Tranfield, E.M., Walker, D.C., 2013. The ultrastructure of animal atherosclerosis: what has been done, and the electron microscopy advancements that could help scientists answer new biological questions. Micron 46, 1–11.

Vanhecke, D., Graber, W., Studer, D., 2008. Close-to-native ultrastructural preservation by high pressure freezing. Methods Cell Biol. 88, 151–164.

Walther, P., 2003. Recent progress in freeze-fracturing of high-pressure frozen samples. J. Microsc. 212, 34–43.

Webster, P., Wu, S., Webster, S., Rich, K., McDonald, K., 2004. Ultrastructural preservation of biofilms formed by non-typeable Hemophilus influenzae. Biofilms 1, 165–182.

Wu, Y., Liang, J., Rensing, K., Chou, T.M., Libera, M., 2014. Extracellular matrix reorganization during cryo preparation for scanning electron microscope imaging of staphylococcus aureus biofilms. Microsc. Microanal. 20, 1348–1355.

Zarnowski, R., Westler, W.M., Lacmbouh, G.A., Marita, J.M., Bothe, J.R., Bernhardt, J., Lounes-Hadj Sahraoui, A., Fontaine, J., Sanchez, H., Hatfield, R.D., Ntambi, J.M., Nett, J.E., Mitchell, A.P., Andes, D.R., 2014. Novel entries in a fungal biofilm matrix encyclopedia. mBio 5, 01314–e01333.

Hrubanová, K., Krzyžánek, V. Inovativní metodika mrazového lámání a cryo-SEM demonstrovaná na biofilmu *Candidy parapsilosis*. *Jemná mechanika a optika*. 2019, 64(1), 15-17. ISSN 0447-6441.

Kamila HRUBANOVÁ, Vladislav KRZYŽÁNEK
Ústav přístrojové techniky AV ČR, v. v. i., Brno

Inovativní metodika mrazového lámání a cryo-SEM demonstrovaná na biofilmu *Candidy parapsilosis*

Předložená studie představuje nové technické řešení umožňující kombinaci mrazového lámání (freeze-fracturing) malých safírových disků s poloměrem 1,4 mm používaných pro vysokotlaké mražení (high pressure freezing, HPF) a zobrazování pomocí kryogenní rastrovací elektronové mikroskopie (cryo-SEM). Práce zahrnuje podrobný popis metodologie a její demonstraci na plně hydratovaných vzorcích kvasinkových biofilmů, kmen Candida parapsilosis, který patří mezi významné mikroorganismy v klinické praxi. Cryo-SEM a HPF jsou považovány za špičkové techniky v elektronové mikroskopii, avšak jejich kombinace není vždy snadno použitelná. Popsané technicko-metodologické řešení umožňuje kombinaci vysokotlakého zmrazování pomocí EM PACT2 (Leica Microsystems) a zobrazování perpendikulárního mrazového lomu pomocí SEM (Jeol), který je vybaven systémem ALTO 2500 (Gatan). Pro uchycení vzorku a jeho následné lámání byl vyvinut speciální držák, jehož použití je demonstrováno na několika experimentech zabývajících se výzkumem ultrastruktury mikrobiálních biofilmů, kde je hlavním cílem vizualizace biofilmu se zaměřením na kvalitu promražení jeho extracelulární polymerní substance (EPS) a detekce oblasti přilnutí mikrobiálních buněk k substrátu/povrchu safírového disku.

Klíčová slova: cryo-SEM, mrazový lom, biofilm

1. ÚVOD

Mikroskopické organismy, kterými se práce zabývá, se vyznačují různorodou formou života. Kromě planktonického způsobu přežívání jsou tyto organismy schopné přilnout k povrchu nebo rozhraní a vytvořit tak organizované společenství, jež je obklopeno matricí extracelulárních polymerních substancí (EPS), které mikroby sami produkují. Takové mikrobiální společenství je nazýváno biofilmem. Prostřednictvím biofilmu mohou mikroorganismy kolonizovat povrchy implantátů a díky EPS jsou mikrobiální buňky chráněny před obrannými mechanizmy imunitního systému a působením antibiotik [1, 2]. Z pohledu mikrobů se tedy jedná o velice výhodnou formu života, avšak v klinické praxi je schopnost tvorby biofilmu považována za důležitý faktor virulence těchto mikroorganismů. Popis struktury biofilmu může přispět k porozumění jeho vzniku a základním biochemickým mechanismům v tomto procesu [3], což by mohlo pomoci k nalezení účinnější léčebné strategie.

Mikrobiální biofilmy bývají zkoumány a zobrazovány různými mikroskopickými technikami [4], např. konfokální laserovou skenovací mikroskopií (CLSM), konvenční rastrovací elektronovou mikroskopií (SEM) [5], transmisní elektronovou mikroskopií (TEM) [6] a dalšími speciálními technikami SEM (cryo-SEM, environmentální SEM (ESEM) a FIB SEM). Jedním z omezení CLSM je jeho nízké užitečné zvětšení. Toto omezení lze snadno překonat pomocí SEM analýzy a získat tak obrázky s vysokým zvětšením, které jsou důležité pro pochopení fyziologie biofilmů. Pro konvenční SEM zobrazování je nutná speciální příprava hydratovaných vzorků [7]. Konvenční postupy přípravy vzorků pro vysoké vakuum v SEM zahrnují kroky, které mohou způsobit podstatné změny v mikrobiální buněčné ultrastruktuře. Chemická fixace pomocí aldehydů a těžkých kovů pomáhá zachovat morfologii buněk a zvyšuje kontrast. Dehydratace organickými rozpouštědly může způsobit diskontinuity buněčné membrány, odstraněním vody dochází ale i k dalším negativním účinkům na morfologii biofilmu. EPS v biofilmu obsahuje přibližně 95 % vody a v důsledku dehydratace vypadá spíše jako vláknitá struktura než jako hustá gelová matrice obklopující buňky [2]. V případě použití nízkých teplot během přípravy vzorku a jeho následné analýzy není biofilm dehydratován, díky tomu je zachována jeho struktura v téměř nativním stavu a navíc i možnost zobrazování s vysokým rozlišením [8, 9]. Bylo prokázáno, že mrazová příprava biofilmu vykazuje výrazně lepší zachování jeho vnitřní organizace i ultrastruktury na buněčné úrovni [10]. Aby se eliminovalo poškození spojené s mrazovou přípravou vzorku, byly vyvinuty různé inovativní metody. Jeden z nejjednodušších způsobů cryo-fixace je rychlé ponoření vzorku do kryogenu [11]. Ponoření preparátu do tajícího dusíku nebo kapalného etanu/propanu je dostatečné pouze pro fixaci velmi tenkých vrstev. Fixace biofilmu ponořením do tajícího dusíku vede k významným laterálním makro-segregacím mikrobů i EPS, použití kapalného etanu vede k mikro-segregaci v EPS a makro-segregacím v případě buněk [12]. K účinnější cryo-fixaci se sníženou tvorbou ledových krystalů může být dosaženo zvýšením tlaku kryogenní kapaliny v průběhu mražení pomocí metody HPF. Experimentální výsledky ukazují, že HPF umožňuje zmrazit vzorky až do 200 µm tloušťky bez viditelného poškození ledem [13, 14]. Tato studie ukazuje, že aplikace výše zmíněné metody mražení, následného mrazového lámání a zobrazování pomocí cryo-SEM se zdá být optimálním řešením pro vizualizaci ultrastruktury biofilmu *C. parapsilosis*.

2. METODA MRAZOVÉHO LÁMÁNÍ

Technika mrazového lámání (angl. freeze-fracturing) sestává z mechanického rozbití zmrazených hydratovaných vzorků a v případě perpendikulárního lomu umožňuje zobrazování vnitřní struktury studovaného preparátu pomocí cryo-SEM. Existují studie, ve kterých bylo navrženo a popsáno několik experimentů s frakturou kolmo orientovaných vzorků [15], ale tyto pokusy byly proveditelné pouze pro vzorky na safírových discích o průměru 6 mm. V případě této studie byl dostupný přístroj HPF EM PACT2 (Leica Microsystems), pomocí něhož je možné zmrazit pouze vzorky umístěné na safírové disky s průměrem 1,4 mm. Proto bylo naším hlavním cílem vyvinout speciální cryo držák pro uchycení těchto malých disků s možností jejich mrazového lámání a navrhnout optimální metodiku pro manipulaci s preparáty v tekutém dusíku. Mrazové lámání bylo prováděno v cryo preparační komoře ALTO 2500 (GATAN), jež je připojená na SEM 7401F (JEOL). Jedná se spíše o náhodnou událost, při níž nebývá snadné zlomit vzorek v definovaném místě a detekovat tak specifickou oblast vzorku.

3. INSTRUMENTÁLNÍ ŘEŠENÍ

Pro konstrukční řešení držáku vzorku byly specifikovány tyto požadavky:

(1) snadné uchycení safírového disku o průměru 1,4 mm v kapalném dusíku,

(2) možnost perpendikulárního lámání safírového disku se vzorkem v přípravné komoře ALTO 2500 za vysokého vakua a nízkých teplot s použitím originálního skalpelového manipulátoru a

(3) možnost zobrazovat obě strany safírového disku v cryo--SEM bez nutnosti vyjmutí vzorku ze systému ALTO 2500 (GA-TAN) a cryo-SEM.

Rozměry a materiál těla držáku zůstaly analogické ke komerčně dostupnému držáku vzorků pro jednoduché cryo-SEM zobrazování z důvodu zachování jeho kompatibility s cryo sestavou ALTO 2500. Na *obr. 1A* je zaznamenán schematický nákres nového držáku, na němž je znázorněn způsob uchycení vzorku na safírovém disku, který umožňuje pozorování perpendikulárního lomu v cryo-SEM. Držák má dvě hlavní části: i) hlavního tělesa s bajonetovým rozhraním, které je kompatibilní s tyčí transferu a kolejnicovým systémem v ALTO 2500 a ii) pohyblivé části vybavené šroubem pro upevnění safírového disku. V průběhu instalace safírového disku do nového držáku vzorku v tekutém dusíku je z důvodu malé velikosti disku velmi obtížné správně určit stranu, na které se nachází vrstva biofilmu. Z tohoto důvodu je možné pohyblivou část nesoucí safírový disk naklonit o ±5° pomocí skalpelového manipulátoru v ALTO 2500, což umožňuje pozorování rozhraní z obou stran rozlomeného safírového disku.
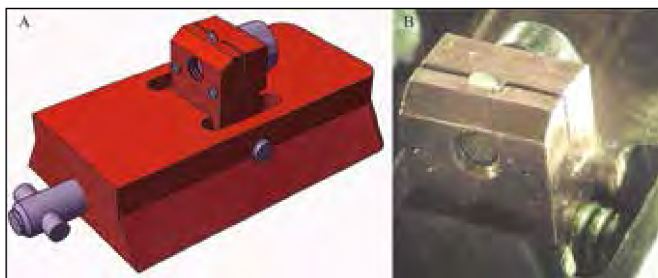

Obr. 1   Schematické zobrazení (A) a reálná fotografie (B) nového držáku vzorku pro uchycení malého safírového disku

4. APLIKACE METODY

Použitelnost navrženého držáku je demonstrována na experimentech zabývajících se vnitřní strukturou biofilmu a samotného kultivačního media v závislosti na zvoleném protokolu mrazové fixace. Pro mrazovou fixaci byly použity ponory do tajícího dusíku a vysokotlaké mražení (HPF). Kvalita zamražení byla evaluována při nízké teplotě pomocí cryo-SEM. Naše experimentální výsledky se shodovaly s poznatkem, že jednoduché ponoření do kapalného kryogenu je použitelné pouze u velmi tenkých vzorků o tloušťce < 10 μm, a to s ohledem na zvolený substrát (nosič vzorku) a chemické složení preparátu. V případě pozorování vnitřní struktury ECM a mikrobiálních buněk je nezbytná kombinace fixace mražením pomocí HPF a perpendikulárního lámání. Pozorovaná tloušťka vrstvy biofilmu na kultivačním substrátu (krycí sklo/safírový disk) byla (10–20) μm. Celkový objem masy preparátu snižuje účinnost chlazení během mražení. Tloušťka nosičů vzorků a jejich tepelná vodivost patří mezi kritické parametry pro kvalitu mrazové fixace, což platí zejména pro imerzní fixaci. Ideální nosič vzorku pro mražení ponorem by měl být vyroben z tenké titanové folie nebo jiných vysoce pevných kovů [16]. Krycí sklo je běžně používaným kultivačním substrátem v mnoha *in vitro* studiích zabývajících se výzkumem mikrobiálních biofilmů [17, 18]. Použití safírových disků se může zdát jako výhodnější varianta z hlediska jejich tepelné vodivosti a také tloušťky. Některé pokusy však naznačují, že u buněk kultivovaných na safírových discích vede fixace mražením

pomocí ponoru do tekutého kryogenu také k segregaci [19]. Tento výsledek odpovídá i našim experimentům (*obr. 2*) [20], proto byla technika založená na HPF shledána optimálním řešením, které umožňuje zachování ultrastruktury biofilmu o tloušťce až 200 μm.
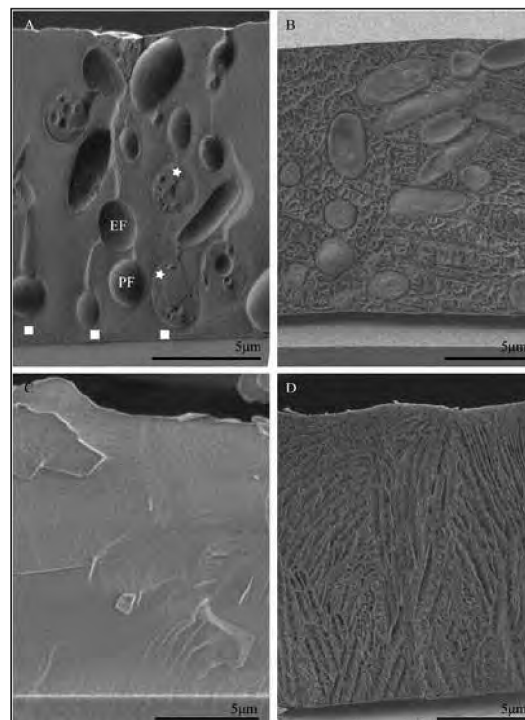
Obr. 2   Mrazový lom kvasinkového biofilmu *Candidy parapsilosis* a čistého kultivačního media (A) *C. parapsilosis* na safírovém disku, fixace HPF (B) *C. parapsilosis* na podložním skle, fixace ponořením do tajícího dusíku. (C) Kultivační médium na safírovém disku zmrazené HPF. (D) Kultivační médium na krycím skle zmrazené ponořením do tajícího dusíku. Endoplazmatické (EF) a protoplazmatické (PF) části lomu vykazují typické invaginace, v rozlomených buňkách lze pozorovat dobře zachovanou ultrastrukturu s viditelnými buněčnými organelami (hvězdy) a poměrně velkými vzdálenostmi mezi buňkami a oblastí adheze ke kultivačnímu substrátu (čtverce). Parametry pozorování: detekce SE, urychlovací napětí (1–2) keV, pracovní vzdálenost 8 mm, vzorky bez pokovení. Převzato z [20]

5. EXPERIMENT

(1) **Mikrobiální kmen *C. parapsilosis* BC11**, který byl vybrán pro tuto studii, pocházel ze sbírek mikrobiologických ústavů Masarykovy univerzity a Fakultní nemocnice u sv. Anny v Brně [21]. Kultura byla uchovávána při teplotě –70 °C v Itest cryotubes (ITEST plus, Hradec Králové). Kultivace byla prováděna při teplotě 37 °C na agarovém substrátu Mueller-Hinton (Oxoid, Basingstoke, Spojené království) po dobu 24 hodin, následně byla mikrobiální kultura resuspendována ve sterilním fyziologickém solném roztoku (PSS) na optickou hustotu 0,5 dle stupnice McFarland. Během experimentu byly použity 24jamkové destičky pro kultivaci tkáňových kultur Nunclon (Nunc, Roskilde, Dánsko) obsahující 1 ml kvasinkového dusíkového základu Difco (Becton, Dickinson a Co., Franklin Lakes, USA) se 4 % glukózy – YNBg), který byl naočkován 100 μl standardizované buněčné suspenze. Jako kultivační substráty byly použity safírové disky o průměru 1,4 mm (č. 16706849, Leica Microsystems Inc., Rakousko), kompatibilní s HPF systémem EM PACT2, a krycí sklo (č. 1014/1818, Hecht--Assistant, Paříž, Francie). Po 24 hodinách inkubace při 37 °C byly substrátové disky/krycí skla z jamek vyjmuty a dále zpracovány.

(2) Pro **cryo fixaci vzorků biofilmu** na pevném substrátu byly použity dvě metody: standardní ponoření do tajícího dusíku a vysokotlaké mražení pomocí HPF. V obou případech byly substráty s kultivovaným biofilmem opatrně a rychle vyjmuty z naočkovaného média.

Zmrazování pomocí tajícího dusíku bylo provedeno v přípravné stanici, která je součástí systému ALTO 2500 (GATAN Inc., USA). Podkladem pro kultivaci vzorků biofilmu bylo krycí sklo o tloušťce 0,17 mm, které bylo před zmrazením vyjmuto z média bez promytí.

Vysokotlaké zmrazení bylo prováděno s přístrojem EM PACT2 HPF (Leica Microsystems Inc., Rakousko) za standardních podmínek. Stejně jako v případě fixace ponořením do kryogenu nebyly vzorky před zmrazením promyté.

(3) Držák se vzorkem byl přesunut do přípravné komory ALTO 2500, kde bylo provedeno **mrazové lámání vzorku** pomocí skalpelu, který je součástí manipulátoru, a následně proběhla **sublimace** po dobu jedné minuty při teplotě –95 °C, která vedla k odhalení strukturálních detailů biofilmu v rovině lomu. Ve všech experimentech bylo možné zobrazit vzorky biofilmu bez pokovení, protože v použitém zvětšení nebylo nabíjení rušivé, díky čemuž bylo možné zobrazování vzorku bez případných artefaktů způsobených pokovením.

(4) Vzorky byly zobrazovány pomocí mikroskopu SEM 7401F (JEOL, Japonsko), který byl vybaven systémem ALTO 2500. Během pozorování byla teplota cryo stolku nastavena na –135 °C, urychlovací napětí na (1–2) keV v režimu detekce sekundárních elektronů při pracovní vzdálenosti 8 mm.

6. SHRNUTÍ VÝSLEDKŮ

Výsledky experimentů této studie ukazují, že popsaná metoda zahrnující cryo-SEM zobrazování v kombinaci s vysokotlakým mražením HPF a perpendikulárním lámáním je vynikající technika analýzy vysoce hydratovaných vzorků, jako jsou kvasinkové biofilmy *Candidy parapsilosis*. Vyvinutý držák pro uchycení safírových disků s průměrem 1,4 mm, jenž je kompatibilní s kryogenním systémem ALTO 2500, může být, stejně jako popsaná metodika, snadno přizpůsoben i pro jiné typy přístrojů HPF a cryo-SEM. Tato metoda umožňuje pozorování prostorové distribuce mikrobiálních buněk uvnitř vrstvy biofilmu a tím i kvantifikaci relativně velkých vzdáleností jejich vzájemného kontaktu, a zároveň hodnotit adhezní oblasti mikrobiálních buněk ke kultivačnímu substrátu, které indikují klíčovou roli vzniku extracelulární matrix. Další aplikací může být několikastupňová sublimace, při níž dochází k rozlišování oblastí biofilmu s vyšší a nižší koncentrací vody, což může přispět k porozumění samotné architektuře mikrobiálního biofilmu.

L i t e r a t u r a

[1] Deleo, F.; Otto, M. W., *Bacterial pathogenesis : methods and protocols*. Humana Press: Totowa, N.J., 2008.

[2] Donlan, R. M.; Costerton, J. W., Biofilms: Survival mechanisms of clinically relevant microorganisms. *Clin Microbiol Rev* **2002**, 15, (2).

[3] Holá, V.; Růžička, F.; Votava, M., The dynamics of *Staphylococcus epidermis* biofilm formation in relation to nutrition, temperature, and time. *Scripta Medica Facultatis Medicae Universitatis Brunensis Masarykianae* **2006**, 79, (3), 169–174.

[4] Schaudinn, C.; Stoodley, P.; Hall-Stoodley, L.; Gorur, A.; Remis, J.; Wu, S.; Auer, M.; Hertwig, S.; Guerrero-Given, D.; Hu, F. Z.; Ehrlich, G. D.; Costerton, J. W.; Robinson, D. H.; Webster, P.,

Death and Transfiguration in Static *Staphylococcus epidermidis* Cultures. *Plos One* **2014**, 9, (6), e100002.

[5] Dohnalkova, A. C.; Marshall, M. J.; Arey, B. W.; Williams, K. H.; Buck, E. C.; Fredrickson, J. K., Imaging hydrated microbial extracellular polymers: Comparative analysis by electron microscopy. *Appl Environ Microb* **2011**, 77, (4), 1254-1262.

[6] Lawrence, J. R.; Swerhone, G. D. W.; Leppard, G. G.; Araki, T.; Zhang, X.; West, M. M.; Hitchcock, A. P., Scanning transmission X-ray, laser scanning, and transmission electron microscopy mapping of the exopolymeric matrix of microbial biofilms. *Appl Environ Microb* **2003**, 69, (9), 5543–5554.

[7] Alhede, M.; Qvortrup, K.; Liebrechts, R.; Hoiby, N.; Givskov, M.; Bjarnsholt, T., Combination of microscopic techniques reveals a comprehensive visual impression of biofilm structure and composition. *Fems Immunol Med Mic* **2012**, 65, (2), 335-342.

[8] Hayat, M. A., *Principles and techniques of scanning electron microscopy. Biological applications. Volume 1*. Van Nostrand Reinhold Company.: 1974.

[9] Kuo, J., *Electron microscopy: Methods and protocols*. Springer Science & Business Media: 2007; Vol. 369.

[10] Webster, P.; Wu, S.; Webster, S.; Rich, K.; McDonald, K., Ultrastructural preservation of biofilms formed by non-typeable *Hemophilus influenzae*. *Method Enzymol* **2004**, 1, (03), 165–182.

[11] Galway, M. E.; Heckman Jr, J. W.; Hyde, G. J.; Fowke, L. C., Advances in High-Pressure and Plunge-Freeze Fixation. *Methods in Cell Biology* **1995**, 49, 3–19.

[12] Wu, Y.; Liang, J.; Rensing, K.; Chou, T. M.; Libera, M., Extracellular Matrix Reorganization during Cryo Preparation for Scanning Electron Microscope Imaging of *Staphylococcus aureus* Biofilms. *Microsc Microanal* **2014**, 20, (5), 1348–1355.

[13] Shimoni, E.; Muller, M., On optimizing high-pressure freezing: from heat transfer theory to a new microbiopsy device. *J Microsc* **1998**, 192, (3), 236–247.

[14] Studer, D.; Michel, M.; Muller, M., High-Pressure Freezing Comes of Age. *Scanning Microscopy* **1989**, 253–269.

[15] Walther, P., Cryo-fracturing and cryo-planing for in-lens cryo-SEM, using a newly designed diamond knife. *Microsc Microanal* **2003**, 9, (4), 279–285.

[16] Handley, K. M.; Turner, S. J.; Campbell, K. A.; Mountain, B. W., Silicifying Biofilm Exopolymers on a Hot-Spring Microstromatolite: Templating Nanometer-Thick Laminae. *Astrobiology* **2008**, 8, (4), 747–770.

[17] Azeredo, J.; Azevedo, N. F.; Briandet, R.; Cerca, N.; Coenye, T.; Costa, A. R.; Desvaux, M.; Di Bonaventura, G.; Hebraud, M.; Jaglic, Z.; Kacaniova, M.; Knochel, S.; Lourenco, A.; Mergulhao, F.; Meyer, R. L.; Nychas, G.; Simoes, M.; Tresse, O.; Sternberg, C., Critical review on biofilm methods. *Crit Rev Microbiol* **2017**, 43, (3), 313–351.

[18] Haque, F.; Alfatah, M.; Ganesan, K.; Bhattacharyya, M. S., Inhibitory Effect of Sophorolipid on *Candida albicans* Biofilm Formation and Hyphal Growth. *Sci Rep-Uk* **2016**, 6.

[19] Kaech, A.; Woelfel, M., Evaluation of Different Freezing Methods for Monolayer Cell Cultures. *Microsc Microanal* **2007**, 13, (S02), 240–241.

[20] Hrubanova, K.; Nebesarova, J.; Ruzicka, F.; Krzyzanek, V., The innovation of cryo-SEM freeze-fracturing methodology demonstrated on high pressure frozen biofilm. *Micron* **2018**, 110, 28–35.

[21] Ruzicka, F.; Horka, M.; Hola, V.; Kubesova, A.; Pavlik, T.; Votava, M., The differences in the isoelectric points of biofilm-positive and biofilm-negative *Candida parapsilosis* strains. *J Microbiol Meth* **2010**, 80, (3), 299–301.

Mgr. Kamila Hrubanová; Ing. Vladislav Krzyžánek, Ph.D.; Ústav přístrojové techniky AV ČR, v. v. i., Královopolská 147, 612 64 Brno; tel. +420 541 514 302; e-mail: hrubanova@isibrno.cz a krzyzanek@isibrno.cz

Jedná se o vědecký článek.

Obruča, S., Sedláček, P., Krzyžánek, V., Mravec, F., Hrubanová, K., Samek, O., Kučera, D., Benešová, P., Márová, I. Accumulation of Poly(3-hydroxybutyrate) Helps Bacterial Cells to Survive Freezing. PLoS ONE. 2016, 11(6), 0157778:1-16. E-ISSN 1932-6203
doi: 10.1371/journal.pone.0157778

Accumulation of Poly(3-hydroxybutyrate) Helps Bacterial Cells to Survive Freezing

**Stanislav Obruca[1]☯*, Petr Sedlacek[1]☯, Vladislav Krzyzanek[2], Filip Mravec[1],
Kamila Hrubanova[2], Ota Samek[2], Dan Kucera[1], Pavla Benesova[1], Ivana Marova[1]**

1 Materials Research Centre, Faculty of Chemistry, Brno University of Technology, Purkynova 118, 612 00,
Brno, Czech Republic, **2** Institute of Scientific Instruments, Academy of Sciences of The Czech Republic,
Vvi, Kralovopolska 147, 612 64, Brno, Czech Republic

☯ These authors contributed equally to this work.
* Stana.O@seznam.cz

Abstract

Accumulation of polyhydroxybutyrate (PHB) seems to be a common metabolic strategy
adopted by many bacteria to cope with cold environments. This work aimed at evaluating
and understanding the cryoprotective effect of PHB. At first a monomer of PHB, 3-hydroxy-
butyrate, was identified as a potent cryoprotectant capable of protecting model enzyme
(lipase), yeast (*Saccharomyces cerevisiae*) and bacterial cells (*Cupriavidus necator*)
against the adverse effects of freezing-thawing cycles. Further, the viability of the frozen–
thawed PHB accumulating strain of *C. necator* was compared to that of the PHB non-accu-
mulating mutant. The presence of PHB granules in cells was revealed to be a significant
advantage during freezing. This might be attributed to the higher intracellular level of 3-
hydroxybutyrate in PHB accumulating cells (due to the action of parallel PHB synthesis and
degradation, the so-called PHB cycle), but the cryoprotective effect of PHB granules seems
to be more complex. Since intracellular PHB granules retain highly flexible properties even
at extremely low temperatures (observed by cryo-SEM), it can be expected that PHB gran-
ules protect cells against injury from extracellular ice. Finally, thermal analysis indicates that
PHB-containing cells exhibit a higher rate of transmembrane water transport, which protects
cells against the formation of intracellular ice which usually has fatal consequences.

Introduction

Microorganisms are exposed to a series of various stress factors in the environment, among
which great temperature oscillations are very frequent. It should be noted that approximately
80% of our planet's biosphere is permanently cold with average temperatures below 5°C and
that even in the remaining regions the temperature fluctuates wildly, occasionally falling close
to, or even below 0°C [1]. Therefore, many microorganisms have developed sophisticated strat-
egies to help them endure low temperatures. These include the capacity to produce and accu-
mulate cryoprotectants, substances which are able to protect cells from the adverse effects of
freezing and low temperature [2]. There are numerous low molecular weight solutes (e.g.
amino acids and their derivatives, sugars, ectoines and their derivatives, etc.) as well as high

molecular weight substances (e.g. proteins and polysaccharides) which are produced by bacteria and exhibit cryoprotective properties [2, 3].

Low temperatures induce distinct responses among bacterial cells depending on the actual temperature. Exposure to cold conditions above 0°C is usually accompanied by an active response from bacterial cells. On the contrary, the response of most prokaryotes is passive at subzero temperatures, which is connected with the formation of ice [4]. As ice crystals grow, a process which occurs initially in the extracellular medium, the concentration of the solutes in the medium is excluded into an ever-decreasing solvent volume which results in effective osmotic stress. This induces so-called "freeze-dehydration" which is an important harmful consequence of cell freezing. Another important damaging mechanism identified during freezing of the cells is formation and propagation of intracellular ice. It is proposed that crystals of intracellular ice cause the physical destruction of membranes, formation of gas bubbles, and might also result in organelle disruption [3]. More generally, the survival of bacterial cells during freezing depends on the cooling rate. Cell survival is maximal when cooling occurs slowly enough to avoid formation of intracellular ice but fast enough to prevent causing injury to the cells by substantial dehydration [5]. Apart from dehydration and intracellular ice formation, cells can also be harmed by reactive oxygen species (ROS) formed in cells during freezing [6]. In addition, a decrease in the size of the unfrozen channels in ice during freezing can cause shrinkage of the cells, resulting in mechanical injury [7].

Polyhydroxyalkanoates (PHAs) are storage polymers accumulated in the form of intracellular granules by a wide range of taxonomically different groups of microorganisms. Among the wide variety of PHAs, the polyester of 3-hydroxybutyrate, poly(3-hydroxybutyrate) (PHB), is the most common and the best studied [8]. The biosynthesis and degradation of intracellular PHB occur in cells simultaneously, and therefore the metabolism of PHB exhibits a cyclic mechanism [9]. It is generally proposed that PHAs serve primarily as a carbon and energy storage material when exogenous carbon sources are depleted. However, there are reports that the capacity for intracellular PHA accumulation and degradation also enhances the resistance of bacterial cells to various stress conditions including low temperatures and freezing.

PHAs have been observed to be essential for maintenance of the redox state in the Antarctic bacterium *Pseudomonas* sp. 14–3 during low-temperature adaptation [10]. Iustman et al. isolated and studied the Antarctic strain *Pseudomonas extremaustralis*, whose high resistance to a wide range of stress conditions including cold was attributed to its capacity to produce PHB [11]. The PHB biosynthetic genes of the bacterium are located within an adaptive genomic island and were probably acquired by horizontal gene transfer, which suggests the importance of PHA accumulation in adaptation to stress conditions, such as those found in the extreme Antarctic environment [12]. Further, Pavez et al. reported that PHAs exert a protective effect against freezing in *Sphingopyxis chilensis* [13]. Numerous PHA-producing bacterial strains have also been isolated from Antarctic freshwater [14] and Antarctic soil [15], which indicates that PHA accumulation is a common metabolic strategy adopted by many bacteria to cope with cold environments.

Hence, in this work we investigated and assessed the potential protective mechanisms of PHB when bacterial cells are exposed to freezing and thawing. We have recently revealed the monomer of PHB– 3-hydroxybutyrate (3HB)–to be a very potent chemical chaperone capable of protecting model enzymes against heat-mediated denaturation and oxidative damage. Due to continuous PHB synthesis and degradation in bacterial cells (the so-called PHB cycle), the 3HB concentration in the PHB accumulating strain *Cupriavidus necator* was more than 16.5-fold higher than in the strain unable to accumulate PHA [16]. In this work, we tested the cryoprotective effect of 3HB for lipase as a model enzyme as well as for selected eukaryotic (*Saccharomyces cerevisiae*) and prokaryotic (*Cupriavids necator*) microorganisms. In addition,

using flow cytometry, thermal analysis, and Cryo-Scanning Electron Microscopy (Cryo-SEM), we tried to shed light on the complex role of intracellular PHB granules with respect to the survival of bacterial cells during freezing and thawing.

Materials and Methods

Materials and microorganisms

Trehalose, 3-hydroxybutyrate, p-nitrophenylpalmitate and lipase from *Rhizopusoryzea* were purchased from Sigma Aldrich, Germany. *Cupriavidus necator* H16 (CCM 3726) was obtained from the Czech Collection of Microorganisms, Brno, Czech Republic. The PHB non-producing strain *Cupriavidus necator* PHB^{-4} (DSM-541) was purchased from the Leibnitz Institute DSMZ-German Collection of Microorganism and Cell Cultures, Braunschweig, Germany. *Saccharomyces cerevisiae* CCY 21-4-47 was purchased from the Culture Collection of Yeast, Bratislava, Slovakia.

Screening of cryoprotective effect of 3HB for lipase against freezing-thawing treatment

Samples of lipase (0.4 mg/ml) in 100 mM of phosphate buffer (pH 7.4) were prepared in the presence (50 and 100 mM) or absence of 3HB and in presence of 100 mM trehalose. The freezing-thawing stabilizing effect of 3HB on lipase was studied by incubating the samples (initial volume 1 ml) at -30°C for 2 h and thawing them at 30°C. After each cycle, aliquots (100 μl) for the determination of residual activity were taken.

The enzyme activity of lipase samples was determined spectrophotometrically according to the established procedure described by Pinsirodom and Parkin with a slight modification [17]. The assays were performed in standard 96-well microplates; the reaction mixture consisted of 230 μL of 100 mM phosphate buffer pH 7.4, 25 μL of 420 μM p-nitrophenylpalmitate substrate solution and 25 μL of suitable diluted enzyme solution. The reaction was started by the addition of substrate and the formation of the product (p-nitrophenol) at 40°C was followed at 405 nm using a Biotek ELx808 microplate reader. Under the specified conditions, 1 unit of enzyme activity was defined as the amount of enzyme releasing 1 μmol of the product per minute. All the analyses were performed in triplicates.

Evaluation of the cryoprotective effect of 3HB for yeast and bacterial cells

The yeast culture *Saccharomyces cerevisiae* was cultivated (25°C, 140 rpm) in 250 mL Erlenmeyer flasks containing 100 mL of YPD medium (20 g/L glucose, 20 g/L peptone, 10 g/L yeast extract) for 24 hours. Then, 2 mL aliquots were taken, washed with PBS buffer, and re-suspended in PBS buffer in the absence or presence of 3HB (50 mM and 100 mM). The cell suspensions were frozen at -30°C for 2 h, then thawed at laboratory temperature and the viability of the yeast culture was analyzed immediately. We performed 5 subsequent freezing-thawing cycles, each sample prepared in triplicate. In a further experiment, we compared the cryoprotective effect of 100 mM of 3HB with trehalose and glycerol applied at the same concentration level. In this experiment, the yeast culture was adapted to the presence of cryoprotectants at 4°C for 1 h, after which freezing-thawing cycles were performed as described above.

Similar experiments were also performed with the PHB-producing bacterial strain *C. necator* H16 and its PHB non-accumulating mutant *C. necator* PHB^{-4}. Erlenmeyer flasks (volume 250 mL) containing 100 mL of Mineral Salt (MS) medium (the MS medium was composed of 20 g fructose, 3 g (NH$_4$)$_2$SO$_4$, 1 g KH$_2$PO$_4$, 11.1 g Na$_2$HPO$_4$· 12 H$_2$O, 0.2 g MgSO$_4$, 1 mL of

microelement solution and 1 L of distilled water; the microelement solution was composed of 9.7 g FeCl$_3$, 7.8 g CaCl$_2$, 0.156 g CuSO$_4 \cdot$ 5 H$_2$O, 0.119 g CoCl$_2$, 0.118 g NiCl$_2$ in 1 L of 0.1 M HCl) were inoculated with 5 mL of the overnight culture of the particular strain of *C. necator* grown in Nutrient Broth medium (NB medium: 10 g peptone, 10 g beef extract, 5 g NaCl in 1 L of distilled water). After 72 h of cultivation, 2 mL aliquots were taken, washed with PBS buffer, and re-suspended in PBS buffer in the absence or presence of 100 mM of 3HB. The cell suspensions were frozen at 30°C for 2 h, then thawed at laboratory temperature, and the viability of the bacterial culture was analyzed immediately. The freezing-thawing cycling was repeated 4 times, each sample prepared in triplicate. In addition, PHB content in the bacterial cultures was determined as described previously [18].

The capacity of *C. necator* H16 and *C. necator* PHB^{-4} to endure different freezing temperatures was also tested. Both bacterial strains were cultured as described above for 72 h, washed and re-suspended in PBS buffer, incubated at -5, -10, -15, and -20°C for 60 minutes, and thawed at laboratory temperature. After that, the viability of each bacterial culture was determined immediately.

The viability of yeast and bacterial cell populations was assessed by means of membrane integrity assay. Flow cytometry analysis using propidium iodide according to Coder was employed [19]. After each freezing-thawing cycle, 100 μl aliquots were taken, washed with PBS buffer, and diluted to a cell count of approx. 5·10^6 per ml. Then, 1 ml of cell suspension was stained by 1 μl of 1 mg/ml propidium iodide in the dark for 5 min. After that, the viability of the cells was analyzed by flow cytometry (Apogee A50, Apogee, GB) using a 488 nm laser for the excitation and the red channel (FL3) for the fluorescence detection.

Thermal analysis of bacterial cells

Basic calorimetric and thermogravimetric assays of bacterial samples were used in order to estimate whether the presence of PHB granules in cells can somehow affect the activity of the cellular water. For this purpose, we used bacterial cultures of *C. necator* H16 cultivated for 72 h in MS and NB medium, respectively. The fact that the strain does not accumulate PHB in NB medium is well documented [20] and was experimentally confirmed by the determination of the total PHB content in the cell by GC-FID as described previously [18]. Samples for the thermal analyses were always washed carefully with deionized water and centrifuged and the excess water was removed.

Differential scanning calorimetry was performed using a temperature-modulated calorimeter (DSC Q2000, TA Instruments, DE) equipped with an RCS90 cooling accessory and assessed by TA Universal Analysis 2000 software. All experiments were performed in hermetically sealed Tzero aluminum pans under a dynamic nitrogen atmosphere. Temperature-modulated DSC in the standard and quasi-isothermal modes, respectively, were applied in order to investigate the thermal effects of the freezing-thawing behavior of the bacterial cultures. In the former technique (MTDSC), the sample is cooled substantially from 20°C to -50°C and then heated back up with an underlying cooling/heating rate of 5°C/min and a temperature modulation of ± 1°C every 60 s. Quasi-isothermal temperature-modulated DSC (QiMTDSC; for details, see e.g. Otun et al. [21]) is a variant of traditional temperature-modulated DSC which involves the holding and modulation of a sample at a specific temperature for extended periods of time. This temperature can be increased or decreased incrementally in the course of the experiment. In the performed QiMTDSC experiment, samples were cooled down from 5°C to -30°C and heated back up in 1°C increments with an isotherm of 10 min at each increment. A temperature modulation of ±1°C every 60 s was applied.

Thermogravimetry (TGA, TA Instruments, Q5000IR) was used to determine the weight loss in the temperature interval 25–700°C under a dynamic dry air atmosphere with a heating

rate of 10°C/min. Weight loss in the interval 25–200°C was used to calculate the total water content in the samples. In addition, an isothermal TGA experiment at 60°C was performed in order to provide further comparison of the dynamics of the drying process for the samples under investigation.

Cryo-SEM

Bacterial cultures of *C. necator* H16 or *C. necator* PHB^{-4} grown on Petri dishes with the mineral medium described above were collected from agar plates, quickly frozen in liquid nitrogen and moved into a cryo-vacuum chamber (ACE600, Leica Microsystems), where they were freeze-fractured and briefly sublimated at -95°C. Further, the samples were moved at high vacuum using a shuttle (VCT100, Leica Microsystems) into a Scanning Electron Microscope (Magellan 400/L, FEI) equipped with a cold stage and the fractured structures were observed in a 1 keV electron beam at -135°C without any metal coating.

Results

Cryoprotective effect of 3HB for lipase

In our previous work, we observed that 3HB serves as a very effective protectant of enzymes (in particular, lipase from *Rhizopus oryzea* and lysozyme) against denaturation caused by high temperature and oxidative damage [16]. Hence, we also tested its cryoprotective efficiency using lipase–the same model enzyme. The enzyme was solubilized in phosphate buffer in the absence and presence of 3HB, which was tested at two concentration levels: 50 and 100 mM. Further, the enzyme was also tested in presence of well-established cryoprotectant trehalose, which was applied at 100 mM. The samples were subjected to repeated freezing-thawing cycles and the activity of the enzyme was determined after each cycle (Fig 1). The freezing-thawing treatment significantly reduced the activity of the enzyme in the control sample (without 3HB) which, after the 7th cycle, exhibited only 45.23% of its initial activity. In contrast, 3HB exhibited a significant concentration-dependent protective effect, since the relative enzyme activity was always higher when 3HB was present in the sample. The higher the dose of 3HB, the higher the enzyme activity that was observed. Surprisingly, when 100 mM of 3HB was applied, the relative enzyme activity of the enzyme in the sample actually increased during the initial 5 freezing-thawing cycles and a significant decrease in the activity was not observed until the 6th cycle; even after the 7th cycle the enzyme still possessed 87% of its relative activity. Protective effect of 100 mM 3HB is comparable to that of 100 mM trehalose, application of which also surprisingly increased enzyme activity during initial freezing-thawing cycles and after the 7th cycle 90% of its initial activity was recorded.

An increase in enzyme activity after freezing in presence of cryoprotectants was observed also by other authors and is ascribed to favorable conformation changes (partial unfolding) of enzyme at the level of active site and/or its neighborhood which leads to a higher affinity between enzyme and substrate [22, 23].

3HB as a protectant of *Saccharomyces cerevisiae*

In the first experiment, we demonstrated the cryoprotective activity of 3HB for enzymes. Therefore, we decided to test its ability also to protect whole cells against damage induced by freezing-thawing cycles. First, we utilized the yeast *Saccharomyces cerevisiae* as a model eukaryotic microorganism. Yeast cells suspended in PBS buffer with and without 3HB (50 and 100 mM) were repeatedly frozen at -30°C and thawed and the viability of the yeast culture was assayed after each cycle. Also in this case, 3HB exhibited a significant cryoprotective effect: the
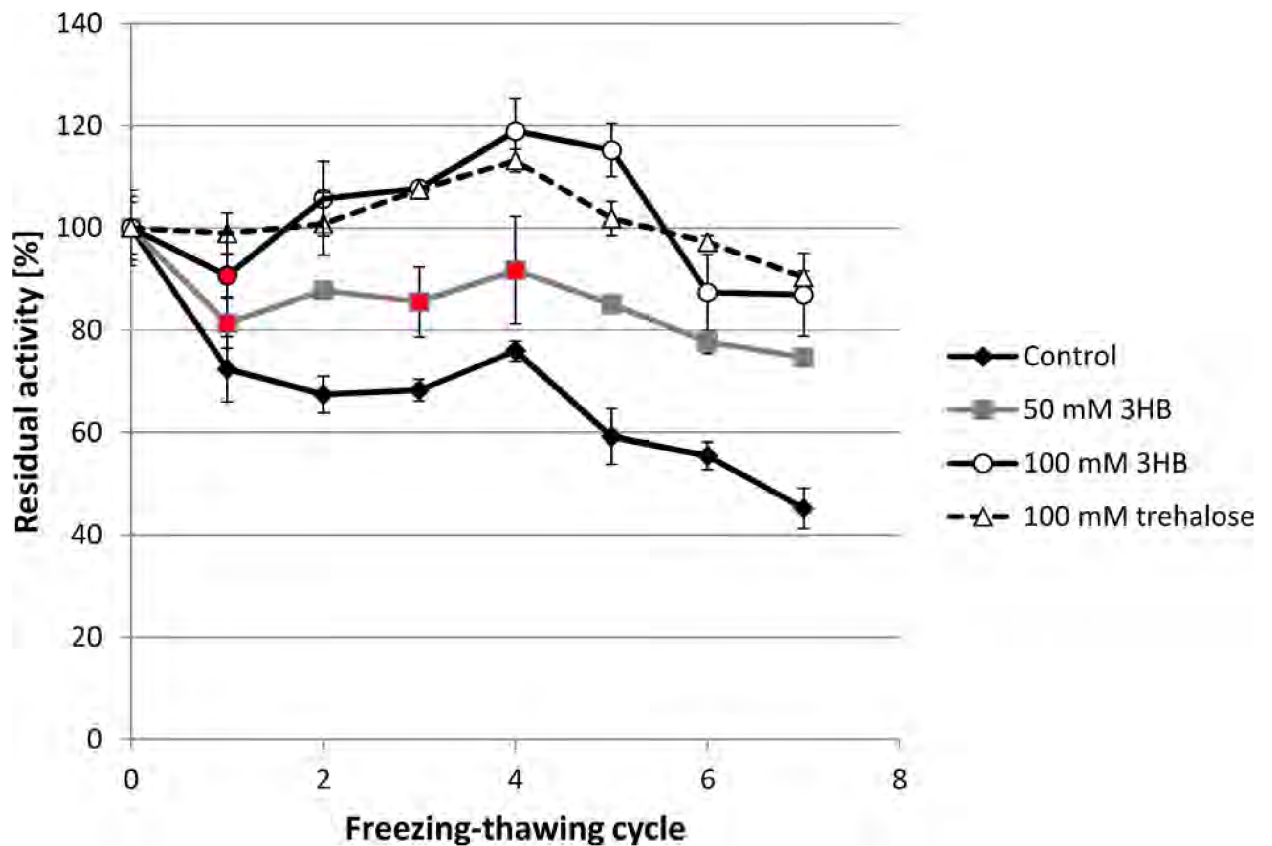
Fig 1. Effect of freezing-thawing treatment on the residual activity of lipase in the absence and presence of 50 mM and 100 mM 3HB. *note: Statistical significance was tested using 2 sample t-test (Minitab), each sample was compared with control, statistically insignificant results are labeled by red.

doi:10.1371/journal.pone.0157778.g001

viability of the yeast culture was always higher in the presence of 3HB than in the control culture (Fig 2A). After 5 freezing-thawing cycles, only 6% of cells in the control culture were viable, whereas the viabilities of the cultures with 50 and 100 mM 3HB were 48.7 and 57.1%, respectively.

In a further experiment, the cryoprotective effect of 3HB was compared with that of two other well-established cryoprotectants–trehalose and glycerol [3]. All the tested solutes were applied at a concentration of 100 mM. Unlike in the previous experiment, before exposure to the freezing-thawing cycles, the yeast culture was left to adapt to the cryoprotectants at 4°C for 1 h (the control culture was treated in the same manner). Such adaptation was reported to increase the effectiveness of most cryoprotectants [2]. A comparison of the protective effects of the tested solutes is presented in Fig 2B. All the tested solutes significantly enhanced the viability of the yeast culture in comparison with the control culture. After the 8th cycle, only 7.9% of cells in the control sample were viable, whereas the viability of yeast culture challenged in the presence of cryoprotectants did not fall below 60%. Among the tested cryoprotectants, 3HB exhibited the greatest protective effect, which was slightly greater than that of trehalose (the proportion of viable cells in the yeast culture after the 8th cycle was 79.3 and 76.0% in 3HB and trehalose, respectively). The protective effect of glycerol was less pronounced, with 61.7% of cells remaining viable after 8 freezing-thawing cycles. Hence, 3HB seems to be a very effective cryoprotectant, even in comparison with trehalose and glycerol, which are considered to be
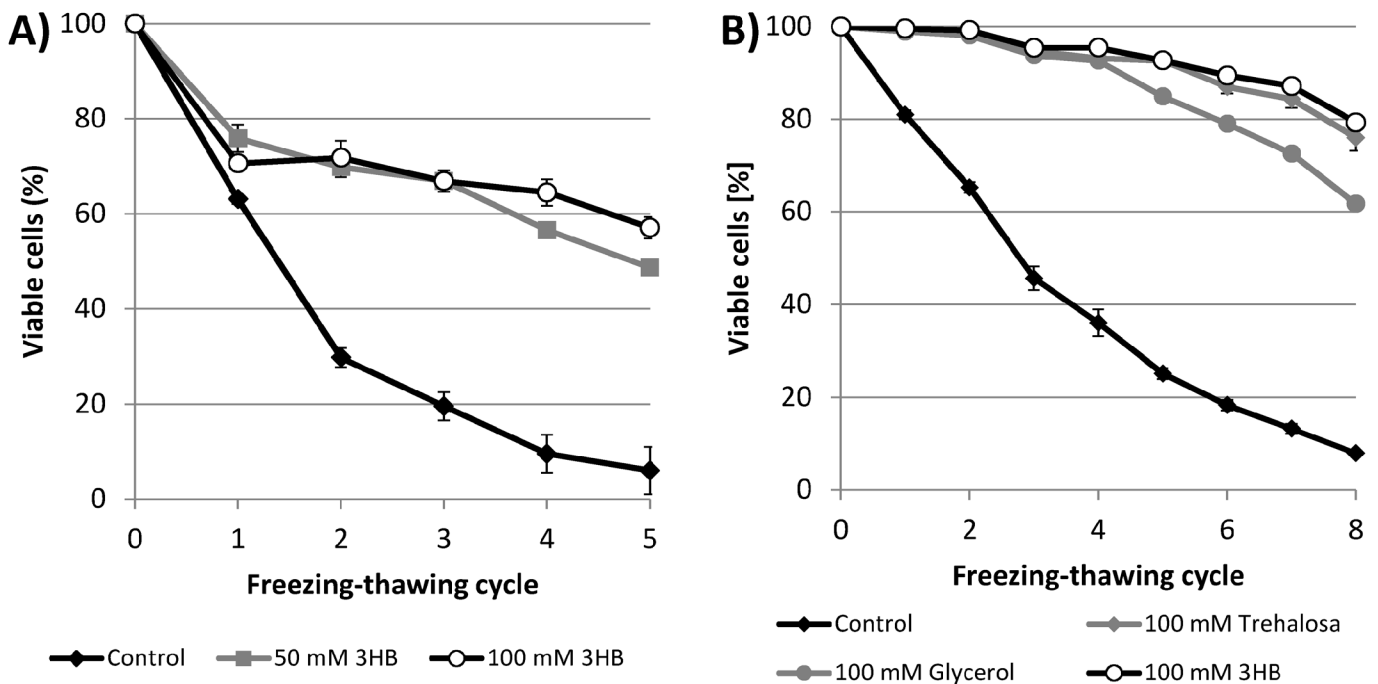
Fig 2. A) Viability of *S. cerevisiae* culture during freezing-thawing challenge in the presence of 3HB applied at 50 mM and 100 mM and in its absence B) Viability of the yeast culture exposed to repeated freezing-thawing in the presence of 3HB, trehalose and glycerol (all protectants were applied at 100 mM concentration) and in absence of a cryoprotectant. *note: Statistical significance was tested using 2 sample t-test (Minitab), each sample was compared with control, all the differences were found statistically significant.

natural cryoprotectants used by various microbes and are also routinely applied in the cryo-preservation of microorganisms [2; 24].

Cryoprotective effect of 3HB and PHB for *Cupriavidus necator*

The protective effect of 3HB during freezing-thawing cycles was also tested with two bacterial cultures: PHB-producing *Cupriavidus necator* H16 and its mutant strain *Cupriavidus necator* PHB^{-4}, which, due to a mutation of the gene encoding for PHB synthase, is not capable of accumulating PHB [25]. The bacterial cultures were cultivated for 72 h, at which point both cultures had reached the stationary phase of their growth. The PHB content in *C. necator* H16, determined by GC-FID, reached 76% of cell dry weight; the PHB content in the culture of *C. necator* PHB^{-4} was negligible (about 0.4% of cell dry weight). Both cultures were exposed to freezing-thawing cycles (the temperature of freezing was -30°C) suspended in PBS buffer in the presence or absence of 100 mM of 3HB. The results are shown in Fig 3A.

Similarly to the previous experiments with *S. cerevisiae*, the application of 3HB significantly improved the survival of both bacterial cultures, as compared to samples without 3HB. Moreover, we observed a significantly higher proportion of viable cells in the bacterial culture capable of accumulating PHB than in the PHB non-accumulating mutant in both experimental settings–with and without 3HB. In addition, bacterial cultures in the absence of 3HB revealed a different profile to their viability curves during the freezing-thawing challenge compared to yeast cultures or bacterial cultures with 3HB. In the yeast cultures and also in the bacterial cultures with 3HB, viability decreased more or less constantly during the whole freezing-thawing test. In contrast, without exogenous 3HB, most bacterial cells lost their viability during the first freezing-thawing cycle (the proportions of viable cells after the 1st cycle were 40.1 and 26.3% in
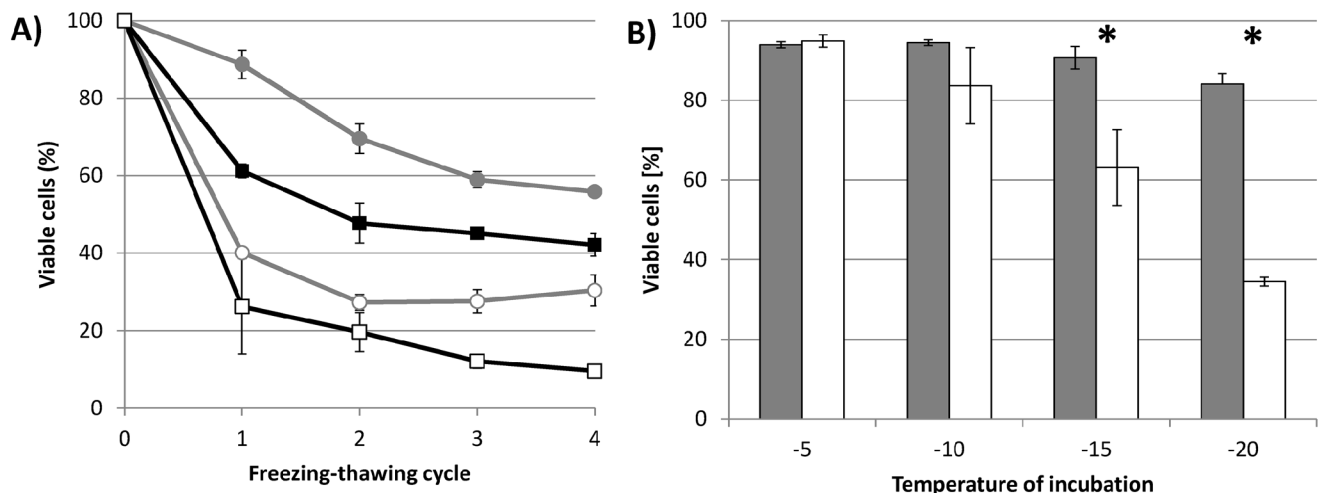
C. necator H16 and *C. necator* PHB^{-4}, respectively). After that the viability of the cultures remained constant or decreased only slowly.

Therefore, we decided to compare the resistance of both bacterial strains without the addition of 3HB during a single freezing-thawing cycle challenge in which different temperatures of freezing (-5, -10, -15, and -20°C) were applied. The bacterial strain capable of PHB accumulation revealed a significantly higher ability to endure freezing than its PHB non-producing mutant strain. With decreasing temperature the differences between the viabilities of the bacterial strains increased (see Fig 3B). When the bacterial strains were exposed to -5°C, the proportions of viable cells in *C. necator* H16 and *C. necator* PHB^{-4} were 94.0 and 94.9%, respectively. However, at -20°C, in the culture of *C. necator* H16 84.1% of cells retained viability, while only 34.5% of cells were identified as viable in *C. necator* PHB^{-4}. Hence, it seems that the presence of PHB granules in cell cytoplasm represents a significant advantage when the cells are exposed to subzero temperatures: the lower the temperature, the more pronounced the protective effect that was observed.

In addition, to investigate whether PHB granules are actively metabolized by bacterial culture *C. necator* H16 during repeated freezing-thawing, we performed experiment in which we determined PHB content in the bacterial culture after the each cycle; data are provided in S1 Fig. Since none decrease in the PHB content was observed, it can be stated that the bacterial culture did not utilize PHB granules to increase intracellular level of 3HB and it seems that in perspective of PHB metabolism response of the bacterial culture to repeated freezing is rather passive than active.

Observation of PHB granules by Cryo-SEM

Cryo-SEM is a very interesting technique providing an ultrastructural insight into various biological samples in a deeply-frozen state. Therefore, we used this method to investigate the morphology of frozen intracellular PHB granules. Fig 4 shows Cryo-SEM microphotographs of PHB non-containing (*C. necator* PHB^{-4}) and containing (*C. necator* H16) bacterial cells. In PHB-containing cells, needle-like plastic deformations were observed, while these structures

Fig 3. A) Viability of PHB-accumulating *C. necator* H16 and PHB non-accumulating *C. necator* PHB^{-4} exposed to repeated freezing-thawing challenge in the presence and absence of 100 mM 3HB. B) Viability of *C. necator* H16 and *C. necator* PHB^{-4} exposed to various sub-zero temperatures without addition of 3HB. *note: Statistical significance was tested using 2 sample t-test (Minitab). Presence of 3HB resulted in statistically significant increase in viability for both tested cultures and for all freezing-thawing cycles. Difference between viability of *C. necator* H16 and *C. necator* PHB–4 was statistically significant for all experimental conditions except for the initial 2 freezing-thawing cycles in absence of 3HB. In Fig 3B viability of *C. necator* H16 was compared with viability of *C. necator* PHB^{-4} for each temperature of incubation; statistically significant differences are labeled by asterisks.
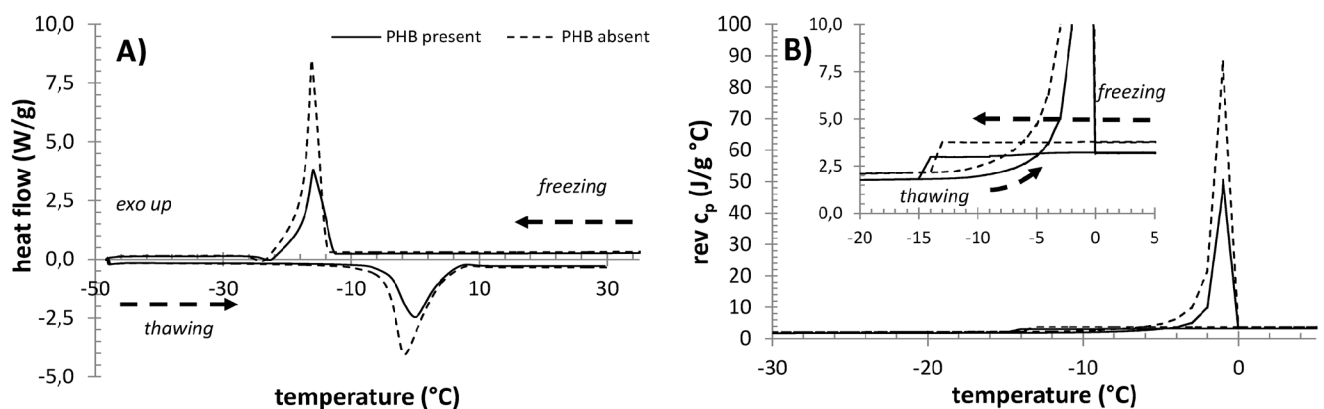
doi:10.1371/journal.pone.0157778.g003
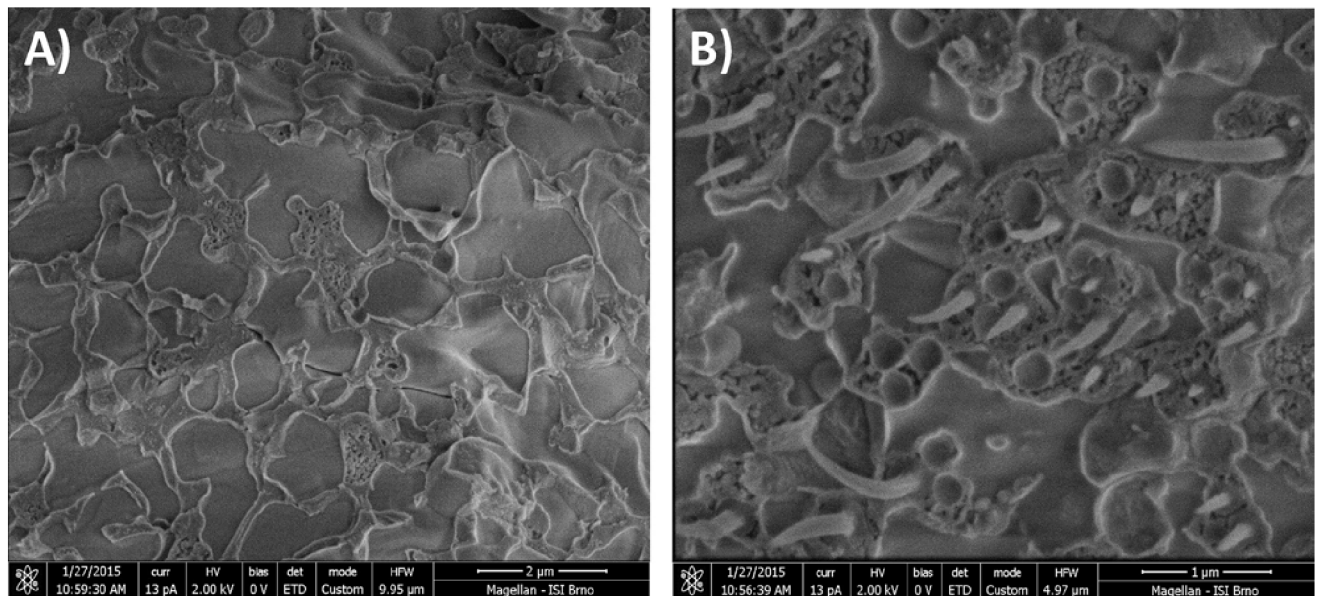
Fig 4. Cryo-SEM microphotographs of A) PHB non-producing *C. necator* PHB^{-4}, B) PHB-accumulating cells of *C. necator* H16.

were absent in cells without polymer, which indicates that these deformations can be clearly attributed to PHB granules. Employing the same experimental approach, similar structures were also observed by [26] in the PHA-producing bacteria *Comamonas acidovorans*. Despite the fact that the mechanism of the genesis of these deformations during freeze-fraction has not yet been explained, we can state that frozen PHB granules exhibit completely different mechanical and physico-chemical properties than any other components of bacterial cytoplasm and that their flexibility, even in deeply-frozen states, is significantly higher than that of PHB isolated from bacterial cells. When PHB polymer is extracted from cells, its elongation-to-break is about 4% [8], while in Cryo-SEM microphotographs we observed elongation corresponding to a value of more than 100%.

Effect of PHB on the freezing/melting of cellular water studied by DSC

A comparison of standard MTDSC thermograms recorded for *C. necator* H16 samples cultivated in the two different media is shown in Fig 5A. The freezing and thawing of water in the

Fig 5. Results of DSC analysis of centrifuged PHB-containing and PHB non-containing cultures of *C. necator*. A) MTDSC thermograms, B) QiMTDSC thermograms.

samples are represented by corresponding exotherms and endotherms, respectively. The shape and position of the freezing exotherm provide little information about the state of water in the system, because the freezing phenomenon is greatly affected by the inevitable and hardly reproducible effect of water supercooling. On the other hand, the endothermic signal, which corresponds to the melting of the frozen water, gives an interesting overview of the activity of water in the sample [27].

Two interesting observations can be derived from the thermograms shown in Fig 5A. First, the melting endotherm which corresponds to the culture sample containing PHB granules is shifted to higher temperatures. Second, the total area of the endotherm (which represents the weight-specific heat consumed during the water melting) is significantly lower. The latter feature is easily explainable by the fact that the relative water content in PHB-containing cells is naturally lower, which correspondingly decreases the area of the ice-melting endotherm. The specific heats of fusion of water in the samples, which were calculated from the total area of the melting endotherm and from the total water content in the sample determined by TGA analysis (see below), did not show any significant differences either between the two analyzed samples or in comparison with the heat of fusion of pure water. This indicates that neither of the samples contains any significant amount of water which does not freeze (often referred to as non-freezing water).

On the other hand, the shift of the ice-melting endotherm towards higher temperatures for the MS medium-cultivated culture represents a significant experimental finding. It was demonstrated that the shift is reproducible–it was found repeatedly, no matter which particular DSC protocol was applied. In all these experiments, not only the peak but also the onset point of the endotherm was always shifted. The particular magnitude of the shift depended on the experimental conditions, e.g. the heating rate. For the results shown in Fig 5A, the peak of the endotherm was shifted by approx. 1.5°C.

An invaluable feature of MTDSC analysis is that it allows separation of the heat-flow signals related to reversible and non-reversible processes, respectively. The deconvolution of the total heat-flow signal, presented in Fig 5A, is shown in S2 Fig. The results of this deconvolution confirm that the freezing of water in the samples is an almost completely non-reversible process that is caused by the above-mentioned supercooling of liquid water. On the other hand, a further difference in the water-melting process between the PHB-containing and non-containing cultures was revealed: the non-reversible component of the melting signal in the absence of PHB was significantly more pronounced.

Effect of PHB on the drying of cells studied by TGA

TGA analysis was utilized in this study to provide further information on the activity of water in the studied bacterial cultures. Fig 6A shows the complete thermograms of PHB-containing and non-containing cells. The presence of PHB in the culture is evident from the significant weight loss at about 300°C, where the labile organic components of the cells (including PHB) are degraded. Additionally, it can be seen that the weight loss step associated with the drying of the sample is completed below 200°C. The total relative content of water, determined from the weight loss in this temperature interval, naturally differed for the two compared bacterial cultures. Nevertheless, when the content of PHB is excluded and the water content is given relative to the residual dry content of the cell, no important difference between the two samples is found. This shows that the presence of PHB granules does not significantly affect the total content of intracellular water.

Nevertheless, it has been proposed by several authors (e.g. by Uribelarrea et al. [28]) that TGA can be used also for the determination of different forms of water in cell samples. For this purpose, the derivation of water loss with temperature or time (i.e. the rate of drying of the
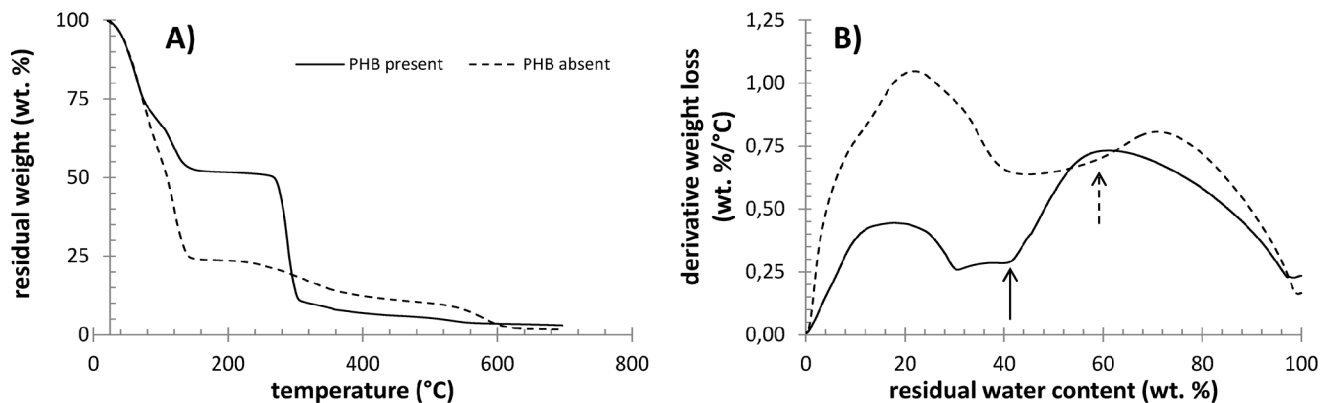
Fig 6. Results of dynamic TGA analysis of centrifuged PHB-containing and PHB non-containing cultures of *C. necator*. A) Weight loss at a heating rate of 10°C/min in the interval 25–700°C, B) derivative weight loss as a function of residual water content (arrows indicate critical water content).

sample) is given as a function of residual water content in the sample, and the critical points of this dependence are taken to be the indicators of moments at which a change in the mechanism of the drying process occurs. It can be seen in Fig 6B that these points can also be found for the tested samples. The arrows in the figure indicate the first critical point of the respective drying curve, when the release of the least strongly bound water is completed.

Discussion

In our previous study we identified 3HB as a very potent chemical chaperone capable of protecting lipase and lysozyme against adverse effects of heat and oxidative damage [16]. Hence, we decided also to test its cryoprotective efficiency for enzymes as well as whole microbial cells. Cryoprotective ability has been observed for a wide spectrum of compatible solutes which are produced and accumulated by various microorganisms to cope with ubiquitous environmental stresses such as high osmolality or temperature fluctuations [29, 30]. The cryoprotective ability of these molecules is not only scientifically interesting from a general stress-response point of view, it also has potential practical applications since proteins and other biological molecules as well as whole cells are routinely preserved in a frozen state. Hence, the application of appropriate cryoprotectants can help to maintain the activity and/or viability of preserved biological samples [2, 31].

Freezing-thawing represents a complex combination of several stress factors which reduce the activity of enzymes. Apart from low temperature and the formation of ice crystals, proteins can also be damaged by increasing concentrations of buffer salts and co-solutes which is accompanied by pH changes and increase of ionic strength [32]. Compatible solutes are usually classified as kosmotropes, which means that interactions of a compatible solute and water are stronger than water-water interaction. This effect on the water network and the ordering of water molecules by compatible solutes, therefore, affect the process of ice formation, thus providing their cryoprotective effect [24, 30]. Furthermore, compatible solutes are capable of stabilizing enzymes by affecting their hydration shell, which might provide protection not only against the adverse effects of low temperature, but also the effects of high osmolality and pH changes, as was reported for ectoines and trehalose by Van Thouc et al. [33].

Although 3HB is usually not ascribed as a typical compatible solute, it seems to be a very efficient cryoprotectant of our model enzyme–lipase from *Rhizopus oryzea* (Fig 1). When 3HB was added at a 100 mM concentration, it was capable of completely protecting lipase against

freezing-thawing mediated damage during the initial 5 freezing-thawing cycles, while in non-protected lipase we observed a decrease in relative activity to 59% of its initial value. Soto et al., reported that 3HB exhibited chemical chaperone activity preventing the aggregation of proteins of *Pseudomonas* sp. CT13 under combined salt and thermal stress [34]. However, to our knowledge, despite the fact that its cryoprotective efficiency is obvious, there are no reports regarding the cryoprotective activity of 3HB.

In comparison with enzymes, the spectrum of potential stresses associated with freezing of the whole cells becomes even wider. During freezing, cells experience either cellular dehydration (as a result of extracellular ice formation and consequent water transport driven by the resulting osmolality difference) or intracellular ice formation (IIF). These factors are oppositely dependent on the cooling rate during freezing (slow cooling leads to dehydration and fast cooling to IIF). While IIF is practically always lethal (cells have a finite volume; the expansion of water during freezing leads to rupture of the cell membrane), dehydration induces different cellular responses according to the particular freezing conditions–above all, the cooling rate [35]. Consequently, extensive cell dehydration causes freezing injury due to exposure to high concentrations of solute, while, on the other hand, partial cell dehydration protects the cell from IIF and is therefore used as a crucial step in cryopreservation protocols [5]. Obviously, the dynamics of the freezing process and of the cell response are crucial for cell survival.

Because of the complex nature of cell freezing, effective cryoprotectants should undertake multiple protective actions [2]. Our results show that 3HB served as a very potent cryoprotectant for *S. cerevisiae* cells (Fig 2); its protective efficiency was comparable with that of glycerol and trehalose, which are routinely used for the cryopreservation of microorganisms. Furthermore, 3HB exhibited even slightly higher cryoprotective activity than trehalose, itself suggested by Jain and Roy to be one of the best cryoprotectants known [24].

Apart from the mechanisms mentioned above, reactive oxygen species (ROS), generated as a consequence of an impaired aerobic respiration chain, also significantly contribute to the injury of cells during the freezing-thawing process [6]. In our previous study we observed that 3HB is, similarly to other compatible solutes such as ectoines [36], capable of protecting model enzymes from oxidative damage cause by hydrogen peroxide or heavy metals [16]. Hence, this important feature can also contribute to the cryoprotective activity of 3HB in yeast cells.

In a further experiment, we tested the cryoprotective potential of 3HB using two bacterial strains, PHB-producing *C. necator* H16 and its PHB non-accumulating mutant strain *C. necator* PHB^{-4}. Similarly as in the yeast culture, and also in both bacterial cultures, the addition of 100 mM 3HB increased the proportion of non-damaged cells in freezing-thawing tests compared with cultures challenged in the absence of 3HB. This observation demonstrates the effectiveness of 3HB as a cryoprotectant of whole microbial cells and shows that 3HB also works in bacterial cells.

However, we also observed a significant difference in the viability of the tested bacterial cultures in the absence of exogenous 3HB. The PHB-producing strain *C. necator* H16 exhibited superior viability to its PHB non-accumulating strain during the entire freezing-thawing test. Thus, it seems that intracellular reserves of PHB also play an important role in the freezing survival of bacteria, which is in agreement with the observations of other authors. Pavez et al. identified PHA accumulation in the bacterium *Sphingopyxis chilensis* (isolated from an oligotrophic aquatic environment where the temperature oscillates around 0°C) as the most important feature protecting cells from freezing conditions [13]. Moreover, PHA-producing bacteria were isolated from Antarctic freshwater [14] and Antarctic soil [15] confirming PHA accumulation as an efficient adaptation strategy for avoiding damage produced by intracellular ice crystals, oxygen-reactive species, and severe dehydration. When exposed to low temperatures, PHAs were observed to be essential for maintenance of the redox state in the Antarctic bacterium *Pseudomonas* sp. 14–3 [10]. In addition, there are several reports describing the

connection between PHA metabolism and cellular alternative sigma factor RpoS stimulating the expression of general stress response-associated genes [11, 37, 38]. Recently, Mezzina et al. reported that phasin, PHA granules associated protein of *Azotobacter* sp. FA-8, revealed chaperone-like activity in-vivo as well as in vitro [39]. However, in our opinion, the cryoprotective mechanism of PHAs is even more complex and is not yet completely understood.

Previously we reported that PHB-accumulating bacterial strain *C. necator* H16 contains a 16.5-fold higher intracellular level of 3HB than its PHB non-accumulating mutant. We estimated the intracellular concentration of 3HB in PHB-accumulating strains to exceed 100 mM [16]. Considering the cryoprotective capacity of 3HB, a complete and functional PHB cycle might be a very important factor providing a naturally higher level of cryoprotectant in cytoplasm. This might substantially contribute to the greater freezing survival of PHB-producing bacterial strains. Nonetheless, it seems that *C. necator* H16 does not actively hydrolyze PHB granules (S1 Fig) to enhance intracellular concentration of 3HB when exposed to repeated freezing, which is in agreement with general expectation that the response of microbial cells to subzero temperatures is usually passive [4].

It is likely that the involvement of PHB in subzero temperature survival is much more complex still. Goh et al. observed that *E. coli* cells harboring PHA biosynthetic genes of *C. necator* but unable to mobilize PHAs exhibited higher stress resistance to oxidative stress [40]. This indicates that only the presence of intracellular PHA granules significantly changes the properties of bacterial cells and influences their stress survival.

Bonthrone et al. reported that intracellular native PHA granules do not comprise rigid, non-flexible, highly crystalized polymer, but are rather formed by highly mobile amorphous elastomer, which is reminiscent of supercooled liquid in terms of its properties [41]. This is in agreement with the extremely flexible behavior of PHB observed by Cryo-SEM (Fig 5). Despite the fact that cells of *C. necator* H16 were fractured at very low temperature (-140°C), we observed pull-out structures corresponding to the elongation of PHB granules of more than 100%. It should be noted that PHB isolated from bacterial cells rapidly crystallizes and its elongation-to-break is about 4% [8]. Hence, intracellular native PHB granules exhibit unique properties which might also provide physical protection of cells against the formation of ice crystals and shearing-stress associated with the freezing of extracellular water. Mazur et al. stated that expanding ice fields during extracellular water freezing results in a decrease in the sizes of unfrozen channels, which may cause shrinkage, deformation, and injury of the cells. PHB granules might represent a highly flexible scaffold protecting bacterial cells from such harm [7].

Our thermal analytical study of bacterial cells also provides some indications of the influence of PHB granules on the state of intracellular water. The shift in the melting endotherm in the MTDSC thermogram to higher temperature, which was observed for the culture containing PHB granules, cannot be revealed solely on the basis of the results of thermal analysis. Nevertheless, several suggestions can be made. One possible explanation is that this effect is related to an alteration of the adhesive forces between water and cellular components in the presence and absence of PHB. The stronger the adhesive force, the more the water molecules are "pulled out" from the ice crystals and the lower the temperature at which the ice melts. Therefore, it can be hypothesized that the "dilution" of the strongly hydrophilic species in the intracellular space by the less hydrophilic surfaces of PHB granules can partially lower the strength of the hydration of the remaining solutes. Deconvolution of the MTDSC signal leads to the similar conclusion. Stronger non-reversible component of the melting signal in the absence of PHB supports the assumption that the released water is more strongly attracted to the cellular components in these cultures than in PHB-containing bacteria.

Also the thermogravimetric analysis of the cell drying experiments revealed similar differences in the state of water between the PHB accumulating and non-accumulation cultures. It is evident from the critical points shown in Fig 6B that the relative content of the least strongly
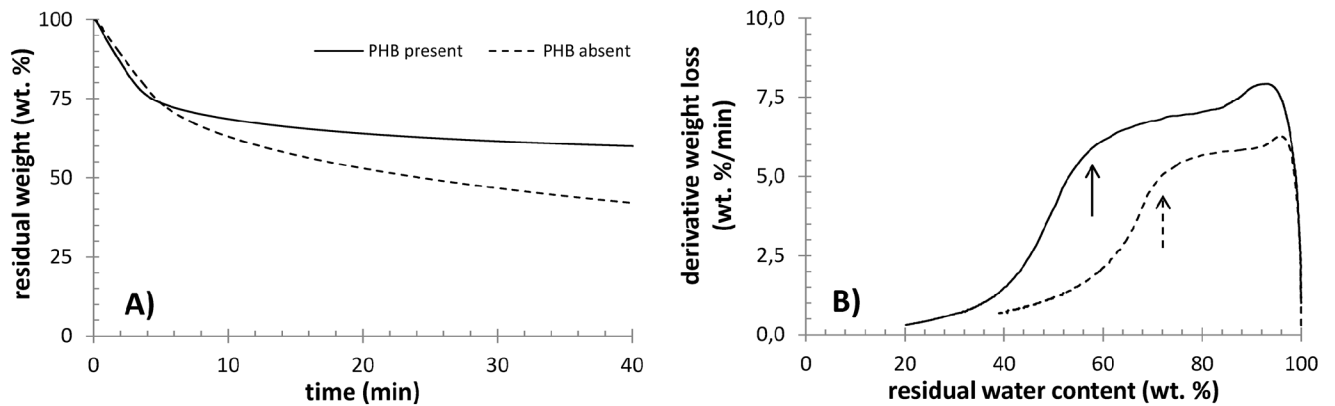
Fig 7. Results of isothermal TGA analysis of centrifuged PHB containing and PHB non-containing cultures of *C. necator*. A) Weight loss at 60°C, B) derivative weight loss as a function of residual water content (arrows indicate critical water content).

doi:10.1371/journal.pone.0157778.g007

bound form of water is higher in PHB-containing bacteria. The same conclusion can be drawn from the results of the isothermal drying experiment, which are presented in Fig 7. Comparison of Figs 6B and 7B indicates that the content of this form of water in the sample depends on the experimental conditions under which the drying occurred. This idea supports the assumption that this drying step is related to water which undergoes a kind of dynamic process such as transport through the cell membrane, desorption from the cell surface, etc.

In sum, the results of calorimetric and thermogravimetric analyses indicate that PHB-containing cells include water which can be more freely released from the cell either during drying or freezing. As discussed above, cell dehydration has diverse effects on cell survival according to the particular freezing conditions. When the cell faces severe dehydration, harmful solute effects cause the cell injury. On the other hand, when water release from the cell is completely suppressed, intracellular ice formation is not prevented and cell damage results from the rupture of the cell membrane. It is well documented that when the influence of the cooling rate is studied, the typical "inverted U" survival curve is obtained for a cell culture [7]. Obviously, a complex balance between the dynamics of external freezing stimuli (represented, for instance, by the rate of cooling) and cell response (the rate of dehydration) is needed in order to minimize the resulting cell mortality. Consequently, the effect of the presence of PHB granules on the state of water inside the cell and on the rate of its transmembrane transport may represent an important contribution to the overall cryoprotective strategy of PHB-producing bacteria.

Supporting Information

S1 Fig. Determination of PHB content (expressed as % of cell dry weight (CDW)) in *C. necator* H16 during freezing-thawing treatment (-30°C).
(DOCX)

S2 Fig. Results of the deconvolution of total MTDSC signals from Fig 5A into reversible (A) and non-reversible (B) components.
(DOCX)

Acknowledgments

Author Contributions

Conceived and designed the experiments: SO PS OS. Performed the experiments: SO PS VK FM KH DK PB. Analyzed the data: SO PS IM. Contributed reagents/materials/analysis tools: VK FM DK PB. Wrote the paper: SO PS VK OS IM.

References

1. De Maayer P, Anderson D, Cary C, Cowan DA. Some like it cold: understanding the survival strategies of psychrophiles. EMBO reports. 2014; 15: 508–517. doi: 10.1002/embr.201338170 PMID: 24671034

2. Hubalek Z. Protectants used in the cryopreservation of microorganisms. Cryobiology. 2003; 46: 205–229. PMID: 12818211

3. Fuller BJ. Cryoprotectants: The essential antifreezes to protect life in the frozen state. CryoLetters. 2004; 25: 375–388. PMID: 15660165

4. Panoff JM, Thammavongs B, Gueguen M, Boutibonnes P. Cold stress responses in mesophilicbacteria. Cryobiology. 1998; 36: 75–83. PMID: 9527869

5. Mori S, Choi J, Devireddy RV, Bischof JC. Calorimetric measurement of water transport and intracellular ice formation during freezing in cell suspension. Cryobiology. 2012; 65: 242–255. doi: 10.1016/j.cryobiol.2012.06.010 PMID: 22863747

6. Baek KH, Skinner DZ. Production of reactive oxygen species by freezing stress and the protective roles of antioxidant enzymes in plants. J Agric Chem Environ. 2012; 1: 34–40.

7. Mazur P. Freezing of living cells: mechanisms and implications. Am J Physiol. 1984; 247: C125–C142. PMID: 6383068

8. Sudesh K, Abe H, Do Y. Synthesis, structure and properties of polyhydroxyalkanoates: biological polyesters. Prog Polym Sci. 2000; 25: 1503–1555.

9. Kadouri D, Jurkevitch E, Okon Y. Ecological and agricultural significance of bacterial polyhydroxyalkanoates. Crit Rev Microbiol. 2005; 31: 55–67. PMID: 15986831

10. Ayub ND, Tribelli PM, Lopez NI. Polyhydroxyalkanoates are essential for maintenance of redox state in the Antarctic bacterium Pseudomonas sp. 14–3 during low temperature adaptation. Extremophiles. 2009; 13: 59–66. doi: 10.1007/s00792-008-0197-z PMID: 18931822

11. Iustman LJR, Ruiz JA. The alternative sigma factor σ^s, affects polyhydroxyalkanoate metabolism in *Pseudomonas putida*. FEMS Microbiol Lett. 2008; 284: 218–224. doi: 10.1111/j.1574-6968.2008.01203.x PMID: 18498401

12. Ayub ND, Pettinari MJ, Mendez BS, Lopez NI. The polyhydroxyalkanoate genes of a stress resistant Antarctic *Pseudomonas* are situated within a genomic island. Plasmid. 2007; 58: 240–248. PMID: 17629557

13. Pavez P, Castillo JL, Gonzales C, Martinez M. Poly-β-hydroxyalkanoate exert protective effect against carbon starvation and frozen coditions in *Sphingopyxischilensis*. Curr Microbiol. 2009; 59: 636–640. doi: 10.1007/s00284-009-9485-9 PMID: 19727947

14. Ciesielski S, Gorniak D, Mozejko J, Swiatecky A, Grzesiak J, Zdanowski M. The diversity of bacteria isolated from Antarctic freshwater reservoirs possessing the ability to produce polyhydroxyalkanoates. Curr Microbiol. 2014; 69: 594–603. doi: 10.1007/s00284-014-0629-1 PMID: 24939384

15. Goh YS, Tan IKP. Polyhydroxyalkanoate production by antarctic soil bacteria isolated from Casey Station and Signy Island. Microbial Res. 2012; 167: 211–219.

16. Obruca S, Sedlacek P, Mravec F, Samek O, Marova I. Evaluation of 3-hydroxybutyrate as an enzyme-protective agent against heating and oxidative damage and its potential role in stress response of poly (3-hydroxybutyrate) accumulating cells. Appl Microbiol Biotechnol. 2016; 100: 1365–1376. doi: 10.1007/s00253-015-7162-4 PMID: 26590589

17. Pinsirodom P, Parkin KL. Lipase assays. Current Protocols in Food Analytical Chemistry. 2001; C3.1.1–C3.1.13.

18. Obruca S, Petrik S, Benesova P, Svoboda Z, Eremka L, Marova I. Utilization of oil extracted from spent coffee grounds for sustainable production of polyhydroxyalkanoates. Appl Microbiol Biotechnol. 2014; 98: 5883–8590. doi: 10.1007/s00253-014-5653-3 PMID: 24652066

19. Coder DM. Assessment of Cell Viability. Current Protocols in Cytometry. 1997;9.2.1–9.2.14

20. Jendrossek D, Pfeiffer D. New insights in the formation of polyhydroxyalkanoate granules (carbonosomes) and novel functions of poly(3-hydroxybutyrate). Environ Microbiol. 2014; 16: 2357–2373. doi: 10.1111/1462-2920.12356 PMID: 24329995

21. Otun SO, Meehan E, Sheng Q, Craig DQM. The Use of quasi-isothermal modulated temperature differential scanning calorimetry for the characterization of slow crystallization processes in lipid-based solid self-emulsifying systems. Pharm Res. 2015; 32: 1316–1324. doi: 10.1007/s11095-014-1535-8 PMID: 25330742

22. Tamiya T, Okahashi N, Sakuma R, Aoyama T, Akahane T, Matsumoto JJ. Freeze denaturation of enzymes and its prevention with additives. Cryobiology. 1985; 22: 446–456. PMID: 2932302

23. Breda M, Vitolo M, Duranti MA, Pitombo RNM. Effect of freezing-thawing on invertase activity. Cryobiology. 1992; 29: 281–290.

24. Jain NK, Roy I. Effect of trehalose on protein structure. Protein Science. 2009; 18:24–36. doi: 10.1002/pro.3 PMID: 19177348

25. Raberg M, Voigt B, Hecker M, Steinbuchel A. A closer look on the polyhydroxybutyrate- (PHB-) negative phenotype of *Ralstonia eutropha* PHB-4. PLOS One. 2014; 9: e95907. doi: 10.1371/journal.pone.0095907 PMID: 24787649

26. Sudesh K, Fukui T, Iwata T, Doi Y. Factors affecting the freeze-fracture morphology of in vivo polyhydroxyalknoate granules. Can J Microbiol. 2000; 46: 304–311. PMID: 10779866

27. Seki S, Kleinhans FW, Mazur P. Intracellular ice formation in yeast cells vs. cooling rate: Predictions from modeling vs. experimental observations by differential scanning calorimetry. Cryobiology. 2009; 58: 157–165. doi: 10.1016/j.cryobiol.2008.11.011 PMID: 19118541

28. Uribelarrea JL, Pacaud S, Goma G. New Method for Measuring the Cell Water-Content by Thermogravimetry. Biotechnol Lett. 1985; 7: 75–80.

29. Roberts MF. Organic compatible solutes of halotolerant and halophilic microorganisms. Saline Systems. 2005; 1: 5. PMID: 16176595

30. Pastor JM, Salvador M, Argandona M, Bernal V, Reina-Bueno M, Csonka LN, et al. Ectoines in cell stress protection: uses and biotechnological production. Biotechnol Adv. 2010; 28: 782–801. doi: 10.1016/j.biotechadv.2010.06.005 PMID: 20600783

31. Sorokulova I, Olesen E, Vodyanoy V. Biopolymers for sample collection, protection, and preservation. Appl Microbiol Biotechnol. 2015; 99: 5397–5406. doi: 10.1007/s00253-015-6681-3 PMID: 25982001

32. Goller K, Galinski EA. Protection of a model enzyme (lactate dehydrogenase) against heat, urea and freeze-thaw treatment by compatible solutes additives. J MolCatal B: Enzym. 1999; 7: 37–45.

33. Van-Thuoc D, Hashim SO, Hatti-Kaul R, Mamo G. Ectoine-mediated protection of enzyme from the effect of pH and temperature stress: a study using *Bacillus halodurans* xylanase as a model. Appl Microbiol Biotechnol. 2013; 97: 6271–6278. doi: 10.1007/s00253-012-4528-8 PMID: 23132342

34. Soto G, Setten L, Lisi C, Maurelis C, Mozzicafreddo M, et al. Hydroxybutyrate prevents protein aggregation in the halotolerant bacterium *Pseudomonas* sp. CT13 under abiotic stress. Exremophiles. 2012; 16: 455–462.

35. Mazur P. Cryobiology–Freezing of biological systems. Science. 1970; 168:939–949. PMID: 5462399

36. Andersson MM, Breccia JD, Hatti-Kaul R. Stabilizing effect of chemical additives against oxidation of lactate dehydrogenase. Biotechnol Appl Biochem. 2000; 32: 145–153. PMID: 11115385

37. Ruiz JA, Lopez NI, Fernandez RO, Mendez BS. Polyhydroxyalkanoate degradation is associated with nucleotide accumulation and enhances stress resistance and survival of *Pseudomonas oleovorans* in natural water microcosm. Appl Environ Microbiol. 2001; 67: 225–230. PMID: 11133449

38. Brigham CJ, Speth DR, Rha CK, Sinskey AJ. Whole-genome microarray and gene deletion studies reveal regulation of the polyhydroxyalkanoate production cycle by the stringent response in *Ralstonia eutropha* H16. Appl Environ Microbiol. 2012; 78: 8033–8044. doi: 10.1128/AEM.01693-12 PMID: 22961894

39. Mezzina MP, Wetzler DE, de Almeida A, Dinjaski N, Prieto MA, Pettinari MJ. A phasin with extra talents: a polyhydroxyalkanoates granule-associated protein has chaperone activity. Environmental Microbiology. 2015; 17: 1765–1776. doi: 10.1111/1462-2920.12636 PMID: 25297625

40. Goh L-K, Purama RK, Sudesh K, Hunter BK, Sanders JKM. Enhancement of Stress Tolerance in the Polyhydroxyalkanoate Producers without Mobilization of the Accumulated Granules. Applied Biochemistry and Biotechnology. 2014; 172(3): 1585–1598. doi: 10.1007/s12010-013-0634-z PMID: 24233544

41. Bonthrone KM, Clauss J, Horowitz DM, Hunter BK, Sanders JKM. The biological and physical chemistry of polyhydroxyalkanoates as seen by NMR spectroscopy. FEMS Microbiology Letters. 1992; 103(2–4): 269–277.

Krzyžánek, V., Skoupý, R., <u>Hrubanová, K</u>. Sestava pro regulaci teploty vzorku. 2018. Brno : Ústav přístrojovén techniky AV ČR, v.v.i., 07.11.2018. 32258. https://isdv.upv.cz/doc/FullFiles/UtilityModels/FullDocuments/FDUM0032/uv032258.pdf

UŽITNÝ VZOR

(19)
ČESKÁ
REPUBLIKA

ÚŘAD
PRŮMYSLOVÉHO
VLASTNICTVÍ

(73) Majitel:
Ústav přístrojové techniky Akademie věd České republiky, v. v. i., Brno, Královo Pole, CZ

(72) Původce:
Ing. Vladislav Krzyžánek, Ph.D., Brno, Královo Pole, CZ
Mgr. Ing. Radim Skoupý, Bystřice nad Pernštejnem, CZ
Mgr. Kamila Hrubanová, Tišnov, CZ

(74) Zástupce:
Kania, Sedlak, Smola - Patentová kancelář, Ing Tomáš Benda, Mendlovo náměstí 907/1a, 603 00 Brno, Staré Brno

(54) Název užitného vzoru:
Sestava pro regulaci teploty vzorku

CZ 32258 U1

Sestava pro regulaci teploty vzorku

<u>Oblast techniky</u>

5

Technické řešení se týká sestavy pro regulaci teploty vzorku pro aplikace kryo rastrovací elektronové mikroskopie.

10   <u>Dosavadní stav techniky</u>

Kryo elektronová mikroskopie přináší důležité informace z biologických i materiálových věd. Velké využití nachází zejména při analýze vzorků s vysokým obsahem vody, ale také například při studiu vlastností polymerů při nízkých teplotách. Základem pro pozorování je udržení přesně
15   stanovené teploty v oblasti zkoumaného vzorku a možnost její účinné regulace.

To je v současné době prováděno pomocí teplotní regulace umístěné v oblasti stolku $\underline{1}$, viz obr. 1, do kterého je poté umisťován odpovídající držák $\underline{2}$, na němž jsou uchycené samotné vzorky $\underline{3}$. Chlazení je prováděno buďto připojením stolku $\underline{1}$ k Dewarově nádobě pomocí pružného a tepelně
20   vodivého spojení, tzv. chladovodu $\underline{4}$, nebo průtokem chladícího média, nejčastěji N2. Topný element $\underline{5}$ zajišťující ohřev na požadovanou teplotu je umístěn na stolku $\underline{1}$ stejně jako teplotní čidlo $\underline{6}$ umožňující měření aktuální teploty. Výsledný systém chlazení-ohřev-měření umožňuje pomocí tepelného regulátoru $\underline{7}$ měřit a udržovat nastavenou teplotu.

25   Nevýhodou uvedeného řešení je, že se proces regulace a měření teploty odehrává v kompletní soustavě zahrnující stolek + držák + vzorek. Celková přesnost a rychlost teplotní regulace je tedy zatížena teplotní setrvačností celého systému obsahujícího velkou masu hmoty, přesností regulační smyčky a nestabilními tepelnými přechody mezi jednotlivými mechanickými částmi soustavy, zejména mezi stolkem a držákem. Během regulace teploty je vyhříván i chlazen nejen
30   držák vzorku, ale i stolek samotný, což přináší nežádoucí časovou prodlevu v reakci na regulační zásah. Regulovanou veličinou je topný výkon implementovaného topného členu.

Dalším nedostatkem stávajícího řešení je, že neumožňuje analýzu zmrazeného vzorku v transmisním módu, tj. pomocí STEM detektoru, a absence informace o teplotě samotného
35   vzorku, jelikož se teplotní čidlo nachází na stolku, nikoliv v blízkosti vzorku umístěného na držáku.

Cílem technického řešení je představit sestavu pro regulaci teploty vzorku výše uvedeného použití, která by nevýhody stavu techniky odstranila.
40

<u>Podstata technického řešení</u>

Výše zmíněné nedostatky odstraňuje do značné míry sestava pro regulaci teploty vzorku pro
45   aplikace kryo rastrovací elektronové mikroskopie obsahující stolek, v němž je umístěn držák vzorku, a dále obsahující topný element, teplotní čidlo a teplotní regulátor, se kterým jsou topný element a teplotní čidlo elektricky propojeny, jehož podstata spočívá v tom, že topný element a/nebo teplotní čidlo jsou umístěny na držáku vzorku.

50   Ve výhodném provedení je propojení mezi teplotním regulátorem a topným elementem a/nebo teplotním čidlem provedeno přes konektor.

V jiném výhodném provedení je konektor umístěn na držáku a mechanicky propojen se stolkem.

55   V jiném výhodném provedení je držák rozšířen o část přečnívající stolek.

V jiném výhodném provedení je držák opatřen drážkou.

V jiném výhodném provedení je na držáku namísto vzorku umístěna alespoň jedna TEM síťka.

V jiném výhodném provedení je sestava provedena z pozlacené slitiny mědi.

Objasnění výkresů

Technické řešení bude dále přiblíženo pomocí obrázků, kde obr. 1 představuje sestavu pro regulaci teploty vzorku pro aplikace kryo rastrovací elektronové mikroskopie podle stavu techniky a obr. 2 představuje sestavu pro regulaci teploty vzorku pro aplikace kryo rastrovací elektronové mikroskopie podle technického řešení s rozšířeným držákem.

Příklad uskutečnění technického řešení

Sestava pro regulaci teploty vzorku pro aplikace kryo rastrovací elektronové mikroskopie podle technického řešení je představena na obr. 2. Jeho provedení je obdobné stavu techniky a obsahuje stolek 1, v němž je umístěn držák 2 vzorku 3. Oproti stavu techniky jsou však topný element 5 a/nebo teplotní čidlo 6 umístěny přímo na držáku 2. Držák 2 je navíc opatřen konektorem 8, k němuž je přes nezobrazené vodiče připojen jak uvedený topný element 5 a teplotní čidlo 6, tak i pomocí kabeláže 9 teplotní regulátor 7. Z důvodu potřeby ukrytí těchto vodičů může být držák 2 opatřen drážkou 10, v níž jsou tyto vodiče vedeny. Kabeláž 9 je výhodně ve formě několikažilového kabelu. Z důvodu potlačení vlivu případných odporů se v našem konkrétním případě jedná o šesti žilový kabel, kde dva vodiče jsou pro topný element 5 a čtyři vodiče pro teplotní čidlo 6. Konektor 8 je dále pomocí například nezobrazených pružných spojů mechanicky propojen se stolkem 1.

Ve výhodném provedení je držák 2 rozšířen takovým způsobem, že jeho část přečnívá stolek 1, což umožňuje provádět analýzu vzorku pomocí STEM detektoru, který je umístěn pod vzorkem v komoře mikroskopu během měření (na obrázku nezobrazeno). V této přečnívající části může být zkoumaný vzorek 3 umístěn na TEM síťce. Rameno držáku 2 slouží rovněž k snadnému umístění topného elementu 5 a teplotního čidla 6.

Sestava je výhodně provedena ze slitiny mědi, neboť ta má poměrně dobrou tepelnou vodivost a je snadno obrobitelná Z důvodu možné oxidace je sestava následně pozlacena (obvykle galvanicky).

Sestava podle technického řešení je určena pro optimalizaci regulace teploty blízkého okolí vzorků určených pro analýzu v rastrovacím elektronovém mikroskopu, tzv. SEM, za velmi nízkých teplot, tzv. cryo-SEM. Rovněž je navržena pro pozorování velmi tenkých vzorků umístěných na TEM síťkách a to tak, aby bylo možné jejich pozorování v transmisním módu pomocí retraktabilního STEM detektoru umístěného pod vzorkem, detektoru pro energiově-disperzní analýzu paprsků rentgenového záření, nebo katodoluminiscenčního detektoru, které jsou umístěny nad vzorkem. Tato kombinace zobrazovacích technik umožňuje stanovení rozličných vlastností studovaného vzorku bez nutnosti s ním manipulovat, v závislosti na specifické konfiguraci detektorů v SEM je možné pozorování více signálů zároveň. Tím se snižuje šance na jeho poškození nebo kontaminaci.

Sestava podle technického řešení umožňuje lépe kontrolovatelný proces sublimace zmražených hydratovaných vzorků, čímž dochází ke zvýšení reprodukovatelnosti cryo-SEM experimentů. Sestava zároveň rozšiřuje využití různých detekčních systémů v SEM, zejména zobrazování tenkých vzorků v transmisním módu, tj. STEM, s možností prvkové, např. EDX,

a katodoluminiscenční, tj. CL, analýzy.

Dále umožňuje:

- přesnější regulaci teploty vzorku tím, že měření teploty dochází přímo na držáku vzorku v jeho těsné blízkosti;

- rychlejší teplotní reakci na změnu topného příkonu v důsledku snížení tepelné kapacity systému, což je dáno umístěním topného tělesa přímo na držáku vzorku;

- možnost výměny vzorku bez ručního rozpojování a spojování přívodních kabelů napojených na konektor, který se nachází na stolku, a to díky jeho protikusu, který je součástí držáku vzorku;

- využitelnost držáku pro analýzu vzorku pomocí transmisního módu (STEM) v SEM s možnosti teplotní regulace;

- využitelnost držáku pro katodoluminiscenční měření díky umístění TEM sítěk velmi blízko horní rovině držáku, tj. umožňuje posun vzorku do ohniska parabolického zrcadla CL detektoru.

NÁROKY NA OCHRANU

1.   Sestava pro regulaci teploty vzorku pro aplikace kryo rastrovací elektronové mikroskopie obsahující stolek (1), v němž je umístěn držák (2) vzorku (3), a dále obsahující topný element (5), teplotní čidlo (6) a teplotní regulátor (7), se kterým jsou topný element (5) a teplotní čidlo (6) elektricky propojeny, **vyznačující se tím**, že topný element (5) a/nebo teplotní čidlo (6) jsou umístěny na držáku (2) vzorku (3).

2.   Sestava podle nároku 1, **vyznačující se tím**, že propojení mezi teplotním regulátorem (7) a topným elementem (5) a/nebo teplotním čidlem (6) je provedeno přes konektor (8).

3.   Sestava podle nároku 2, **vyznačující se tím**, že konektor (8) je umístěn na držáku (2) a mechanicky propojen se stolkem (1).

4.   Sestava podle některého z výše uvedených nároků, **vyznačující se tím**, že držák (2) je rozšířen o část přečnívající stolek (1).

5.   Sestava podle nároku 4, **vyznačující se tím**, že držák (2) je opatřen drážkou.

6.   Sestava podle některého z výše uvedených nároků, **vyznačující se tím**, že na držáku (2) namísto vzorku (3) je umístěna alespoň jedna TEM sítka.

7.   Sestava podle některého z výše uvedených nároků, **vyznačující se tím**, že sestava je provedena z pozlacené slitiny mědi.
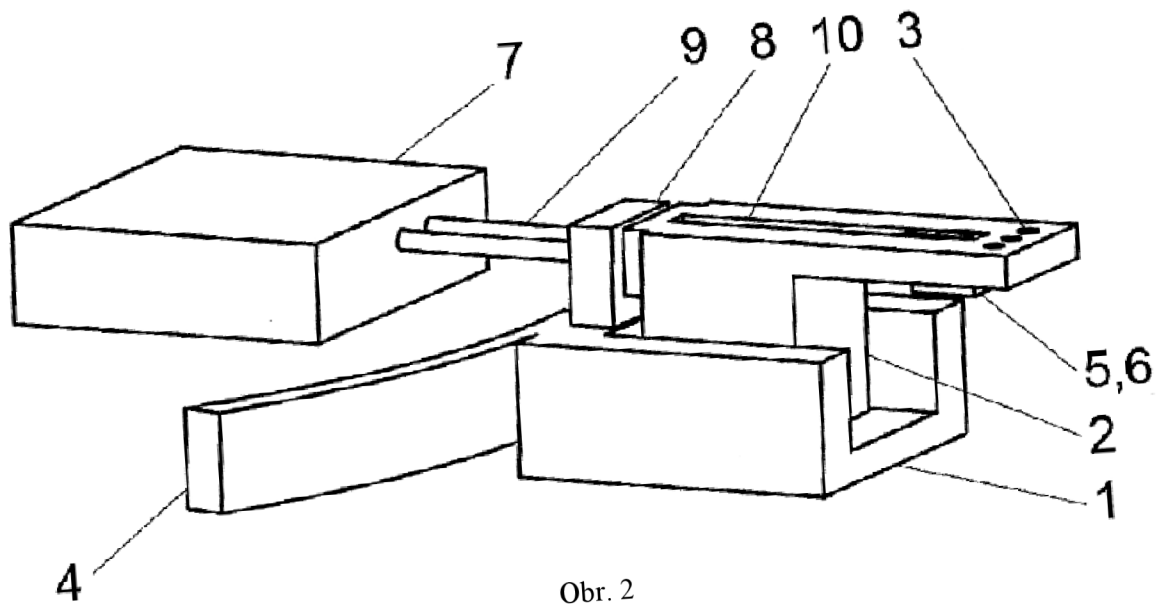
1 výkres
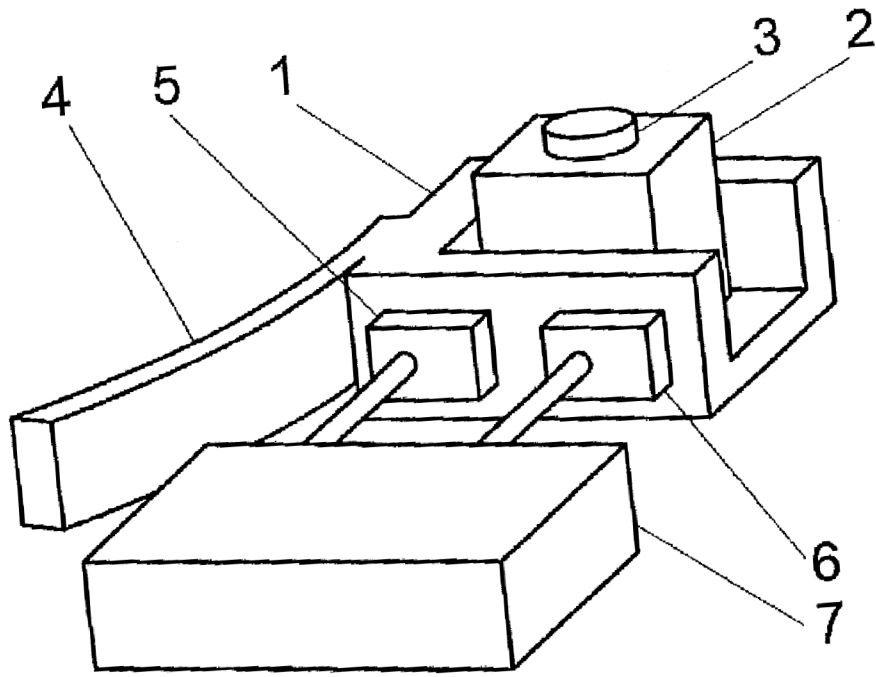
Obr. 1

Obr. 2

Hrubanová, K., Krzyžánek, V., Nebesářová, Jana, Růžička, F., Pilát, Z., Samek, O. Monitoring *Candida parapsilosis* and *Staphylococcus epiderm*idis Biofilms by a Combination of Scanning Electron Microscopy and Raman Spectroscopy. Sensors. 2018, 18(12), 4089. ISSN 1424-8220 doi: 10.3390/s18124089

Monitoring *Candida parapsilosis* and *Staphylococcus epidermidis* Biofilms by a Combination of Scanning Electron Microscopy and Raman Spectroscopy

Kamila Hrubanova [1] [ID], **Vladislav Krzyzanek** [1] [ID], **Jana Nebesarova** [2], **Filip Ruzicka** [3], **Zdenek Pilat** [1] [ID] **and Ota Samek** [1,*]

[1] Institute of Scientific Instruments of the Czech Academy of Sciences, CZ-61264 Brno, Czech Republic; hrubanova@isibrno.cz (K.H.); krzyzanek@isibrno.cz (V.K.); pilat@isibrno.cz (Z.P.)
[2] Biology Centre of the Czech Academy of Sciences, CZ-37005 Ceske Budejovice, Czech Republic; nebe@paru.cas.cz
[3] Department of Microbiology, Faculty of Medicine, Masaryk University and St. Anne's Faculty Hospital, CZ-65691 Brno, Czech Republic; fruzic@fnusa.cz
* Correspondence: osamek@isibrno.cz; Tel.: +420-541-514-284

Abstract: The biofilm-forming microbial species *Candida parapsilosis* and *Staphylococcus epidermidis* have been recently linked to serious infections associated with implanted medical devices. We studied microbial biofilms by high resolution scanning electron microscopy (SEM), which allowed us to visualize the biofilm structure, including the distribution of cells inside the extracellular matrix and the areas of surface adhesion. We compared classical SEM (chemically fixed samples) with cryogenic SEM, which employs physical sample preparation based on plunging the sample into various liquid cryogens, as well as high-pressure freezing (HPF). For imaging the biofilm interior, we applied the freeze-fracture technique. In this study, we show that the different means of sample preparation have a fundamental influence on the observed biofilm structure. We complemented the SEM observations with Raman spectroscopic analysis, which allowed us to assess the time-dependent chemical composition changes of the biofilm in vivo. We identified the individual spectral peaks of the biomolecules present in the biofilm and we employed principal component analysis (PCA) to follow the temporal development of the chemical composition.

Keywords: Raman spectroscopy; biofilm; sample preparation; scanning electron microscopy; cryo-SEM

1. Introduction

Yeast and bacteria are microorganisms that can live as planktonic cells or in an organized formation called biofilm [1]. During their adherence to surfaces or interfaces and their subsequent proliferation, the cells embed themselves into an amorphous extracellular matrix (ECM) [2], which is composed of extracellular polymeric substances (EPS) produced by the cells [3,4]. The presence of ECM is often considered an important characteristic of a mature biofilm [5]. Among the main components of EPS is a mixture of polysaccharides, proteins, and extracellular DNA [6,7]. Since these substances are all highly hydrophilic, the biofilm water content can sometimes be as high as 90% of the total biofilm mass [1,8].

Microbes in natural ecosystems appear to have a pronounced tendency to colonize various surfaces and each other. The interest in such microbial communities—biofilms—has increased over the last three decades, because the biofilms are important in many aspects of health, biotechnology, etc. [9].

The presence of biofilms can lead to human health problems, e.g., biofilm on teeth [10], also known as plaque and a factor in tooth decay and parodontosis, as well as the development of biofilm on medical devices such as catheters or implants [11]. On the other hand, biofilms can be useful, as they are already extensively used in wastewater treatment [12,13] and play a role in biofuel production such as methane generation by methanogenesis [14] or in food production [15]. Life in biofilms is favorable for microbes, bringing advantages such as enhanced persistence and resistance to environmental threats such as antimicrobial agents [16], toxic substances, thermal and oxidative stress [2,17]. Although the composition of biofilms varies depending on the system under study, in general the major component of a biofilm is water. Apart from water and the bacterial cells, the biofilm matrix is a complex formed principally by exopolysaccharides [18]. Moreover, other macromolecules such as proteins, DNA and various products from the lysis of bacteria are present in the biofilm matrix [19]. Studies of biofilms suggest that the biofilm matrix architecture is variable and it contains channels that enable water, nutrients and oxygen flow through the biofilm [20]. However, the detailed architecture of the channels inside the ECM, and the processes operating within them have not yet been fully elucidated [16,20]. Therefore, in this study we have combined suitable microscopic and spectroscopic techniques that could be useful for studying the biofilms.

We examined the biofilm with emphasis on the differences in the apparent structure of the ECM, linked to various sample preparation protocols for SEM. The yeast *Candida parapsilosis* and bacterium *Staphylococcus epidermidis* have been studied in this project. These species are frequently found among the normal human microbiota [21,22]. However, in a medical context, the ability to form biofilms allows these microbes to colonize the surfaces of implants, consequently causing difficult-to-treat infections, especially in immunocompromised patients [23,24]. The presence of EPS protects the microbial cells from the natural defenses of the human immune system as well as from the effects of antibiotic treatments [25,26] and thus it complicates the therapy [1,8]. Understanding the biofilm structure can contribute to the research of biofilm formation and the underlying biochemical mechanisms. This will help to develop a more efficient treatment strategy for biofilm infections [27,28].

Microbial biofilms are usually investigated by various microscopic techniques including confocal laser scanning microscopy (CLSM) and conventional scanning electron microscopy (SEM) [13,29,30], transmission electron microscopy (TEM) [31], Focused Ion Beam (FIB)-SEM [3] and by special SEM techniques, such as cryo-SEM or environmental-SEM [3,32–34]. The main limitation of the light microscopy techniques is the restricted magnification [35]. This can be resolved by the use of SEM, which provides high-magnification images of the individual bacteria and yeast cells and their location and interaction within the ECM, which is important for understanding the morphology and physiology of biofilms [2,36]. However, a conventional SEM, where the sample is observed in high vacuum at room temperature, is limited due to the need for a dry sample [37]. Biofilms are rich in water and the conventional sample preparation for SEM that includes desiccation as a prerequisite for imaging can cause substantial changes in the ECM and the microbial cell ultrastructure, leading to artifacts [5,34]. Chemical fixation with aldehydes and osmium tetroxide treatment help to preserve cell morphology and enhance contrast [38,39], while dehydration with ethanol or acetone series is used for the gradual replacement of the water inside the sample. However, this mode of preparation also causes some artifacts, such as cell membrane discontinuities [40], and it has other deleterious effects on morphology. In the case of cryo-fixation, the biofilm is not dehydrated but kept frozen to obtain high-resolution images closer to the native state of the sample [37,39,41]. It has been proven that in cryo-fixed biofilms, the bacterial ultrastructure preservation and the biofilm organization improved significantly [42]. To reduce the damage inherent to these treatments, various innovative cryogenic sample preparation methods have been developed [41,43,44]. One of the simplest cryo-fixation techniques is plunging the sample into a liquid cryogen [45]. In general, plunging into liquid nitrogen is not usually sufficient because of the Leidenfrost effect: a thermally insulating film of vaporized nitrogen forming around the sample, preventing fast cooling and allowing water ice crystals to form inside the specimen [46]. However, cryogens like liquid ethane/propane are often used, for example in electron tomography,

for fixation of very thin layers [42]. Substantially more effective freezing can be achieved by increasing the pressure during exposure to the liquid cryogen. This can be performed by the high-pressure freezing (HPF) technique [47–50].

We coupled the SEM morphological examination of biofilms with chemical characterization by Raman microspectroscopy. Raman microspectroscopy employs a laser beam that is focused with the microscope objective lens in order to excite and collect Raman scattering from a small volume of the sample. Raman spectra from living microorganisms contain multiple spectral peaks corresponding to unique interatomic vibrations in biomolecules, e.g., nucleic acids, proteins, carbohydrates, and lipids [51–54]. It has been shown that Raman microspectroscopy and Raman imaging can be regarded as the methods of choice for many studies of microorganisms, cells and other biological samples [51,55–65]. Detailed databases of Raman spectral features encountered in biological samples had been published before [60]. When characterizing biofilms using Raman microspectroscopy, the common approach is to analyze the biofilm as a whole. The spectra can be acquired point-by-point at selected positions or using line-scan techniques such as Renishaw StreamLine. In such cases, the Raman signal originates from the cells as well as from the ECM. Nevertheless, it may be useful to separate the ECM contribution from the Raman spectra, in order to fully understand the biochemical processes in the cells embedded in the biofilm matrix. It is well known that such cells express phenotypes that differ from those of their planktonic counterparts, i.a. the increased resistance to chemical treatments.

We employed SEM to study the ECM content and distribution in the biofilm, and the way it translates into its Raman spectral characteristics. The SEM images helped us to estimate the relative proportion of the ECM, which is in most cases ranges between 20% and 50% of the total biofilm volume. This means that in the Raman spectra, we observe the signal both from the bacterial cells and from the ECM, proportion of which depends on the growth stage of the biofilm. The proportion of the ECM increases with the age of the biofilm.

2. Materials and Methods

2.1. Biofilm Cultivation

Two biofilm-positive microbial strains that are often involved in serious infections [27,36,66] were selected as model organisms and examined in this study: the well-characterized *ica* operon-positive, biofilm and slime producing *Staphyloccocus epidermidis* strain CCM 7221 (Czech Collection of Microorganisms, Brno, Czech Republic) [4] and *Candida parapsilosis* BC11 from the Collection of the Microbiology Institute, Masaryk University and St. Anne's University Hospital (Brno, Czech Republic) [66]. The strains included in this study were stored at $-70\,^{\circ}$C in cryo-tubes (ITEST plus, Hradec Králové, Czech Republic). Prior to each experiment, the strains were thawed quickly at $37\,^{\circ}$C and cultivated on Mueller-Hinton agar (Oxoid, Basingstoke, UK) at $37\,^{\circ}$C for 24 h. The microbial cultures were re-suspended in a sterile physiological saline solution (PSS) to the optical density 0.5 of the McFarland scale [54].

In our experiments with the yeast biofilm, the wells of 24-well polystyrene tissue culture plates Nunclon (Nunc, Roskilde, Denmark) containing 1 mL of Yeast Nitrogen Base medium Difco (Becton, Dickinson and Co., Franklin Lakes, NJ, USA) with 4% glucose (YNBg) and sterile substrate discs were inoculated with 100 µL of standardized cell suspension. Bacterial cultures were cultivated in 1 mL of brain-heart infusion (BHI) medium (Oxoid) with 4% glucose (BHIg) under the same conditions. We used standard cover slips or sapphire discs with the diameter 1.4 mm (No. 16706849, Leica Microsystems, Vienna, Austria) and 6 mm (No. 16770158, Leica Microsystems) as a substrate for HPF freezing and a cover slip (No. 1014/1818, Hecht-Assistant, Paris, France) for plunge freezing and conventional protocols for SEM; cover slips are widely used as a cultivation substrate for in vitro biofilm experiments [67–69]. After 24 h of incubation at $37\,^{\circ}$C the substrate discs were removed from wells and further processed.

2.2. Conventional SEM

All the samples were imaged by several different high vacuum scanning electron microscopes (SEM) at room temperature. Specifications of the SEM devices and information on the imaging parameters are stated along with each procedure below in the text. Figure 1 summarizes all the sample preparation protocols for conventional SEM used in our experiments.
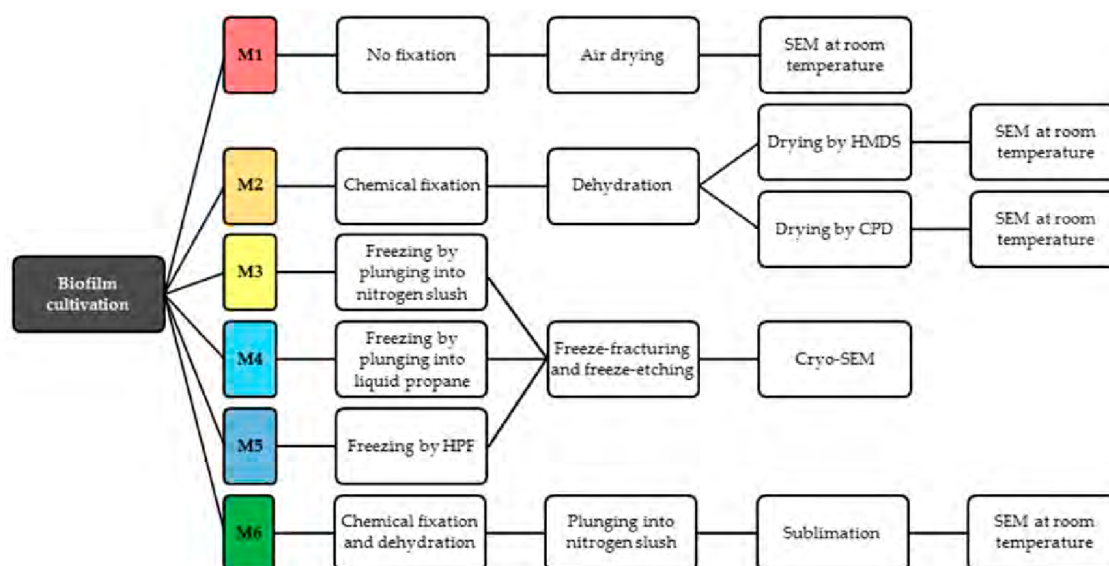

Figure 1. Diagram of microbial biofilm sample preparation for SEM.

2.2.1. Method 1—Air-Drying (M1)

The simplest way to visualize the biofilm in vacuum of electron microscope is without any fixation of the structure. The microbial cultures of *S. epidermidis* and *C. parapsilosis* were cultivated in a medium for 24 h on a cover glass. Subsequently, the samples were air dried for 30 min. Imaging of the SE signal was performed by a VEGA TS 5130MM scanning electron microscope (SEM) (Tescan Orsay Holding, Brno, Czech Republic) at the acceleration voltage of 10 kV with the use of a homemade cathode lens with the deceleration voltage in the range around 3 kV and the working distance of 10 mm.

2.2.2. Method 2—Chemical Preparation (M2)

The microbial cultures of *S. epidermidis* and *C. parapsilosis* after 24-h cultivation under the same conditions as described in previous experiments were prepared according to the standard protocol [37,70,71]. Our samples were fixed in 2.5% glutaraldehyde (Sigma-Aldrich, St. Louis, MO, USA), post-fixed in 1% osmium tetroxide (OsO_4; Sigma-Aldrich) and thoroughly but carefully washed by PBS buffer (Sigma-Aldrich). The process of dehydration by ethanol (VWR Chemicals, Leuven, Belgium) series (30%, 50%, 70%, 80%, 90%, 95%, each step 15 min, and three times 100%) prepared the samples for drying. Here two methods of drying are compared. The first was done by hexamethyldisilazane (SPI-Chem, West Chester, PA, USA; HMDS; CAS 999-97-3) which was diluted with acetone (Sigma-Aldrich). Therefore, before applying this treatment it was necessary to replace the ethanol with acetone in four steps with increasing proportion of acetone (ratio ethanol/acetone 2:1; 1:1; 1:2; pure acetone) [37,70,71]. The second methodology for sample drying is the critical point drying (CPD) using CO_2. The samples, prepared by conventional protocols [37,70] were coated by 10 nm of Au before imaging in a VEGA TS 5130MM SEM at the acceleration voltage 10 kV or in a Magellan 400L SEM (Thermo Fisher Scientific, Hillsboro, OR, USA) at 2 kV.

2.3. Cryo-SEM

Our experiments with imaging at low temperature by cryo-SEM show the comparison of the biofilm structure at the same cultivation conditions but with different preparation protocols. We tested multiple cryo-fixation techniques; the workflow is summarized in Figure 1.

2.3.1. Method 3—Plunging into Nitrogen Slush (M3)

Freezing in the nitrogen slush was performed in the slushing station, a part of the ALTO 2500 cryo-preparation system (GATAN Inc., Pleasanton, CA, USA) [72,73]. The substrate for the cultivation of the biofilm samples was a cover glass of thickness 0.17 mm that was removed from the medium without any rinsing immediately before the freezing step. After freezing, the sample was transferred into an ALTO 2500 cryo-preparation chamber, perpendicularly freeze-fractured and subjected to a short sublimation at −95 °C for 3 min. The imaging was performed by SEM 7401F (JEOL, Akishima, Japan). The cryo-stage in the SEM was cooled at −135 °C, the anti-contamination aperture at −145 °C during specimen observation. The secondary electron (SE) micrographs were recorded at an electron energy range between 1 and 2 keV (low dose), and the working distance of approximately 6–8 mm over the fracture plane.

2.3.2. Method 4—Plunging into Liquid Ethane (M4)

Freezing in liquid ethane was performed in a homemade plunger. The substrate for cultivation of the biofilm samples was a cover glass of thickness 0.17 mm, which was removed from the medium without any rinsing immediately before the freezing step. After the freezing, the sample was mounted in a standard manner into a cryo-sample holder inside the nitrogen slush, then transferred into an ALTO 2500 cryo-preparation chamber, perpendicularly freeze-fractured and subjected to a short sublimation at −95 °C for 3 min. The imaging was performed by SEM 7401F (JEOL, Akishima, Japan) at the same conditions as described above.

2.3.3. Method 5—Cryo-Preparation by HPF (M5)

The high pressure freezing was performed by the HPF instrument EM PACT2 (Leica Microsystems) in standard conditions according to the instructions given in the operation manual. With the HPF EM PACT2, it is only possible to freeze sapphire disks with a diameter of 1.4 mm and therefore they were used as the substrate for the biofilm cultivation. Just as in the case of the plunging fixation the samples were not rinsed before freezing. After freezing, the sample was mounted into a homemade cryo-sample holder in liquid nitrogen [34], then transferred into a cryo-preparation chamber ALTO 2500, perpendicularly freeze-fractured and subjected to short sublimation at −95 °C for 3 min. Imaging was performed by SEM 7401F (JEOL) under the same conditions as described above. Our experiment with high-pressure freezing of the biofilm of *Staphylococcus epidermidis* was carried out by means of a HPF EM ICE (Leica Microsystems). In this case we used 6 mm sapphire discs as a cultivation substrate. After the freeze-fracturing in the ACE 600 cryo-preparation chamber (Leica Microsystems) the samples were sublimated for 5 min at −95 °C and then transferred by the VCT 100 shuttle (Leica Microsystems) into a Magellan 400L cryo-SEM (Thermo Fisher Scientific). The fractured structures were observed with a 2 keV electron beam at −120 °C and a working distance of around 7 mm.

2.4. Method 6—Combined Preparation: Chemical and Cryo-Methods (M6)

Our experiments with combined sample preparation started with biofilm cultivation on the cover glass under the same cultivation conditions as described above, followed by chemical fixation by 2.5% glutaraldehyde and 1% OsO_4 in PBS buffer and thorough washing with PBS. In the next step, the samples were dehydrated by ethanol series (30%, 50%, 70%, 80%, 90%, 95% *v/v* ethanol; 15 min each, and three times with 100% ethanol) and frozen by plunging into the nitrogen slush. After mounting into a standard cryo-sample holder, the samples were transferred into a vacuum

chamber (ACE 600) where they were sublimated overnight. The samples were then moved under high vacuum using a shuttle (VCT 100) into the SEM (Magellan 400L) and observed with a 2 keV electron beam at room temperature. Working distance was around 6 mm. The samples were metal coated by 2 nm of Pt.

2.5. Analysis of the Yeast Biofilm by Raman Spectroscopy

We used a commercial Renishaw Raman microspectrometer (Renishaw inVia, Renishaw plc., Wotton-under-Edge, UK), with a 785 nm diode laser as the excitation source. The laser beam was focused on the sample with a microscope lens (Leica, Wetzlar, Germany, 50×, NA 0.5), the laser spot diameter was 2 μm × 10 μm (note that this laser spot shape is characteristic for the Renishaw InVia instrument [51,64,65]).

The laser was focused on the surface of the biofilm, which was grown on CaF_2 substrate. The samples were measured in two stages: first immediately after the cells were transferred to the substrate (no biofilm), and subsequently after 6 h of growth at 37 °C, when the fresh biofilm structures were formed. The spectra were measured for 30 s from different parts of the sample. The power of the excitation laser reached approximately 100 mW under the objective lens. The Raman spectra were treated with Savitzky-Golay filter to remove noise and with rolling circle filter for background fluorescence removal [74], and subsequently analyzed by principal component analysis [75]. The software was written using MatLab (MathWorks, Natick, MA, USA).

3. Results and Discussion

3.1. Conventional SEM (M1 and M2)

SEM was found suitable for examination of the microbial biofilms, allowing visualization of microbial cell surfaces and the surrounding ECM with high resolution. Conventional sample preparation protocols for fully hydrated biological material involve following primary steps such as chemical fixation, dehydration and drying. This process modifies the biological material for the low pressure in the SEM chamber during the imaging. The advantages of a microbial biofilm specimen prepared in this manner are its stability, easy manipulation at room temperature, and the possibility of additional coating, which helps to visualize details in the surface structure. Contrarily, the use of chemical treatments and multiple rinsing steps exacerbates the artifacts, especially in the sensitive ECM structure and some parts of the biofilm layer may be completely destroyed.

The presented micrographs (Figure 2) show the comparison of influences of various preparation protocols on the microbial biofilm structure. The easiest way of biofilm preparation for SEM observation is air drying on a cover glass. In the micrographs (Figure 2a,b), the surface structures of the biofilm layer look similar for bacteria and yeast; the air drying caused a collapse of the three-dimensional structure. Moreover, in case of *Candida parapsilosis* we see that the extracellular space is filled by a dry matrix and the residues of the cultivation medium (Star in Figure 2b). It was not possible to visualize the clear surfaces of microbial cells (Square in Figure 2b) because they were covered by ECM and dry cultivation medium.

The chemical fixation and dehydration by ethanol series allowed preservation of the three-dimensional structure of the biofilm. However, in many areas of the cultivation substrate, the biofilm layer was destroyed and washed away due to the rinsing process during the sample preparation. ECM was partially preserved as a compact and roughened fiber-like matter in the extracellular space (Figure 2c–f, stars). The use of HMDS as a drying solution is a gentler way than CPD, the biofilm layer was less perturbed. Furthermore, the choice of the drying technique following the chemical preparation did not influence ECM quality. Therefore, drying by HMDS is a preferable method of the biofilm preparation for room temperature imaging by SEM whenever cryo-methods cannot be applied. The conventional SEM can be used for observing the surface of bacterial and yeast biofilm and obtaining high-resolution images of the spatial distribution of microbes. It can

clearly be seen that the sample preparation represents a crucial parameter in the preservation of the three-dimensional structure of the biofilm. The influence of the chemical treatment is most obvious on the spatial architecture of the biofilm and the compact structure of the ECM. The significant disadvantages of the chemical preparation are the partial loss of the biofilm from the cultivation substrate and the time requirements for this process.
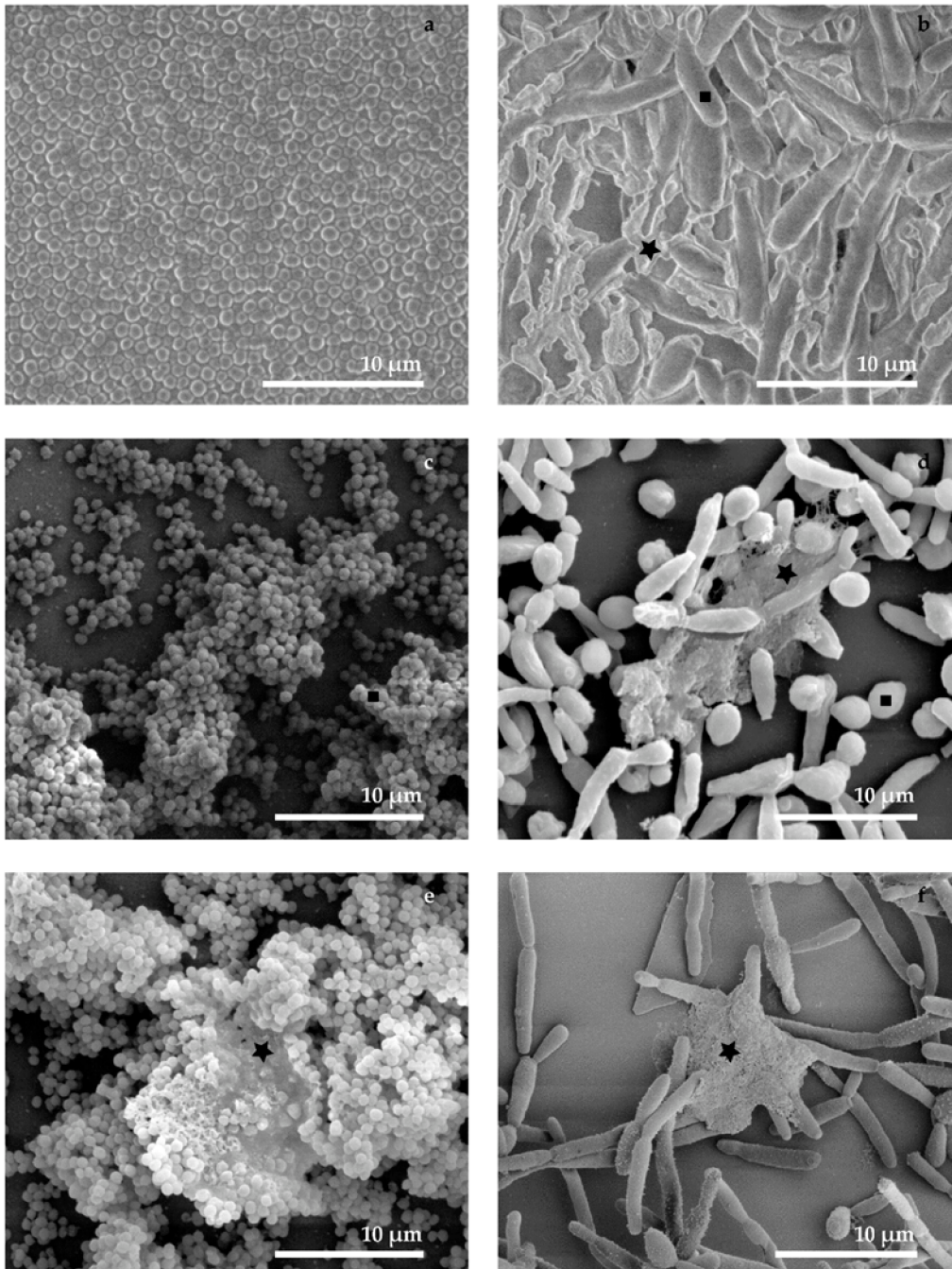
Figure 2. SEM micrographs show the comparison of preparation protocols for microbial biofilm structure (in the left column *S. epidermidis* and in the right column *C. parapsilosis*): (**a**,**b**) no chemical preparation and air drying; measurement parameters: 10 kV with the use of a homemade cathode lens with the deceleration voltage in the range around 3 kV, WD 10 mm; (**c**,**d**) chemical sample preparation and drying by CPD; measurement parameters: (**a**) 10 kV or (**b**) 2 kV, WD 8 mm; (**e**,**f**) chemical sample preparation and drying by HMDS. Marks: stars—ECM, squares—cells; measurement parameters: 2 kV, WD 8 mm.

3.2. Cryo-SEM (M3, M4 and M5)

The use of low-temperature preparation by cryo-SEM for observing biological samples brings a number of advantages compared to conventional SEM at room temperature. The samples do not have to be fixed by chemicals treatment and rinsed several times by a buffer. Moreover, the dehydration series is eliminated and the lengthy drying is no longer needed, therefore the artifacts associated with these processes are eliminated. On the other hand, the observation of biological structures in SEM at low temperatures requires specialized equipment and has its limitations and drawbacks. It is well known that suboptimal freezing speed during the cryo-fixation causes disruptions to the soft hydrated material due to the water ice crystallization [45]. Therefore, the choice of a particular cryo-fixation technique is crucial to obtain unperturbed structure of the frozen specimen.

The comparison of the freezing methods for yeast and bacterial biofilms is the main aim of this section of our study. The perpendicular freeze-fracture of the samples (24 h old biofilms of *Staphylococcus epidermidis* and *Candida parapsilosis*) frozen by plunging into nitrogen slush are shown in Figure 3a,b.

The inner structure of the microorganisms (Marks—squares in Figure 4) seems to be sufficiently preserved in the range of magnification around 5000×. The thickness of the biofilm layer is approximately 10 μm. The structure of the ECM containing the extracellular biopolymers and the cultivation medium has a sponge-like character. We consider this structure to represent a micro-segregation (±0.5 μm) caused by ice crystal growing during the slow freezing process. The method based on plunging the sample into liquid ethane should be appropriate for freezing a sample with thickness up to 10 μm [45]. In our micrographs the final structures after fixation by plunging into liquid ethane look very similar to previous experiments, probably due to the existence of a cultivation substrate such as described in literature [76]. Nevertheless, the use of sapphire discs as a cultivation substrate for plunge-freezing seems to be more suitable from the perspective of their thermal conductivity. However, several experiments show that the plunge freezing fixation of cells cultivated on sapphire discs lead to ice crystal segregation as well [77]; this result also corresponds to our experiments. Noticeably better preservation of the whole microbial biofilm, including the extracellular matrix, is clearly visible in Figure 3e,f (marks—stars). High-pressure freezing ranks among the cutting-edge sample preparation techniques for cryo-SEM. Besides the fast cooling rate, a positive influence is apparently brought by the use of sapphire discs with better thermal conductivity compared to other substrates. The structure of ECM (Figure 3e,f, marks—stars) is very smooth within the magnification used and we were able to detect only minimal disruptions due to the ice crystallization. Moreover, it is possible to recognize the denser parts of the biofilm that can be observed in the surroundings of the microbial cells [34].
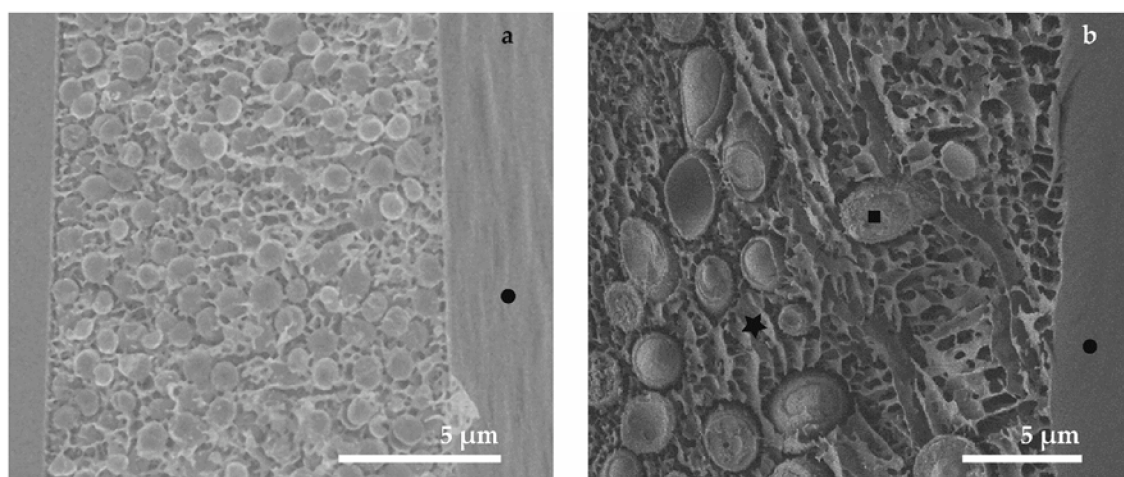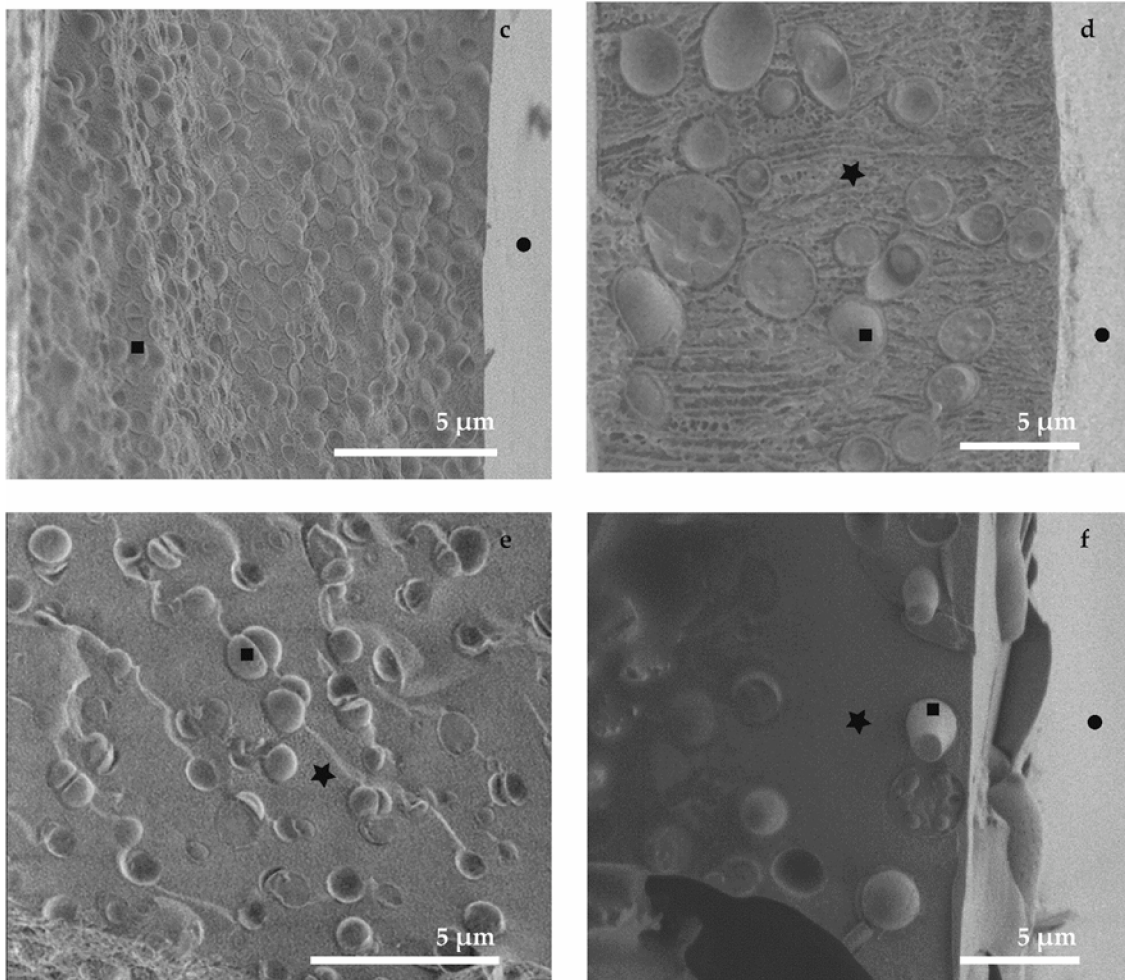

Figure 3. *Cont.*

Figure 3. SEM micrographs showing the comparison of preparation protocols applied to microbial biofilms (in the left column *S. epidermidis* and in the right column *C. parapsilosis*): (**a**,**b**) plunge freezing into nitrogen slush; (**c**,**d**) plunge freezing into liquid ethane; (**e**,**f**) freezing by HPF. Marks: stars—fully hydrated ECM, squares—microbes, dots—surface of biofilm layer; measurement parameters 1 to 2 keV and 6–8 mm.

Cryo-methods in SEM are capable of providing information about the ultrastructure of the microbial biofilm interior, assuming that freeze-fracturing is applied. It is possible to visualize the areas where microbes adhere to the surface of the cultivation substrate and the contact fields between individual microbial cells. On the other hand, examination of the biofilm surface (Figure 3, marks—circles) could not be performed, because the biofilm layer was covered by frozen liquid (the cultivation medium with a content of EPS).
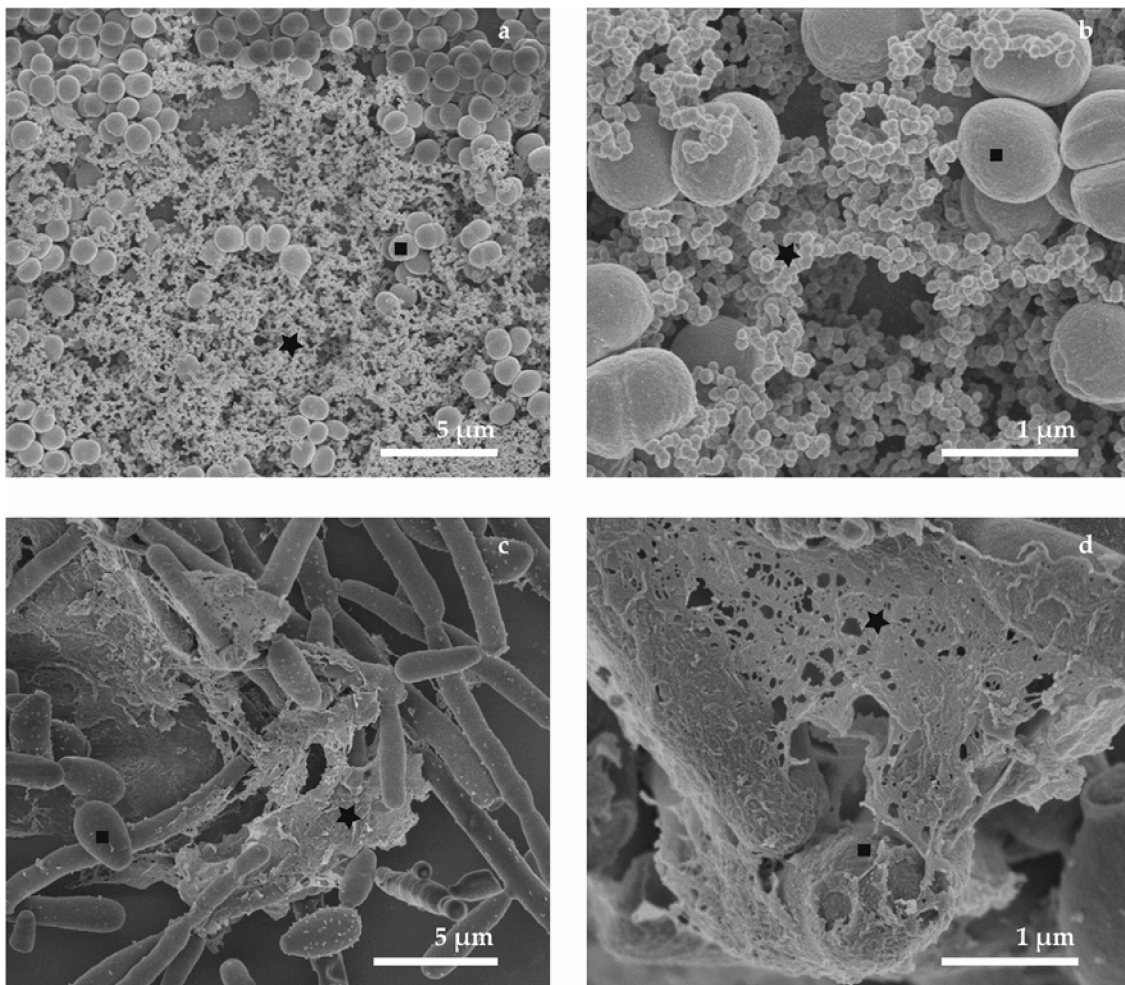
Figure 4. SEM micrographs show the comparison of the bacterial and yeast biofilm structure after the combined sample preparation: (**a**,**b**) *S. epidermidis*; (**c**,**d**) *C. parapsilosis*. In the left column, images are displayed in a lower magnification, while the details are shown in the right column; measurement parameters: 2 keV, WD 6 mm.
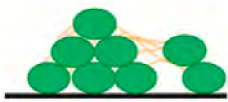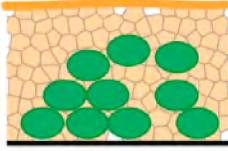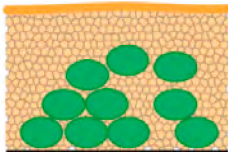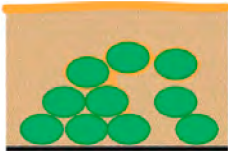
3.3. Combined Preparation—Chemical and Cryo-Methods (M6)

Alternative sample preparation protocol is the combination of chemical fixation by solution of GA and OsO_4 and dehydration by the ethanol series such as in the case of biological sample preparation for conventional SEM techniques by the standard chemical method. When the total water content was replaced by 100% ethanol, the samples in our experiments were frozen by plunging into the nitrogen slush, and transferred to the cryo-preparation chamber where they were sublimated overnight until they were completely dry. The sublimation process started at $-140\ °C$, then temperature increased to $-80\ °C$ with a speed of heating 4 $°C/min$ for 6 h and finally samples were left to warm up to the room temperature spontaneously. Additional coating (4 nm, carbon) allowed a production of high-magnification micrographs of our biofilm samples. From our results it can be concluded that the M6 protocol is the most favorable means of biofilm preparation with the aim of surface visualization. The micrographs in Figure 4 show the spatial distribution of microbes and ECM similar to conventional preparation for room-temperature SEM. The ECM (Figure 4, marks—stars) of the bacterial biofilm seems to have an aggregation character which can arise from the chemical treatment during the preparation. The fiber-like structure of the extracellular matrix that covered and interconnected the yeasts bodies looks very similar to the ECM in samples prepared by CPD, but biofilm samples were washed away to a lesser extent due to the absence of chemical drying or CPD. We were not able to detect any evidence of a gel-like matrix covering the microbial cells as described in many

publications [1,24,78]. This is to be expected, because the whole freeze-drying procedure was applied in this method. We found that the visualized structures are the remnants of the cultivation medium and the condensed matrix components. The limitations of the six different preparation techniques for SEM on bacterial and yeast biofilms (M1–M6), the benefits and influence on the biofilm structure are summarized in Table 1.

Table 1. Comparison of benefits and limitations of sample preparation protocols for SEM (Methods M1–M6) and their influence on biofilm structure as shown in schematic drawings. Our best candidates for sample preparation techniques are labelled green.

M	Advantage	Disadvantage	Schema
M1—air-drying	Speed of sample preparation Simplicity Repeatability of measurement in SEM at room temperature Suitable for **surface imaging**	The loss of the 3D structure Deformation of microbial biofilm Deformation of ECM The possibility of imaging only the sample surface (not interior)	Deformation of biofilm
M2—conventional chemical preparation	Repeatability of measurement in SEM at room temperature The 3D structure is preserved. Suitable for **surface imaging**	Long-term procedure Damage of soft biofilm sample due to multi-steps washing Artefacts with chemicals treatment (the change of gel-like ECM into fiber structures) The sample surface imaging	Biofilm is washed out
M3—plunging LN$_2$; cryo-SEM	Speed of sample preparation The 3D structure of microbial cells is preserved Possibility of biofilm **interior imaging** (used freeze-fracturing technique also suitable for M3–M5)	Artefacts with freezing procedure Freezing is sufficient for very thin samples Limitation for surface imaging because of water content in biofilm samples	"Large" ice crystals
M4—plung. Ethane; cryo-SEM	Speed of sample preparation The 3D structure of microbial cells is preserved Possibility of biofilm **interior imaging**	Artifacts with freezing procedure (smaller ice crystals inside biofilm than by M3) Freezing of thin samples Limitation in surface imaging because of water content in biofilm samples	"Small" ice crystals
M5—HPF freezing and cryo-SEM	Speed of sample preparation 3D structure of microbial cells/ECM is nicely preserved The best freezing technique for samples with thickness up to 200 μm (exp. tested) Biofilm **interior imaging**	Limitation in surface imaging (water content in biofilm) Limitations connected with HPF machine–cultivation substrate (sapphire discs for freeze fracturing; Al or Cu-gold discs)	**Optimal** prep. of biofilm for **interior imaging**
M6—Combined preparation	Speed of sample preparation 3D structure of biofilm Biofilm **surface imaging** Repeatability of measurement in SEM at room temperature after freeze-drying Less washed out biofilm	Artifacts from chemical fixation (the change of gel-like ECM) The imaging of sample surface	**Applicable** prep. of chemically fixed biofilm for **surface imaging**

### 3.4. Analysis of the Yeast and Bacterial Biofilms by Raman Spectroscopy

We assessed the chemical composition of the biofilms using Raman microspectroscopy. Our central objective was to identify the main components of the biofilm. We compared the Raman spectra from the freshly inoculated substrate, containing only the microbial cells, but no ECM, with relatively fresh (6 h old) biofilm, containing a definite proportion of the ECM, see Figure 5. To this end, we assigned the individual peaks of the measured spectra, see Table 2, and we employed PCA to pinpoint the differences in the chemical composition, see Figure 6. The associated PCA loadings reveal the essential changes associated with the ECM production, see Figure 7. We found the main difference between the freshly inoculated substrate and 6 h old biofilm is in the production of proteins, sugars, and lipids (peaks 6, 7, and 8 on Figure 5). This stems from the generation of various polysaccharides, proteoglycans, lipopolysaccharides and lipoproteins as the basis of the ECM.
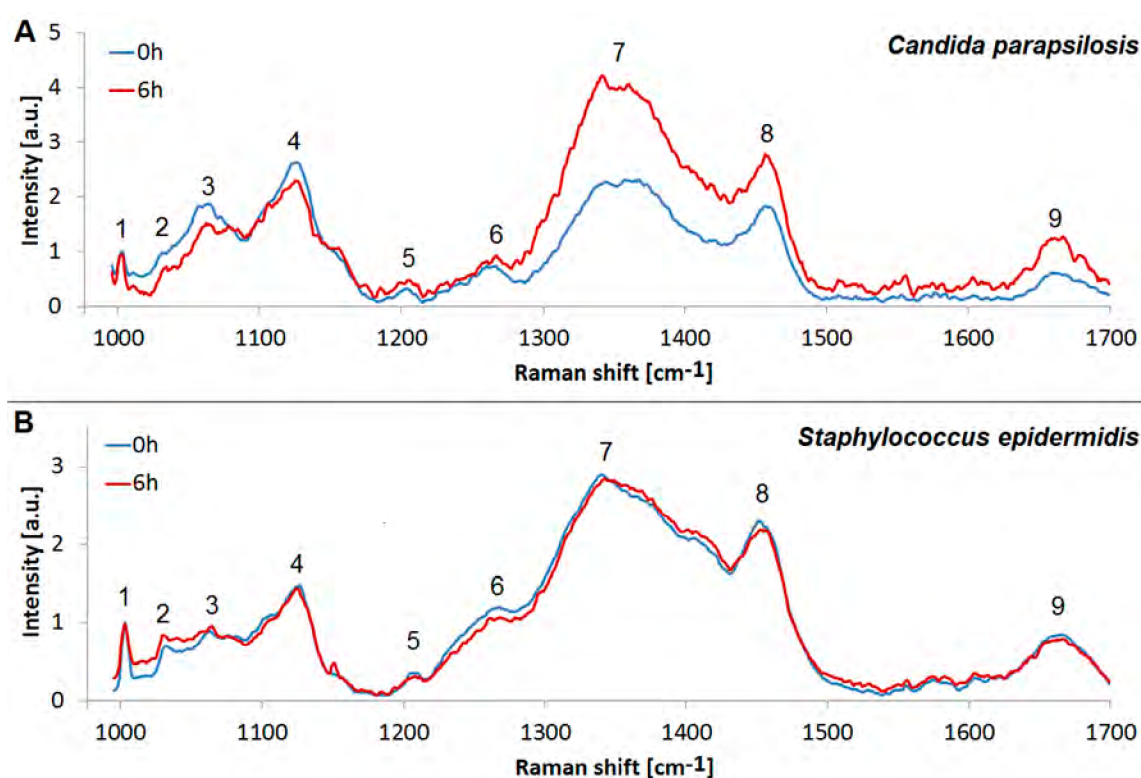
Figure 5. Raman spectra of biofilms. (**A**): *Candida parapsilosis*; (**B**): *Staphylococcus epidermidis*. Comparison of the freshly inoculated substrates containing no ECM (0 h, blue) with 6 h old biofilm, showing the start of the ECM production (6 h, red). The Raman peaks associated with biomolecules are numbered, see Table 2 for the assignments. The spectra were averaged from six separate measurements.

Table 2. Assignments of Raman peaks of *C. parapsilosis* and *S.epidermidis* biofilms [51].

| No.	Wavenumber [cm^{-1}]	Peaks Assignment
1	1002	Symmetric-ring breathing of Phe
2	1033	C-H in-plane stretch of Phe
3	1065	C-C stretch of lipids
4	1125	C-N stretch of proteins
5	1205	Proteins
6	1267	Lipids, Amide III
7	1340–1360	Proteins, Carbohydrates
8	1456	CH_2 scissoring, Lipids
9	1660	Amide I, Lipids
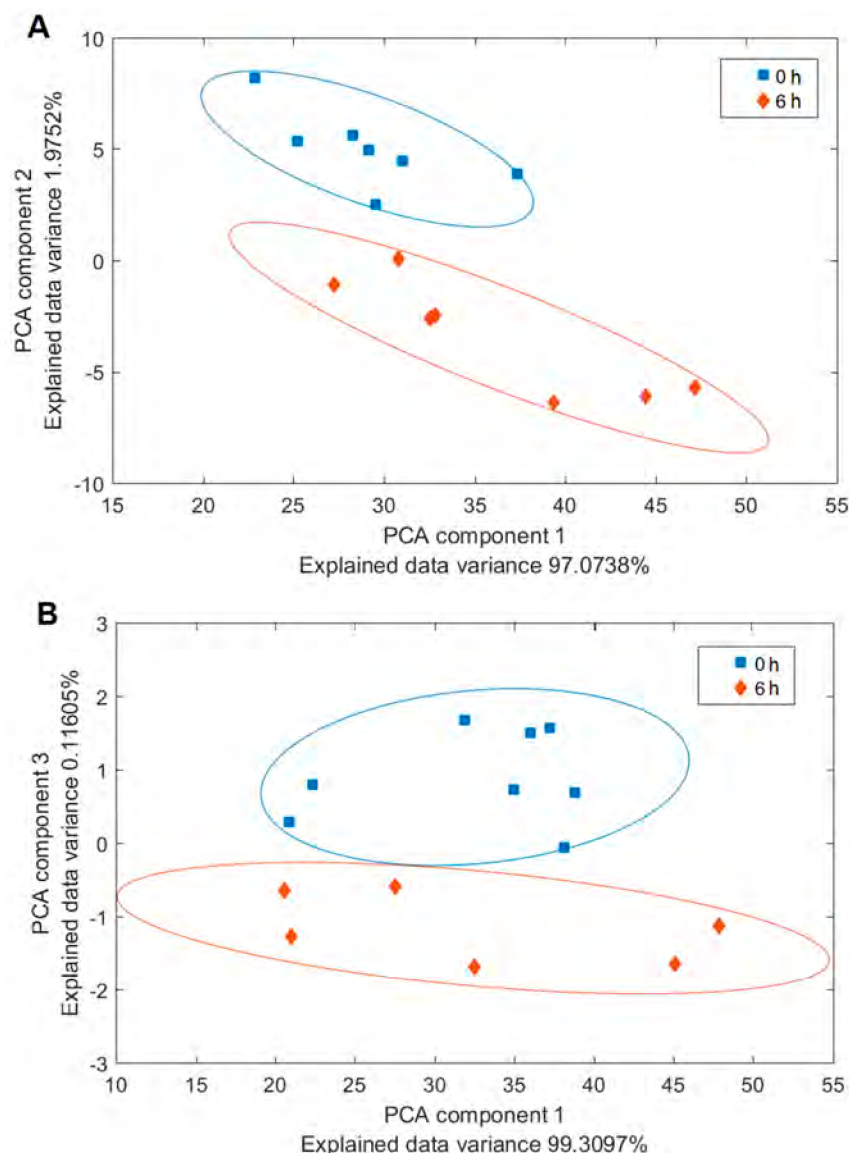
Figure 6. PCA plots for the two species (**A**) *Candida parapsilosis* and (**B**) *Staphylococcus epidermidis*. The clusters of spectra are associated with the two incubation times. Blue squares/0 h—initial cultures with no ECM; red diamonds/6 h—6 h old cultures with starting ECM formation.

While the differences in the spectra of *Candida parapsilosis* at 0 h and 6 h are very pronounced, especially in the region 1340–1360 cm^{-1} and 1456 cm^{-1}, *Staphylococcus epidermidis* spectra at 0 h and 6 h show only marginal differences (Figure 5), although they are clearly visible with the aid of the PCA analysis (Figures 6 and 7). This discrepancy is probably caused by the differences in the optimal conditions for biofilm production by the two studied species. *Candida parapsilosis*, which is eukaryotic, may have developed more complex strategies to react to suboptimal or stressful conditions in general, including the ability to generate biofilm more quickly and efficiently, compared to *Staphylococcus epidermidis*, in which the biofilm production may be linked only to a specific set of growth conditions. We conclude that while we were able to stimulate the biofilm growth in *Candida parapsilosis*, in the Raman experiments we did not meet the optimal conditions for biofilm production in *Staphylococcus epidermidis*. However, it is obvious from the SEM observations, that given enough time, the biofilm growth around the *Staphylococcus epidermidis* cells is abundant.

The chemical changes associated with the formation of biofilm can be easily observed in the PCA loadings in Figure 7. While the *Candida parapsilosis* biofilm appears to be composed mainly of

fungal exopolysaccharides that lack nitrogen in their structure (peaks at 1340–1360 cm^{-1}) [60,79], the biofilm of *Staphylococcus epidermidis* is relatively richer in nitrogen containing polysaccharides such as poly-*N*-acetylglucosamine (peaks around 1400 cm^{-1}) [60,80]. The ECM of *Candida parapsilosis* is composed of several groups of chemical components, including presumably the lipoproteins and proteoglycans. In contrast, the ECM of *Staphylococcus epidermidis* appears to be more chemically uniform. This uniformity apparently stems from the relative simplicity of the bacterial (prokaryotic) metabolism compared to the eukaryotic metabolism of *Candida parapsilosis*.
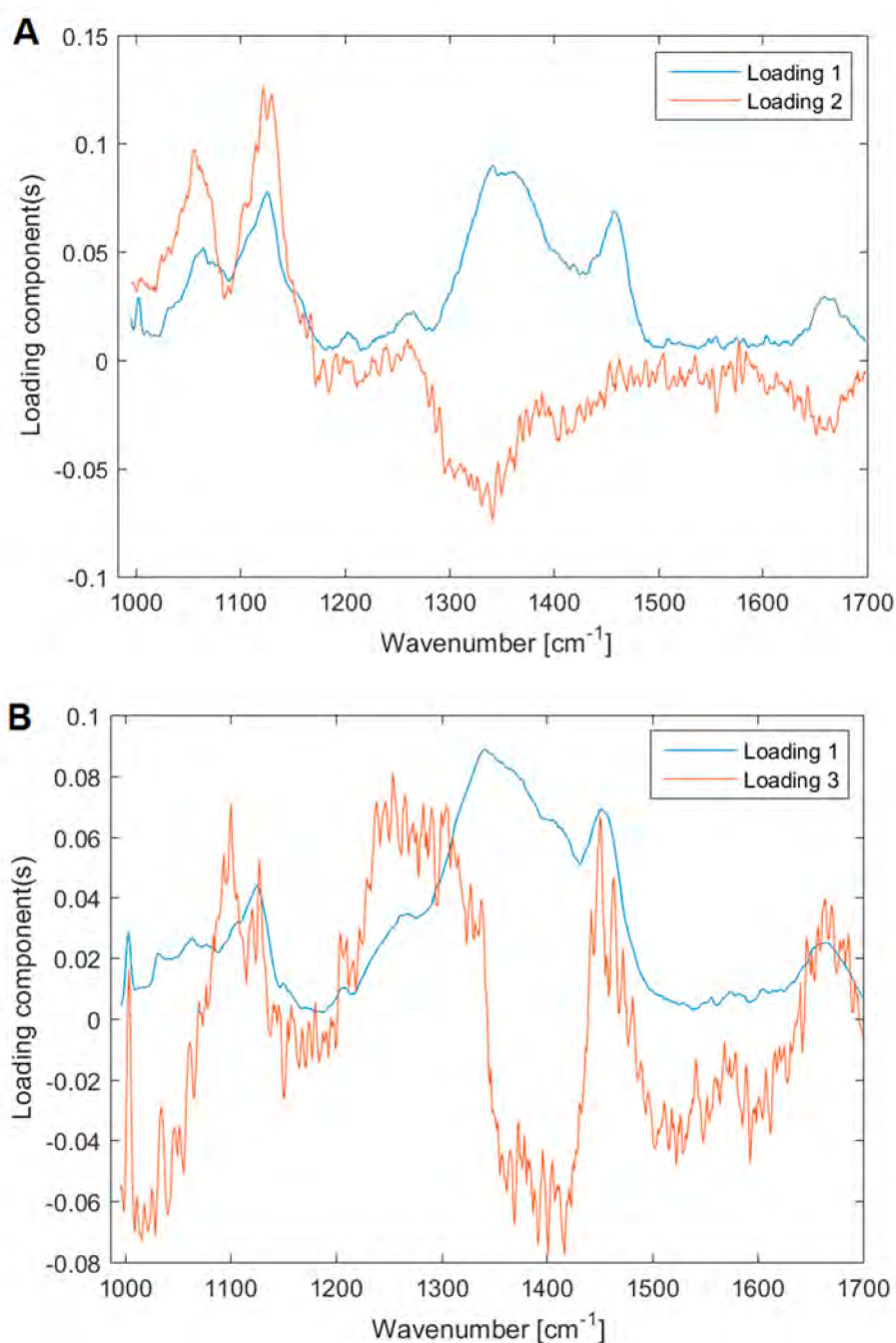
Figure 7. PCA loadings for the two species (**A**) *Candida parapsilosis* and (**B**) *Staphylococcus epidermidis*. The main differences between the cells that did not yet formed the biofilm and the ones that already produce it are presented mainly in the quantity of the generated proteins, sugars and lipids.

4. Conclusions

In order to study the microbial biofilm structure of *Candida parapsilosis* and *Staphylococcus epidermidis* we have investigated different sample preparation techniques for SEM. The effect of sample preparation for conventional SEM allowing surface imaging at room temperature was compared with cryo-SEM techniques employing plunging into various liquid cryogens and HPF. For the cryo-SEM imaging of the biofilm inner structure we have selected the freeze-fracturing technique. We made a comparison of applied techniques for microbial biofilm studies which indeed showed different influences on the final structure of the biofilm. Based on our findings the best candidate for biofilm evaluation can be selected.

We showed that a combination of Raman spectroscopy with selected SEM techniques can provide a deeper insight into the chemistry and composition of biofilms. Such studies involving the influence of variations in the amount of extracellular material during the different stages of biofilm growth are currently under way in our laboratories, making use of a combination of SEM and Raman spectroscopy. We believe that the detailed view of the biofilm structure and composition can advance the better understanding of biofilm structures.

References

1. Donlan, R.M.; Costerton, J.W. Biofilms: Survival mechanisms of clinically relevant microorganisms. *Clin. Microbiol. Rev.* **2002**, *15*, 167–193. [CrossRef] [PubMed]
2. Costerton, J.W.; Stewart, P.S.; Greenberg, E.P. Bacterial biofilms: A common cause of persistent infections. *Science* **1999**, *284*, 1318–1322. [CrossRef] [PubMed]
3. Alhede, M.; Qvortrup, K.; Liebrechts, R.; Hoiby, N.; Givskov, M.; Bjarnsholt, T. Combination of microscopic techniques reveals a comprehensive visual impression of biofilm structure and composition. *FEMS Immunol. Med. Microbiol.* **2012**, *65*, 335–342. [CrossRef] [PubMed]
4. Ruzicka, F.; Horka, M.; Hola, V. Extracellular Polysaccharides in Microbial Biofilm and Their Influence on the Electrophoretic Properties of Microbial Cells. In *Capillary Electrophoresis of Carbohydrates*; Volpi, N., Ed.; Humana Press: New York, NY, USA, 2011; pp. 105–126.
5. Donelli, G. *Microbial Biofilms: Methods and Protocols*; Humana Press: New York, NY, USA, 2014.
6. Flemming, H.C.; Meier, M.; Schild, T. Mini-review: Microbial problems in paper production. *Biofouling* **2013**, *29*, 683–696. [CrossRef] [PubMed]
7. Qin, Z.; Ou, Y.; Yang, L.; Zhu, Y.; Tolker-Nielsen, T.; Molin, S.; Qu, D. Role of autolysin-mediated DNA release in biofilm formation of Staphylococcus epidermidis. *Microbiology* **2007**, *153*, 2083–2092. [CrossRef] [PubMed]
8. Hola, V.; Ruzicka, F.; Tejkalova, R.; Votava, M. Biofilm formation in nosocomial pathogens of respiratory tract. *Int. J. Antimicrob. Agents* **2007**, *29*, S142. [CrossRef]
9. Wimpenny, J. Microbial Metropolis. *Adv. Microb. Physiol.* **2009**, *56*, 29–84. [PubMed]
10. Marsh, P.D. Plaque as a biofilm: Pharmacological principles of drug delivery and action in the sub- and supragingival environment. *Oral Dis.* **2003**, *9*, 16–22. [CrossRef] [PubMed]

11. Francolini, I.; Donelli, G. Prevention and control of biofilm-based medical-device-related infections. *FEMS Immunol. Med. Microbiol.* **2010**, *59*, 227–238. [CrossRef] [PubMed]

12. Barghi, A.; Sadati, R.; Larki, R.A. Biological Wastewater Treatment through Biofilm. *Iran. J. Public Health* **2016**, *45*, 101.

13. Voběrková, S.; Hermanová, S.; Hrubanová, K.; Krzyžánek, V. Biofilm formation and extracellular polymeric substances (EPS) production by *Bacillus subtilis* depending on nutritional conditions in the presence of polyester film. *Folia Microbiol.* **2015**. [CrossRef] [PubMed]

14. Cresson, R.; Dabert, P.; Bernet, N. Microbiology and performance of a methanogenic biofilm reactor during the start-up period. *J. Appl. Microbiol.* **2009**, *106*, 863–876. [CrossRef] [PubMed]

15. Bao, J.; Liu, N.; Zhu, L.; Xu, Q.; Huang, H.; Jiang, L. Programming a Biofilm-Mediated Multienzyme-Assembly-Cascade System for the Biocatalytic Production of Glucosamine from Chitin. *J. Agric. Food Chem.* **2018**, *66*, 8061–8068. [CrossRef] [PubMed]

16. De la Fuente-Nunez, C.; Cardoso, M.H.; de Souza Candido, E.; Franco, O.L.; Hancock, R.E. Synthetic antibiofilm peptides. *Biochim. Biophys. Acta* **2016**, *1858*, 1061–1069. [CrossRef] [PubMed]

17. Huq, A.; Whitehouse, C.A.; Grim, C.J.; Alam, M.; Colwell, R.R. Biofilms in water, its role and impact in human disease transmission. *Curr. Opin. Biotechnol.* **2008**, *19*, 244–247. [CrossRef] [PubMed]

18. Sutherland, I.W. Biofilm exopolysaccharides: A strong and sticky framework. *Microbiology* **2001**, *147*, 3–9. [CrossRef] [PubMed]

19. Branda, S.S.; Vik, A.; Friedman, L.; Kolter, R. Biofilms: The matrix revisited. *Trends Microbiol.* **2005**, *13*, 20–26. [CrossRef] [PubMed]

20. Sutherland, I.W. The biofilm matrix—An immobilized but dynamic microbial environment. *Trends Microbiol.* **2001**, *9*, 222–227. [CrossRef]

21. Adam, B.; Baillie, G.S.; Douglas, L.J. Mixed species biofilms of Candida albicans and Staphylococcus epidermidis. *J. Med. Microbiol.* **2002**, *51*, 344–349. [CrossRef] [PubMed]

22. Holá, V.; Růžička, F.; Votava, M. The dynamics of Staphylococcus epidermis biofilm formation in relation to nutrition, temperature, and time. *Scr. Med. Fac. Med.Univ. Brun. Masaryk.* **2006**, *79*, 169–174.

23. Liu, H.Y.; Zhao, Y.F.; Zhao, D.; Gong, T.; Wu, Y.C.; Han, H.Y.; Xu, T.; Peschel, A.; Han, S.Q.; Qu, D. Antibacterial and anti-biofilm activities of thiazolidione derivatives against clinical staphylococcus strains. *Emerg. Microbes Infect.* **2015**, *4*, e1. [CrossRef] [PubMed]

24. Ruzicka, F.; Horka, M.; Hola, V.; Kubesova, A.; Pavlik, T.; Votava, M. The differences in the isoelectric points of biofilm-positive and biofilm-negative Candida parapsilosis strains. *J. Microbiol. Methods* **2010**, *80*, 299–301. [CrossRef] [PubMed]

25. Deleo, F.; Otto, M.W. *Bacterial Pathogenesis: Methods and Protocols*; Humana Press: Totowa, NJ, USA, 2008.

26. Paiva, L.C.F.; Vidigal, P.G.; Donatti, L.; Svidzinski, T.I.E.; Consolaro, M.E.L. Assessment of in vitro biofilm formation by Candida species isolates from vulvovaginal candidiasis and ultrastructural characteristics. *Micron* **2012**, *43*, 497–502. [CrossRef] [PubMed]

27. Bandara, H.M.H.N.; Lam, O.L.T.; Watt, R.M.; Jin, L.J.; Samaranayake, L.P. Bacterial lipopolysaccharides variably modulate in vitro biofilm formation of Candida species. *J. Med. Microbiol.* **2010**, *59*, 1225–1234. [CrossRef] [PubMed]

28. Lattif, A.A.; Mukherjee, P.K.; Chandra, J.; Swindell, K.; Lockhart, S.R.; Diekema, D.J.; Pfaller, M.A.; Ghannoum, M.A. Characterization of biofilms formed by Candida parapsilosis, C. metapsilosis, and C. orthopsilosis. *Int. J. Med. Microbiol.* **2010**, *300*, 265–270. [CrossRef] [PubMed]

29. Dohnalkova, A.C.; Marshall, M.J.; Arey, B.W.; Williams, K.H.; Buck, E.C.; Fredrickson, J.K. Imaging hydrated microbial extracellular polymers: Comparative analysis by electron microscopy. *Appl. Environ. Microb.* **2011**, *77*, 1254–1262. [CrossRef] [PubMed]

30. Schaudinn, C.; Stoodley, P.; Hall-Stoodley, L.; Gorur, A.; Remis, J.; Wu, S.; Auer, M.; Hertwig, S.; Guerrero-Given, D.; Hu, F.Z.; et al. Death and Transfiguration in Static *Staphylococcus epidermidis* Cultures. *PLoS ONE* **2014**, *9*, e100002. [CrossRef] [PubMed]

31. Lawrence, J.R.; Swerhone, G.D.W.; Leppard, G.G.; Araki, T.; Zhang, X.; West, M.M.; Hitchcock, A.P. Scanning transmission X-ray, laser scanning, and transmission electron microscopy mapping of the exopolymeric matrix of microbial biofilms. *Appl. Environ. Microb.* **2003**, *69*, 5543–5554. [CrossRef]

32. Karcz, J.; Bernas, T.; Nowak, A.; Talik, E.; Woznica, A. Application of lyophilization to prepare the nitrifying bacterial biofilm for imaging with scanning electron microscopy. *Scanning* **2012**, *34*, 26–36. [CrossRef] [PubMed]

33. Krzyzanek, V.; Sporenberg, N.; Keller, U.; Guddorf, J.; Reichelt, R.; Schonhoff, M. Polyelectrolyte multilayer capsules: Nanostructure and visualisation of nanopores in the wall. *Soft Matter* **2011**, *7*, 7034–7041. [CrossRef]

34. Hrubanova, K.; Nebesarova, J.; Ruzicka, F.; Krzyzanek, V. The innovation of cryo-SEM freeze-fracturing methodology demonstrated on high pressure frozen biofilm. *Micron* **2018**, *110*, 28–35. [CrossRef] [PubMed]

35. Biel, S.S.; Wilke, K.; Dunckelmann, K.; Wittern, K.P.; Wepf, R. Light and electron microscopy: Histochemistry on the identical biopsy after high-pressure freezing. *J. Histochem. Cytochem.* **2004**, *52*, S62.

36. Hawser, S.P.; Douglas, L.J. Biofilm Formation by Candida Species on the Surface of Catheter Materials in-Vitro. *Infect. Immunity* **1994**, *62*, 915–921.

37. Kuo, J. *Electron Microscopy: Methods and Protocols*; Springer Science & Business Media: Berlin, Germany, 2007; Volume 369.

38. Montesinos, E.; Esteve, I.; Guerrero, R. Comparison between Direct Methods for Determination of Microbial Cell-Volume—Electron-Microscopy and Electronic Particle Sizing. *Appl. Environ. Microb.* **1983**, *45*, 1651–1658.

39. Webster, P.; Wu, S.; Webster, S.; Rich, K.; McDonald, K. Ultrastructural preservation of biofilms formed by non-typeable Hemophilus influenzae. *Method Enzymol.* **2004**, *1*, 165–182. [CrossRef]

40. Graham, L.L.; Beveridge, T.J. Effect of Chemical Fixatives on Accurate Preservation of Escherichia-Coli and Bacillus-Subtilis Structure in Cells Prepared by Freeze-Substitution. *J. Bacteriol.* **1990**, *172*, 2150–2159. [CrossRef] [PubMed]

41. Hayat, M.A. *Principles and Techniques of Scanning Electron Microscopy. Biological Applications, Volume 1*; Van Nostrand Reinhold Company: New York, NY, USA, 1974.

42. Wu, Y.; Liang, J.; Rensing, K.; Chou, T.M.; Libera, M. Extracellular Matrix Reorganization during Cryo Preparation for Scanning Electron Microscope Imaging of Staphylococcus aureus Biofilms. *Microsc. Microanal.* **2014**, *20*, 1348–1355. [CrossRef] [PubMed]

43. Fassel, T.A.; Edmiston, C.E. Ruthenium red and the bacterial glycocalyx. *Biotech. Histochem.* **1999**, *74*, 194–212. [CrossRef] [PubMed]

44. Reese, S.; Guggenheim, B. A novel TEM contrasting technique for extracellular polysaccharides in in vitro biofilrns. *Microsc. Res. Tech.* **2007**, *70*, 816–822. [CrossRef] [PubMed]

45. Galway, M.E.; Heckman, J.W., Jr.; Hyde, G.J.; Fowke, L.C. Advances in High-Pressure and Plunge-Freeze Fixation. *Methods Cell Biol.* **1995**, *49*, 3–19. [PubMed]

46. Wang, A.B.; Lin, C.H.; Chen, C.C. The critical temperature of dry impact for tiny droplet impinging on a heated surface. *Phys. Fluids* **2000**, *12*, 1622–1625. [CrossRef]

47. Dahl, R.; Staehelin, L.A. High-pressure freezing for the preservation of biological structure: Theory and practice. *J. Electron Microsc. Tech.* **1989**, *13*, 165–174. [CrossRef] [PubMed]

48. Moor, H. Theory and Practice of High Pressure Freezing. In *Cryotechniques in Biological Electron Microscopy*; Steinbrecht, R., Zierold, K., Eds.; Springer: Berlin/Heidelberg, Germany, 1987; pp. 175–191.

49. Studer, D.; Michel, M.; Muller, M. High-Pressure Freezing Comes of Age. *Scanning Microsc.* **1989**, 253–269.

50. Shimoni, E.; Muller, M. On optimizing high-pressure freezing: From heat transfer theory to a new microbiopsy device. *J. Microsc.* **1998**, *192*, 236–247. [CrossRef] [PubMed]

51. Samek, O.; Mlynarikova, K.; Bernatova, S.; Jezek, J.; Krzyzanek, V.; Siler, M.; Zemanek, P.; Ruzicka, F.; Hola, V.; Mahelova, M. Candida parapsilosis Biofilm Identification by Raman Spectroscopy. *Int. J. Mol. Sci.* **2014**, *15*, 23924–23935. [CrossRef] [PubMed]

52. Rebrosova, K.; Siler, M.; Samek, O.; Ruzicka, F.; Bernatova, S.; Jezek, J.; Zemanek, P.; Hola, V. Differentiation between Staphylococcus aureus and Staphylococcus epidermidis strains using Raman spectroscopy. *Future Microbiol.* **2017**, *12*, 881–890. [CrossRef] [PubMed]

53. Notingher, I.; Hench, L.L. Raman microspectroscopy: A noninvasive tool for studies of individual living cells in vitro. *Expert Rev. Med. Devices* **2006**, *3*, 215–234. [CrossRef] [PubMed]

54. Mc, F.J. The nephelometer: An instrument for estimating the number of bacteria in suspensions used for calculating the opsonic index and for vaccines. *J. Am. Med. Assoc.* **1907**, *49*, 1176–1178.

55. Maquelin, K.; Kirschner, C.; Choo-Smith, L.P.; Ngo-Thi, N.A.; van Vreeswijk, T.; Stammler, M.; Endtz, H.P.; Bruining, H.A.; Naumann, D.; Puppels, G.J. Prospective study of the performance of vibrational spectroscopies for rapid identification of bacterial and fungal pathogens recovered from blood cultures. *J. Clin. Microbiol.* **2003**, *41*, 324–329. [CrossRef] [PubMed]

56. De Gelder, J.; De Gussem, K.; Vandenabeele, P.; Vancanneyt, M.; De Vos, P.; Moens, L. Methods for extracting biochemical information from bacterial Raman spectra: Focus on a group of structurally similar biomolecules—Fatty acids. *Anal. Chim. Acta* **2007**, *603*, 167–175. [CrossRef] [PubMed]

57. Tuma, R. Raman spectroscopy of proteins: From peptides to large assemblies. *J. Raman Spectrosc.* **2005**, *36*, 307–319. [CrossRef]

58. Notingher, I. Raman Spectroscopy cell-based Biosensors. *Sensors* **2007**, *7*, 1343–1358. [CrossRef]

59. Neugebauer, U.; Schmid, U.; Baumann, K.; Ziebuhr, W.; Kozitskaya, S.; Holzgrabe, U.; Schmitt, M.; Popp, J. The influence of fluoroquinolone drugs on the bacterial growth of S-epidermidis utilizing the unique potential of vibrational spectroscopy. *J. Phys. Chem. A* **2007**, *111*, 2898–2906. [CrossRef] [PubMed]

60. De Gelder, J.; De Gussem, K.; Vandenabeele, P.; Moens, L. Reference database of Raman spectra of biological molecules. *J. Raman Spectrosc.* **2007**, *38*, 1133–1147. [CrossRef]

61. Perna, G.; Lastella, M.; Lasalvia, M.; Mezzenga, E.; Capozzi, V. Raman spectroscopy and atomic force microscopy study of cellular damage in human keratinocytes treated with $HgCl_2$. *J. Mol. Struct.* **2007**, *834*, 182–187. [CrossRef]

62. Pyrgiotakis, G.; Bhowmick, T.K.; Finton, K.; Suresh, A.K.; Kane, S.G.; Bellare, J.R.; Moudgil, B.M. Cell (A549)-particle (Jasada Bhasma) interactions using Raman spectroscopy. *Biopolymers* **2008**, *89*, 555–564. [CrossRef] [PubMed]

63. Pilat, Z.; Bernatova, S.; Jezek, J.; Kirchhoff, J.; Tannert, A.; Neugebauer, U.; Samek, O.; Zemanek, P. Microfluidic Cultivation and Laser Tweezers Raman Spectroscopy of *E. coli* under Antibiotic Stress. *Sensors* **2018**, *18*, 1623. [CrossRef] [PubMed]

64. Rebrosova, K.; Siler, M.; Samek, O.; Ruzicka, F.; Bernatova, S.; Hola, V.; Jezek, J.; Zemanek, P.; Sokolova, J.; Petras, P. Rapid identification of staphylococci by Raman spectroscopy. *Sci. Rep.* **2017**, *7*, 14846. [CrossRef] [PubMed]

65. Samek, O.; Obruca, S.; Siler, M.; Sedlacek, P.; Benesova, P.; Kucera, D.; Marova, I.; Jezek, J.; Bernatova, S.; Zemanek, P. Quantitative Raman Spectroscopy Analysis of Polyhydroxyalkanoates Produced by Cupriavidus necator H16. *Sensors* **2016**, *16*, 1808. [CrossRef] [PubMed]

66. Ruzicka, F.; Hola, V.; Votava, M.; Tejkalova, R. Importance of biofilm in Candida parapsilosis and evaluation of its susceptibility to antifungal agents by colorimetric method. *Folia Microbiol.* **2007**, *52*, 209–214. [CrossRef]

67. Azeredo, J.; Azevedo, N.F.; Briandet, R.; Cerca, N.; Coenye, T.; Costa, A.R.; Desvaux, M.; Di Bonaventura, G.; Hebraud, M.; Jaglic, Z.; et al. Critical review on biofilm methods. *Crit. Rev. Microbiol.* **2017**, *43*, 313–351. [CrossRef] [PubMed]

68. Haque, F.; Alfatah, M.; Ganesan, K.; Bhattacharyya, M.S. Inhibitory Effect of Sophorolipid on Candida albicans Biofilm Formation and Hyphal Growth. *Sci. Rep.* **2016**, *6*, 23575. [CrossRef] [PubMed]

69. Ludecke, C.; Jandt, K.D.; Siegismund, D.; Kujau, M.J.; Zang, E.; Rettenmayr, M.; Bossert, J.; Roth, M. Reproducible Biofilm Cultivation of Chemostat-Grown *Escherichia coli* and Investigation of Bacterial Adhesion on Biomaterials Using a Non-Constant-Depth Film Fermenter. *PLoS ONE* **2014**, *9*, e84837. [CrossRef] [PubMed]

70. Bray, D.F.; Bagu, J.; Koegler, P. Comparison of Hexamethyldisilazane (Hmds), Peldri-Ii, and Critical-Point Drying Methods for Scanning Electron-Microscopy of Biological Specimens. *Microsc. Res. Tech.* **1993**, *26*, 489–495. [CrossRef] [PubMed]

71. Hazrin-Chong, N.H.; Manefield, M. An alternative SEM drying method using hexamethyldisilazane (HMDS) for microbial cell attachment studies on sub-bituminous coal. *J. Microbiol. Methods* **2012**, *90*, 96–99. [CrossRef] [PubMed]

72. Osumi, M.; Konomi, M.; Sugawara, T.; Takagi, T.; Baba, M. High-pressure freezing is a powerful tool for visualization of Schizosaccharomyces pombe cells: Ultra-low temperature and low-voltage scanning electron microscopy and immunoelectron microscopy. *J. Electron Microsc.* **2006**, *55*, 75–88. [CrossRef] [PubMed]

73. Psenicka, M.; Tesarova, M.; Tesitel, J.; Nebesarova, J. Size determination of *Acipenser ruthenus* spermatozoa in different types of electron microscopy. *Micron* **2010**, *41*, 455–460. [CrossRef] [PubMed]

74. Brandt, N.N.; Brovko, O.O.; Chikishev, A.Y.; Paraschuk, O.D. Optimization of the rolling-circle filter for Raman background subtraction. *Appl. Spectrosc.* **2006**, *60*, 288–293. [CrossRef] [PubMed]

75. Wold, S.; Esbensen, K.; Geladi, P. Principal Component Analysis. *Chemom. Intell. Lab.* **1987**, *2*, 37–52. [CrossRef]

76. Kaech, A.; Ziegler, U. High-Pressure Freezing: Current State and Future Prospects. *Methods Mol. Biol.* **2014**, *1117*, 151–171. [PubMed]

77. Kaech, A.; Woelfel, M. Evaluation of Different Freezing Methods for Monolayer Cell Cultures. *Microsc. Microanal.* **2007**, *13*, 240–241. [CrossRef]

78. Donlan, R.M. Biofilms: Microbial life on surfaces. *Emerg. Infect. Dis.* **2002**, *8*, 881–890. [CrossRef] [PubMed]

79. Mahapatra, S.; Banerjee, D. Fungal exopolysaccharide: Production, composition and applications. *Microbiol. Insights* **2013**, *6*, 1–16. [CrossRef] [PubMed]

80. Maira-Litran, T.; Kropec, A.; Abeygunawardana, C.; Joyce, J.; Mark, G.; Goldmann, D.A.; Pier, G.B. Immunochemical properties of the staphylococcal poly-*N*-acetylglucosamine surface polysaccharide. *Infect. Immunity* **2002**, *70*, 4433–4440. [CrossRef]

Biofilm formation and extracellular polymeric substances (EPS) production by *Bacillus subtilis* depending on nutritional conditions in the presence of polyester film

Stanislava Voběrková [1] · **Soňa Hermanová** [2] · **Kamila Hrubanová** [3] · **Vladislav Krzyžánek** [3]

Abstract The influence of biofilm formation as the mode of microorganism growth on degradation of synthetic polymers represents an important research topic. This study focuses on the effect of biofilm developed by *Bacillus subtilis* (BS) cultivated submerged under various nutrition conditions on biodeterioration of poly(ε-caprolactone) film. Polymer in the film form (thickness 0.7 mm) was incubated for 21 days either continuously or by regularly renewed system. The scission of polyester chain bonds took place in all biotic media and was enhanced by biofilm formation in nutrient-rich media.

Abbreviations

BS	*Bacillus subtilis*
MM	Mineral medium
MM+YE	Mineral medium enriched by yeast extract
NBG	Nutrient broth medium enriched by glucose
NB	Nutrient broth
PCL	Poly(ε-caprolactone)
EPS	Extracellular polymeric substances
eDNA	Extracellular DNA

✉ Stanislava Voběrková
stanislava.voberkova@mendelu.cz

[1] Institute of Chemistry and Biochemistry, Faculty of Agronomy, Mendel University in Brno, Zemědělská 1/1665, 613 00 Brno, Czech Republic

[2] Department of Polymers, Faculty of Chemical Technology, University of Chemistry and Technology Prague, Technická 5, 16628 Prague, Czech Republic

[3] Institute of Scientific Instruments of ASCR, Královopolská 147, 61264 Brno, Czech Republic

Introduction

Bacillus subtilis which is a nonpathogenic, Gram-positive soil bacterium belongs to group of attractive microorganisms, which are capable of forming architecturally complex communities of cells known as biofilm (Kearns et al. 2005). Within a biofilm, bacterial cells display higher resistance to adverse environmental effects than their planktonic counterparts. Biofilm formation may represent a survival strategy in a nutritionally limited environment (Speranza et al. 2011). The extracellular matrix, where cells are embedded during biofilm development form an integral part of a biofilm (Marvasi et al. 2010). This matrix consists of extracellular polymeric substances (EPS) where polysaccharides are responsible for both adhesion and cohesion interactions, proteins serve as carbon and energy source, and extracellular DNA seems to play an important role in the establishment of the whole biofilm structure. However, extracellular DNA production by *B. subtilis* is incorrectly understood (Zafra et al. 2012). It was stated that EPS is both secreted by bacteria and is the product of cell lysis and hydrolytic activities even without the presence of accessible solid surfaces (Flemming et al. 2007).

The role of EPS in the cell surface adhesion process has been extensively researched by biofilm scientific literature (Czaczyk and Myszka 2007; Marvasi et al. 2010). However, up to now, only a few of these papers have provided actual information on relationship between biofilm formation, EPS production, and biodeterioration of polymer materials in relation to nutritional factors (Allan et al. 2002; Jung et al. 2013). Bacterial biofilm has a significant impact on utilization and lifetime period of polymer material in medical, industrial, and environmental settings (Rinaudi et al. 2006). Although biofilm formation on polymer surfaces (Sivan 2011) does not lead to its biodegradation, it contributes to changes in surface conditions and in this way influences the biodegradation rate.

To our knowledge, only few studies have dealt with the effect of microbial growth mode on the biodeterioration of polymer surfaces. Lefévre et al. (2002) reported that the biodegradation rate of poly(ε-caprolactone) film decreased, and also, biodegradation extent was more limited under conditions, which favored the biofilm formation, than under those, where no biofilm was detected.

Therefore, this research has been carried out to study the effect of various nutrition conditions on the biofilm formation and related PCL film biodeterioration by submerged cultivation of *B. subtilis* CCM 1999.

Materials and methods

Inoculum preparation and cultivation media

B. subtilis CCM 1999 (BS) was obtained from the culture collection of the Czech Collection of Microorganisms (CCM), at Masaryk University Brno, Faculty of Science. Tested culture was maintained on nutrient agar at 30 °C for 3 days before the start of the experiments.

For inoculum preparation, 1 mL of distilled sterile water was added into nutrient agar inoculated with *B. subtilis*. The colonies were rubbed carefully with a sterile vaccination loop and transferred into 100 mL of nutritious medium in a sterile Erlenmeyer flask (250 mL), and bacterial inoculum was cultivated (30 °C, 160 rpm, 6 h). After this time, 1 mL of cultivation media (600×10^6 CFU/mL) was used for inoculation of cultivation medium in L-tubes and biodeterioration tests. Bacterial density was measured by McFarland densitometer (DEN-1B, LABOSERV s.r.o Brno).

Used mineral medium (MM) consisted of KH_2PO_4 (0.7 g), K_2HPO_4 (0.7 g), $MgSO_4\cdot7H_2O$ (0.7 g), NH_4NO_3 (1 g), NaCl (0.005 g), $FeSO_4\cdot7H_2O$ (0.002 g), $ZnSO_4\cdot7H_2O$ (0.002 g), $MnSO_4\cdot7H_2O$ (0.001 g), and distilled water (1000 mL). For MM+YE medium, yeast extract (10 g) was added. Nutritious medium (NB medium) was prepared from peptone (3.0 g), yeast extract (1.0 g), NaCl (0.5 g), and distilled water (100 mL). For NBG medium, glucose (2.0 g) was added to NB medium. All the media were sterilized in an autoclave at 121 °C and 103.4 kPa for 20 min.

Poly(ε-caprolactone)

Poly(ε-caprolactone) (PCL) containing hydroxyl end groups was prepared by the ring-opening polymerization of ε-caprolactone (97 %, Sigma-Aldrich). Polyester films were prepared by melt-pressing (temperature 64 °C, 3 min, pressure 0.35 MPa) of dried powder, which was previously twice reprecipitated by methanol. Specimens with the following dimensions ($10\times10\times0.7$ mm) were sterilized by UV irradiation for 30 min at each side and

subjected to incubation. PCL was subjected to analysis and degradation experiment in the film form.

For the DSC experiments, DSC Q100 (TA Instruments) was used. About 4 mg of sample was encapsulated in standard aluminium pans. Samples were heated and cooled at the rate of 10 °C/min under nitrogen gas flow (50 mL/min). Measurement was as follows: (i) 0–100 °C, (ii) 100–0 °C, (iii) 0–100 °C, and (iv) 100–0 °C. Crystallinity of films was evaluated according to the following equation, where ΔH_m is measured melting enthalpy and ΔH_m^0 (139.5 J/g) is melting enthalpy for hypothetically 100 % crystalline sample:

$$\chi(\%) = \Delta H_m \Big/ \Delta H_m^0 \times 100$$

Thermal characteristics of tested PCL film are summarized in Table 1. Melting (T_m) and crystallization (T_c) temperatures were taken as the temperature of the peak value.

FTIR spectra were analyzed using FTIR spectrometer Nicolet 6700 (Thermo Scientific, USA) equipped with a diamond crystal GladiATR (PIKE Technologies, USA). ATR-FTIR spectra were measured with a resolution of 4 cm^{-1} in the range of 4000–400 cm^{-1} (64 scans).

Molar masses were determined by size exclusion chromatography (SEC) on Waters Breeze chromatographic system equipped with RI detector. Separation was performed on two PSS Lux LIN M 5 μm (7.8×300 mm) columns at 35 °C in THF at an elution rate of 1 mL/min using polystyrene as standards for calibration.

Surface of PCL films exposed to BS-inoculated media was evaluated by SEM. Samples were washed by distilled water and air-dried and then coated by 4 nm platinum to enhance the image contrast. Sample surfaces were investigated in the SEM Magellan 400/L (FEI) at the electron energy of 2 keV by recording the secondary electron micrographs at various magnifications.

Procedures

Cultivation of *B. subtilis*

BS was cultivated (160 rpm) at 30 °C in the presence or without PCL specimen for 21 days. One specimen was added per tube with 6 mL of medium at pH 7.0. Submerged

Table 1 Thermal characteristics of studied PCL film

	T_m^{1st} [°C]	χ^{1st} [%]	T_c^{1st} [°C]	T_m^{2nd} [°C]	χ^{2nd} [%]	T_c^{2nd} [°C]
PCL	64	71	38	59	55	38

Melting temperature T_m, crystallization temperature T_c, and crystallinity χ were determined from the first (1st) and the second (2nd) heating

cultivation was performed either continuously, or BS-inoculated medium was regularly renewed every week. PCL specimens were withdrawn after 21 days and rinsed with distilled water and dried until the constant mass. For control abiotic test, noninoculated growth media with sodium azide (0.02 % *w/w*) were used.

Extracellular polymeric substances

The presence of EPS was determined after 7, 24, 168, and 504 h of incubation time. After BS-inoculated medium centrifugation (7800*g*, 4 °C, 20 min), an aliquot of cell-free supernatant was withdrawn (12 mL) and incubated with ethanol at 4 °C overnight. Final suspension was centrifuged (7800*g*, 4 °C, 20 min), and 10 mL of distilled water was added for resuspending. The content of proteins, polysaccharides, and extracellular DNA was determined. Protein content was quantified according to Lowry method with bovine serum albumin as a standard (Lowry et al. 1951). Polysaccharide concentration was determined according to Dubois method (Dubois et al. 1956) with glucose as a standard.

Average was counted from results of six measurements, where set of three measurements for one test tube was done.

Extracellular DNA extraction

The bacterial culture (1 mL) was separated by centrifugation (10,000*g*, 4 °C, 5 min). Removed cells from supernatants were lysed in pellets form in 100 μL of lysis solution (50 mmol/L glucose, 25 mmol/L Tris–HCl buffer, pH 8.0; 10 mmol/L EDTA, pH 8.0, and lysozyme 2 mg/mL) for 5 min at laboratory temperature. After the incubation period, 150 μL of alkaline lysis solution (0.2 mol/L NaOH, 1 % sodium dodecyl sulfate) was added. The tubes were gently vortexed to mix completely and incubated for 5 min at 0 °C. After this time, 150 μL of solution (5 mol/L sodium acetate adjusted at pH 4.8 with acetic acid) was added to neutralize the solution. The suspension was carefully mixed by inversion for a few seconds during which it became almost clear and slightly viscous. The tube was maintained for 5 min at 0 °C, and then, it was centrifuged (10,000*g*, 4 °C, 5 min). The supernatant was carefully removed and transferred to the clear Eppendorf tube; 900 μL of ethanol (96 %) was added; and the solution was gently mixed. The tube was held at −20 °C for 15 min, and precipitate was collected by centrifugation (10,000*g*, 4 °C, 5 min) and supernatant removed by aspiration. The pellets were dissolved in 40 μL of buffer (10 mmol/L Tris–HCl, pH 8.0; 1 mmol/L EDTA; pH 8.0), and the concentration of isolated DNA was estimated by spectrophotometry (NanoDrop 2000, Thermo Fisher Scientific).

Results and discussion

Bacterial growth and pH profile during cultivation

Accelerated tests concerning polymer biodeterioration and biodegradation at the laboratory scale are frequently conducted under conditions both optimized for the growth of the particular microorganisms and those where the polymer represents the sole carbon source. From this point of view, the influence of the nutritional factors on the cell growth of *B. subtilis* (BS) culture was researched in four different incubation media, where carbon to nitrogen ratio increased in order as follows: mineral medium (MM)<yeast extract enriched mineral medium (MM+YE)<nutrient broth (NB)<nutrient broth supplemented with glucose (NBG). The carbon and nitrogen content was chemically determined by chromic sulfuric acid digest and a modified Kjeldahl method, respectively. The results of bacterial growth can be seen from Fig. 1. Bacterial population growing in media with peptone (NB, NBG) as an important source of organic nitrogen, showed prolonged stationary phase of bacterial growth in comparison to those in mineral (MM+YE) medium, where only yeast extract was present. This corresponds to the results of study on wild-type strain of *B. subtilis* RB14, where a soybean peptone supported cellular growth more than less nutritious casein peptone during the fermentation of different nitrogen sources (Zahora et al. 2009).

The presence of melt-pressed poly(ε-caprolactone) film in cultivation media seemed to have negligible effect on biomass growth under experimental conditions (Fig. 1). It is worth mentioning that the turbidimetric measurement provided indirect information about bacterial growth, which could be influenced also by presence of dead cells and biofilm matrices, which had gradually developed during the experimental period.

pH profiles of all tested media (Fig. 2) were measured as an additional information since changes in pH during cultivation documented the bacterial metabolism and could also influence the biofilm formation. In all media tested, it was clearly observed that by means of metabolite production during the growth and biotransformation, BS significantly affected the environment. Decrease in pH value of BS-inoculated NBG and NB media, which was measured within a few first hours of incubation, can be attributed to the higher cellular growth and related to higher catabolic activity. Production of acids may also play a role, especially when all the glucose was used up, which was testified by the significant pH decrease observed in BS-inoculated NBG medium (Blencke et al. 2003; Yan et al. 2013). The pH value gradually increased to 8.7–9.2 in all tested media. This would be probably due to ammonification and degradation of nitrogenous medium component by BS. The pH profile of control abiotic media with initial pH of 7.0 containing PCL specimen was almost constant or slightly lowered to 6.6.
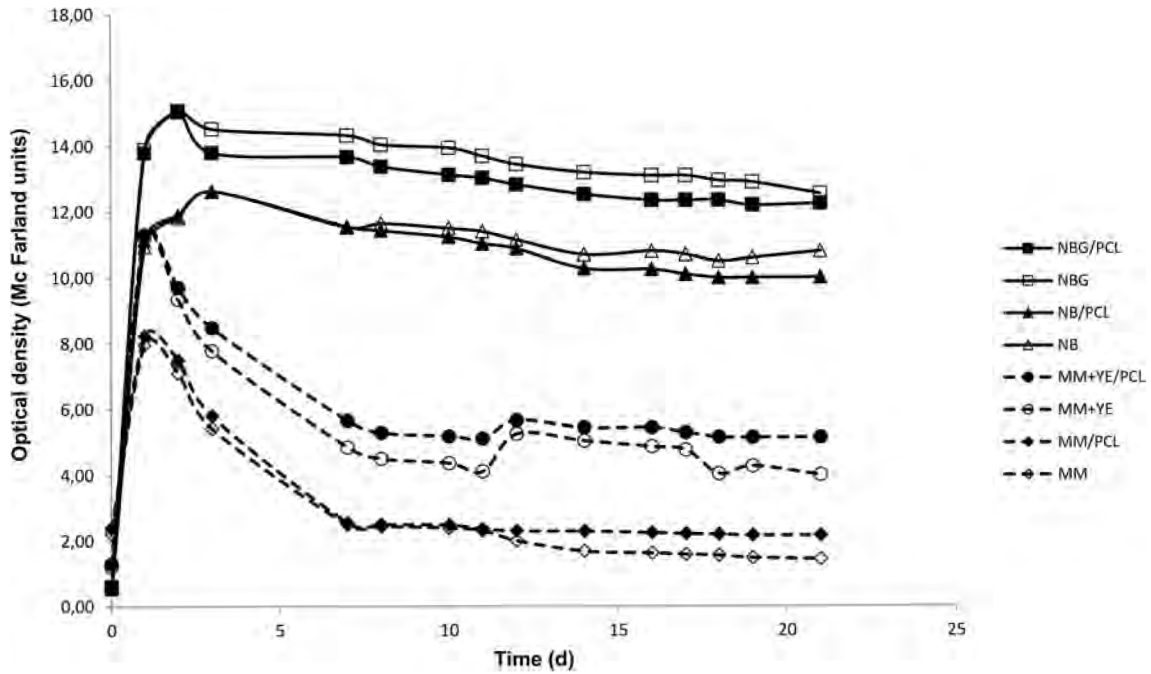
Fig. 1 Growth profile of BS culture in different cultivation media in presence of PCL and in media without PCL; bacterial growth is expressed in McFarland units

Biofilm formation and EPS production

Biofilm generation on PCL film surface was monitored by SEM. Extensive tests of different preparation techniques (Echlin 2009) showed that the PCL film was not inert toward chemicals used within the standard protocols for chemical preparation. Acetone, commonly used for sample dehydration, dissolves PCL and thus cannot be used in this case. Also,
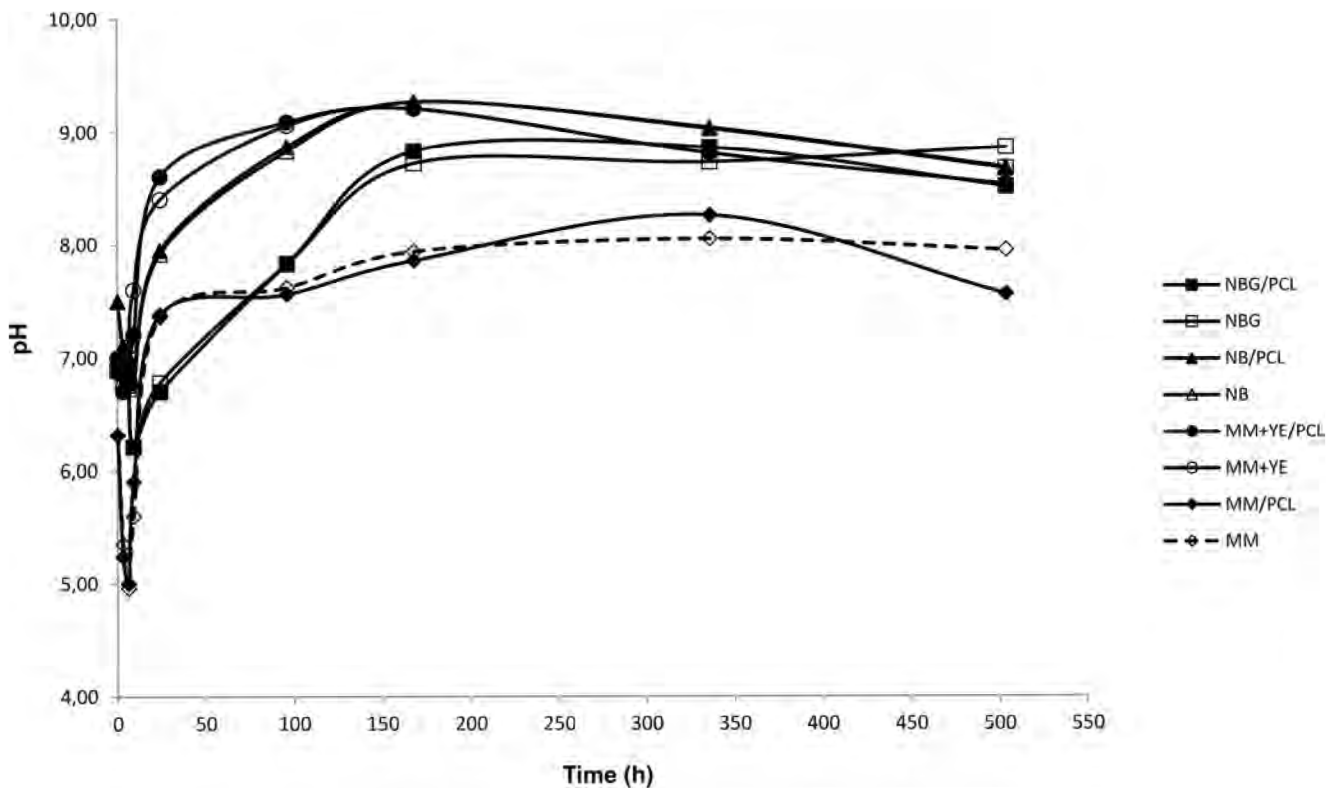
Fig. 2 pH profile of BS growing in different cultivation media with and without PCL

drying in solutions with low surface pressure, which requires miscibility with acetone like hexamethyldisilazane, was not possible to be applied. Critical point drying method commonly used for drying biological samples cannot be used due to instability of the PCL films under the high pressure and temperature that are demanded for the technique. Therefore, incubated PCL samples were washed by distilled water and air-dried before SEM analysis.

Almost intact PCL surface after 24 h as well as after 3 days of cultivation test suggests only planktonic growth of BS, whereas most studies reported the biofilm occurrence after 24–48 h of cultivation period (Bridier et al. 2013). Biofilm formation was not observed in PCLs immersed in both BS-inoculated mineral media (MM, MM+YE) during the whole incubation period. The presented results are in contradiction to several studies, where nutritionally limited environment supported the biofilm formation (Ryu et al. 2004; Jung et al. 2013). The main reason presented was that the surface colonization provided increased concentration of nutrients previously absorbed by solid surface together with apparent lack of carbon and nitrogen sources in mineral media bulk which corresponds to the low planktonic growth.

For PCLs immersed in inoculated nutritious media (NB, NBG), cracks were developed after 1-week period (as indicated by an arrows in Fig. 3a, b), and the biofilm formation was detected after 14 days (Fig. 3c, d). Biofilm formation proceeded independently of media renewing and also the presence of glucose does not seem to have a noticeable effect. Dense and compact biofilm was generated in NBG medium, whereas biofilm in NB medium showed more porous structure. Due to the presence of glucose as an easily accessible carbon source, higher substrate transfer rates were assumed and consequently, compact and dense biofilm was formed. On the contrary, porous biofilm was observed in a substrate with transfer-limited regime, where only peptone and yeast extract were present (NB medium).

According to SEM observations, biofilm developed on the PCL films inoculated for 21 days in nutrient media showed mucous features. Present hydrated matrix (Fig. 3e) with bacterial cell embedded in the biofilm (Fig. 3f) documented the architecture of BS biofilm. EPS matrix was also observed, which formed environment for bacteria (Fig. 3g) along with a network of channels (Fig. 3h). According to Romero (2013), they contribute to aeration, elimination of trash, transit of nutrients, and signaling.

Alkaline pH did not inhibit the BS adhesion and had no effect on biofilm formation under cultivation conditions. The inhibiting effect of the alkaline pH on the *Staphylococcus aureus* and *Staphylococcus epidermidis* bacterial attachment and normal development of biofilm was reported by Nostro et al. (2012).

To make the information on biofilm development complete, the content of EPS was determined after 7, 24, 168, and 504 h of BS cultivation. Production of EPS essential for biofilm formation can be seen from Fig. 3c, d. As several authors reported (Kodali et al. 2009; Sheng et al. 2010), yields of EPS extracted from biofilm depend on the method of extraction. Precipitation by ethanol was chosen for this study, because this precipitation process removes only the biopolymer (exo-polysaccharides and proteins) and not corresponding monomers, present in the fermentation medium.

High production of EPS was observed during exponential phase of cell growth. It means that EPS synthesis depends on proliferating process of cells. The lowest amount of EPS was found for BS-inoculated MM and MM+YE media, independently of the PCL presence, which correlates with no biofilm formation during 21 days (Figs. 4, 5, and 6).

The content of EPS was considerably higher in the presence of PCL film in BS-inoculated nutritious media (NB, NBG) than that measured for media without the polymer. During stationary phase of cell growth a slight increase in concentration of polysaccharides, which act as a binding agent for bacterial population on a solid surface, was detected in the presence of PCL films (Fig. 4).

Extracellular protein content determined from ethanol extracts precipitation is expressed in $mg/10^8$ cells (Fig. 5). The amount of precipitated extracellular proteins increased during exponential and in the early stationary phase of cell growth, and then remained constant during the whole cultivation period. Their content was higher in the presence of PCL film, where formation of its layer on solid surface is supposed. This layer might convert the solid/medium interface into a region of gel-like nature to interact with other specific polymers of the bacteria surfaces. Significant increase in the concentration of extracellular DNA (eDNA) after a week of incubation in the presence of PCL samples was observed (Fig. 6), which correlates well with the presence of biofilm.

Surprisingly, glucose, which has been reported as a possible main precursor of EPS production (Miqueleto et al. 2010), increased production of polysaccharides and extracellular proteins but had little or no effect on secretion of eDNA. This observation may be related to the little-known way how different species release DNA into the environment and also the diverse role of eDNA in biofilm formation.

Changes in polymer characteristics

Poly(ε-caprolactone) had relatively low molar mass (M_n 20 kg/mol) and high crystallinity (71 %). Due to its hydrophobic and semicrystalline character, PCL is assumed to be stable against abiotic hydrolysis at temperatures of 25–30 °C. To evaluate the impact of base-catalyzed hydrolysis on polyester chain degradation, PCL was also immersed in abiotic media with pH profile following that of BS-inoculated ones for 21 days. No mass loss and almost negligible changes in molar mass of aged samples confirmed the PCL resistance to hydrolysis both at neutral and at alkaline conditions through the entire incubation period (Table 2).

Fig. 3 SEM images of PCL samples immersed in nutrient media (NBG, NB) inoculated by *B. subtilis* after 7, 14, and 21 days of experiment: the image of cracks on PCL sample in NB (**a**) and in NBG (**b**) medium after 7 days of incubation; the image of character of biofilm in NB (**c**) and in NBG (**d**) medium after 14 days of incubation; the image of mucous matrix (NBG medium) illustrated the presence of biofilm after 21 days (**e**); the presence of bacteria in biofilm in NBG medium after 21 days (**f**); SEM observation of EPS substances in NB medium after 21 days (**g**); presence of channels in biofilm in NBG medium after 21 days (**h**)
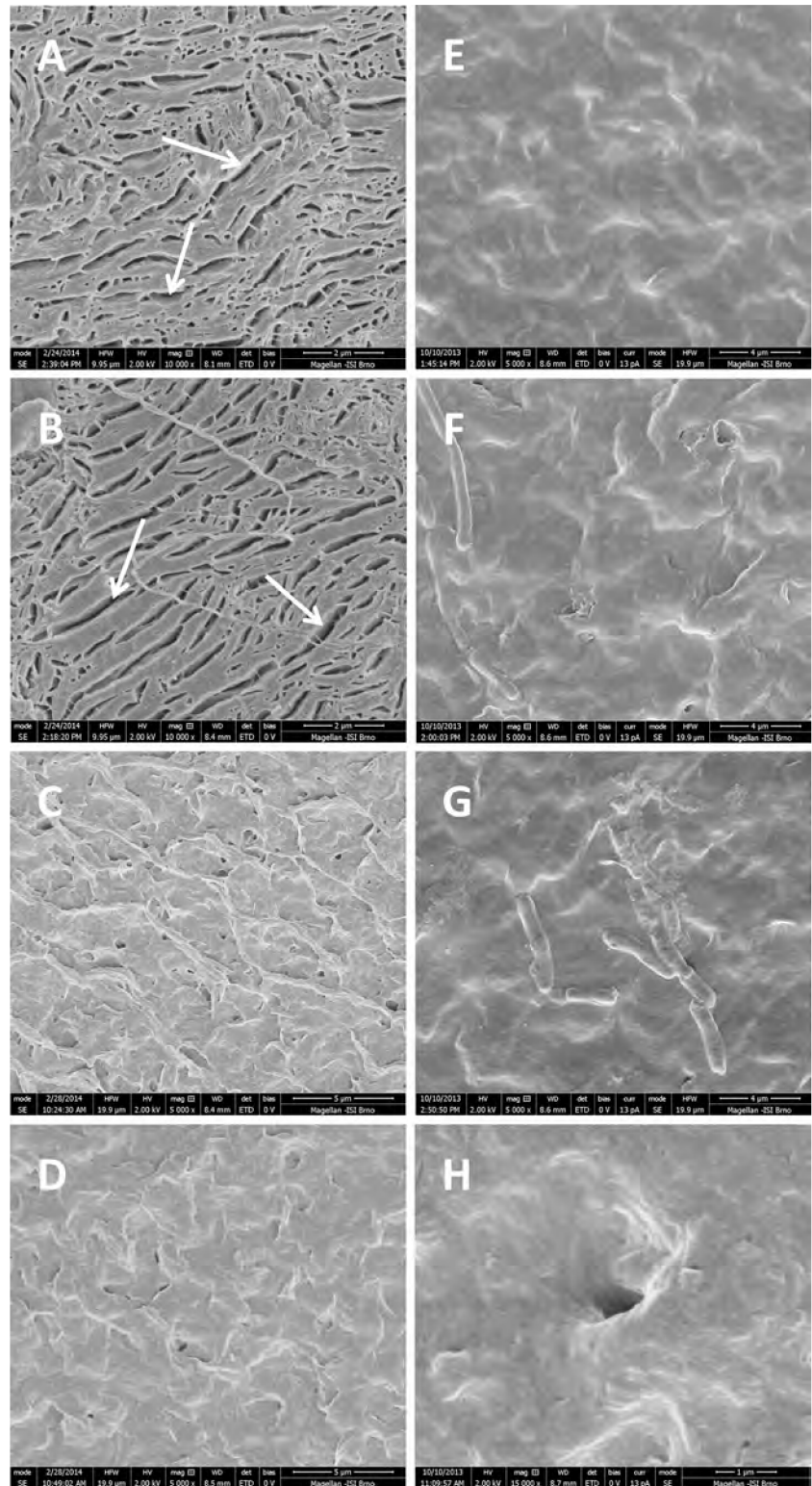
The biodeterioration action of *B. subtilis* (BS) on PCL film was recorded on the base of the gradual sample mass loss and the surface erosion, which were measured in all inoculated media. The decrease in bacterial aged PCL molar mass was negligible, and it implied that the chain scission occurred only in the surface layer of PCL films after the extracellular enzymes adsorption. It could be also suggested that extracellular enzymes acting in the vicinity of polyester chain ends mainly through the chain-unzipping mechanism. Consequently,
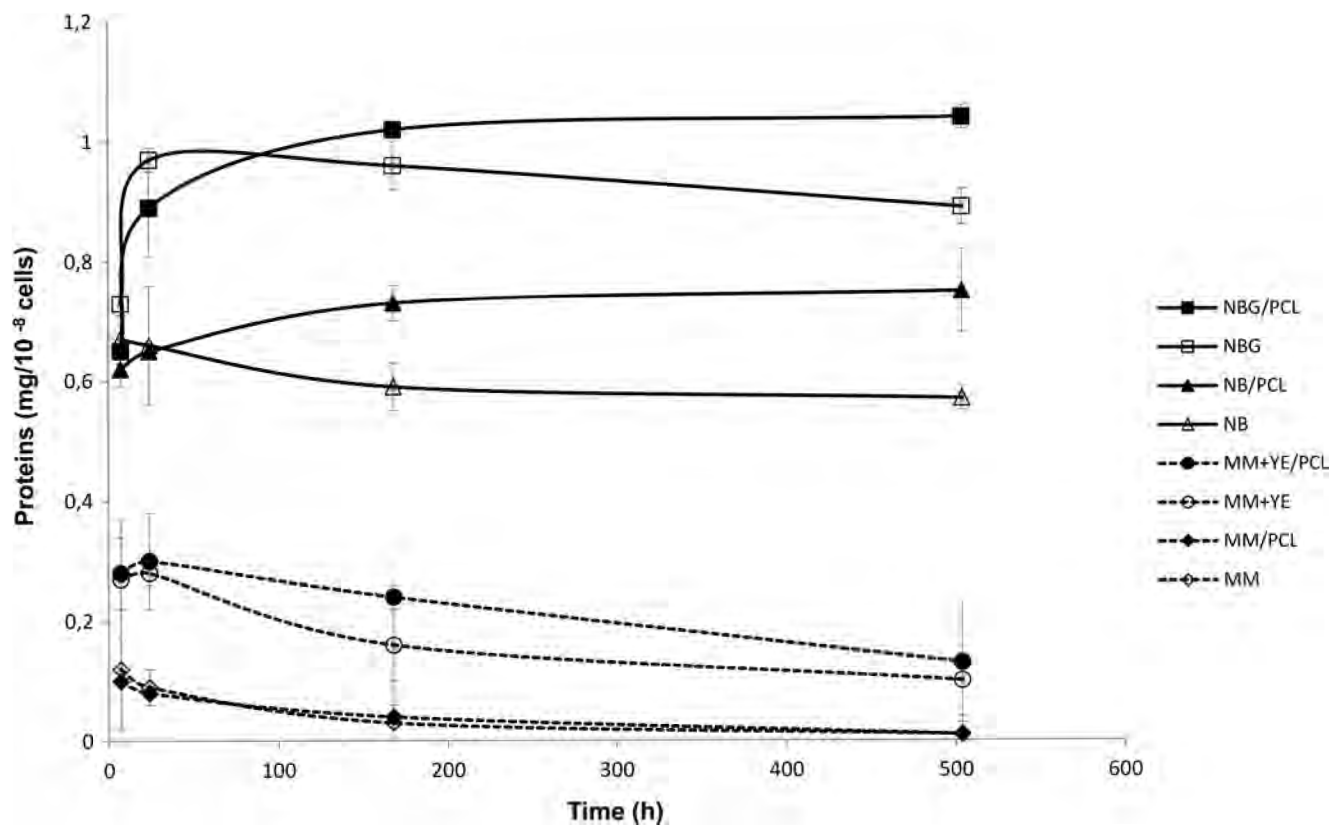
Fig. 4 Concentration of extracellular polymeric substances (EPS)—polysaccharides was monitored in cell-free supernatant removed from different cultivation media with and without PCL. *Error bars* represent standard deviation of six measurements
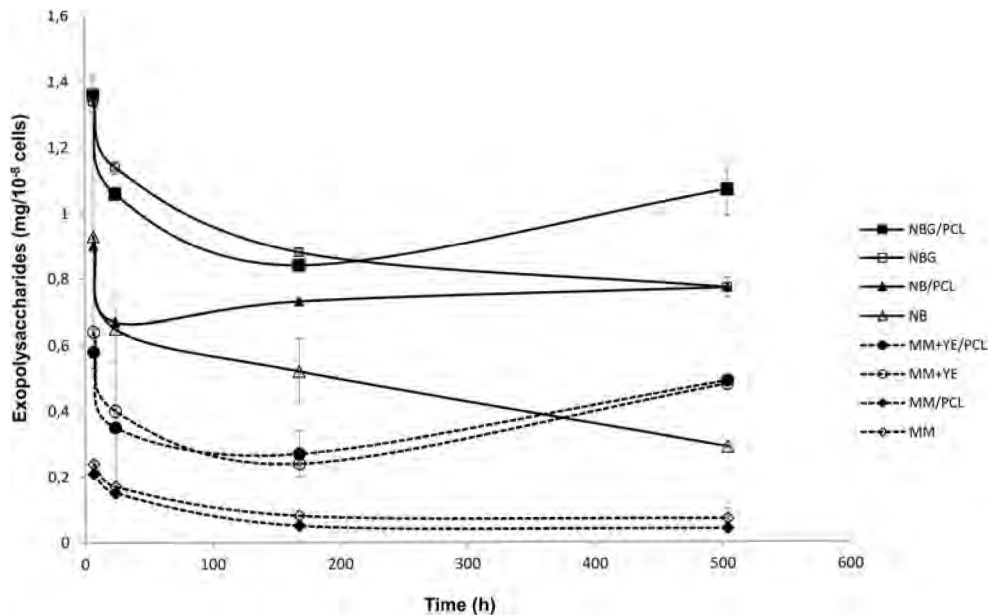
generated soluble degradation products were released into the surrounding medium as was evidenced by the sample mass loss (Table 2). Development of randomly distributed microcracks on the PCL films exposed to BS-inoculated nutrient-poor media (as indicated by an arrows in Fig. 7a, b), which confirms the surface erosion process, occurred almost independently of microbial culture renewing.

For PCL films immersed in biotic nutritious media (NB, NBG), the cracks were also developed after 1 week

Fig. 5 Concentration of extracellular polymeric substances (EPS)—proteins was monitored in cell-free supernatant removed from different cultivation media with and without PCL. *Error bars* represent standard deviation of six measurements
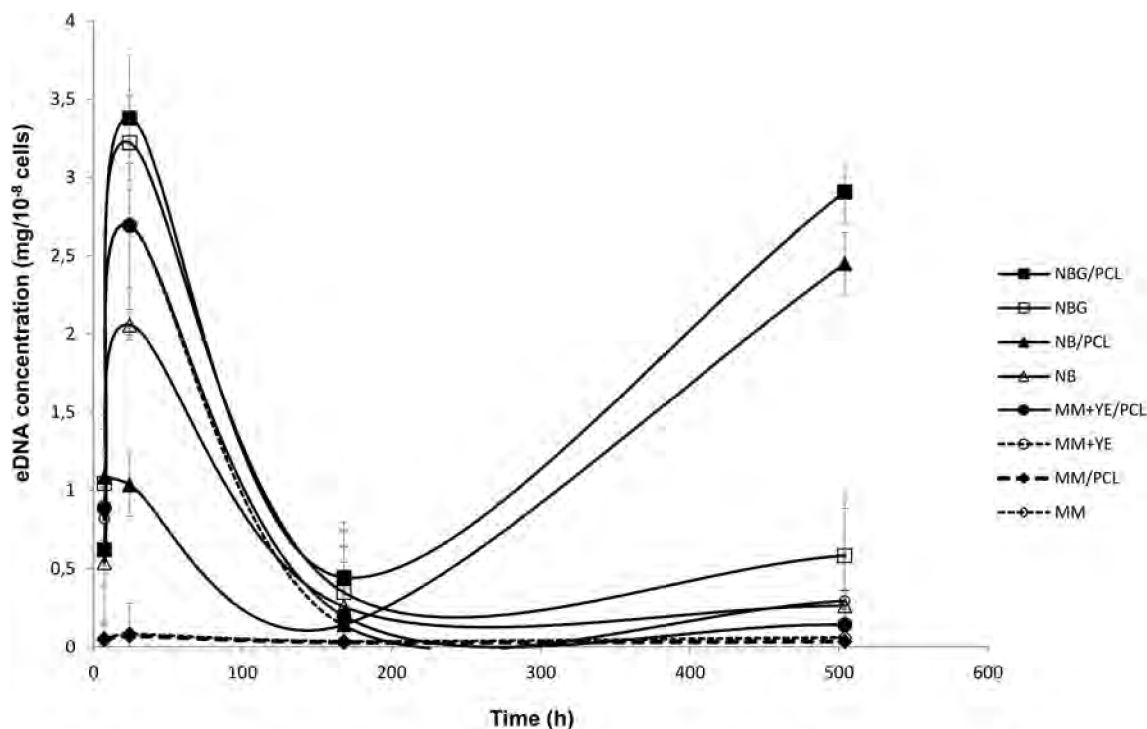
Fig. 6 Concentration of extracellular polymeric substances (EPS)—DNA was monitored in cell-free supernatant removed from different cultivation media with and without PCL. *Error bars* represent standard deviation of six measurements

of incubation period (Fig. 3a, b), and continuous biofilm was apparent on the film surface after an additional week (Fig. 3c, d). The presence of biofilm enhanced the rate of biodeterioration process as documented by the highest mass loss of PCL specimens aged in both biotic nutritious media without renewing (Table 2). With nutritious media renewing, the degrading capability of BS for PCL chains dropped and the sample mass loss was almost the same as that in renewed mineral medium with yeast extract.

Table 2 Changes in molar mass and mass loss of PCL samples exposed to *Bacillus subtilis* and those exposed to comparable abiotic conditions

| Sample	Mass loss[a] (%)	M_n^{SEC} (g/mol)	M_w^{SEC} (g/mol)
PCL (0d)	–	20,100	27,300
BS-NBG	7.0±1.3	18,100	25,700
BS-NBG (changed)	3.2±0.6	19,900	27,100
NBG-control (pH 7)	0.0	20,300	27,300
NBG-control (real pH)	0.0	19,700	26,000
BS-NB	10.3±0.3	19,600	26,900
BS-NB (changed)	4.8±0.3	19,900	27,000
NB-control (pH 7)	0.0	20,700	27,800
NB-control (real pH)	0.0	19,700	26,400
BS-MS+YE	1.0±0.7	18,700	26,500
BS-MS+YE (changed)	3.4±1.3	19,000	26,100
MS+YE-control (pH 7)	0.0	20,900	27,500
MS+YE-control (real pH)	0.0	19,400	26,500
BS-MS	0.3±0	20,400	27,500
BS-MS (changed)	0.7±0.1	20,200	27,400
MS-control	1.0±0.1	20,400	27,300

[a] Mass loss is calculated according to the equation as follows: $100 \times \left(\frac{m_o - m_d}{m_o} \right)$, where m_0 means mass of the film before experiment and m_d means mass of the dried sample after the experiment
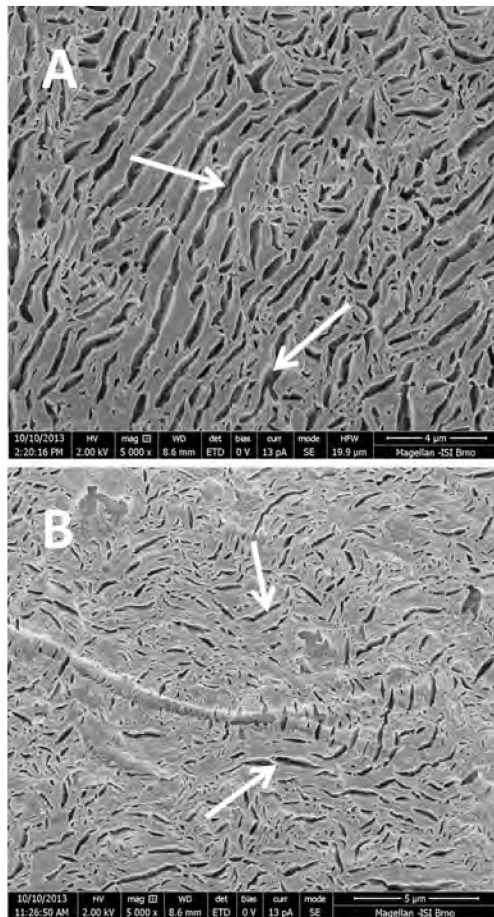
Fig. 7 Surface morphology of PCL films after 21 days of exposure to BS: in mineral medium (MM) (**a**) and in mineral medium with yeast extract (MM+YE) (**b**)

PCL films before and after microbial cultivation in mineral media ATR-FTIR spectra were evaluated with emphasis on regions, where carbonyl stretching and
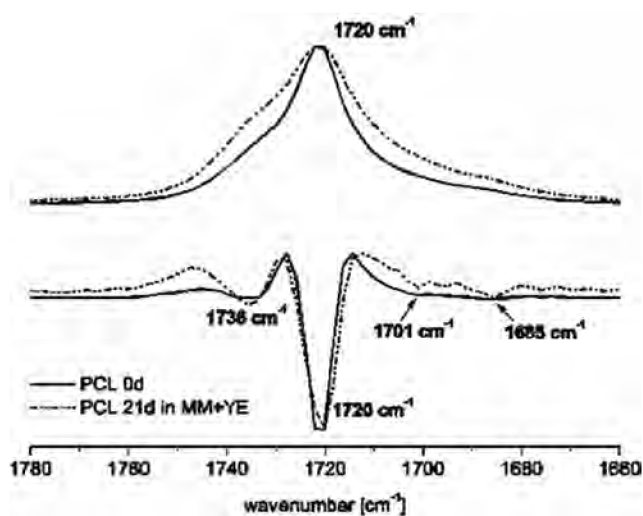
Fig. 8 ATR-FTIR spectrum of PCL film before degradation and representative degraded sample: carbonyl peak centered at 1720 cm^{-1} and the second derivate of this peak

bending vibration bands were present. In the second derivate, the splitting of absorption peak at 1720 cm^{-1} into two peaks, first at 1736 cm^{-1} (amorphous state) and the second one at 1721 cm^{-1} (crystalline state) confirmed semicrystalline character of PCL film under research (Fig. 8) (Rohindra et al. 2005). The increase in absorption from 1721 cm^{-1} relative to 1736 cm^{-1} in the spectrum of microbial aged PCL film reflected increase in crystallinity of surface layer in comparison to the sample before degradation. This can be attributed to the microbial attack and erosion of amorphous domains which are more vulnerable to degradation than crystalline ones. Further, a new peak at 1701 cm^{-1} is attributed to carbonyl stretching in carboxylic group. The minor peak at 1685 cm^{-1} belonged to amide band and suggested the presence of protein traces adsorbed by the sample surface. The generation of carboxylic end groups confirmed chain scission process during the sample exposure to microorganism. Presence of these groups enhanced hydrophilic character of the film surface, which was more susceptible to further water absorption and also to enzyme attack.

It is worth mentioning, that the changes observed support only small-scale hydrolysis scission of ester bonds in accordance with relatively low mass loss of samples.

Conclusion

The results obtained by this research led to the following conclusions:

– The availability of nutrients and C/N ratio in cultivation medium is highly decisive for the biofilm formation and also for its character. Biofilm formation was not observed in mineral media with low nutrient availability and low C/N ratio. PCL film seemed to have a negligible effect on both planktonic bacterial growth enhancement and inhibition but affected the mode of growth through its function of solid carrier for biofilm formation after approx. 14 days of continuous cultivation only in nutritious media.

– EPS were produced during whole cultivation period (21 days), and their content was considerably higher in the presence of PCL film in nutrient media.

– An increased production of extracellular proteins and polysaccharides was determined while there was a presence of glucose in cultivation medium (NBG). The production of eDNA was not influenced.

– The surface erosion rate of PCL samples increased under conditions when the biofilm formation on the polyester film was favored.

References

Allan VJM, Callow ME, Macaskie LE, Paterson-Beedle M (2002) Effect of nutrient limitation on biofilm formation and phosphatase activity of a *Citrobacter* sp. Microbiology 148:277–288

Blencke HM, Homuth G, Ludwig H, Mäder U, Hecker M, Stülke J (2003) Transcriptional profiling of gene expression in response to glucose in *Bacillus subtilis*: regulation of the central metabolic pathways. Metabol Eng 5:133–150

Bridier A, Meylheuc T, Briandet R (2013) Realistic representation of *Bacillus subtilis* biofilms architecture using combined microscopy (CLSM, ESEM and FESEM). Micron 48:65–70

Czaczyk K, Myszka K (2007) Biosythesis of extracellular polymeric substances (EPS) and its role in microbial biofilm formation. Polish J Environ Stud 16(6):799–806

Dubois M, Gilles KA, Hamilton JK, Rebers PA, Smith F (1956) Colorimetric method for determination of sugars and related substances. Anal Chem 28(3):350–357

Echlin P (2009) Handbook of sample preparation for scanning electron microscopy and X-ray microanalysis. Springer, US

Flemming HC, Neu TR, Wozniak DR (2007) The EPS matrix: the "house of biofilm cells". J Bacteriol 189(22):7945–7948

Jung JH, Choi NY, Lee SY (2013) Biofilm formation and exopolysaccharide (EPS) production by *Cronobacter sakazakii* depending on environmental conditions. Food Microbiol 34:70–80

Kearns DB, Chu F, Branda SS, Kolter R, Losick R (2005) A master regulator for biofilm formation by *Bacillus subtilis*. Mol Microbiol 55(3):739–749

Kodali V, Prabhakar Das S, Sen R (2009) An exopolysaccharide from a probiotic: Biosynthesis dynamics, composition and emulsifying activity. Food Res Inter 42(5-6):695–700

Lefévre C, Tidjani A, Vander Wauven C, David C (2002) The interaction mechanism between microorganisms and substrate in the biodegradation of polycaprolactone. J Appl Polym Sci 83:1334–1340

Lowry OH, Rosenbrough NJ, Farr AL, Randall RJ (1951) Protein measurement with Folin phenol reagent. J Biol Chem 193(1):265–275

Marvasi M, Visscher PT, Martinez LC (2010) Exopolymeric substances (EPS) from *Bacillus subtilis*:polymers and genes encoding their synthesis. FEMS Microbiol Lett 313(1):1–9

Miqueleto AP, Dolosic CC, Pozzi E, Foresti E, Zaiat M (2010) Influence of carbon sources and C/N ratio on EPS production in anaerobic sequencing batch biofilm reactors for wastewater treatment. Biores Technol 101:1324–1330

Nostro A, Cellini L, Di Giulio M, D'Arrigo M, Marino A, Blanco AR, Favaloro A, Cutroneo G, Bisignano G (2012) Effect of alkaline pH on staphylococcal biofilm formation. APMIS 120:733–742

Rinaudi L, Fujishige NA, Hirsch AM, Banchio E, Zorreguieta A, Giordano W (2006) Effects of nutritional and environmental conditions on *Sinorhizobium meliloti* biofilm formation. Res Microbiol 157:867–875

Rohindra D, Sharma P, Khurma J (2005) Soil and microbial degradation study of poly(ε-caprolactone) – poly(vinyl butyral) blends. Macromol Symp 224(1):323–332

Romero D (2013) Bacterial deteriminants of the social behaviour of *Bacillus subtilis*. Res Microbiol 167:788–798

Ryu JH, Kim H, Beuchat LR (2004) Attachment and biofilm formation by *Escherichia coli* O157:H7 on stainless steel as influenced by exopolysaccharide production, nutrient availability, and temperature. J Food Protect 67:2123–2131

Sheng GP, Yu HQ, Li XY (2010) Extracellular polymeric substances (EPS) of microbial aggregates in biological wastewater treatment systems: a review. Biotechnol Adv 28:882–894

Sivan A (2011) New perspectives in plastic biodegradation. Curr Opin Biotechnol 22:422–426

Speranza B, Corbo MR, Sinigaglia M (2011) Effects of nutritional and environmental conditions on *Salmonella* sp. biofilm formation. J Food Sci 76(1):M12–M16

Yan Z, Zheng XW, Chen JY, Han JS, Hai BZ (2013) Effect of different *Bacillus* strains on the profile of organic acids in a liquid culture of Daqu. J Inst Brew 119(1-2):78–83

Zafra A, Lamprecht-Grandío M, González de Figueras C, González-Pastor JE (2012) Extracellular DNA release by undomesticated *Bacillus subtilis* is regulated by early competence. PLoS ONE 7(11), e48716

Zahora US, Rahman M, Shahedur Ano T (2009) Biofilm formation and lipopeptide antibiotic iturin A production in different peptone media. J Environ Sci Suppl 4:S24–S28

Morphological and Production Changes in Stressed Red Yeasts Monitored Using SEM and Raman Spectroscopy

K. Hrubanova[1], O. Samek[1], A. Haronikova[2], S. Bernatova[1], P. Zemanek[1], I. Marova[2], V. Krzyzanek[1]

[1.] Institute of Scientific instruments, The Czech Academy of Sciences, v.v.i., Brno, Czech Republic.
[2.] Centre for Material Research, Brno University of Technology, Brno, Czech Republic.

We report on our investigations of the influence of different cultivation conditions on lipids, using scanning electron microscopy (SEM) and Raman spectroscopy techniques. Here, SEM uses electron beam to gain information about morphology of cells which reflects cells response on the applied stress. Consequently, Raman spectroscopy [1] was used for the determination of carotenoids and lipids present in the biomass. Thus, our study targets some factors which could lead to efficient industrial production of carotenoids and lipids in selected biotechnological production.

Applied stress and other environmental factors can induce changes in cell composition, metabolism and physiology [2]. In our investigations we focused on red/carotenogenic yeasts which also produce high amount of lipidic compounds. Carotenoids are membrane-bound lipid-soluble pigments, which can act as effective antioxidants and scavenge singlet oxygen. In red yeast controlled physiological and nutrition stress can be used for enhanced pigment and also oil production. Namely, in our experiments osmotic stress was induced in the two different media with different carbon to nitrogen (C/N) ratio which led to production of yeast lipids or carotenoids. Note, that also morphology of cells can be changed. Both media contain the same: salts, glucose and ammonium sulfate with different C/N ratio. First growth medium (medium 1) indicate a positive results to carotenoids production and second medium (medium 2) with high C/N ratio lead to an increased lipid production. Our experimental results are presented in Figure 1 and Figure 2.

For SEM imaging the samples of *Cystofilobasidium infirmominiatum* were prepared in the following way: (i) the samples were cultivated aerobically at 25°C in the two different media for 144 hours. (b) cells suspensions were fixed in 2.5 % glutaraldehyde in PBS for 2 hours and 30 min in 1 % OsO_4, dehydrated by ethanol series and dried in HDMS on the glass slides. Both images of prepared samples were scanned without any metal coating at electron beam energy 1 keV and beam current 6.3 pA in SEM Magellan (FEI). The samples of *Sporobolomyces shibatanus* were cultivated as mentioned above and observed by cryo scanning electron microscopy (cryo-SEM). The sample was quickly frozen in liquid nitrogen, moved into a vacuum chamber (ACE600, Leica Microsystems) where it was freeze-fractured and sublimated at -95°C for 5 minutes. In the next step, the sample was moved at high vacuum using a shuttle (VCT100, Leica Microsystems) into the SEM (Magellan, FEI) equipped with a cold stage and the fractured structure was observed with 1 keV electron beam at -120°C and beam current 6.3 pA without any metal coating.

Our results are quite encouraging, however, further systematic studies are required in order to fully monitor cell response mechanisms on applied stress. Such studies are currently under way in our laboratories, exploiting combination of SEM and Raman spectroscopy approaches.

References:
[1] O. Samek *et al*, Sensors **10** (2010), p. 8635-8651.
[2] I. Marova *et al*, J of Environmental Management **95** (2012), p. S338.
[3] This work received support from the Ministry of Health, Ministry of Education, Youth and Sports of the Czech Republic (LO1212) together with the European Commission and the Czech Science Foundation (ALISI No. CZ.1.05/2.1.00/01.0017) and the Grant Agency of the Czech Republic (GA14-20012S and GA15-20645S). A.H. and I.M. were supported by the project "Materials Research Centre at FCH BUT- Sustainability and Development" - no. LO1211 of the Ministry of Education, Youth and Sports of the Czech Republic. KH acknowledges the support of FEI/CSMS scholarship.
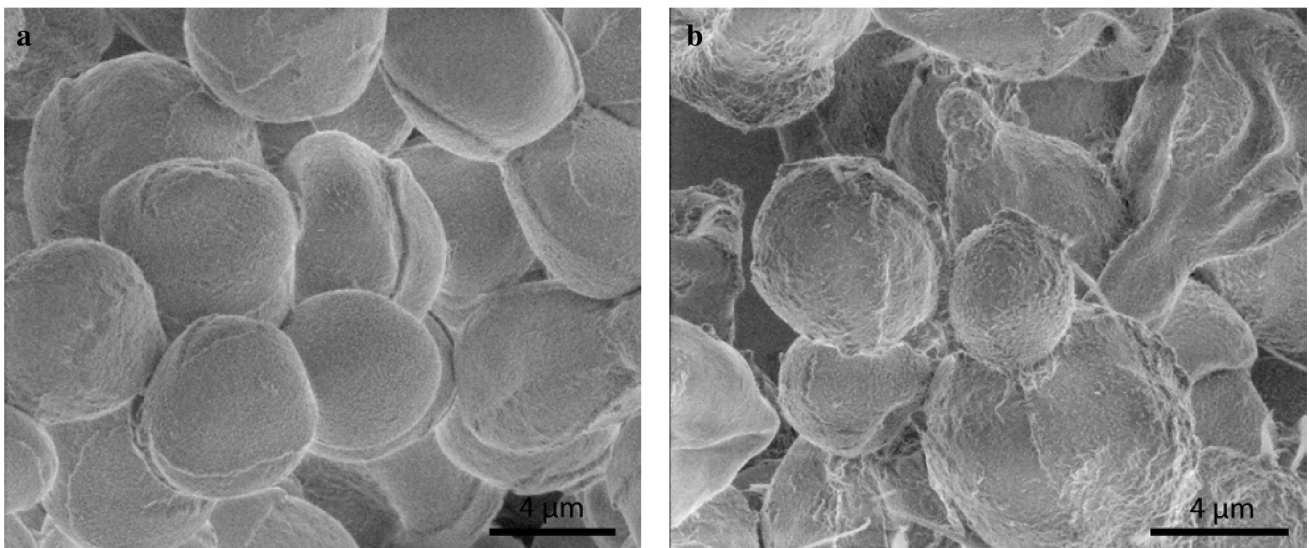
Figure 1. a) SEM image of *Cystofilobasidium infirmominiatum* (medium 1); b) SEM image of *Cystofilobasidium infirmominiatum* (medium 2), here different surface morphology is clearly visibly due to the applied stress.
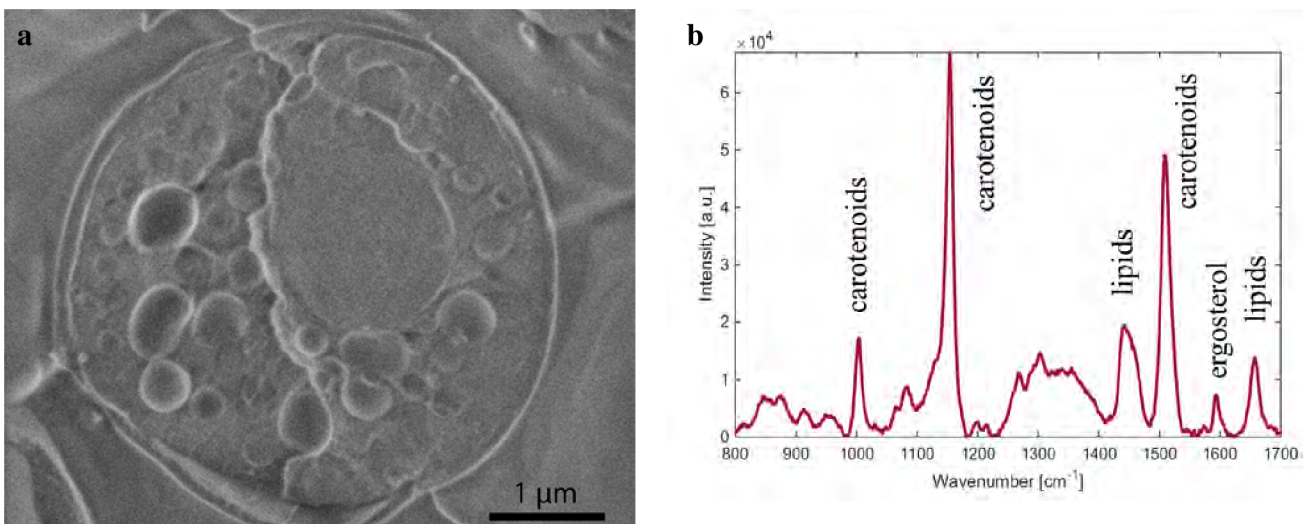
Figure 2. *Sporobolomyces shibatanus* (cultivated in lipid enhancing medium 2), a) Cryo-SEM image of one cell clearly showing lipid bodies, b) presence of applied stress on the same organism led to important overproduction of beta-carotene, ergosterol and lipids which can be confirmed by Raman spectroscopy.